MycoKeys 49: 1–14 (2019)
doi: 10.3897/mycokeys.49.31904
http://mycokeys.pensoft.net

RESEARCH ARTICLE

A peer-reviewed open-access journal
MycoKeys
Launched to accelerate biodiversity research

Two new endophytic *Colletotrichum* species from *Nothapodytes pittosporoides* in China

Sixuan Zhou[1,2], Lijun Qiao[1], Ruvishika S. Jayawardena[3], Kevin D. Hyde[3], Xiaoya Ma[1,3], Tingchi Wen[1], Jichuan Kang[1]

1 *Engineering Research Center of the Utilization for Characteristic Bio-Pharmaceutical Resources in Southwest, Ministry of Education/College of Life Sciences, Guizhou University, Guiyang, Guizhou Province 550025, China* **2** *Institute of Animal Husbandry and Veterinary, Guizhou Academy of Agricultural Sciences, Guiyang, Guizhou province 550006, China* **3** *Center of Excellence in Fungal Research, Mae Fah Luang University, Chiang Rai 57100, Thailand*

Corresponding author: *Jichuan Kang* (jckang@gzu.edu.cn)

Academic editor: *T. Lumbsch* | Received 25 November 2018 | Accepted 20 February 2019 | Published 11 March 2019

Citation: Zhou S, Qiao L, Jayawardena RS, Hyde KD, Ma X, Wen T, Kang J (2019) Two new endophytic *Colletotrichum* species from *Nothapodytes pittosporoides* in China. MycoKeys 49: 1–14. https://doi.org/10.3897/mycokeys.49.31904

Abstract

Two new endophytic species, *Colletotrichum jishouense* **sp. nov.** and. *C. tongrenense* **sp. nov.** were isolated from *Nothapodytes pittosporoides* in Guizhou and Hunan provinces, China. Detailed descriptions and illustrations of these new taxa are provided and morphological comparisons with similar taxa are explored. Phylogenetic analysis with combined sequence data (ITS, GAPDH, ACT and TUB2) demonstrated that both species formed distinct clades in this genus. This is the first record of *Colletotrichum* species from *N. pittosporoides* in China.

Keywords

Ascomycota, Multi-loci, Phylogeny, Morphology, Taxonomy

Introduction

Nothapodytes pittosporoides (Oliv.) Sleum (Icacinacceae) has been used as Traditional Chinese Medicine (TCM) and is mainly distributed in southern China (Fang 1981). It is quickly gaining attention as the characteristic compounds of camptothecin and its derivatives (CIDs) in *N. pittosporoides* (Dong et al. 2015) are used as anti-cancer drugs in the world market (Demain and Vaishnav 2011). It is recognised that endophytes reside in the internal tissues of living plants and potentially have the capability to produce the same functional compounds as their hosts (Stierle et al. 1993, 1995; Kusari et al.

2008; Bhalkar et al. 2016; Uzma et al. 2018). The endophytic fungi in *N. pittosporoides* were therefore studied for their secondary metabolites with pharmaceutical potential.

Endophytic fungi were isolated from different parts of *Nothapodytes pittosporoides* (Zhou et al. 2017; Qiao et al. 2018) collected from different sites. A high diversity of fungi were found, of which several species of *Colletotrichum* were isolated and identified.

Colletotrichum species are globally distributed and occur in various plants as endophytes (Tibpromma et al. 2018). *Colletotrichum* is the sole genus in the family Glomerellaceae (Glomerellales, Sordariomycetes, Wijayawardene et al. 2018) and was introduced by Corda (1831) with the type species *C. lineola* (Jayawardena et al. 2016, 2017, Wijayawardene et al. 2017). Recently, several studies have analysed this genus and these are summarised in Hyde et al. (2014), who accepted 163 names. Since this review, about 30 more species have been introduced (Baroncelli et al. 2017; Douanlameli et al. 2017; Jayawardena et al. 2017; Silva et al. 2018).

In this study, we introduce two novel species, *C. jishouense* sp. nov. and *C. tongrenense* sp. nov. isolated as endophytes from *N. pittosporoides*. These species are based on both morphological features and molecular sequence data evidence.

Material and methods

Sample collection

Fresh healthy plant samples (leaves, stems and roots) of *Nothapodytes pittosporoides* were collected in Tongren City, Guizhou Province and Jishou City, Hunan Province, China. Materials were kept in zip-lock bags on ice. Fungal isolation was carried out within 24 hours of collection.

Isolation and cultivation of fungal endophytes

Each part of the plant was surface sterilised to eliminate epiphytic microorganisms. The samples were washed thoroughly in running tap water, followed by immersion in 70% (v/v) ethanol for 3 min to sterilise the surfaces, then rinsed with sterilised distilled water for 1 min. Samples were dried on sterilised filter paper and then placed in 3% hydrogen peroxide for 7 min, washed in sterilised distilled water and dried on a sterilised filter paper again. Each plant tissue was then cut into small cubes (0.5 × 0.5 cm) using a sterilised blade. The cubes were placed on potato dextrose agar (PDA) medium in Petri dishes containing with antibiotic (100 mg/l chloramphenicol) and incubated at 25 °C until fungal growth emerged from the plant segments. The endophytic fungi were isolated and sub-cultured on fresh PDA plates at 25 °C in darkness. Fungal isolates were stored on PDA and covered with sterilised water at 4 °C.

The type specimens are deposited in Guizhou Agricultural College (GACP), Guiyang, China. Ex-type living cultures are deposited at Guizhou Medical University Culture Collection (GMBC). Mycobank numbers are provided.

DNA extraction, PCR amplification, and sequencing

Genomic DNA was extracted from fresh fungal mycelia using the BIOMIGA Fungus Genomic DNA Extraction Kit (GD2416, Biomiga, USA), following the manufacturer's instructions. DNA samples were stored at -20 °C until used for polymerase chain reaction (PCR). Four loci, rDNA regions of internal transcribed spacers (ITS), partial β-tubulin (TUB2), actin (ACT) and glyceraldehyde-3-phosphate dehydrogenase (GAPDH) genes were amplified by PCR with primers ITS1 (Gardes and Bruns 1993) + ITS4 (White et al. 1990), Bt-2a + Bt-2b (Glass and Donaldson 1995), ACT-512F + ACT-783R (Carbone and Kohn 1999) and GDF1 + GDR1 (Guerber et al. 2003), respectively. The components of a 50 µl volume PCR mixture were used as follows: 2.0 µl of DNA template, 1 µl of each forward and reverse primer, 25 µl of 2 × Easy *Taq* PCR Super Mix (mixture of Easy *Taq* TM DNA Polymerase, dNTPs and optimised buffer, Beijing Trans Gen Biotech Co., Chaoyang District, Beijing, China) and 19 µl sterilised water. PCR thermal cycle programmes for ITS and ACT gene amplification were provided as: initial denaturation at 95 °C for 3 min, followed by 35 cycles of denaturation at 95 °C for 30 s, annealing at 52 °C for 50 s, elongation at 72 °C for 45 s and final extension at 72 °C for 10 min. The PCR thermal cycle programme for GAPDH gene amplification was provided as: initial denaturation at 95 °C for 3 min, followed by 35 cycles of denaturation at 94 °C for 30 s, annealing at 60 °C for 30 s, elongation at 72 °C for 45 s and final extension at 72 °C for 10 min. The PCR thermal cycle programme for TUB2 gene amplification was provided as: initial denaturation 95 °C for 3 min, followed by 35 cycles of denaturation at 94 °C for 30 s, annealing at 55 °C for 45 s, elongation at 72 °C for 45 s and final extension at 72 °C for 10 min. The quality of PCR products were checked with 1.5% agarose gel electrophoresis stained with ethidium bromide. PCR products were sent for sequencing to Sangon Co., Shanghai, China.

Sequence alignment and phylogenetic analyses

Sequence data of the four loci were blasted in the GenBank database and all top hits, including the corresponding type sequences, were retrieved (Table 1). Multiple sequence alignments for ITS, TUB2, ACT and GAPDH were constructed and carried out using the MAFFT v.7.110 online programme (http://mafft.cbrc.jp/alignment/server/, Katoh and Standley 2013) with the default settings. Four datasets of ITS, TUB2, ACT and GAPDH of *Colletotrichum* spp. were combined and manually adjusted using BioEdit v.7.0.5.3 (Hall 1999), then assembled using SequenceMatrix1.7.8 (Vaidya et al. 2011). The final alignments contained 1593 characters with gaps, ITS with 522 sites, TUB2 with 510 sites, ACT with 269 sites and GAPDH with 292 sites. Fifty-four taxa and 1593 sites were used for phylogenetic analyses. Gaps were treated as missing data in maximum likelihood (ML), Bayesian Inference (BI) and parsimony trees. The phylogeny website tools "ALTER" (Glez-Peña et al. 2010) were used to convert the alignment file from Fasta to PhyLip file for RAxML analysis and Nexus for MrBayes. All loci were tested based on single maximum likelihood (ML) trees and Bayesian Inference (BI) methods.

Table 1. Taxa used for phylogenetic analyses in the study.

Species name	Isolate No.[b]	GenBank Accession No.			
		ITS	GAPDH	ACT	TUB
Colletotrichum agaves	AR3920	DQ286221	–[a]	–	–
C. anthrisci	CBS 125334*	GU227845	GU228237	GU227943	GU228139
C. aracearum	LC1041	KX853167	KX893586	KX893578	KX893582
C. arxii	CBS 132511	KF687716	KF687843	KF687802	KF687881
C. brevisporum	BCC 38876*	JN050238	JN050227	JN050216	JN050244
C. chlorophyte	IMI 103806*	GU227894	GU228286	GU227992	GU228188
C. citricola	SXC151*	KC293576	KC293736	KC293616	KC293656
C. citri-maximae	AGMy0254*	KX943582	KX943578	KX943567	KX943586
C. cliviae	CBS 125375*	JX519223	JX546611	JX519240	JX519249
C. coccodes	CBS 369.75	HM171679	HM171673	HM171667	JX546873
C. colombiense	CBS 129818*	JQ005174	JQ005261	JQ005522	JQ005608
C. conoides	CAUG17*	KP890168	KP890162	KP890144	KP890174
C. constrictum	CBS 128504*	JQ005238	JQ005325	JQ005586	JQ005672
C. cordylinicola	ICMP18579*	JX010226	JX009975	HM470235	JX010440
C. dematium	CBS 125.25*	GU227819	GU228211	GU227917	GU228113
C. dracaenophilum	CBS 118199	JX519222	JX546707	JX519238	JX519247
C. euphorbiae	CPC 21823	KF777146	KF777131	KF777125	KF777247
C. excelsum-altitudum	CGMCC 3.15130*	HM751815	KC843502	KC843548	JX625211
C. fructi	CBS 346.37*	GU227844	GU228236	GU227942	GU228138
C. fuscum	CBS 133701*	KM105174	KM105524	KM105384	KM105454
C. fusiforme	MFLU 13-0291*	KT290266	KT290255	KT290251	KT290256
C. gigasporum	CBS 133266	KF687715	KF687822	–	KF687866
C. godetiae	CBS 133.44*	JQ948402	JQ948733	JQ949723	JQ950053
C. grevilleae	CBS 132879*	KC297078	KC297010	KC296941	KC297102
C. hymenocallidicola	MFLUCC 12–0531*	KT290264	KT290263	–	–
C. jishouense	**GZU_HJ2_G2**	**MH482931**	**MH681657**	**MH708134**	**MH727472**
C. jishouense	**GZU_HJ2_G3**	**MH482929**	**MH681658**	**MH708135**	**MH727473**
C. jishouense	**GZU_HJ2_G4**	**MH482932**	**MH681659**	**MH708136**	**MH727474**
C. jishouense	**GZU_HJ3_J5**	**MH482930**	**MH492706**	**MH708137**	–
C. kahawae	C1266.1	JX010231	JX010012	JX009452	JX010444
C. ledebouriae	CPC 25671*	KX228254	–	KX228357	–
C. liaoningense	CAUOS2*	KP890104	KP890135	KP890097	KP890111
C. lindemuthianum	CBS 144.31*	JQ005779	JX546712	JQ005842	JQ005863
C. magnisporum	CBS 398.84	KF687718	KF687842	KF687803	KF687882
C. malvarum	CBS 521.97*	KF178480	KF178504	KF178577	KF178601
C. neosansevieriae	CPC 25127*	KR476747	KR476791	KR476790	KR476797
C. nymphaeae	CBS 515.78	JQ948197	JQ948527	JQ949518	JQ949848
C. orchidophilum	CBS 632.80*	JQ948151	JQ948481	JQ949472	JQ949802
C. pisicola	CBS 724.97*	KM105172	KM105522	KM105382	KM105452
C. pseudoacutatum	CBS 436.77*	JQ948480	JQ948811	JQ949801	JQ950131
C. pseudomajus	CBS 571.88	KF687722	KF687826	KF687801	KF687883
C. radices	CBS 529.93	KF687719	KF687825	KF687785	KF687869
C. rhombiforme	CBS 129953*	JQ948457	JQ948788	JQ949778	JQ950108
C. sansevieriae	MAFF 239721*	NR_152313	–	–	–
C. spinosum	CBS 515.97*	KF178474	KF178498	KF178571	KF178595
C. tanaceti	CBS 132693*	JX218228	JX218243	JX218238	JX218233
C. trichellum	CBS 217.64*	GU227812	GU228204	GU227910	GU228106
C. tongrenense	**GZU_TRJ1-37**	**MH482933**	**MH705332**	**MH717074**	**MH729805**
C. tropicicola	L58	JN050240	JN050229	JN050218	JN050246
C. truncatum	CBS 151.35	GU227862	GU228254	GU227960	GU228156
C. vietnamense	CBS 125478	KF687721	KF687832	KF687792	KF687877
C. yunnanense	CBS 132135*	JX546804	JX546706	–	JX519248
Monilochaetes infuscans	CBS 869.96	JQ005780	JX546612	JQ005843	JQ005864

Notes: New strains are in bold. * ex-type strains. [a] No data in GenBank. [b] BCC: BIOTEC Culture Collection, National Center for Genetic Engineering and Biotechnology (BIOTEC), Khlong Luang, Pathumthani, Thailand; CBS: Culture collection of the Centraalbureau voor Schimmelcultures, Fungal Biodiversity Centre, Utrecht, The Netherlands; CGMCC: China General Microbiological Culture Collection; CPC: Working collection of Pedro W. Crous, housed at CBS; IMI: Culture collection of CABI Europe UK Centre, Egham, UK; LC: Working collection of Lei Cai, housed at CAS, China; MAFF: MAFF GenBank Project, Ministry of Agriculture, Forestry and Fisheries, Tsukuba, Japan; MFLUCC: Mae Fah Luang University Culture Collection, Chiang Rai, Thailand; MFLU: Herbarium of Mae Fah Luang University, Chiang Rai, Thailand; ICMP: International Collection of Microorganisms from Plants, Auckland, New Zealand.

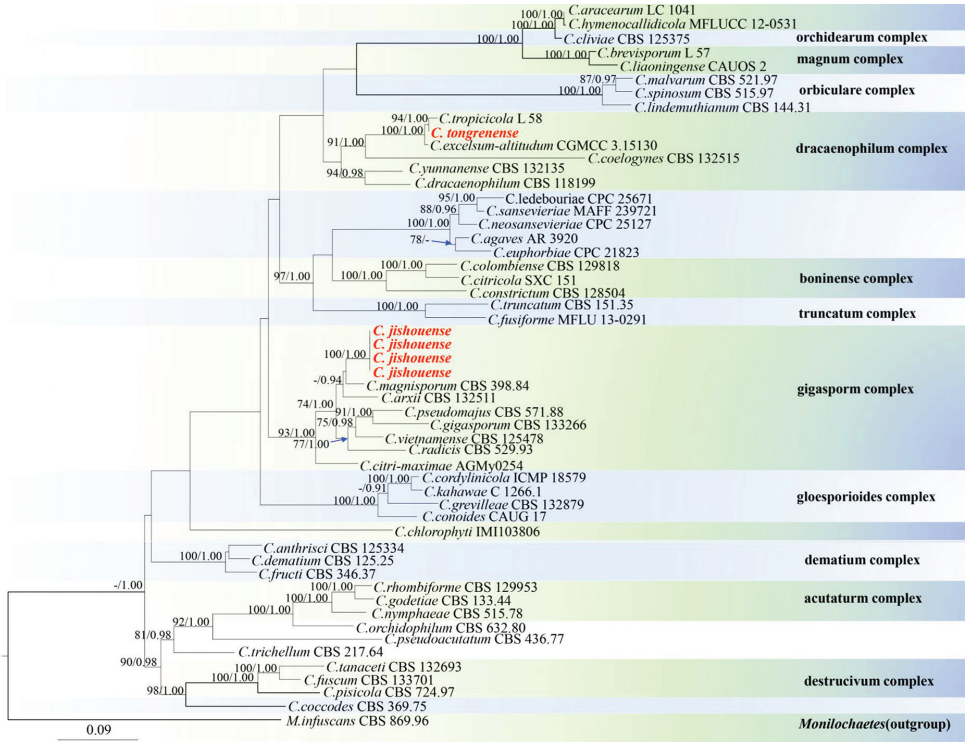

Figure 1. Phylogram generated from Maximum Likelihood (RAxML) analysis based on combined ITS, ACT, TUB2 and GAPDH DNA sequence data of *Colletotrichum*. Bayesian Posterior Probabilities (BSPP) greater than 0.90 and Maximum Likelihood Bootstrap Support values (MLBS) greater than 70% are shown above branches. New isolates are in red. The tree is rooted with *Monilochaetes infuscans* CBS 869.96.

Maximum Likelihood (ML) analysis was performed on the website of CIPRES Science Gateway v.3.3 (http://www.phylo.org/portal2/, Miller et al. 2010) using RAxML-HPC Blackbox version 8.2.10. All free model parameters were estimated by RAxML and ML estimate of 25 per site rate categories. Final ML searches were conducted using the GTRGAMMA model. Bootstrap Support values (BS) equal to or greater than 60% are given above each node (Fig. 1).

For Bayesian Inference (BI), a Markov Chain Monte Carlo (MCMC) algorithm was used to generate phylogenetic trees with Bayesian probabilities using MrBayes 3.2.6 (Ronquist et al. 2012) for the combined sequence datasets. MrModeltest v.2.3 (Nylander 2004) was used to carry out the statistical selection of the best-fit model of nucleotide substitution. GTR+G model was selected for ITS, a GTR+I+G model for TUB2, a HKY+I+G model for ACT and GAPDH were incorporated into the analysis. Models of nucleotide substitution for each gene determined by MrModeltest v. 2.3 were included for each set of gene sequence data. Two runs were executed simultaneously for 1,000,000 generations and sampled every 100 generations. Of the trees, 25% were discarded as burn-in and the remaining trees were used to calculate the posterior probabilities. Convergence was assumed when the standard deviation of split

sequences was less than 0.01. Phylogenetic trees were visualised using FigTree v1.4.0 (http://tree.bio.ed.ac.uk/software/figtree/, Rambaut 2012). The final alignment was deposited in Treebase (http://www.treebase.org, submission number 23622).

Morphological analysis

Isolates were grown on PDA, water agar (WA) with bamboo and corn malt agar medium (CMA) for examination of morphological characters. Colonies were examined after 7, 14 and 21 d at 25 °C in darkness. The morphological characters of mycelia, conidiophores, conidiogenous cells and conidia were observed and photographed using a Nikon NI-SS microscope and processed with Adobe Photoshop CS3 Extended version 10.0 software (Adobe Systems, USA).

Results

Sample collection and isolation

Four hundred and forty endophytic fungi were isolated from different parts of *Nothapodytes pittosporoides* in Jishou, Hunan Province and Tongren, Guizhou Province, belonging to twenty-four genera based on ITS sequences analysis. *Colletotrichum* was a common genus amongst the isolates. Herein, five endophytic taxa were isolated and identified as *Colletotrichum* of which GZU_HJ2_G2, GZU_HJ2_G3 and GZU_HJ2_G4 were isolated from roots and GZU_HJ3_J5 from stems of *N. pittosporoides* in Jishou, Hunan Province. GZU_TRJ1-37 was isolated from stems of *N. pittosporoides* in Tongren, Guizhou Province.

Phylogenetic analyses

Phylogenetic analysis of four loci (ITS, GAPDH, ACT and TUB2) sequence datasets included 54 taxa, 1,593 positions including gaps (ITS: 1–522, TUB2: 523–1032, ACT: 1033–1301, GAPDH: 1302–1593) and *Monilochaetes infuscans* (CBS 869.96) was selected as the outgroup taxon. The 50% majority rule consensus Bayesian phylogram presented in Fig. 1 and the topology is recovered with the RAxML tree. Values of the Bayesian PP ≥ 0.70 from MCMC analyses and bootstrap support values of RAxML ≥ 90% are given on the branches.

Representatives of complexes and species in *Colletotrichum* (Noireung et al. 2012; Tao et al. 2013; Liu et al. 2014; Jayawardena et al. 2016; Douanla-meli et al. 2017) are included in the phylogenetic analyses (Fig. 1). Four isolates, GZU_HJ2_G2, GZU_HJ2_G3, GZU_HJ2_G4 and GZU_HJ3_J5, were identified as distinct new species and are described as *Colletotrichum jishouense* sp. nov., and as *C. tongrenense* sp. nov., based on their morphology and molecular phylogeny.

Taxonomy

***Colletotrichum jishouense* SX. Zhou, JC. Kang & K.D. Hyde, sp. nov.**
MycoBank number: MB828723
Fig. 2

Etymology. '*Jishouense*' referring to Jishou City, site of collection of type species.

Description. Endophytic fungus in root of *Nothapodytes pittosporoides*. ***Sexual morph:*** Undetermined. ***Asexual morph:*** Vegetative hyphae 0.5–1.2 µm diam. (n=10), hyaline, smooth-walled, septate, branched. *Chlamydospores* not observed. *Conidiophores* formed on a basal cushion, hyaline to pale brown, clavate or cylindrical, septate and irregularly branched. *Conidiogenous cells* 4–11 × 2–3 µm ($\bar{x}$= 6.7 ± 3.0 × 2.6 ± 0.4 µm, n=20), L/W ratio= 2.5, hyaline, smooth-walled, clavate to mostly ampulliform or cylindrical. *Conidia* hyaline, smooth-walled, aseptate, straight, cylindrical, some clavate, the apex and base rounded, 5–14 × 3–5 µm ($\bar{x}$ = 10.8 ± 1.8 × 3.7 ± 0.5 µm, n = 40), L/W ratio= 2.9. *Appressoria* not observed.

Culture characteristics. Colonies on PDA, reaching 55–60 mm diam. in 14 days at 25 °C in darkness, circular, mycelium superficial and partially immersed, more or less planar, brown in the medium but covered with abundant, pale and lanose to cottony aerial mycelium, reverse greenish pale brown, margin entire and irregular.

Material examined. CHINA, Hunan Province, Jishou City (28°55'24"N, 109°10'24"E), isolated from healthy roots of *Nothapodytes pittosporoides*, 27 May 2016, S.X. Zhou (Holotype GACP GZU_HJ2_G3 dried culture), ex-type living culture, GMBC0209, living culture, GZU_HJ2_G2, living culture, GZU_HJ2_G4.

China, Hunan Province, Jishou City (28°55'24"N, 109°10'24"E), isolated from healthy stem of *Nothapodytes pittosporoides*, 27 May 2016, S.X. Zhou, living culture, GZU_HJ3_J5.

Notes. *Colletotrichum jishouense* belongs in the *gigasporum* species complex. *C. jishouense* has shorter and narrower conidiogenous cells and conidia than all the related species in the *C. gigasporum* complex (Liu et al. 2014). Phylogenetically, our four new isolates clustered together with *C. magnisporum* (CBS 398.84). The pairwise dissimilarities of DNA sequences between *C. jishouense* and *C. magnisporum* were 2 bp, 20 bp, 5 bp and 9 bp in ITS, TUB2, ACT and GAPDH, respectively. They are phylogenetically distinct species and, therefore, *C. jishouense* sp. nov. is introduced.

***Colletotrichum tongrenense* S.X. Zhou, J.C. Kang & K.D. Hyde, sp. nov.**
MycoBank number: MB828725
Fig. 3

Etymology. '*tongrenense*' referring Tongren City, site of collection of type species.

Description. Endophytic in leaves and stems of *Nothapodytes pittosporoides*. ***Sexual morph:*** Undetermined. ***Asexual morph:*** On WA, vegetative hyphae 1.4–6 µm diam. (n=10), smooth-walled, septate, branched, hyaline. *Chlamydospores* not

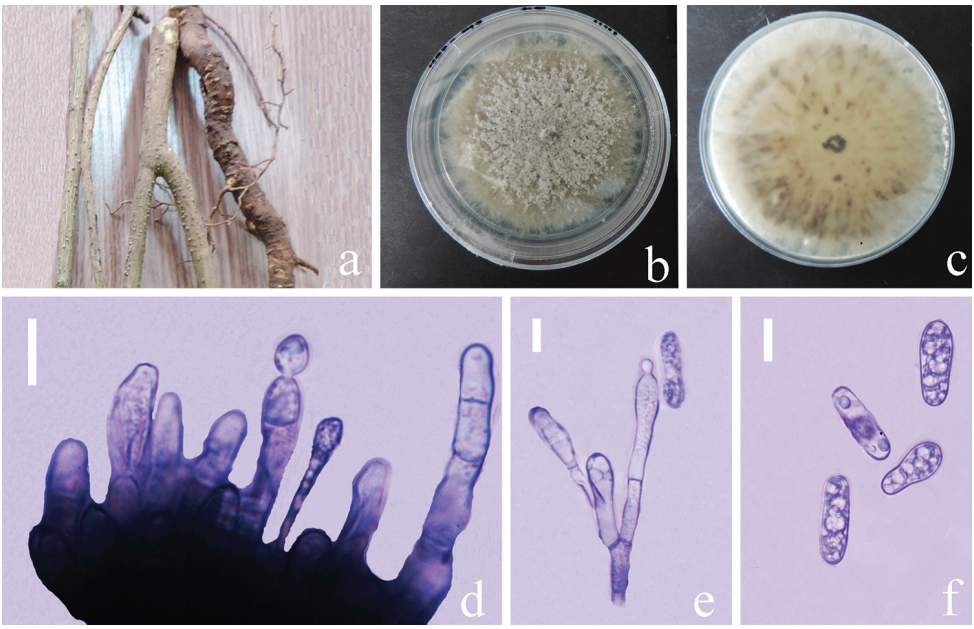

Figure 2. *Colletotrichum jishouense* (GACP GZU_HJ2_G3, holotype) **a** stems and roots of *Nothapodytes pittosporoides* **b,c** colonies on PDA **d** conidiophores in cotton blue **e** conidiophores with conidia in cotton blue **f** conidia in cotton blue. Scale bars: 10 μm (**d**), 5 μm (**e, f**).

observed. *Setae* unbranched, septate, tapering to rounded at apical end, pale brown to dark brown, smooth-walled, 45–90 μm long, 5.9–6.2 μm wide at widest part, 2.6–5.8 μm wide at bottom, 1.5–1.6 μm wide at apex. *Conidiophores* pale brown, septate, branched. *Conidiogenous cells* pale, hyaline, smooth-walled, erect, clavate or cylindrical, 2–11 × 1–2 μm ($\bar{x}$ = 6.3 ± 4.4 × 1.7 ± 0.4 μm, n = 20), L/W ratio= 3.7. *Conidia* hyaline, aseptate, smooth-walled, variable in size and shape, thick-walled, ellipsoidal to subglobose, the apex and base rounded, slightly constricted in the middle, 11–14 × 5–7 μm ($\bar{x}$ = 13.1 ± 1.0 × 5.5 ± 0.6 μm, n = 40), L/W ratio= 2.4.

Culture characteristics. Cultures on WA at 25 °C in darkness, reaching 15–18 mm diam. in 21 days, white to grey, asymmetrical surface, reverse dark grey to black.

Colonies on PDA at 25 °C reaching 45–55 mm diam. in 12 days in darkness, circular, more or less planar, surface dark brown, covered with abundant, pale grey, lanose to cottony aerial mycelium, margin smooth, entire and pale white. Reverse dark grey, margin pale white.

Cultures on CMA, 10–15 mm diam. in 21 days, covered with dark brown aerial mycelium, sparse, reverse light brown, margin irregular.

Material examined. CHINA, Guizhou province, Tongren (27°35'37"N, 109°10'58"E, elevation 332.8 m), isolated from healthy stems of *Nothapodytes pittosporoides*, 27 May 2016, S.X. Zhou and L.J. Qiao (Holotype GACP GZU-TRJ1-37 dried culture), ex-type living culture, GMBC0209.

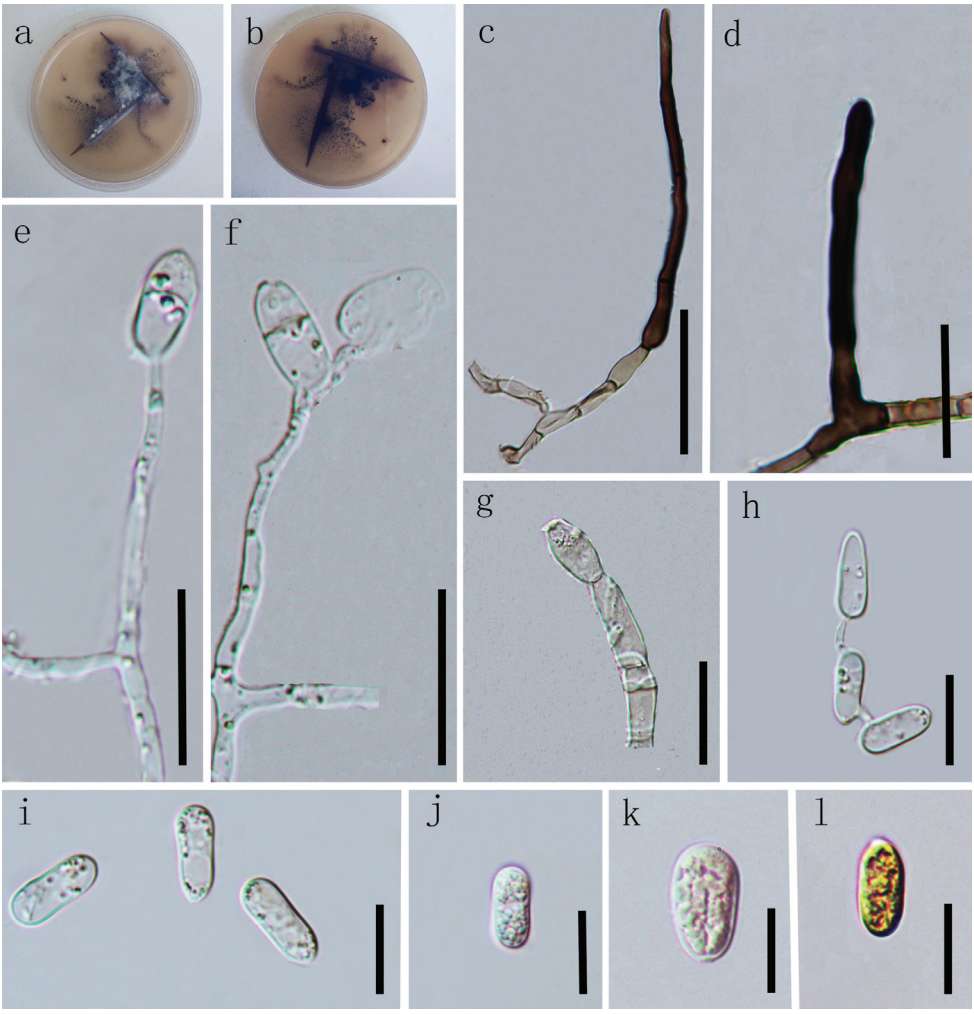

Figure 3. *Colletotrichum tongrenense* (GACP GZU_TRJ1-37, holotype) **a, b** colonies on WA **c–g** Conidiophores **h–l** Conidia. Scale bars: 40 μm (**c**), 20 μm (**d, g**), 10 μm (**e, f**), 10 μm (**h–l**).

Notes. *Colletotrichum tongrenense* belongs to the *C. dracaenophilum* species complex (Damm et al. 2019). Morphologically, *C. tongrenense* resembles *C. tropicicola* and *C. excelsum-altitudum* in conidia characters, but it can be distinguished from *C. tropicicola* in having setae and longer conidia (15–19 μm *vs* 11–14 μm) (Noireung et al. 2012). *C. tongrenense* is distinguished from *C. excelsum-altitudum* (Tao et al. 2013) in having smaller conidiophores (2–11 × 1–2 μm vs 8.5–25 × 4–5 μm). Phylogenetically, the new isolate GZU_TRJ1-37 clusters together with *C. tropicicola* with good bootstrap support (94% MLBS, 1.00 PP) (Fig. 1) and the phylogenetic analysis supports it as a distinct species. There are 6, 4, 2 and 5 base pairs differences in ITS, TUB2, ACT and GAPDH gene regions, respectively, between the new isolate and the type strain of *C. tropicicola*, which confirms that they are separate species. Therefore, it is introduced as a novel species.

Discussion

Colletotrichum appears to have a wide host range and a geographic distribution (Yang et al. 2009, Hyde et al. 2014, Jayawardena et al. 2016). This study reports on five endophytic *Colletotrichum* isolates which were isolated from *Nothapodytes pittosporoides*. Two new species were introduced, named *C. jishouense* and *C. tongrenense*, respectively, based on morphological characters and multilocus (ITS, TUB2, ACT and GAPDH) phylogenetic analyses. The *C. gigasporum* species complex is associated with various host plants as pathogens and endophytes and also isolated from air and stored grain, indicating that the members are not host-specific and apparently have different life styles (Than et al. 2008, Yang et al. 2009, Liu et al. 2014, Jayawardena et al. 2016). The *C. dracaenophilum* species complex contains a few apparently host-specific species and these species seem to be uncommon (Damm et al. 2019). The complex includes *C. coelogynes*, *C. dracaenophilum*, *C. excelsum-altitudinum*, *C. tropicicola* and *C. yunnanense*. A further strain, *C. tongrenense* was identified to the *C. dracaenophilum* species complex in the study, based on the multilocus phylogeny and morphological features. Amongst them, *C. excelsum-altitudinum* was described from healthy leaves of *Bletilla ochracea* (Orchidaceae) in Guizhou, China (Tao et al. 2013.), *C. tropicicola* were described from leaves of *Citrus maxima* and *Paphiopedilum* sp. in Thailand and a further strain from *C.* sp. in Mexico (Noireung et al. 2012, Damm et al. 2019). The *C. coelogynes* strain CBS 132504 is an endophytic *Colletotrichum* isolate from both *Dendrobium* spp. in China (Yuan et al. 2009, Gao and Guo, unpublished data). *C. yunnanense* was described from healthy leaves of *Buxus* sp. in Yunnan, China (Liu et al. 2007).

Morphological features and genes sequence data are recognised as a basis for describing new species, but sometimes morphological features of *Colletotrichum* are not stable and may change under different growth conditions (Liu et al. 2014). DNA sequence comparison and multi-gene phylogenetic analyses can provide sufficient evidence to show distinct taxa (Jeewon and Hyde 2016). However, single gene data, including ITS, are usually insufficient for species identification in most of the *Colletotrichum* species complexes (Hyde et al. 2009). Multi-locus phylogenies are therefore necessary to describe *Colletotrichum* species (Jayawardena et al. 2016).

The composition of endophytic microorganisms may depend on the plant age, tissue, host type and time of isolation (Rosenblueth and Martinez-Romero 2006). The new species, *Colletotrichum tongrenense* lives in stems and *C. jishouense* lives in roots and stems of *Nothapodytes pittosporoides*. Nothing is known about their infection strategies on the host. It is also the first report of *Colletotrichum* species from *N. pittosporoides*. This study enriches the host diversity of *Colletotrichum*.

Acknowledgements

This work was funded by grants of the National Natural Science Foundation of China (NSFC Grants nos. 31670027 &31460011 & 30870009). Sixuan Zhou thanks Dr. Shaun Pennycook, Prof. Jiangming Lv, Yongzhong Lu and Jianfei Gao for their help.

References

Bhalkar BN, Patil SM, Govindwar SP (2016) Camptothecine production by mixed fermentation of two endophytic fungi from *Nothapodytes nimmoniana.* Fungal Biology120: 873–883. https://doi.org/10.1016/j.funbio.2016.04.003

Baroncelli R, Talhinhas P, Pensec F, Sukno SA, Floch GL, Thon MR (2017) The *Colletotrichum acutatum* species complex as a model system to study evolution and host specialization in plant pathogens. Frontiers in Microbiology 8: 2001. https://doi.org/10.3389/fmicb.2017.02001

Carbone I, Kohn LM (1999) A method for designing primer sets for speciation studies in filamentous ascomycetes. Mycologia 91: 553–556. https://doi.org/10.2307/3761358

Corda ACI (1831) Die Pilze Deutschlands. In: Sturm J (Ed.) Deutschlands Flora in Abbildungen nach der Natur mit Beschreibungen. Sturm, Nürnberg 3 (12): 33–64.

Damm U, Sato T, Alizadeh A, Groenewald JZ, Crous PW (2019) The *Colletotrichum dracaenophilum*, *C. magnum* and *C. orchidearum* species complexes. Studies in Mycology 92(5): 1–46. https://doi.org/10.1016/j.simyco.2018.04.001

Demain AL, Vaishnav P (2011) Natural products for cancer chemotherapy. Microbial Biotechnology 4(6): 687–699. https://doi.org/10.1111/j.1751-7915.2010.00221.x

Douanla-meli C, Unger JG (2017) Phylogenetic study of the *Colletotrichum* species on imported citrus fruits uncovers a low diversity and a new species in the *Colletotrichum gigasporum* complex. Fungal Biology 121(10): 858–868. https://doi.org/10.1016/j.funbio.2017.06.003

Fang WP (1981) Flora Republicae. Popularis Sinicae 46. Science Press, Beijing, Tomus, 49 pp.

Gardes M, Bruns TD (1993) ITS primers with enhanced specificity for basidiomycetes – application to the identification of mycorrhizae and rusts. Molecular Ecology 2: 113–118. https://doi.org/10.1111/j.1365-294X.1993.tb00005.x

Glass NL, Donaldson GC (1995) Development of primer sets designed for use with the PCR to amplify conserved genes from filamentous ascomycetes. Applied Environmental Microbiology 61: 1323–1330.

Glezpeña D, Gómezblanco D, Reboirojato M, Fdezriverola F, Posada D (2010) ALTER: program-oriented conversion of DNA and protein alignments. Nucleic Acids Research 38: 14–18. https://doi.org/10.1093/nar/gkq321

Guerber JC, Liu B, Correll JC, Johnston PR (2003) Characterization of diversity in *Colletotrichum acutatum* sensu lato by sequence analysis of two gene introns, mtDNA and intron RFLPs, and mating compatibility. Mycologia 95(5): 872–895. https://doi.org/10.1080/15572536.2004.11833047

Guo DY, Ling TJ, Cai XH (2015) Chemical constituents of *Nothapodytes pittosporoides* (Icacinaceae). Biochemical Systematics and Ecology 61: 293–296. https://doi.org/10.1016/j.bse.2015.06.039

Hall TA (1999) BioEdit: a user-friendly biological sequence alignment editor and analysis program for Windows 95/98/NT. Nucleic Acids Symposium Series 41: 95–98.

Hyde KD, Cai L, Cannon PF, Crouch JA, Crous PW, Damm U, Goodwin PH, Chen H, Johnston PR, Jones EBG, Liu ZY, McKenzie EHC, Moriwaki J, Noireung P, Pennycook SR, Pfenning LH, Prihastuti H, Sato T, Shivas RG, Tan YP, Taylor PWJ, Weir BS, Yang YL, Zhang JZ (2009) *Colletotrichum* names in current use. Fungal Diversity 39: 147–182.

Hyde KD, Nilsson RH, Alias SA, Ariyawansa HA, Blair JE, Cai L, de Cock AWAM, Dissanayake AJ, Glockling SL, Goonasekara ID, Gorczak M, Hahn M, Jayawardena RS, van Kan JAL, Laurence MH, Lévesque CA, Li XH, Liu JK, Maharachchikumbura SSN, Manamgoda DS, Martin FN, McKenzie EHC, McTaggart AR, Mortimer PE, Nair PVR, Pawłowska J, Rintoul TL, Shivas RG, Spies CFJ, Summerell BA, Taylor PWJ, Terhem RB, Udayanga D, Vaghefi N, Walther G, Wilk M, Wrzosek M, Xu JC, Yan JY, Zhou N (2014) One stop shop: backbones trees for important phytopathogenic genera: I. Fungal Diversity 67: 21–125. https://doi.org/10.1007/s13225-014-0298-1

Index Fungorum (2017) http://www.indexfungorum.org/names/Names.asp

Jayawardena RS, Camporesi E, Elgorban AM, Bahkali AH, Yan J, Hyde KD (2017) A new species of *Colletotrichum* from *Sonchus* sp. in Italy. Phytotaxa 314(1): 55–63. https://doi.org/10.11646/phytotaxa.314.1.3

Jayawardena RS, Hyde KD, Damm U, Cai L, Liu M, Li XH, Zhang W, Zhao WS, Yan JY (2016) Notes on currently accepted species of *Colletotrichum*. Mycosphere 7: 1192–1260. https://doi.org/10.5943/mycosphere/si/2c/9

Jeewon R, Hyde KD (2016) Establishing species boundaries and new taxa among fungi: recommendations to resolve taxonomic ambiguities. Mycosphere 7(11): 1669–1677. https://doi.org/10.5943/mycosphere/7/11/4

Kusari S, Lamshöft M, Zühlke S, Spiteller M (2008) An endophytic fungus from *Hypericum perforatum* that produces hypericin. Journal of Natural Products 71:159–16. https://doi.org/10.1021/np070669k

Katoh K, Standley DM (2013) MAFFT multiple sequence alignment software version 7: improvements in performance and usability. Molecular Biology and Evolution 30(4): 772–780. https://doi.org/10.1093/molbev/mst010

Liu F, Cai L, Crous PW, Damm U (2014) The *Colletotrichum gigasporum* species complex. Persoonia 33: 83–97. https://doi.org/10.3767/003158514X684447

Liu X, Xie X, Duan J (2007) *Colletotrichum yunnanense* sp. nov., a new endophytic species from *Buxus* sp. Mycotaxon 100: 137–144.

Miller MA, Pfeiffer W, Schwartz T (2010) Creating the CIPRES Science Gateway for inference of large phylogenetic trees. 2010 Gateway Computing Environments Workshop (GCE), IEEE, 2010. https://doi.org/10.1109/GCE.2010.5676129

Noireung P, Phoulivong S, Liu F, Cai L, McKenzie EHC, Chukeatirote E, Jones EBG, Bahkali AH, Hyde KD (2012) Novel species of *Colletotrichum* revealed by morphology and molecular analysis. Cryptogamie, Mycologie, 33(3):347–362. https://doi.org/10.7872/crym.v33.iss3.2012.347

Nylander JAA (2004) MrModeltest v2. Program distributed by the author. Evolutionary Biology Centre, Uppsala University, Uppsala.

Qiao LJ, Zhou SX, Wen TC, Kang JC, Lei BX (2018) Diversity of endophytic fungi from *Nothapodytes pittosporoides* in Guizhou Province. Mycosystema 37(1): 43–51.

Rambaut A (2012) FigTree version 1.4. http://tree.bio.ed.ac.uk/software/figtree

Ronquist F, Teslenko M, van der Mark P, Ayres DL, Darling A, Höhna S, Larget B, Liu L, Suchard MA, Huelsenbeck JP (2012) MrBayes3.2: efficient Bayesian phylogenetic inference and model choice across a large model space. Systematic Biology 61(3): 539–542. https://doi.org/10.1093/sysbio/sys029

Rosenblueth M, Martinez-Romero E (2006) Bacterial endophytes and their interactions with hosts. Acta Pharmacologica Sinica 19: 827–837. https://doi.org/10.1094/MPMI-19-0827

Silva MD, Cruz ES, Veloso TGR, Miranda L, Pereiram OL, Bocayuva MF, Kasuya MCM (2018) *Colletorichum serranegrense* sp. nov., a new endophytic species from the roots of the endangered Brazilian epiphytic orchid *Cattleya jongheana*. Phytotaxa 351(2): 163–170. https://doi.org/10.11646/phytotaxa.351.2.4

Stamatakis A (2014) RAxML version 8: a tool for phylogenetic analysis and post-analysis of large phylogenies. Bioinformatics 30(9): 1312–1313. https://doi.org/10.1093/bioinformatics/btu033

Stierle A, Strobel G, Stierle D (1993) Taxol and taxane production by *Taxomyces andreanae*, an endophytic fungus of Pacific yew. Science 260: 214–216. https://doi.org/10.1126/science.8097061

Stierle A, Strobel G, Stierle D, Grothaus P, Bignami G (1995) The search forataxol-producing microorganism among the endophytic fungi of the Pacific yew, *Taxus brevifolia*. Journal of Nature Products 58: 1315–1324. https://doi.org/10.1021/np50123a002

Tao G, Liu ZY, Liu F, Gao YH, Cai L (2013) Endophytic *Colletotrichum* species from *Bletilla ochracea* (Orchidaceae), with descriptions of seven new species. Fungal Diversity 61(1): 139–164. https://doi.org/10.1007/s13225-013-0254-5

Than PP, Prihastuti H, Phoulivong S, Taylor PWJ, Hyde KD (2008) *Chilli anthracnose* disease caused by *Colletotrichum* species. Journal of Zhejiang University-Science B 9: 764–788. https://doi.org/10.1631/jzus.B0860007

Tibpromma S, Hyde KD, Bhat JD, Mortimer PE, Xu JC, Promputtha I, Doilom M, Yang JB, Tang AMC, Karunarathna SC (2018) Identification of endophytic fungi from leaves of Pandanaceae based on their morphotypes and DNA sequence data from southern Thailand. Mycokeys 33: 25–67. https://doi.org/10.3897/mycokeys.33.23670

Uzma F, Mohan CD, Hashem A, Konappa NM, Rangappa S, Kamath PV, Singh BP, Mudili V, Gupta VK, Siddaiah CN (2018) Endophytic fungi-alternative sources of cytotoxic compounds: a review. Frontiers in Pharmacology, 9: 309. https://doi.org/10.3389/fphar.2018.00309

Vaidya G, Lohman DJ, Meier R (2011) SequenceMatrix: concatenation software for the fast assembly of multi-gene datasets with character set and codon information. Cladistics 27: 171–180. https://doi.org/10.1111/j.1096-0031.2010.00329.x

White TJ, Bruns T, Lee S, Taylor JW (1990) Amplification and direct sequencing of fungal ribosomal RNA genes for phylogenetics. PCR protocols: a guide to methods and applications. Academic Press, San Diego,California 18: 315–322. https://doi.org/10.1016/B978-0-12-372180-8.50042-1

Wijayawardene NN, Hyde KD, Lumbsch T, Liu JK, Maharachchikumbura SSN, Ekanayaka AH, Tian Q, Phookamsak R (2018) Outline of Ascomycota – 2017. Fungal Diversity 88: 167–263. https://doi.org/10.1007/s13225-018-0394-8

Wijayawardene NN, Hyde KD, Rajeshkumar KC, Hawksworth DL, Madrid H, Kirk PM, Braun U (2017) Notes for genera: ascomycota. Fungal Diversity 86(1): 1–594. https://doi.org/10.1007/s13225-017-0386-0

Wijayawardene DNN, Song Y, Bhat DJ, McKenzie EHC, Chukeatirote E, Wang Y, Hyde KD (2013) *Wojnowicia viburni* sp. nov. from China and its phylogenetic placement. Sydowia 65: 181–190.

Yang YL, Liu ZY, Cai L, Hyde KD, Yu ZN, McKenzie EHC (2009) *Colletotrichum* anthracnose of Amaryllidaceae. Fungal Diversity 39: 123–146.

Yuan ZL, Chen YC, Yang Y (2009) Diverse non-mycorrhizal fungal endophytes inhabiting an epiphytic, medicinal orchid (*Dendrobium nobile*): estimation and characterization. World Journal of Microbiology & Biotechnology 25(2): 295–303. hhttps://doi.org/10.1007/s11274-008-9893-1

Zhou SX, Qiao LJ, Kang JC, Hyde KD, Ma XY (2017) A new species of *Monilochaetes* from *Nothapodytes pittosporoides*. Phytotaxa 326(2): 129–136. https://doi.org/10.11646/phytotaxa.326.2.4

MycoKeys 49: 15–48 (2019)
doi: 10.3897/mycokeys.49.32115
http://mycokeys.pensoft.net

RESEARCH ARTICLE

A peer-reviewed open-access journal
MycoKeys
Launched to accelerate biodiversity research

Six new species of *Arthrinium* from Europe and notes about *A. caricicola* and other species found in *Carex* spp. hosts

Ángel Pintos[1], Pablo Alvarado[2], Juan Planas[3], Rene Jarling[1]

1 *Departamento de Investigación Mycologica, Cultivos Pima SL, Son Peretó 50 bajos, 07013 Palma de Mallorca, Spain* **2** *ALVALAB, La Rochela 47, 39012 Santander, Spain* **3** *Carrer can Socies 12, 07010 Palma de Mallorca, Spain*

Corresponding author: *Ángel Pintos* (info@cultivospima.com)

Academic editor: *G. Mugambi* | Received 4 December 2018 | Accepted 29 January 2019 | Published 12 March 2019

Citation: Pintos A, Alvarado P, Planas J, Jarling R (2019) Six new species of *Arthrinium* from Europe and notes about *A. caricicola* and other species found in *Carex* spp. hosts. MycoKeys 49: 15–48. https://doi.org/10.3897/mycokeys.49.32115

Abstract

Several new *Arthrinium* specimens were collected from various locations in Mediterranean and temperate Europe. A collection of the type species, *A. caricicola*, was obtained from dead leaves of *Carex ericetorum* in Berlin. Sequences of four genetic markers, ITS, 28S rDNA, tef1 and tub2 were produced from almost all collections and analyzed with those available in public databases. Results are employed to support six new species: *A. balearicum*, *A. descalsii*, *A. esporlense*, *A. ibericum*, *A. italicum* and *A. piptatheri*. The type species, *A. caricicola*, is related to other species occurring on *Carex* sp.; these might represent an independent lineage from *Apiospora* and the remaining species of *Arthrinium*. Finally, the sexual morph of *A. marii* is described and illustrated for the first time.

Keywords

Apiosporaceae, Ascomycota, Sordariomycetes, Xylariales, ITS, 28S rDNA, tef1, tub2

Introduction

The genus *Arthrinium* Kunze (Apiosporaceae, Sordariomycetes) differs from other anamorphic genera because of the presence of basauxic conidiophores, which arise from structures called conidiophore mother cells (Schmidt and Kunze 1817; Hughes 1953;

Minter 1985). This infrequent type of conidiogenesis can be found also in *Cordella* Speg., *Dictyoarthrinium* S. Hughes, *Pteroconium* Sacc. ex Grove, and *Spegazzinia* Sacc. (Ellis 1971), but *Pteroconium* and *Cordella* are now considered synonyms of *Athrinium* (Seifert et al. 2011; Crous and Groenewald 2013). *Apiospora* Sacc., the sexual state of *Arthrinium*, is also considered a synonym based on the one fungus-one name policy (Hawksworth et al. 2011; Crous and Groenewald 2013), and *Nigrospora* Zimm. is thought to be the closest relative (Wang et al. 2017).

There are about 80 valid species names of *Arthrinium*. The most significant contributions to species diversity of *Arthrinium* before the DNA-era were those of Schmidt and Kunze (1817), Kunze and Schmidt (1823), Fuckel (1870, 1874), Ellis (1963, 1965, 1971, 1976), and Larrondo and Calvo (1990, 1992). Genetic evidence allowed to confirm some of these taxa and propose multiple new species, e.g. Crous and Groenewald (2013), Singh et al. (2013), Dai et al. (2016, 2017), Jiang et al. (2018), and Wang et al. (2018). Smith et al. (2003) produced the first genetic data (18S and 28S rDNA) of *A. phaeospermum* (Corda) M.B. Ellis, supporting that this genus, as well as *Apiospora*, represent a separate family within Xylariales. This was later confirmed by Spatafora et al. (2006) and Zhang et al. (2006) who added new information from gene-coding DNA markers (18S and 28S rDNA, tef1, rpb2). Singh et al. (2013) published a ITS rDNA phylogeny including several type sequences obtained by Ogawa et al. (unpublished), such as those of *A. marii* Larrondo & Calvo, *A. hispanicum* Larrondo & Calvo, *A. mediterranei* Larrondo & Calvo, *A. serenense* Larrondo & Calvo, and *A. phaeospermum*, and introduced the new species *A. rasikravindrae* Shiv M. Singh, L.S. Yadav, P.N. Singh, Rah. Sharma & S.K. Singh (as *rasikravindrii*). Soon afterwards, Crous and Groenewald (2013) published a comprehensive re-evaluation of *Arthrinium* based on multigenic data, introducing eight new species and providing genetic data from several type strains of other taxa. They formally proposed the synonymy between *Arthrinium* and *Apiospora*, giving priority to *Arthrinium*, but provided no data of the type species, *A. caricicola* Kunze & J.C. Schmidt. Sharma et al. (2014) published the new species *A. jatrophae* R. Sharma, G. Kulk. & Shouche and built a phylogenetic tree based on rDNA that showed three main clades: one formed by *A. urticae* M.B. Ellis, a second including *A. puccinioides* Kunze & J.C. Schmidt and *A. japonicum* Pollack & C.R. Benj., and a third including the remaining known species of *Arthrinium* and *Apiospora*. Multigenic data of the first two clades was first obtained by Ogawa et al. (unpublished), and also Crous and Groenewald (2013), although they did not include these data in their phylogenetic analyses. Some new species of *Arthrinium* were described in the next years (Crous et al. 2015; Senanayake et al. 2015; Hyde et al. 2016; Dai et al. 2016, 2017; Wang et al. 2018; Jiang et al. 2018), and the multilocus phylogenetic analysis revealed that the sister clade of *Arthrinium* was *Nigrospora* in Apiosporaceae (Wang et al. 2017).

Morphological features traditionally employed to discriminate between species of *Arthrinium* include conidial shape, conidiophores, presence or absence of sterile cells and the presence of setae. Two great groups of species can be discriminated: 1) those with irregularly shaped conidia (including the type species *A. cariciola* and several oth-

ers mainly associated with *Carex* spp. (Cyperaceae, Poales), such as *A. austriacum* Petr., *A. fuckelii* Gjaerum, *A. globosum* Koskela, *A. japonicum*, *A. kamtschaticum* Tranzschel & Woron., *A. morthieri* Fuckel, *A. muelleri* M.B. Ellis, *A. naviculare* Rostr., *A. puccinioides* and *A. sporophleum* Kunze), and 2) the remaining species with globose to ellipsoid conidia, mainly associated with other plants in the Poales (Cyperaceae, Poaceae, Restionaceae), e.g. *A. pterospermum* (Cooke & Massee) Arx, *A. phragmitis* Crous, *A. sacchari* (Speg.) M.B. Ellis, *A. saccharicola* F. Stevens, *A. kogelbergense* Crous, and *A. hysterinum* (Sacc.) P.M. Kirk, or even a wider diversity of potential hosts, such as *A. arundinis* (Corda) Dyko & B. Sutton, *A. phaeospermum*, *A. rasikravindrae* and *A. malaysianum* Crous.

Spatafora et al. (2006) and Zhang et al. (2006) were the first to obtain genetic data from the type species of *Apiospora*, *Ap. montagnei* Sacc. (CBS 212.30, AFTOL-ID 951) and suggested that it belongs in a distinct family within Xylariales. Sequences of a few other species of *Apiospora* are also available, including *Ap. sinensis* K.D. Hyde, J. Fröhl. & Joanne E. Taylor (HKUCC 3143 in Smith et al. 2003), *Ap. setosa* Samuels, McKenzie & D.E. Buchanan (ICMP 6888 /ATCC 58184 ex type PDD 41017 in Huhndorf et al. 2004), and *Ap. tintinnabula* Samuels, McKenzie & D.E. Buchanan (ICMP 6889-96 ex type PDD 41022 in Jaklitsch and Voglmayr 2012). Jaklitsch and Voglmayr (2012) produced a 28S rDNA phylogeny where the type species *Ap. montagnei* seemed not significantly different from *Ap. sinensis* but distinct from the other species sequenced. In addition, some *Apiospora* sexual morphs have been biologically linked with putatively prioritary *Arthrinium* taxa: *A. hysterinum* = *Ap. bambusae* (Turconi) Sivan. (Sivanesan 1983; Kirk 1986; Réblová et al. 2016), *A. arundinis* = *Ap. montagnei* (Hyde et al. 1998), and *A. sinense* = *Ap. sinense* (Réblová et al. 2016). However, none of these putative synonymies has been confirmed with genetic data, as some type collections are missing or too old for standard DNA analysis.

The aim of the present study was to study new *Arthrinium* samples found in temperate and southern Europe, including one specimen of *A. caricicola* and several putatively new species, and compare them morphologically and genetically with existing taxa. In some cases, e.g. *Ap. tintinnabula*, type collections were loaned and additional sequences obtained to delimit the genetic boundaries of some species.

Materials and methods

Pure culture isolation

During the surveys conducted in 2017 and 2018, 34 fresh specimens were collected from various plant hosts in Germany, Italy, Portugal and Spain. To isolate the sexual morph, ascomata were removed from the stromata using a sterile razor blade, transferred to a water droplet mounted on a microscope slide, torn apart with forceps to release the ascospores from asci, and pipetted on a 2% malt extract agar (MEA) plate supplemented with 200 mg/L penicillin G and streptomycin sulphate. Germinated

ascospores were then transferred to MEA 2% plates, which were sealed with plastic film and incubated at room temperature. To isolate the asexual morph, plate cultures were superficially scrapped with a needle to dislodge conidia that were transferred to a drop of water. The suspension was then picked up with a syringe, and small droplets sown on a MEA 2% plate supplemented with 200 mg/L penicillin G and streptomycin sulphate. The germinated conidia were then transferred to 2% MEA plates, which were sealed with laboratory film and incubated at room temperature. Cultures were deposited at CBS-KNAW Fungal Biodiversity Centre, Utrecht, The Netherlands (CBS).

Morphological observations

Hand sections of stromata or conidiomata were made using a razor blade and mounted in water on a microscope slide. Observations were made with a Zeiss Axioscop microscope using differential interference contrast (DIC), images were taken with a FLIR camera with A. Coloma open source software. Measurements were taken with FIJI ImajeJ software, reported with maximum and minimum values in parentheses, and the range representing the mean plus and minus the standard deviation, followed by the number of measurements in parentheses. For certain images of conidiophores, the image stacking software Zerene Stacker v. 1.04 (Zerene Systems LLC, Richland, WA, USA) was used. Morphological descriptions were based on cultures sporulating on 2% MEA medium at room temperature. The original specimens were deposited at the fungarium of the Real Jardin Botanico de Madrid (MA-Fungi).

DNA isolation, amplification and phylogenetic analyses

Total DNA was extracted from dry specimens employing a modified protocol based on Murray and Thompson (1980). PCR amplification was performed with the primers ITS1F and ITS4 (White et al. 1990; Gardes and Bruns 1993) for ITS region, while LR0R and LR5 (Vilgalys and Hester 1990; Cubeta et al. 1991) were used to amplify the 28S rDNA region, T1, Bt2a, and Bt2b (Glass and Donaldson 1995; O'Donnell and Cigelnik 1997) for the β-tubulin gene (tub2), and EF1-728F, EF1-983F and EF1-1567R (Rehner and Buckley 2005) for the translation elongation factor 1a (tef1) gene. PCR reactions were performed under a program consisting of a hot start at 95 °C for 5 min, followed by 35 cycles at 94 °C, 54 °C and 72 °C (45, 30 and 45 s respectively) and a final 72 °C step 10 min. PCR products were checked in 1% agarose gels, and positive reactions were sequenced with one or both PCR primers. Chromatograms were checked searching for putative reading errors, and these were corrected.

BLAST (Altschul et al. 1990) was used to select the most closely related sequences from INSDC public databases. Sequences came mainly from Crous and Groenewald (2013), Singh et al. (2013), Sharma et al. (2014), Crous et al. (2015), Senanayake et al. (2015), Dai et al. (2016, 2017), Hyde et al. (2016), Réblová et al. (2016), Jiang et

al. (2018), and Wang et al. (2018), as well as Ogawa et al. (unpublished). Two distinct alignments were built in MEGA 5.0 (Tamura et al. 2011) and aligned with Clustal W with manual corrections: 1) a multigenic alignment including ITS, 28S rDNA, tub2 and tef1 data (without introns) from all Apiosporaceae and related families, and 2) a second alignment built with the same DNA markers (with introns) including only species related with *A. sacchari* (/saccharii clade). Introns were removed from tef1 and tub2, and GBlocks (Castresana 2000) was employed to remove 201 ambiguously aligned sites from ITS rDNA in the Apiosporaceae alignment, but not in the alignment of the /sacchari clade, in order to resolve this complex with all the phylogenetic signal available. The final alignment of the Apiosporaceae included five partitions with 217/461 (ITS rDNA), 229/846 (28S rDNA), 78/252 (tub2), 43/147 (tef1 EF1-728F to EF1-983F), and 76/413 (tef1 EF1-983F to EF1-1567R) variable sites, while the final alignment of the /sacchari clade had 35/535 (ITS rDNA), 18/837 (28S rDNA), 99/719 (tub2), 68/429 (tef1 EF1-728F to EF1-983F), and 4/407 (tef1 EF1-983F to EF1-1567R) variable sites. The aligned loci were loaded in PAUP* 4.0b10 (Swofford 2001) and subjected to MrModeltest 2.3 (Nylander 2004). Model GTR+G+I was selected and implemented in all partitions in MrBayes 3.2.6 (Ronquist and Huelsenbeck 2003), where a Bayesian analysis was performed (data partitioned, two simultaneous runs, six chains, temperature set to 0.2, sampling every 100th generation) until convergence parameters were met after about 3.43M generations (Apiosporaceae) or 0.9M (/sacharii clade), standard deviation having fell below 0.01. Finally, a full search for the best-scoring maximum likelihood tree was performed in RAxML (Stamatakis 2006) using the standard search algorithm (data partitioned, GTRMIX model, 2000 bootstrap replications). Significance threshold was set above 0.95 for posterior probability (PP) and 70% bootstrap proportions (BP).

Results

Phylogeny

The analysis of ITS, 28S rDNA, tef1 and tub2 data from the entire family Apiosporaceae (Fig. 1) produced a phylogeny with two main significantly supported clades: 1) composed of *A. puccinioides*, *A. japonicum* and newly sequenced specimens matching the species *A. cariciola*, *A. curvatum* var. *minus*, and *A. sporophleum*, and 2) a second clade containing all other sequences of *Arthrinium* and *Apiospora*. Among the other specimens analyzed, some matched the genetic concept of *A. hysterinum*, *A. phragmitis*, *A. arundinis*, *A. rasikravindrae*, or *A. marii*. Five new lineages were also found, which are formally proposed as new taxa below.

The analysis of ITS, 28S rDNA, tef1 and tub2 of the species around *A. sacchari* (/sacchari clade) (Fig. 2) showed that the clade of *A. marii* contains the types of *A. hispanicum* and *A. mediterranei*, but receives low overall support, maybe because of the incomplete data from these two species. Samples CBS 113535 and CBS 114803 were identified as *A. marii* too, but seem to represent an independent lineage.

Table 1. Details of strains included in this study. Types are in bold.

Species	Isolate	CBS culture	Herbarium code	Host	ITS rDNA	28S rDNA	tef1	tub2
A. arundinis	AP11118A	CBS 145128	MA-Fungi 91722	*Bambusa* sp.	MK014835	MK014868	MK017945	MK017974
***A. balearicum*, holotype**	**AP24118**	**CBS 145129**	**MA-Fungi 91723**	***Undetermined poaceae***	**MK014836**	**MK014869**	**MK017946**	**MK017975**
A. caricicola	AP23518	CBS 145127	MA-Fungi 91725	*Carex ericetorum*	MK014838	MK014871	MK017948	MK017977
A. curvatum var. *minus*	AP25418	CBS 145131	MA-Fungi 91726	hojas de *Carex* sp.	MK014839	MK014872	MK017949	MK017978
***A. descalsii*, holotype**	**AP31118A**	**CBS 145130**	**MA-Fungi 91724**	***Ampelodesmos mauritanicus***	**MK014837**	**MK014870**	**MK017947**	**MK017976**
***A. esporlense*, holotype**	**AP16717**	**CBS 145136**	**MA-Fungi 91727**	***Phyllostachys aurea***	**MK014845**	**MK014878**	**MK017954**	**MK017983**
A. hysterinum	AP15318	CBS 145132	MA-Fungi 91728	*Phyllostachys aurea*	MK014840	MK014873	MK017950	MK017979
			ICMP6889	*Bambusa*	MK014841	MK014874	MK017951	MK017980
	AP29717	CBS 145133	MA-Fungi 91729	*Phyllostachys aurea*	MK014842	MK014875	MK017952	MK017981
	AP2410173	CBS 145134	MA-Fungi 91730	*Phyllostachys aurea*	MK014843	MK014876		
	AP12118	CBS 145135	MA-Fungi 91731	*Phyllostachys aurea*	MK014844	MK014877	MK017953	MK017982
***A. ibericum*, holotype**	**AP10118**	**CBS 145137**	**MA-Fungi 91732**	***Arundo donax***	**MK014846**	**MK014879**	**MK017955**	**MK017984**
***A. italicum*, holotype**	**AP221017**	**CBS 145138**	**MA-Fungi 91733**	***Arundo donax***	**MK014847**	**MK014880**	**MK017956**	**MK017985**
	AP29118	CBS 145139	MA-Fungi 91734	*Phragmites australis*	MK014848	MK014881	MK017957	MK017986
A. marii	AP13717	CBS 145140	MA-Fungi 91735	*Arundo donax*	MK014849	MK014882	MK017958	MK017987
	AP10118A			*Phragmites australis*	MK014850	MK014883	MK017959	MK017988
	AP11717A	CBS 145141	MA-Fungi 91737	*Ampelodesmos mauritanicus*	MK014851	MK014884	MK017960	MK017989
	AP191017		MA-Fungi 91738	*Phragmites australis*	MK014852	MK014885	MK017961	MK017990
	AP261017	CBS 145142	MA-Fungi 91739	*Piptatheri miliaceum*	MK014853	MK014886	MK017962	MK017991
	Vog2	CBS 145143	MA-Fungi 91740	*Phragmites australis*	MK014854	MK014887	MK017963	MK017992
	AP31118	CBS 145144	MA-Fungi 91736	*Ampelodesmos mauritanicus*	MK014855	MK014888	MK017964	MK017993
A. phragmitis	AP281217A1	CBS 145145	MA-Fungi 91741	*Phragmites australis*	MK014856	MK014889	MK017965	MK017994
	AP2410172A	CBS 145146	MA-Fungi 91742	*Phragmites australis*	MK014857	MK014890	MK017966	MK017995
	AP3218	CBS 145147	MA-Fungi 91743	*Phragmites australis*	MK014858	MK014891	MK017967	MK017996
	AP29717A	CBS 145148	MA-Fungi 91744	*Arundo donax*	MK014859	MK014892	MK017968	MK017997
***A. piptatheri*, holotype**	**AP4817A**	**CBS 145149**	**MA-Fungi 91745**	***Piptatherum miliaceum***	**MK014860**	**MK014893**	**MK017969**	
A. puccinioides	AP26418	CBS 145150	MA-Fungi 91746	*Carex arenaria*	MK014861	MK014894	MK017970	MK017998
A. rasikravindrii	AP8817	CBS 145151	MA-Fungi 91747	*Phyllostachys aurea*	MK014862	MK014895		
	AP10418	CBS 145152	MA-Fungi 91748	*Phyllostachys aurea*	MK014863	MK014896	MK017971	MK017999
	AP2410171	CBS 145153		*Phyllostachys aurea*	MK014864	MK014897	MK017972	MK018000
A. sporophleum	AP21118	CBS 145154	MA-Fungi 91749	*Juncus* sp.	MK014865	MK014898	MK017973	MK018001

Table 2. Details of all strains included in the phylogenetic analyses. Sequences generated in this study are shown in bold.

Species	voucher/culture	ITS rDNA	28S rDNA	tub2	tef1
Apiospora setosa	ICMP 4207		DQ368631	DQ368620	
Apiospora tintinnabula	**ICMP6889**	**MK014841**	**MK014874**	**MK017951**	**MK01980**
Arthrinium 'vietnamense'	IMI 99670	KX986096	KX986111	KY019466	
Arthrinium arundinis	CBS 106 12	KF144883	KF144927	KF144973	KF145015
Arthrinium arundinis	**CBS 145128**	**MK014835**	**MK014868**	**MK017945**	**MK017974**
Arthrinium arundinis	CBS 449 92	KF144887	KF144931	KF144977	KF145019
Arthrinium arundinis	CBS 450 92	AB220259	KF144932	KF144978	KF145020
Arthrinium arundinis	CBS 124788	KF144885	KF144929	KF144975	KF145017
Arthrinium arundinis	CBS 133509	KF144886	KF144930	KF144976	KF145018
Arthrinium arundinis	CBS 114316	KF144884	KF144928	KF144974	KF145016
Arthrinium arundinis	CBS 464 83	KF144888	KF144933	KF144979	KF145021
Arthrinium arundinis	CBS 732 71	KF144889	KF144934	KF144980	KF145022
Arthrinium arureum	CBS 24483	AB220251	KF144935	KF144981	KF145023
Arthrinium balearicum	**CBS 145129**	**MK014836**	**MK014869**	**MK017946**	**MK017975**
Arthrinium camelliae-sinensis	LC8181	KY494761	KY494837	KY705229	KY705157
Arthrinium camelliae-sinensis	LC5007	KY494704	KY494780	KY705173	KY705103
Arthrinium caricicola	**CBS 145127**	**MK014838**	**MK014871**	**MK017948**	**MK017977**
Arthrinium curvatum var. *minus*	**CBS 145131**	**MK014839**	**MK014872**	**MK017949**	**MK017978**
Arthrinium descalsii	**CBS 145130**	**MK014837**	**MK014870**	**MK017947**	**MK017976**
Arthrinium dichotomanthi	LC8175	KY494755	KY494831	kY705223	KY705151
Arthrinium dichotomanthi	LC4950	KY494697	KY494773	KY705167	KY705096
Arthrinium esporlense	**CBS 145136**	**MK014845**	**MK014878**	**MK017954**	**MK017983**
Arthrinium euphorbiae	IMI 285638b	AB220241	AB220335	AB220288	
Arthrinium garethjonesii	JHB004	KY356096	KY356091		
Arthrinium garethjonesii	HKAS 96289	NR_154736	NG_057131		
Arthrinium guizhouense	LC5322	KY494709	KY494785	KY705178	KY705108
Arthrinium guizhouense	LC5318	KY494708	KY494784	KY705177	KY705107
Arthrinium hydei	CBS 114990	KF144890	KF144936	KF144982	KF145024
Arthrinium hydei	LC7103	KY494715	KY4947911	KY705183	KY705114
Arthrinium hyphopodii	MFLUCC 15-003	NR_154699			
Arthrinium hyphopodii	JHB003 Art	KY356098	KY356093		
Arthrinium hysterinum	**CBS 145133**	**MK014842**	**MK014875**	**MK017952**	**MK01981**
Arthrinium hysterinum	**CBS 145135**	**MK014844**	**MK014877**	**MK017953**	**MK01982**
Arthrinium hysterinum	**CBS 145132**	**MK014840**	**MK014873**	**MK017950**	**MK01879**
Arthrinium hysterinum	**CBS 145134**	**MK015843**	**MK014876**		
Arthrinium ibericum	**CBS 145137**	**MK014846**	**MK014879**	**MK017955**	**MK017984**
Arthrinium italicum	**CBS 145138**	**MK014847**	**MK014880**	**MK017956**	**MK017985**
Arthrinium italicum	**CBS 145139**	**MK014848**	**MK014881**	**MK017957**	**MK017986**
Arthrinium japonicum	IFO30500	AB220262	AB220309	AB220309	
Arthrinium japonicum	IFO31098	AB220264	AB220311	AB220311	
Arthrinium jatrophae	CBS 134262	NR_154675			
Arthrinium jatrophae	MMI00051	AB743995			
Arthrinium jiangxiense	LC4577	KY494693	KY494769	KY705163	KY705092
Arthrinium jiangxiense	LC4494	KY494691	KY494766	KY705160	KY705089
Arthrinium kogelbergense	CBS 113332	KF144891	KF144937	KF144983	KF145025
Arthrinium kogelbergense	CBS 113333	KF144892	KF144938	KF144984	KF145026
Arthrinium kogelbergense	CBS 113335	KF144893	KF144939	KF144985	KF145027
Arthrinium kogelbergense	CBS 117206	KF144895	KF144941	KF144987	KF145029
Arthrinium longistromum	MFLU 15-1184	NR_154716			
Arthrinium longistromum	MFLUCC 11-0481	KU940141	KU863129		
Arthrinium malaysianum	CBS 102053	KF144896	KF144942	KF144988	KF145030
Arthrinium malaysianum	CBS 251.29	KF144897	KF144943	KF144989	KF145031

Arthrinium marii	CPC 18902	KF144901	KF144948		
Arthrinium marii	**CBS 145140**	**MK014849**	**MK014882**	**MK017958**	**MK017987**
Arthrinium marii	CBS 114803	KF144899	KF144945	KF144991	KF145033
Arthrinium marii	CBS 113535	KF144898	KF144944	KF144990	KF145032
Arthrinium marii	**CBS 145141**	**MK014851**	**MK014884**	**MK017960**	**MK017989**
Arthrinium marii	**CBS 145142**	**MK014853**	**MK014886**	**MK017962**	**MK017991**
Arthrinium marii	**CBS 145143**	**MK014854**	**MK014887**	**MK017963**	**MK017992**
Arthrinium marii	**CBS 145144**	**MK014855**	**MK014888**	**MK017964**	**MK017993**
Arthrinium mediterranei	IMI 326875	AB220243	AB220337	AB220290	
Arthrinium neosubglobosa	HKAS 96354	NR_154737	NG_057131		
Arthrinium neosubglobosa	JHB006	KY356089	KY356094		
Arthrinium obovatum	LC8177	KY494757	KY494833	KY705225	KY705153
Arthrinium obovatum	LC4940	KY494696	KY494772	KY705166	KY705095
Arthrinium ovatum	CBS 115042	KF144903	KF144950	KF144995	KF145037
Arthrinium phaeospermum	CBS 114317	KF144906	KF144953	KF144998	KF145040
Arthrinium phaeospermum	CBS 114318	KF144907	KF144954	KF144999	KF145041
Arthrinium phaeospermum	CBS 114315	KF144905	KF144952	KF144997	KF145039
Arthrinium phaeospermum	CBS 114314	KF144904	KF144951	KF144996	KF145038
Arthrinium phragmitis	**CBS 145145**	**MK014856**	**MK014889**	**MK017965**	**MK017994**
Arthrinium phragmitis	**CBS 145146**	**MK014857**	**MK014890**	**MK017966**	**MK017995**
Arthrinium phragmitis	CBS 135458	KF144909	KF144956	KF145001	KF145043
Arthrinium phragmitis	**CBS 145147**	**MK014858**	**MK014891**	**MK017967**	**MK017996**
Arthrinium phragmitis	**CBS 145148**	**MK014859**	**MK014892**	**MK017968**	**MK017997**
Arthrinium piptatheri	**CBS 145149**	**MK014860**	**MK014893**	**MK017969**	
Arthrinium pseudosinense	CBS 135459	KF144910	KF144957		KF145044
Arthrinium pseudospegazzinii	CBS 102052	KF144911	KF144958	KF145002	KF145045
Arthrinium pterospermum	CBS 123185	KF144912	KF144959	KF145003	
Arthrinium pterospermum	CBS 134000	KF144913	KF144960	KF145004	KF145046
Arthrinium puccinioides	**CBS 145150**	**MK014861**	**MK014894**	**MK017970**	**MK017998**
Arthrinium rasikravindrae	CBS 33761	KF144914	KF144961		
Arthrinium rasikravindrae	**CBS 145151**	**MK014862**	**MK014895**		
Arthrinium rasikravindrae	CPC 21602	KF144915			
Arthrinium rasikravindrae	**CBS 145152**	**MK014863**	**MK014896**	**MK017971**	**MK017999**
Arthrinium rasikravindrae	LC7115	KY494721	KY494797	KY708159	KY705118
Arthrinium rasikravindrae	**CBS 145153**	**MK014864**	**MK014897**	**MK017972**	**MK018000**
Arthrinium sacchari	CBS 30149	KF144917	KF144963	KF145006	KF145048
Arthrinium sacchari	CBS 21230	KF144916	KF144962	KF145005	KF145047
Arthrinium sacchari	CBS 66474	KF144919	KF144965	KF145008	KF145050
Arthrinium sacchari	CBS 37267	KF144918	KF144964	KF145007	KF145049
Arthrinium saccharicola (1)	CBS 19173	KF144920	KF144966	KF145009	KF145051
Arthrinium saccharicola (1)	CPC 18977	KF144923			
Arthrinium saccharicola (2)	CBS 33486	AB220257	KF144967	KF145010	KF145052
Arthrinium saccharicola (2)	CBS 83171	KF144922	KF144969	KF145012	KF145054
Arthrinium saccharicola (2)	CBS 46383	KF144921	KF144968	KF145011	KF145053
Arthrinium serenense	ATCC 76309	AB220240	AB220334	AB220287	
Arthrinium serenense	IMI 326869	AB220250	AB220344	AB220297	
Arthrinium sporophleum	**CBS 145154**	**MK014865**	**MK014898**	**MK017973**	**MK018001**
Arthrinium subglobosa	MFLUCC 11-0397	KR069112	NG_057070		
Arthrinium subglobosa ('*hyphopodii*')	MFLUCC 15-003	KR069111			
Arthrinium subroseum	LC7292	KY494752	KY494828	KY705220	KY705148
Arthrinium subroseum	LC7215	KY494740	KY494816	KY705208	KY705236
Arthrinium thailandicum	LC5630	KY494714	KY494790	KY806200	KY705113
Arthrinium thailandicum	MFLUCC 15-0202	KU940145	KU863133		

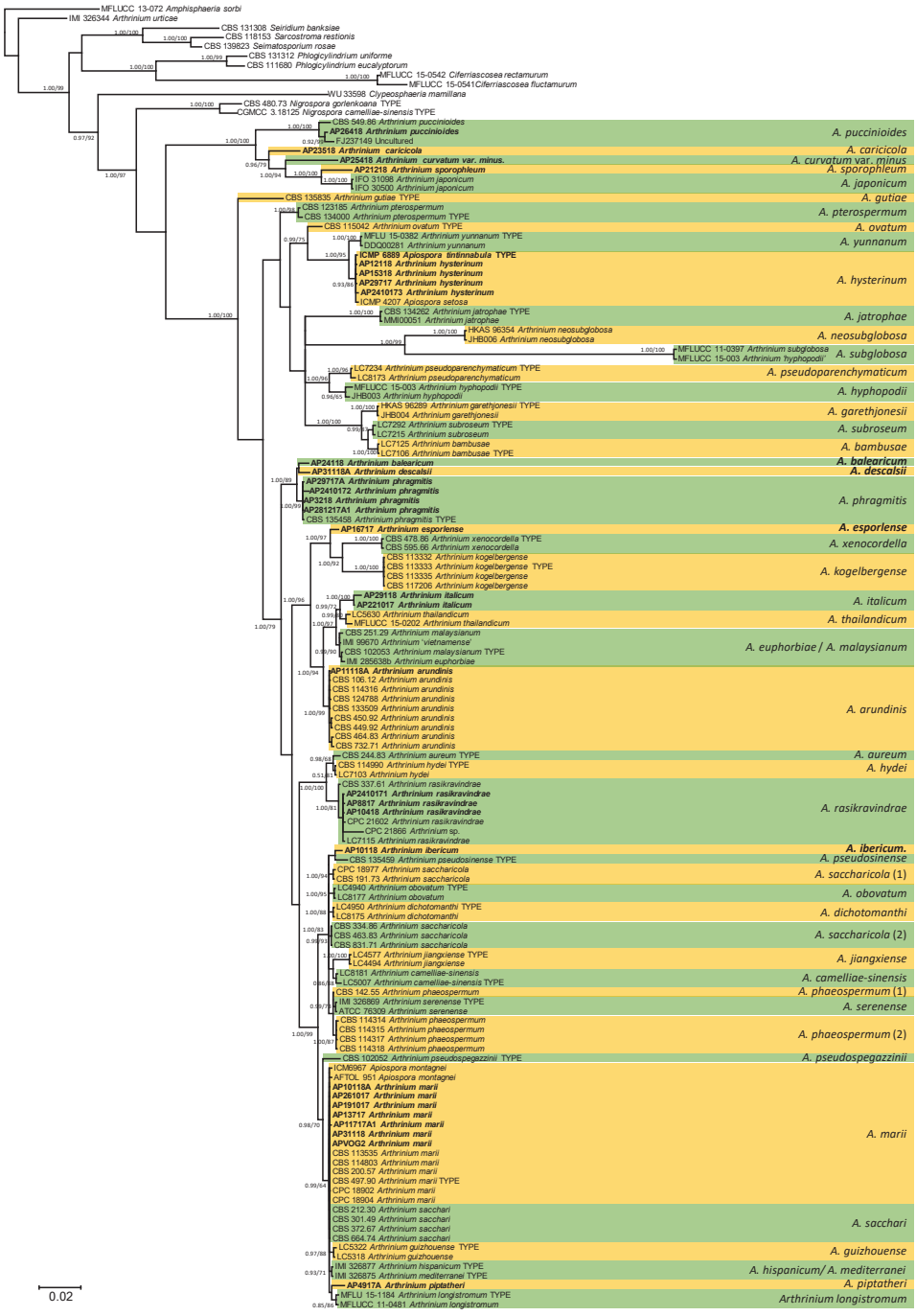

Figure 1. 50% majority rule consensus phylogram obtained in MrBayes from 25725 trees after the analysis of ITS rDNA, 28S rDNA, tef1 and tub2 sequences (introns excluded) of the family Apiosporaceae. Nodes were annotated if supported by > 70% ML BP or > 0.95 bayesian PP, but non-significant support values are exceptionally represented inside parentheses. Bold names represent samples sequenced in the present study.

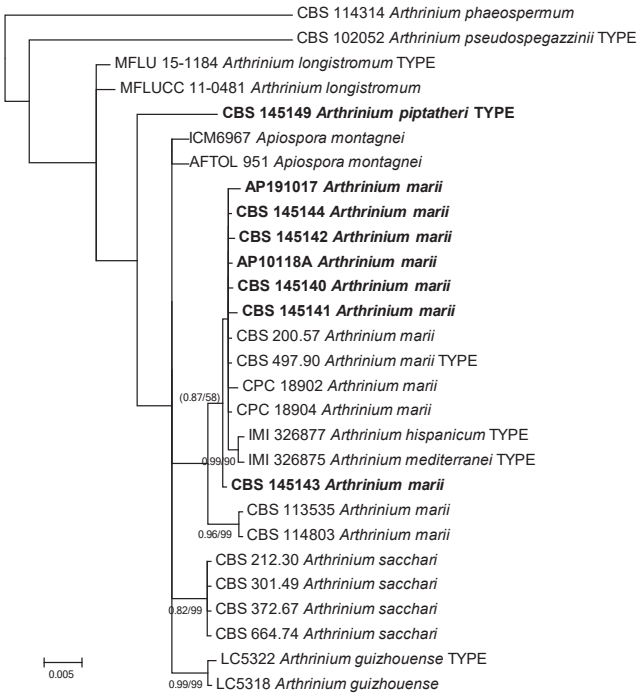

Figure 2. 50% majority rule consensus phylogram obtained in MrBayes from 6750 trees after the analysis of ITS rDNA, 28S rDNA, tef1 and tub2 sequences (introns included) of the /sacchari clade. Nodes were annotated if supported by > 70% ML BP or > 0.95 bayesian PP, but non-significant support values are exceptionally represented inside parentheses. Bold names represent samples sequenced in the present study.

Taxonomy

Arthrinium balearicum **Pintos & P. Alvarado, sp. nov.**
MycoBank: MB 828866
Fig. 3

Etymology. Refers to the Balearic Islands (Spain), where the holotype was found.

Diagnosis. Sexual morph: *Stromata* forming black, linear, confluent raised areas on host surface, with the longer axis broken at the apex, (500–)600–1500(–2000) µm × (200–)320–450(–500) µm (n = 20). *Ascomata* globose to subglobose, with flattened base, blackish brown, (120–) 140–180 (–200) µm in diameter (n = 30). *Peridium* 8–15 µm thick, consisting of 4–5 layers of cells arranged in *textura angularis*, externally dark brown, hyaline in the inner part. *Ostiole* single, central, 30–60 µm in diameter, with a periphysate channel 20–30 µm long. *Peryphises* broad, colourless. *Hamathecium* composed of dense hypha-like, broad septate paraphyses, deliquescing early, 4–6 µm thick. *Asci* 8-spored, unitunicate, clavate, broadly cylindrical, with an inconspicuous pedicel, rounded apex,

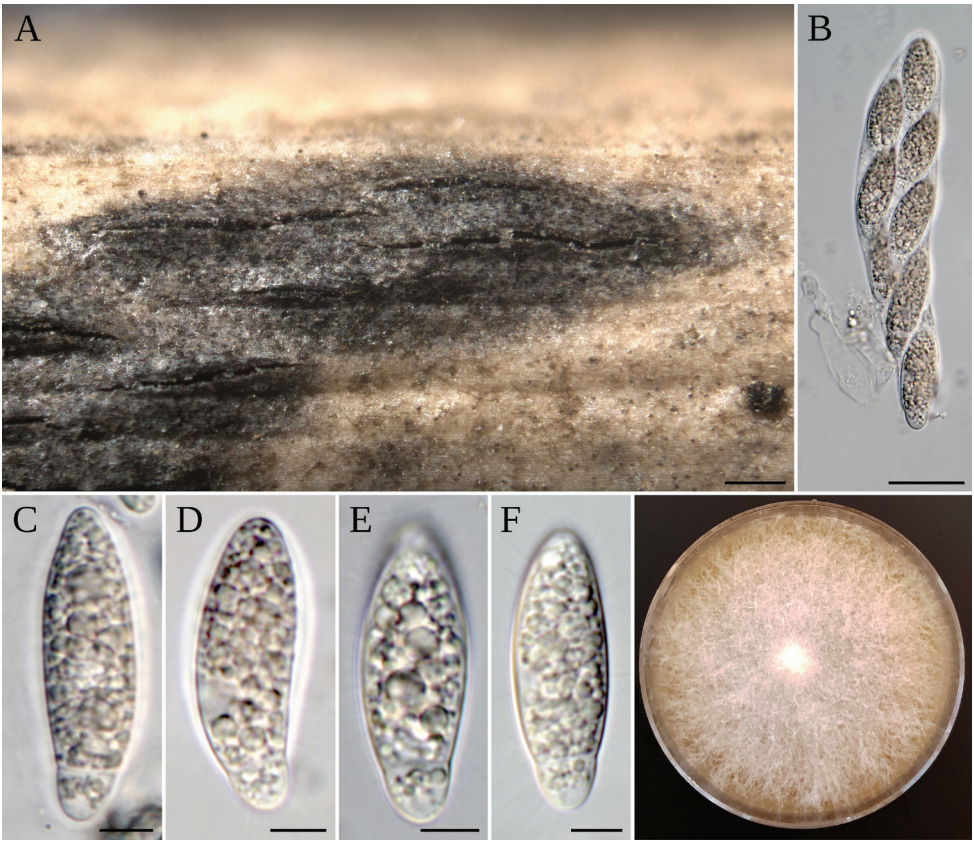

Figure 3. *A. balearicum* **A** stromata on host; **B** asci **C–F** ascospores **G** colony on MEA. Scale bars: 200 µm (**A**); 20 µm (**B**); 5 µm (**C–F**).

thin-walled, without an apical apparatus, measuring (77–)80–98(–105) × (14–)15–19(–21) µm (*n* = 22). *Ascospores* 1–3-seriate, hyaline, apiospore smooth-walled, fusiform, elliptical, reniform, straight or curved, bicellular, wider at the center of the longest cell, measuring (23–)26–30(–32) × (7–)9–10(–12) µm (*n* = 35), basal cell 3–6 µm long, sometimes containing a droplet. Asexual morph: not observed. Culture characteristics: colonies flat spreading on MEA 2%, with moderate aerial mycelium, reverse withish.

Type. Spain: Balearic Islands: Mallorca, Llucmajor, on undetermined Poaceae, 24 Jan. 2018, *A. Pintos* (MA-Fungi 91723 holotype, AP24118 isotype, CBS 145129 ex-type culture).

Notes. *Arthrinium balearicum* is related with *A. descalsii*, but has some genetic differences with this species having only 93% (482/518 bp) of its ITS rDNA, 99% (821/823 bp) of 28S rDNA, 97% (688/707 bp) of tef1, and 98% (406/413 bp) of tub2 similar. It is also phylogenetically close to *A. phragmitis*, a species with a similar ascospore size, (23–)26–30(–32) × (7–)9–10(–12) µm in *A. balearicum* and (22–)23–28(–30) µm × (6–)7–9(–10) µm in *A. phragmitis*. Unfortunately, the asexual morph of *A. balearicum* could not be studied to compare it with that of *A. phragmitis*.

Arthrinium caricicola **Kunze & J.C. Schmidt, Mykologische Hefte (Leipzig) 1: 9 (1817)**
Fig. 4

Description. Asexual morph: *colonies* on the host punctiform, pulvinate, 140–400 µm in diameter, blackish brown. *Mycelium* formed by hyaline smooth, branched hyphae, 2–5 µm in diameter. *Conidiophore mother cells* arising from a superficial or erumpent mycelial mat, subspherical to lageniform in shape, hyaline with brown pigments at the base, measuring (4–)5–7(–8) × (8–)9–11(–12) µm (n = 45). *Conidiophores* erect or ascending, simple, straight or flexuous, cylindrical, smooth-walled, colourless excepting for the thick, brown to dark brown, transversal septa, 15–100 × 3–5 µm (n = 50). *Conidia* fusiform or broadly spindle-shaped, smooth-walled, broader at the mid-

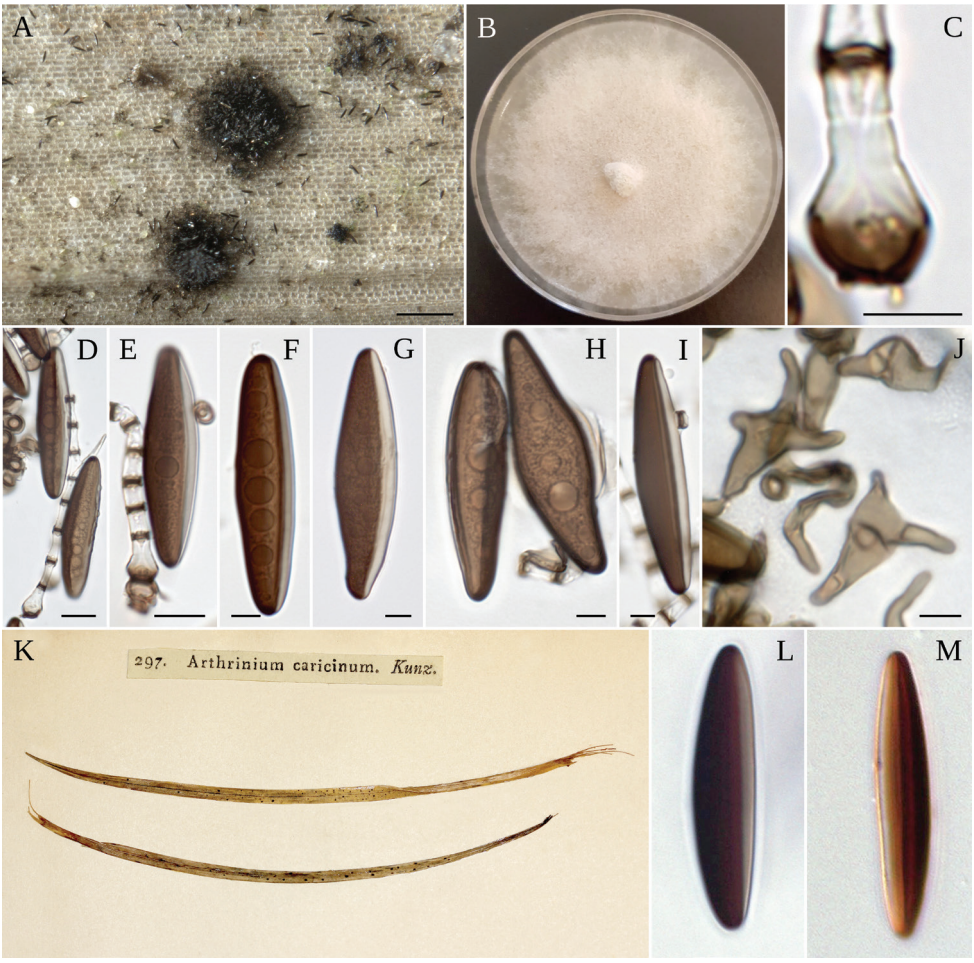

Figure 4. *A. caricicola* **A** colony on host **B** colony on MEA **C** conidiophore mother cell **D, E** conidiophore mother cell, conidiophore bearing conidia, conidia **F–H** conidia **I** conidia with scar **J** lobate sterile cells. Scale bars: 200 µm (**A**); 5 µm (**C–I**); 10 µm (**J**). **K** *A. caricicola* syntype, colonies on host; **L, M** conidia.

dle, tapering towards the narrowly rounded ends, dark brown with a hyaline rim, (37–)44–51(–55) µm in frontal view, (8–)9–11(–12) µm in side view (*n* = 50). *Sterile cells* smaller, 15–19 × 10–13 µm, and paler than conidia, bicuspidate or irregularly lobed. *Culture characteristics*: flat colonies spreading on MEA 2%, with moderately abundant, white cottony aerial mycelium, reverse whitish too, circular in shape with irregular edge.

Notes. The conidia of *A. caricicola* and *A. japonicum* have a similar fusiform shape and length, but differ in width ((8–)9–11(–12) µm vs 12–16(–20) µm). Conidia of *A. mytilimorphum* have also a similar shape, but turns out shorter and thinner (20–30 × 6–8.5 µm). The morphological characters of the syntype of *A. caricicola* deposited by Fries in the Herbarium of Uppsala University as Fung. Scleromyc. Suecici, fully match the specimen collected in this study. The closely related species *A. sporophleum* has very different lemon-shaped conidia, while those of *A. curvatum* var. *minus* are curved, and those of *A. puccinioides* are polygonal.

Specimens examined. Germany: *Brandenburg*: south of Liberose, on dead leaves of *Carex ericetorum*, 14 May 2018, *R. Jarling* (MA-Fungi 91725).

***Arthrinium curvatum* var. *minus* M.B. Ellis, Trans. Brit. Mycol. Soc. 34: 501 (1951)**
Fig. 5

Physalospora scirpi Arx, Gen. Fungi Sporul. Cult. (Lehr): 116 (1970).
Pseudoguignardia scirpi Gutner, Mater. Mikol. Fitopat. Ross. 6(1): 311 (1927).

Description. Asexual morph: *Colonies* are compact, round, dark to black, 80–320 in diameter. *Mycelium* is composed of hyaline to pale brown smooth hyphae 2–7 µm in diameter. *Conidiophore mother cells* spherical to lageniform, hyaline with brown pigments at the base, measuring (4–)5–7(–8) × (4–)5–6(–7) µm (*n* = 30). *Conidiophores* cylindrical unbranched, straight or flexuous, hyaline and smooth walled, with a single brown transversal septa, measuring 30–100 × 2–4 µm. (*n* = 30). *Conidiogenous cells* cylindrical 1–1.5 × 1–1.5 µm (*n* = 20). *Conidia* borne along the sides of conidiophores, curved, rounded at the ends, brown, with a hyaline germ slit and a clearly visible scar, (8–)9–10(–11) µm long in frontal view, (5–)6–7(–8) µm in side view (*n* = 30). *Sterile cells* rounded, paler than conidia. *Culture characteristics* flat colonies spreading on MEA 2% with moderate aerial mycelium, reverse withish.

Notes. *Arthrinium curvatum* var. *minus* can be confused with *A. curvatum* var. *curvatum*, but conidia of var. *minus* measure (8–)9–10(–11) × (5–)6–7(–8) µm, while those of *A. curvatum* var. *curvatum* measure 11–15 × 6–8 µm. Gutner (1927) described *Pseudoguignardia scirpi*, a sexual morph of *A. curvatum*, later combined as *Physalospora scirpi* (Arx 1970). *Arthrinium curvatum* var. *minus* is closely related with *A. sporophleum* (with lemon-shaped conidia) and *A. japonicum* (with larger fusiform conidia) and to a lesser extent also with *A. caricicola* (with larger fusiform conidia) and *A. puccinioides* (with polygonal conidia). Ellis et al. (1951) described *A. curvatum* var. *minus*, a taxon

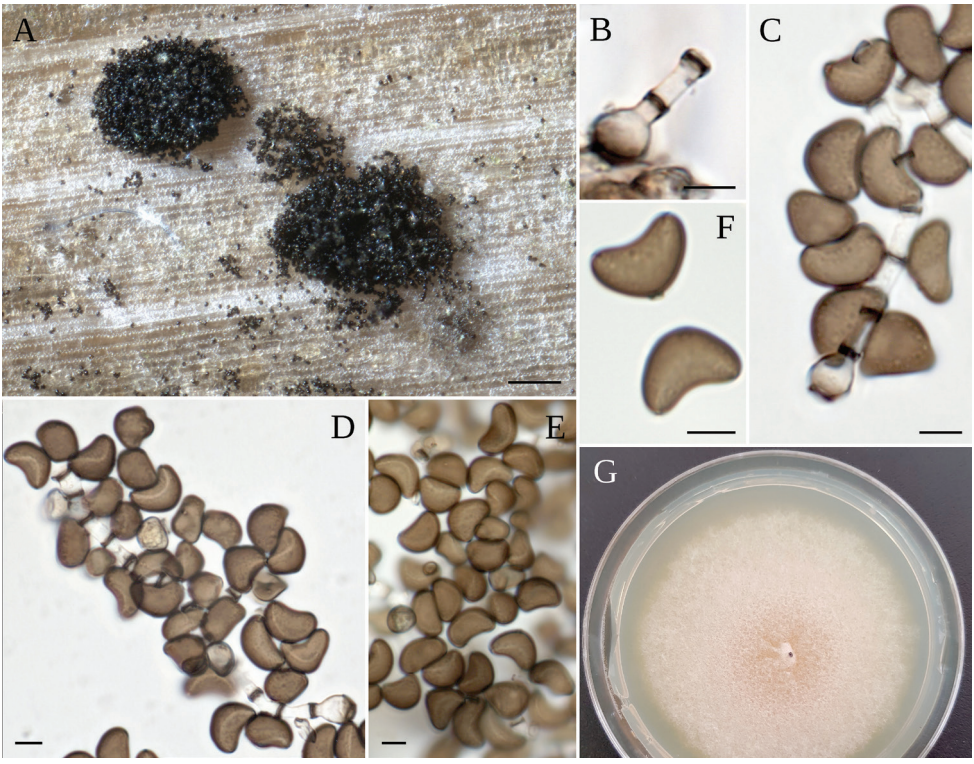

Figure 5. *A. curvatum* var. *minus* **A** colony on host **B** conidiophore mother cell **C, D** conidiophore mother cell, conidiophore bearing conidia **E, F** curved conidia **G** colony on MEA. Scale bars: 200 µm (**A**); 5 µm (B–F).

with similarly shaped but smaller conidia than *A. curvatum*. The specimen studied in the present work matches the shape and size of conidia reported by Ellis et al. (1951) for *A. curvatum* var. *minus*, rather than those of *A. curvatum* var. *curvatum*.

Specimens examined. Germany: Brandenburg: south of Liberose, on dead leaves of *Carex* sp., 28 Mar. 2018, *R. Jarling* (MA-Fungi 91726).

***Arthrinium descalsii* Pintos & P. Alvarado, sp. nov.**
MycoBank: MB 828867
Fig. 6

Etymology. Named to honor the eminent mycologist Enric Descals Callisen.

Diagnosis. Sexual morph: *Stromata* forming black fusiform spots that merge with each other with age, forming an erumpent black mass visible at the naked eye, 2–10 × 0.2–0.5 mm in size, with the long axis broken at the top revealing the ostioles of pseudothecia. *Ascomata* pseudothecia, subglobose with a flattened base, arranged in rows, brown to dark brown, 150–220 µm high × 150–250 µm wide (n = 20). *Peridium* with

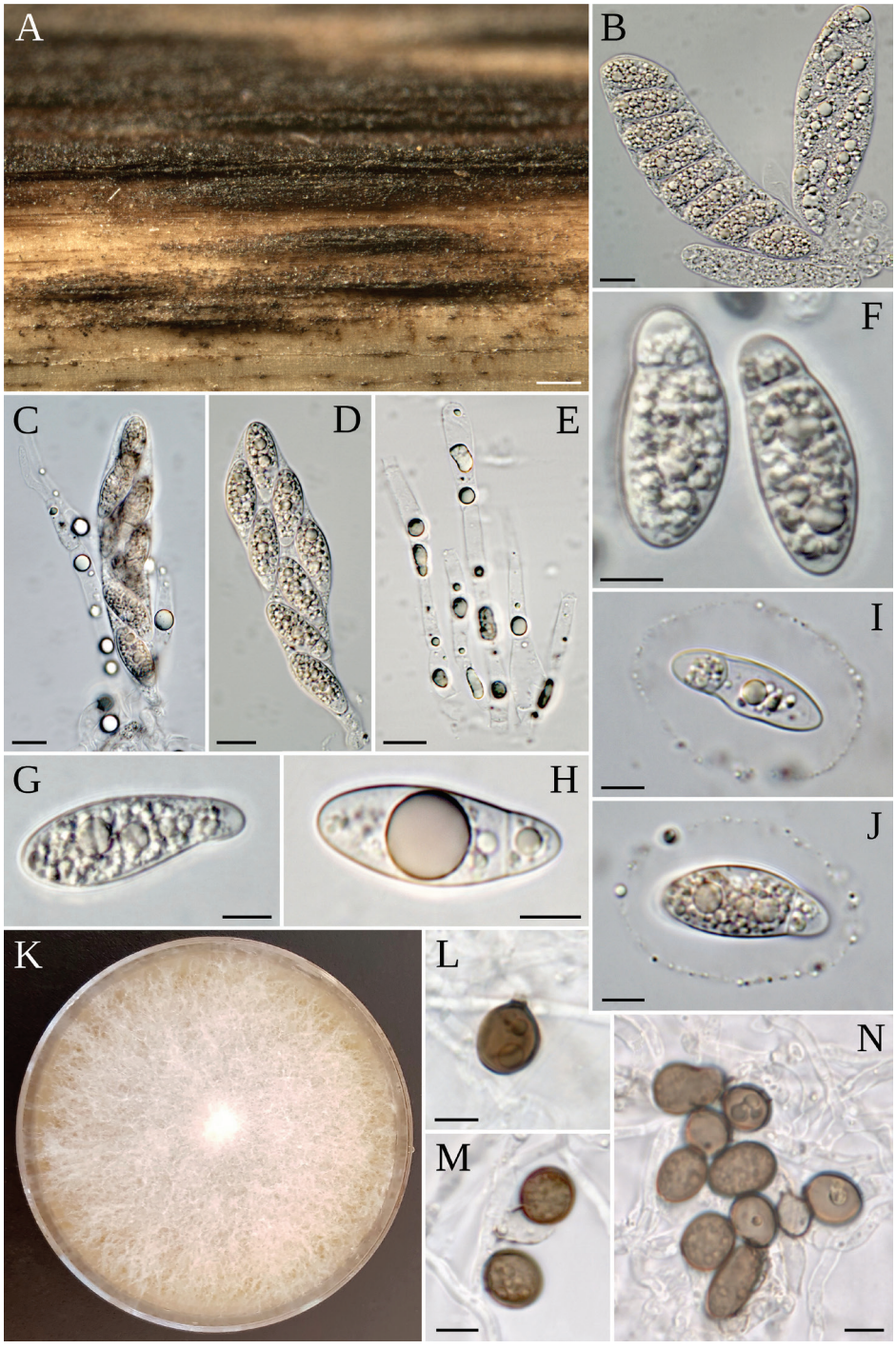

Figure 6. *A. descalsii* **A** stromata on host **B–D** asci with ascospores **E** paraphyses **F, G** ascospores **I, J** ascospores with sheath **K** colony on MEA 2%; coniogenous cell giving rise to conidia; conidiogenous cells giving rise to conidia and conidia cluster **G** conidia. Scale bars: 200 µm (**A**); 10 µm (**B–E**); 5 µm (**F–J**); 5 µm (**L–N**).

several layers of cells arranged in *textura angularis*, with a conspicuous ostiole 50–80 µm in diameter, periphysate. *Hamathecium* paraphyses hyphae-like, septate, hyaline. *Asci* cylindrical, clavate, with a short or indistinct pedicel, with rounded apices, measuring (73–)82–95(–111) × (16–)17–20(–23) µm (*n* = 30). *Ascospores* uniseriate to biseriate, hyaline, smooth-walled, apiosporic, composed of a large curved upper cell and smaller lower cell, fusiform to slightly curved in shape with narrowly rounded ends, guttulated, sometimes with a thick gelatinous sheath, (17–)18–22(–24) × (6–)7–9(–10) µm, and a basal cell 3–5 µm (*n* = 45). Asexual morph: *Mycelium* hyaline, septate, branched, hyphae 1.5–4.5 µm in diameter *Conidiophores* reduced to the conidiogenous cells. *Conidiogenous cells* solitary on hyphae, ampuliform, hyaline to brown, 5 × 4 µm. *Conidia* brown, smooth, guttulate, globose to ellipsoid (5–)7(–8) µm long (*n* = 20) in face view, lenticular with a paler equatorial slit and 6-7 µm long in side view (*n* = 10). *Sterile cells* elongated, sometimes mixed among conidia. *Culture characteristics*: ascospores germinating on MEA 2% within 24–48 h. *Colonies* flat, spreading, with sparse aerial mycelium, pale siena.

Notes. *Arthrinium descalsii* is closely related with *A. phragmitis* and *A. balearicum*. It was found in the Mediterranean grass *Ampelodesmos mauritanicus*, although additional samples are needed before concluding if it could be exclusively associated with this endemic host. Ascospore size is often smaller than that of *A. balearicum*, (23–)26–30(–32) × (7–)9–10(–12) µm, but it matches that reported in the protologue of *A. phragmitis*, (20–)22–24(–25) × (7–)8–9(–10) µm. However, the conidiophores of *A. descalsii* are reduced to conidiogenous cells, while those of *A. phragmitis* measure about 10–45 × 1.5–2 µm, and conidia are slightly smaller in face view, measuring (5–)7(–8) µm long in *A. descalsii* and up to 8–10(–11) µm in *A. phragmitis*.

Type. Spain: Balearic Islands: Mallorca, es Capdella, on dead stems of *Ampelodesmos mauritanicus*, 31 Jan. 2018, *A. Pintos* (MA-Fungi 91724 holotype, AP31118A isotype, CBS 145130 ex-type culture).

Arthirnium esporlense **Pintos & P. Alvarado, sp. nov.**
MycoBank MB 828868
Fig. 7

Etymology. In reference to Esporles, the village of Mallorca (Spain) where it was found.

Diagnosis. Asexual morph: *Mycelium* consisting of smooth, hyaline, branched septate hyphae about 1.5–4 µm in diameter. *Conidiophores* reduced to conidiogeous cells. *Conidiogenous cells* polyblastic, aggregated in clusters on hyphae, smooth, hyaline to pale brown, ampuliform, cylindrical or lageniform, measuring 4–22 × 4–8 µm. *Conidia* brown, smooth, globose with a pale equatorial slit and (8–)9–12(–13) µm long in frontal view, lenticular and 6–8 µm long in side view (*n* = 30). *Sterile cells* elongated, sometimes mixed among conidia, paler than them. *Culture characteristics*: colonies flat, spreading, with moderate aerial mycelium, on MEA 2% surface white with yellowish patches, reverse concolour with age.

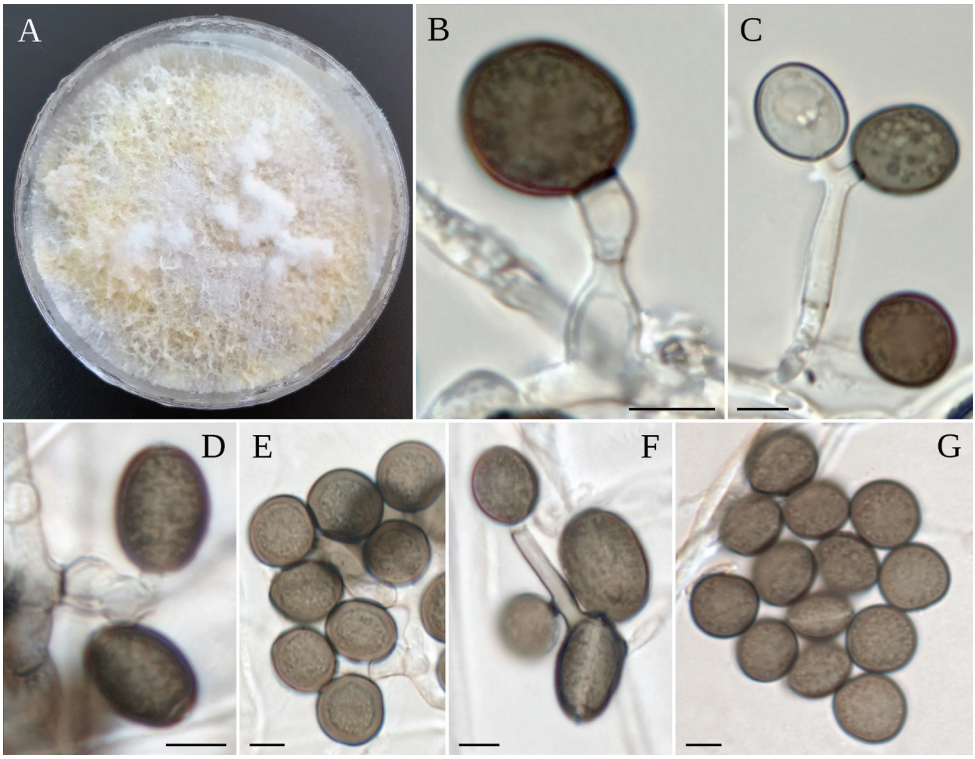

Figure 7. *A. esporlense* **A** colony on MEA **B–F** coniogenous cell giving rise to conidia **G** conidia. Scale bars: 5 µm (**B–G**).

Type. Spain: Balearic Islands: Mallorca, Esporles, on dead culms of *Phyllostachys aurea*, 16 July 2017, *A. Pintos* (MA-Fungi 91727 holotype, AP16717 isotype, CBS 145136 ex-type culture).

Notes. *Arthrinium esporlense* is closely related with *A. xenocordella* and *A. kogelbergense*. However, *A. esporlense* does not produce brown setae as *A. xenocordella*, a species until now known only from soil samples (Crous and Groenewald 2013). *Arthrinium esporlense* morphologically differs from *A. kogelbergense* by producing slightly bigger conidiogenous cells (4–22 × 4–8 µm vs 5–12 × 4–5 µm). These three species are genetically related (1.00 PP, 96 BP) to the group formed by *A. arundinis*, *A. thailandicum* D.Q. Dai & K.D. Hyde, *A. malaysianum* and the new species *A. italicum* proposed below.

Arthrinium hysterinum **(Sacc.) P.M. Kirk, Trans. Brit. Mycol. Soc. 86: 409 (1986)**
Fig. 8

Melanconium hysterinum Sacc., Bolm Soc. broteriana, Coimbra, sér. 1 11: 21 (1893) [Basionym].

Scyphospora hysterina (Sacc.) Sivan., Trans. Brit. Mycol. Soc. 81: 331 (1983).
Melanconium bambusae Turconi, Atti Ist. bot. R. Univ. Pavia, sér. 2 16: 251 (1916).
Scirrhia bambusae Turconi, Atti Ist. bot. R. Univ. Pavia, sér. 2 16: 531 (1916).
Scirrhodothis bambusae (Turconi) Trotter, in Saccardo, Syll. Fung. 24: 611 (1926).
Placostroma bambusae (Turconi) R. Sprague, Diseases Cereals Grasses N. Amer.: 121 (1950).
Apiospora bambusae (Turconi) Sivan., Trans. Brit. Mycol. Soc. 81: 331 (1983).
Scyphospora phyllostachydis L.A. Kantsch., Bolêz. Rast. 17: 88 (1928).
Cordella johnstonii M.B. Ellis, Mycol. Pap. 103: 31 (1965).
Apiospora setosa Samuels et al., New Zealand J. Bot. 19: 142 (1981).
Apiospora tintinnabula Samuels et al., New Zealand J. Bot. 19: 142 (1981).

Description. Sexual morph: *Stromata* black, fusiform, forming rows of densely arranged perithecial ascomata parallel to the main axis of the host, measuring (400–)600–2500(–3000) × (250–)320–450(–550) µm (*n* = 30). *Ascomata* globose to subglobose, with a flattened base, blackish brown, (130–)250–290(–320) µm in diameter (*n* = 30). *Peridium* consisting of 3 or 4 layers of cells arranged in *textura angularis*, dark brown in the external side, hyaline in the inside, ostiole single, central, 10–30 µm in diameter, with a periphysate channel 20–35 µm long. *Peryphises* broad, colourless. *Hamathecium* composed of dense hypha-like, broad septate paraphyses, early deliquescing. *Asci* 8-spored, unitunicate, clavate, broadly cylindrical, pedicel indistinct, apical rounded, thin-walled, without an apical apparatus, measuring (76–)85–98(–115) × (20–)22–26(–28) µm (*n* = 22). *Ascospores* uni- to tri-seriate, hyaline, apiosporic, smooth-walled, fusiform, elliptical, reniform, straight or curved, smooth-walled, sometimes with an internal droplet, bicellular, the widest part located in the central part of the longest cell, some ascospores have a mucose sheath covering them, (28–)32–34(–38) × (8–)9–11(–13) (*n* = 35) µm, basal cell 5–7 µm. Asexual morph: *Mycelium* branched, septate. *Conidiomata* on host surrounding the stromata of the sexual phase, parallel to the longitudinal axis of the stem, subepidermal, opening by longitudinal splitting of the epidermis and revealing a black conidial mass, (450–)630–950(–1000) × (275–)345–550 (–600) µm (*n* = 35). *Conidiophore mother cell* arising from the stroma, ampuliform, lageniform, cupulate or cylindrical, sometimes with granular pigments at the apex, (5)6–10(–16) × (3–)5–7(–8) µm (*n* = 24). *Conidiophores* basauxic, polyblastic, cylindrical, hyaline to light brown, smooth or with granular pigments in all their length, straight or flexuous, septate or not, sometimes exceeding 90 µm in length × 2–4 µm wide (*n* = 43). *Conidia* globose to obovoid, dark brown, with a central scar at the base, (15–)16–20(–21) in frontal view, (14–)15–18(–19) in side view (*n* = 40). *Sterile cells* gray, irregularly angled and lobed, (15–)17–41(–42) × (10–)14–23(–25) µm (*n* = 30). *Culture characteristics*: colonies in MEA 2% flat, spreading, first white and cottony, later became dark pink, *mycelium* branched, septate, hyaline, reverse dark.

Notes. After the works of Samuels (1981), Sivanesan (1983), Kirk (1986) and Réblová et al. (2016), *Ap. bambusae*, *Ap. setosa* and *Ap. tintinnabula*, as well as *Scyphos-*

Figure 8. *A. hysterinum* lenticular-shaped colonies on host **A** stromata and conidiomata **B, C** asci **D–G** ascospores **H** colony on MEA **I** black masses of conidia in culture **K, L** conidiophore mother cell **M** rugose conidiogenous cell **N–P** conidia with lobate sterile cells **O** conidia. Scale bars: 200 µm (**A**); 10 µm (**B, C**); 5 µm (**D–G**); 200 µm (**I**); 5 µm (**K, M, O**); 10 µm (**P**).

pora phyllostachydis, are all considered synonyms of *A. hysterinum*. *Arthrinium hysterinum* is phyllogenetically close to *A. yunnanum* D.Q. Dai & K.D. Hyde, but morphologically differs from the latter because of its thinner asci (76–115 × 20–28 vs 85–100 × 30–35 µm). In addition, *A. hysterinum* has longer conidiophores up to 90 µm long, and lobed sterile cells while in *A. yunnanum* conidiophores do not exceed 50 µm, and sterile cells are lacking.

Specimens examined. New Zealand: Waikato: Paeroa, on dead culm of *Bambusa* sp., 28 Feb. 1980, *E.H.C. McKenzie & P.R. Johnston* (ICMP 6889 ex-type culture).

Spain: Galicia: Santiago de Compostela, on dead culms of *Phyllostachys aurea*, 12 Jan. 2018, *A. Pintos* (MA-Fungi 91731, AP12118). Balearic Islands: Mallorca, Esporlas, on dead culms of *Phyllostachys aurea*, 29 July 2017, *A. Pintos* (MA-Fungi 91729, AP29717). Mallorca, Jardin Botanico de Soller, on dead culms of *Phyllostachys aurea*, 24 Oct. 2017, *A. Pintos* (MA-Fungi 91730, AP2410173). Mallorca, Soller, on dead culms of *Phyllostachys aurea*, 15 Mar. 2018, *A. Pintos* (MA-Fungi 91728, AP15318).

Arthrinium ibericum **Pintos & P. Alvarado, sp. nov.**
MycoBank MB 828869
Fig. 9

Etymology. In reference to the Iberian Peninsula, where the holotype was collected.

Diagnosis. Sexual morph: *Stromata* solitary to gregarious, immersed or semi-immersed, fusiform to ellipsoid in shape, black, with the long axis broken at the top, 2–5 × 0.5–1 mm. *Ascomata* perithecial, subglobose with a flattened base, arranged in rows, brown to dark brown, exudating a white cirrhus of ascospores, 170–300 µm in diameter and 200–300 µm high. *Peridium* consisting in 3 or 4 layers of cells arranged in *textura angularis*. *Ostiole* single, central, 12–30 µm in diameter, with a periphysate channel. *Hamathecium* composed of dense, septate, branched paraphyses. *Asci* 8-spored, clavate or cylindrical, lacking an apical apparatus, shortly pedicelate, measuring (82–)90–125(–128) × (14–)15–19(–21) µm (n = 30). *Ascospores* uniseriate to biseriate, hyaline, smooth-walled, apiosporic, composed of a large curved upper cell and small lower cell, fusiform or slightly curved in shape with narrowly rounded ends, uniguttulated, lacking a gelatinose sheath, measuring (28–)29–34(–37) × (5–)6–8(–9) µm, and a basal cell 5–7 µm (n = 45). Asexual morph: *Mycelium* hyaline, septate, branched, hyphae 2–4 µm in diameter. *Conidiophores* reduced to the conidiogenous cells. *Conidiogenous cells* aggregated in clusters on hypha or solitary, ampuliform or cylindrical, 6–12 × 3 µm. *Conidia* brown, smooth, globose to ellipsoid (9–)10(–12) µm long (n = 30) in face view, lenticular, with a paler equatorial slit, and (6–)7(–8) µm long (n = 40) in side view. *Sterile cells* elongated, rolled up, sometimes mixed among conidia. *Culture characteristics*: ascospores germinating on MEA 2% within 24–48 h. *Colonies* flat, spreading, with sparse aerial mycelium, pale siena with white patches.

Type. Portugal. *Viana do Castelo*: Valença do Minho, on dead culms of *Arundo donax*. 10 Jan. 2018, *A. Pintos* (MA-Fungi 91732 holotype, AP10118 isotype, CBS 145137 ex-type culture).

Notes. *Arthrinium ibericum* belongs to the large clade around *A. sacchari*, where it shows a relation with the subclade of *A. phaeospermum*, *A. saccharicola*, and the modern species *A. serenense*, *A. camelliae-sinensis*, *A. jiangxiense*, *A. dichotomanthii*, *A. obovatum* and *A. pseudosinense*. The size of conidia is more or less similar to that of *A. camelliae-sinensis*, where these measure about 9.0–13.5 µm in frontal view, but con-

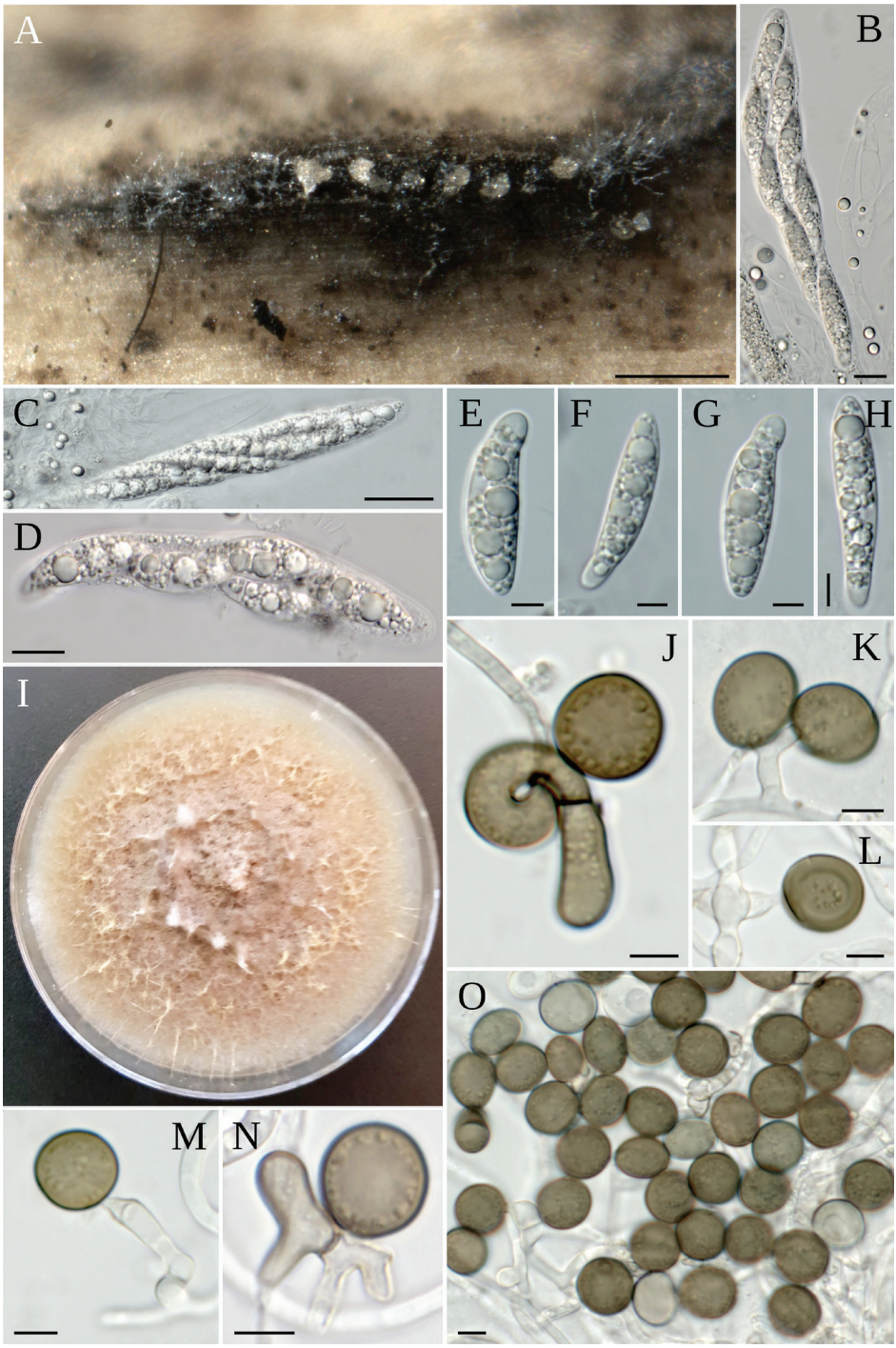

Figure 9. *A. ibericum* **A** ascomata with oozing ascospores **B–D** asci **E–H** ascospores **I** colony on MEA **J–M** conidiogenous cells giving rise to conidia **N** sterile cell with conidia **O** conidia. Scale bars: 200 µm (**A**); 10 µm (**B–D**); 20 µm (**C**); 5 µm (**E–H**); 5 µm (**J–O**).

idiogenous cells are a bit smaller in this species, measuring about 4.0–9.5 × 3.0–6.0 µm. *Arthrinium pseudosinense* has slightly smaller asci measuring 85–100 × 15–20 µm, and ellipsoid conidia covered with a mucilaginous sheath. *Arthrinium saccharicola* has hyphae slightly wider, about 3–5 µm. The genetic identity of *A. phaeospermum* is still dubious because of the lack of a proper type, but the lineages of this species in the work of Crous and Groenewald (2013) have slightly smaller conidiogenous cells measuring 5–10 × 3–5 µm, and a different iron-grey colour of colonies in MEA.

Arthrinium italicum **Pintos & P. Alvarado, sp. nov.**
MycoBank MB 828870
Fig. 10

Etymology. In reference to Italy, the country where the holotype was found.

Diagnosis. Sexual morph: *Stromata* solitary to gregarious, inmersed to erumpent, fusiform, with long axis broken at the top by one or two cracks, 0.5–4 × 0.2–0.5 mm (*n* = 20). *Ascomata* uniseriate or irregularly arranged beneath stromata, pseudothecial, black, globose to subglobose with a flattened base, 150–200 µm high × 230–300 µm wide. *Peridium* composed of 5 or 6 layers of brown cells arranged in textura angularis, with a conspicuous peryphisate ostiole. *Hamathecium* paraphyses hyphae-like. *Asci* broadly cylindrical, clavate or subglobose, pedicel indistinct, apically rounded (70–)72–93(–96) × (14–)15–18(–20) µm (*n* = 30). *Ascospores* apiosporic, clavate to fusiform with narrowly rounded ends, composed of a large upper cell and small lower cell, hyaline, smooth-walled, surrounded by a gelatinose sheath, measuring (20–)21–25(–26) × (5–)6– 9(–10) µm, basal cell 3–5 µm (*n* = 45). Asexual morph: *Mycelium* consisting of smooth, hyaline, branched, septate hyphae 1.5–4 µm in diameter. *Conidiophores* straight or flexuous, cylindrical, colourless except for the thick brown transversal septa, smooth-walled, 10–50 × 1–3 µm. *Conidiogenous cells* ampuliform, cylindrical or doliform, hyaline to brown, (3–)4–7(–9) × (1.5–)2–3(–5) µm (*n* = 30). *Conidia* brown, smooth, globose in face view, lenticular in side view, 4–6 × 3–4 µm (*n* = 65), with a pale equatorial slit. *Culture characteristics*: on MEA 2%, sparse aerial mycelia, surface dirty white, reverse pale yellowish.

Type. Italy: Sicily: On dead culms of *Arundo donax*, 19 June 2016, *H. Voglmayr* (MA-Fungi 91733 holotype, AP221017 isotype, CBS 145138 ex-type culture).

Notes. *Arthrinium italicum* is phylogenetically close to *A. thailandicum*, and to a lesser extent to *A. malaysianum*. Stromata of *A. thailandicum* are smaller than those of *A. italicum*, measuring 0.45–0.99 × 0.3–0.55 mm, ascomata are perithecical, its conidiogenous cells are longer (11.5–39 × 2–3.5 µm) and branched, and conidia measure 5–9 × 5–8 µm. The conidia of *A. malaysianum* are similar in size, but this species does not produce conidiophores.

Other specimens examined. Spain: Balearic Islands: Mallorca, Puerto de Andratx, on dead culms of *Phragmites australis*, 29 Jan. 2018, *A. Pintos* (MA-Fungi 91734, AP29118).

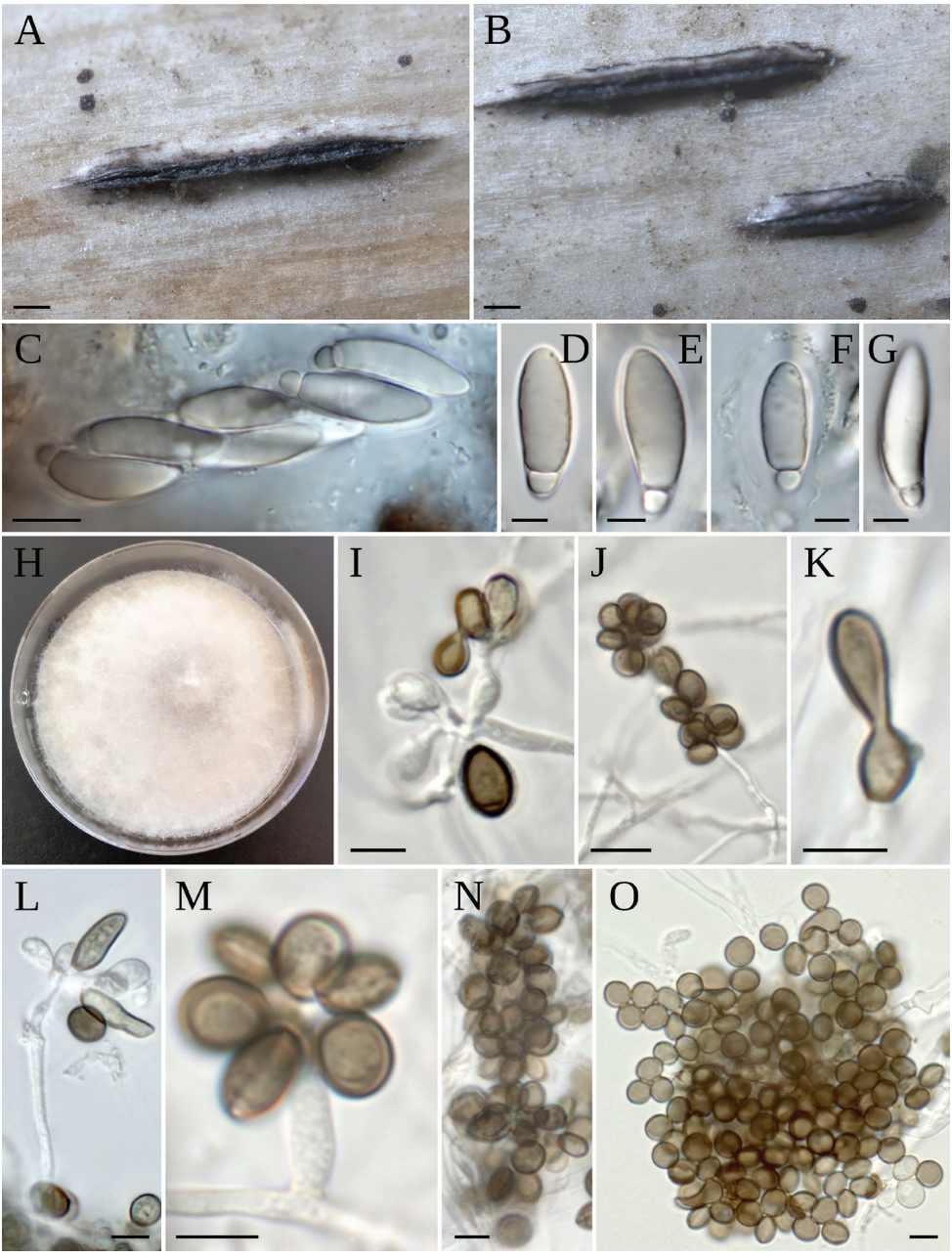

Figure 10. *A. italicum* **A, B** stromata on host **C** asci **D, E, G** ascospores **F** ascospores with sheath **H** colony on MEA **I–M** conidiogenous cell giving rise to conidia **N, O** conidia. Scale bars: 200 µm (**A, B**); 5 µm (**D–G**); 5 µm (**H–L, N, O**); 10 µm (**M**).

Arthrinium marii **Larrondo & Calvo, Mycologia 82: 397 (1990)**
Fig. 11

Description. Sexual morph: *Stromata* forming black fusiform spots, visible at the naked eye, with a long axis broken at the top revealing the ostioles of pseudothecia, 2–6 × 0.2–0.5 mm in size. *Ascomata* subglobose, sometimes with a flattened base, brownish to reddish brown, 150–190 µm high × 160–250 µm wide (*n* = 20). *Peridium* with several layers of cells arranged in *textura angularis*, with a conspicuous ostiole 50–7–80 µm diameter, periphysate. *Hamathecium* paraphyses not prominent, hyphae-like, septate, hyaline. *Asci* 8-spored, unitunicate, broadly cylindrical to clavate, with rounded apex and a short pedicel, (60–)70–100(–115) × (16–)18–20(–22) µm (*n* = 30). *Ascospores* fusiform to elliptical, with narrowly rounded ends, hyaline, with multiple guttules, surrounded by a mucilaginous sheath, (16)19–23(–24) × (6–)7–8(–10) µm, basal cell 2–5 (*n* = 30). Asexual morph: *Mycelium* consisting of smooth, hyaline, branched, septate hyphae measuring 1.5–5 µm in diameter. *Conidiophores* straight or flexuous, cylindrical, colourless except for the thick brown transverse septa, measuring 10–40 × 2–3 µm. *Conidiogenous cells* ampuliform to cylindrical, hyaline to brown, (3–)4–7(–11) × (1.4–)2–4(–5) µm (*n* = 30). *Conidia*, brown, smooth, granular, globose in face view, lenticular in side view, measuring (6–)7–8(–9) × 4–5(–6) µm, with a pale equatorial slit. *Sterile cells* elongated, brown. *Culture characteristics*: ascospores germinating on MEA 2% within 24–48 h. *Colonies* flat, spreading, with sparse aerial mycelium, reverse concolour with agA.

Notes. *Arthrinium marii* was proposed by Larrondo and Calvo (1990) who described its asexual morph. This apparently frequent species has been isolated from the atmosphere, pharmaceutical excipients, home dust, and beach sand, as well as from various plant hosts (Crous 2013). In the present work the sexual morph is described for the first time. Genetically, samples identified as *A. marii* seem to represent two distinct clades (Fig. 2), with differences in tub2 and tef1 genes, but it should be further investigated with additional data before concluding if these clades should be interpreted as intraspecific variability, partially isolated lineages, or fully isolated species. Similarly, the incomplete data from the type specimens of *A. hispanicum* and *A. mediterranei* do not allow one to conclude if these apparently related species represent a single taxon or even belong to *A. marii*.

Specimens examined. Austria: Oberösterreich: St. Willibald, on dead culms of *Phragmites australis*, 10 July 2016, *H. Voglmayr*, (MA-Fungi 91738, AP191017).

Italy: Sicily: casa de la Monache, on dead culms of *Phragmites australis*, 16 July 2016, *H. Voglmayr* (MA-Fung 91740, APVog2).

Portugal: Viana do Castelo: Valença do Minho, on dead culms of *Phragmites australis*, 10 Jan. 2018, *A. Pintos* (AP10118A).

Spain: Balearic Islands: Mallorca, Esporlas, on dead culms of *Arundo donax*, 13 July 2017, *A. Pintos* (MA-Fungi 91735, AP13717). Ibidem., 29 July 2017, *A. Pintos* (AP29717). Palma de Mallorca, on *Ampelodesmos mauritanicus*, 11 July 2017, *A. Pintos* (MA-Fungi 91737, AP11717A). Palma de Mallorca, on dead culms of *Phragmites australis*, 26 July 2017, *A. Pintos* (MA-Fungi 91739, AP261017).

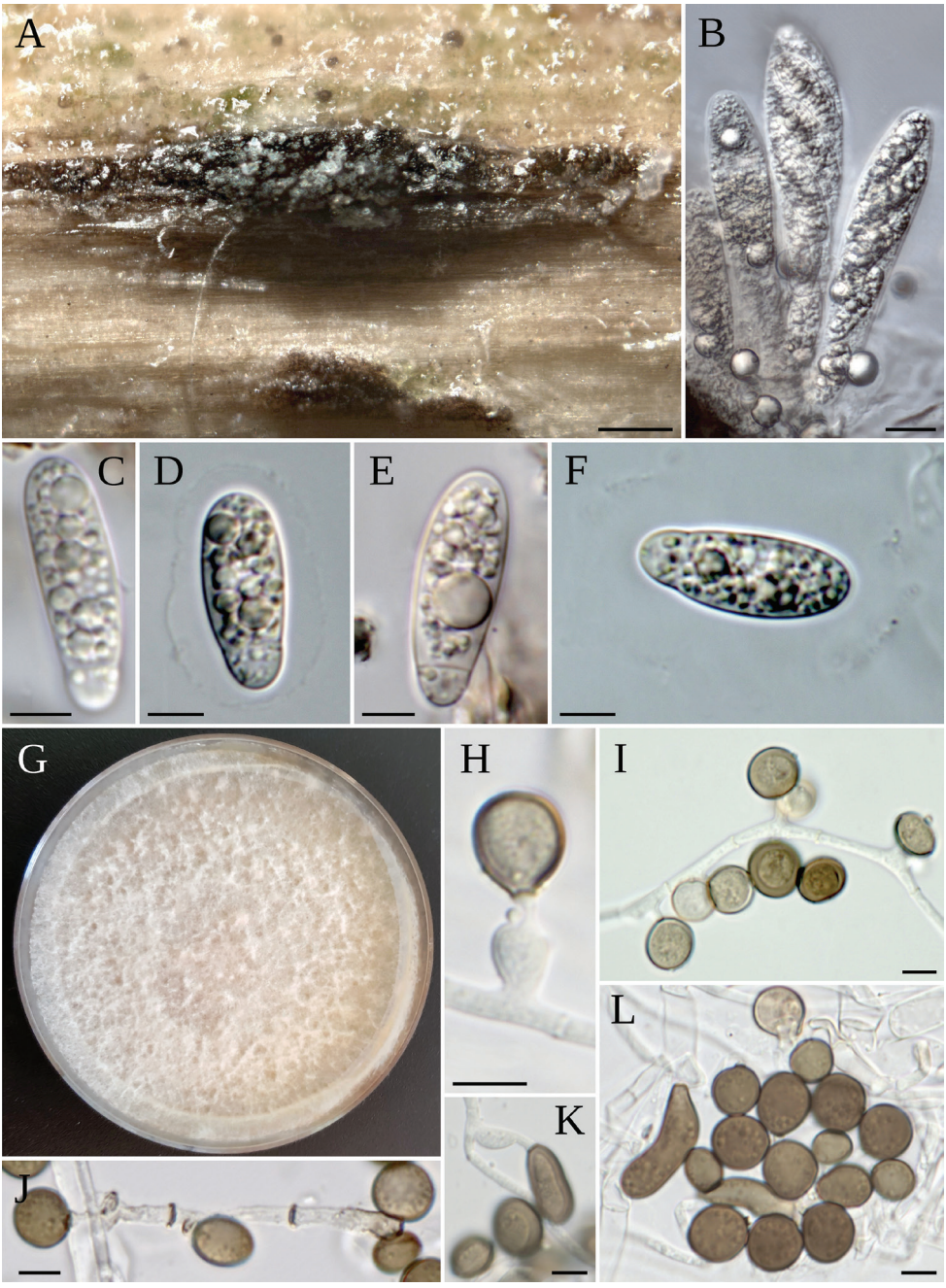

Figure 11. *A. marii* **A** stromata on host **B** asci **C–F** ascospores **G** colony on MEA **H–I, K** conidiogenous cells giving rise to conidia **J** conidiophore bearing conidia **L** conidia and sterile cells. Scale bars: 200 µm (**A**); 10 µm (**B**); 5 µm (**C–F**); 5 µm (**H–L**).

Arthrinium piptatheri **Pintos & P. Alvarado. sp. nov.**
MycoBank MB 828871
Fig. 12

Etymology. Named after *Piptatherum*, the host plant from which it was first isolated.

Diagnosis. Asexual morph: *Mycelium* consisting of smooth, hyaline, branched, septate hyphae measuring 1–4 µm in diameter. *Conidiophore mother cells* hyaline to brown, aggregated in clusters or solitary on hyphae, ampuliform, cylindrical or doliform, 4–11 × 2–5 µm, growing above one or several hyaline cylindrical cells. *Conidiophore* reduced to a conidiogenous cell. *Conidiogenous cells* basauxic, polyblastic, sympodial, cylindrical, discrete, sometimes branched, smooth-walled, measuring 6–27 × 2–5 µm (n = 25). *Conidia* globose to ellipsoidal, pale brown to brown, with a thin hyaline germ-slit, 6–8 × 3–5 µm (n = 30). *Sterile cells* eloganted, brown, sometimes mixed among conidia, 13–16 × 4–5 µm (n = 30). *Culture characteristics*: on MEA 2%, colonies flat, spreading, with sparse aerial mycelium, reverse concolour with agar.

Type. Spain: Balearic Islands: Mallorca: Llucmajor, on dead stems of *Piptatherum miliaceum*, 4 Aug. 2017, *A. Pintos* (MA-Fungi 91745 holotype, AP4817A isotype, CBS 145149 ex-type culture).

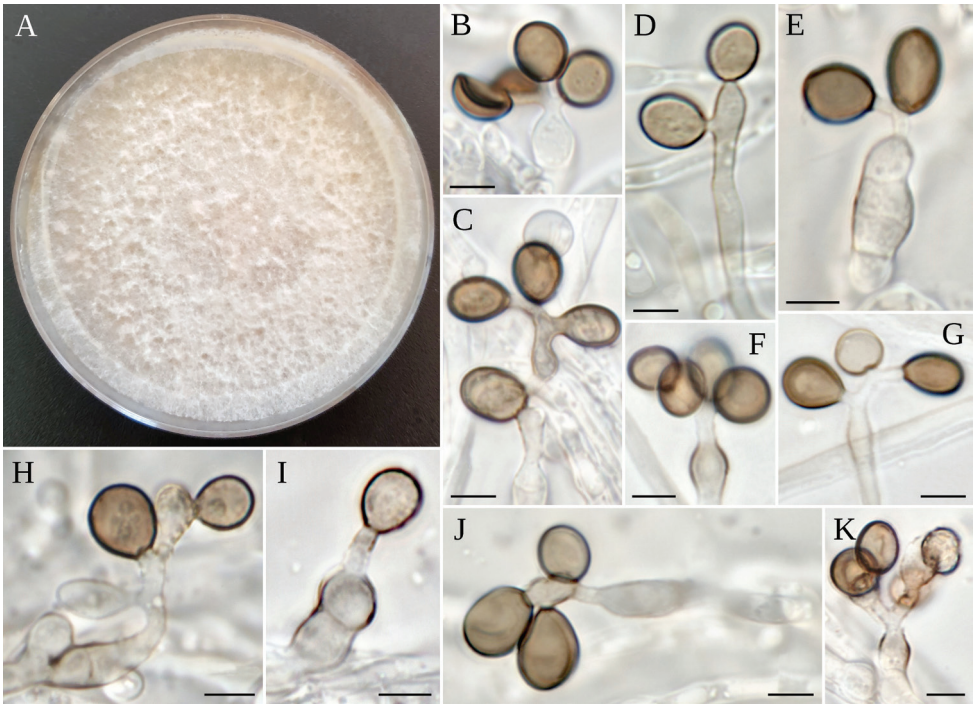

Figure 12. *A. piptatheri* **A** colony on MEA **B–K** conidiogenous cells giving rise to conidia. Scale bars: 5 µm (**B–K**).

Notes. *Arthrinium piptatheri* is genetically close, but genetically distinct from *A. marii*, *A. sacchari*, *A. guizhouense*, *A. hispanicum*, *A. mediterranei*, *A. longistromum* D.Q. Dai & K.D. Hyde, and to a lesser extent *A. pseudospegazzinii* (Fig. 2) and the clade around *A. phaeospermum* (Fig. 1). The incomplete genetic data available is probably the cause behind the lack of significant support for some of these taxa. Morphologically, *A. piptatheri* differs from *A. marii* because of its sympodial, branched conidiogenous cells. *Arthrinium guizhouense* has shorter conidiogenous cells (3.5–8.0 µm). Finally, some sequences of *Ap. montagnei* are related also with this group (Fig. 2), but this species is considered the sexual morph of *A. arundinis*, with a very different genetic profile in Crous and Groenewald (2013), so its actual identity should be further investigated.

Arthrinium puccinioides **Kunze & J.C. Schmidt, Mykologische (Leizpig) 2: 103 (1823)**
Fig. 13

Conoplea puccinioides DE Candolle, 1905, Flore Francaise, Ed. 3, Tome 2, p.73, ex Mérat, Novuvelle Flore des environs de Paris, 1821, p. 16.
Goniosporium puccinioides (Kunze & J. C.Schmidt) Link, in Willdenow, Sp.pl., Edn 4 6(1): 44 (1824).
Gonatosporium puccinioides (Kunze & J. C.Schmidt) Corda, Icon. Fung. (Prague) 3:8 (1839).

Description. Asexual morph: *Mycelium* consisting on smooth hyaline, branched, septate hyphae measuring 1.5–5 µm in diameter. *Colonies* are small, rounded or ovoid, dark brown, 50–400 µm in diameter. *Conidiophore mother cells* subspherical, lageniform or barrel-shaped, 4–5 × 3–5 µm (n = 30). *Conidiophores* cylindrical, straight or flexuous, septate, hyaline excepting for the thick brown or dark brown transversal septa, 20–140 × 3–4 µm (n = 30). *Conidiogenous cells* cylindrical, occurring between the conidiophore septa, 0.9–1.8 µm. *Conidia* dark brown, smooth, polygonal with rounded angles to hemispherical, measuring (8–)9–11(–12) × 8–9 µm, with one or two concentric pale rings. *Sterile cells* spherical, triangular or polygonal, with refractive bodies inside, paler than conidia, 6–9 µm in diameter. *Culture characteristics* colonies flat spreading on MEA 2%, with moderate aerial mycelium, reverse whitish, no esporulate on culture.

Notes. *Arthrinium puccinioides* is the only species of *Arthrinium* with polygonal conida. It shows a genetic relationship with other species found in *Carex* sp. hosts, such as *A. caricicola*, *A. curvatum* var. *minus*, *A. japonicum* or *A. sporophleum*. The present sample fits the original description of *A. puccinioides* by Kunze and Schmidt (1823) as well as those by Ellis et al. (1951), Ellis (1965), and Scheuer (1996).

Specimens examined. Germany: *Berlin*: Köpenick, Stellingdamm, on dead leaves of *Carex arenaria*, 26 April 2017, *R. Jarling* (MA-Fungi 91746, AP26418).

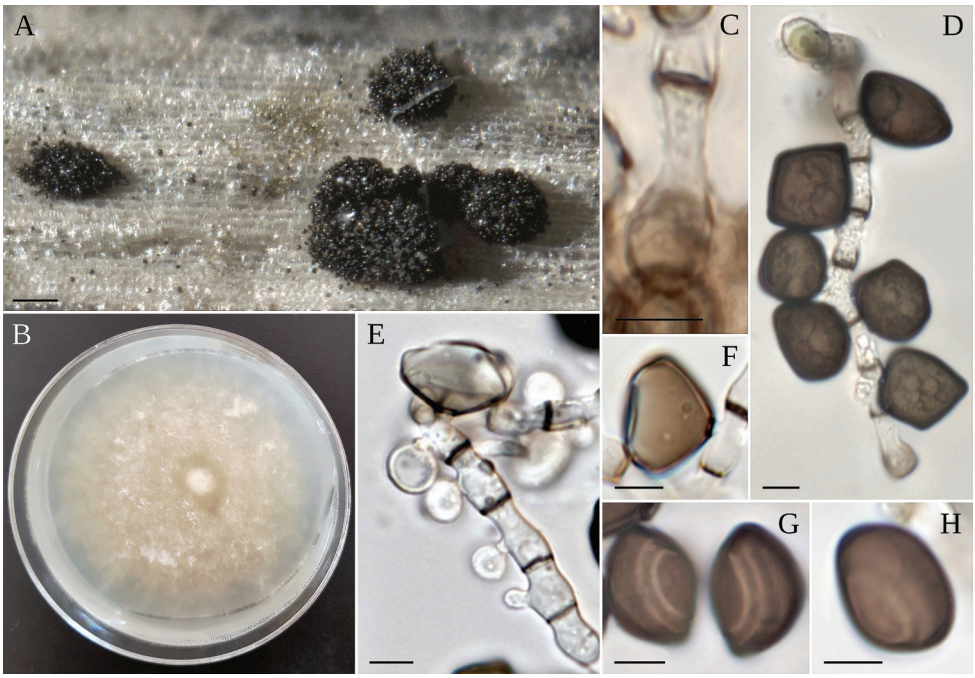

Figure 13. *A. puccinioides* **A** colony on host **B** colony on MEA **C** conidiophore mother cell **D–F** conidiophore bearing conidia **G–H** conidia in side view. Scale bars: 100 µm (**A**); 5 µm (**C–H**).

Arthrinium sporophleum **Kunze, 1823, in Kunze & Schmidt's Mykologische Hefte, 2, p. 104; Fries, 1832, Systema Mycol., 3, p. 377**
Fig. 14

Sporophleum gramineum Nees, 1824, apud Link in Linne, Species Plantarum, ed. 4 (Willdenow's), 6, 1, p. 45.
Torula eriophori Berkeley, 1836, Fungi in J. E. Smith's English Flora, 5 (2), p. 359.
Arthrinium sporophleoides Fuckel, Jb. nassau. Ver. Naturk. 27–28: 78 (1874) [1873–74]

Description. Asexual morph: *Mycelium* consisting on smooth hyaline branched hyphae, 2–5 µm in diameter. *Colonies* oval to irregular, dark blakish brown, 300–1200 × 150–650 µm. *Conidiophore mother cells* sub-cylindrical, hyaline to pale brown, measuring 5–7 × 5–7 µm (n = 20). *Conidiophores* straight to flexuous, cylindrical, hyaline except for the thick brown to dark brown transversal septa, 30–130 × 2–4 µm (n = 20). *Conidia* brown, smooth, lemon-shaped in face view, measuring (10–)11–14(–15) × (5–)6–8(–9) µm (n = 45), triangular with the outer edge curved and rounded angles in side view, measuring 5–8 µm thick. *Sterile cells* paler than conidia, subspherical or triangular, 5–8 µm wide. *Culture characteristics*: on MEA 2% colonies cottony, white with grey patches, reverse pale grey.

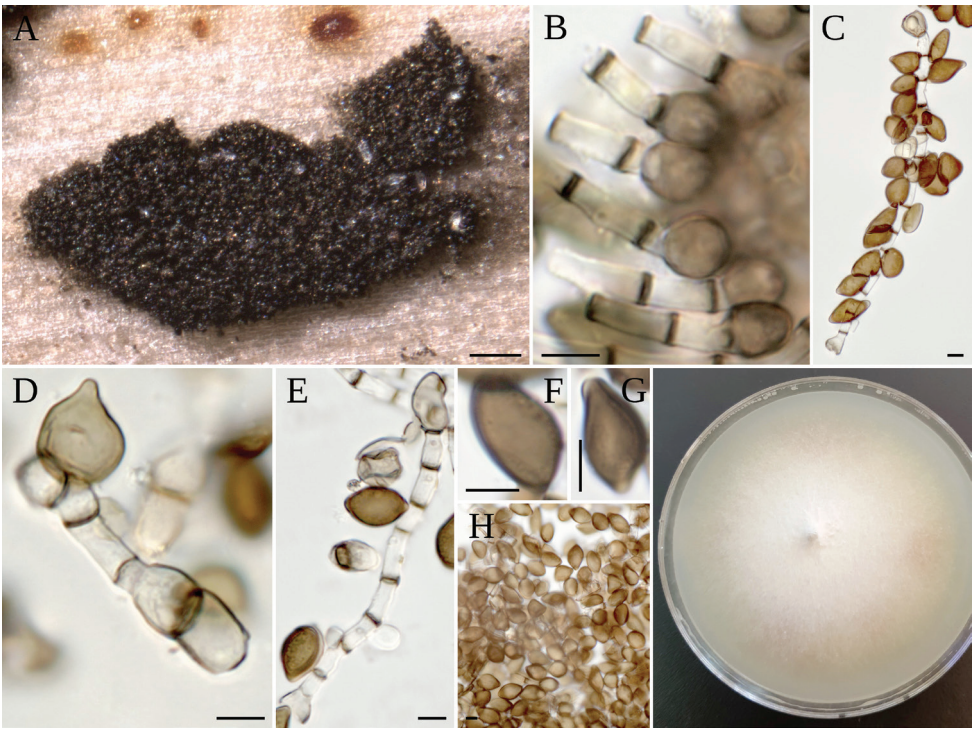

Figure 14. *A. sporophleum* **A** colony on host **B** conidiophore mother cells **C–E** conidiophore mother cells with conidiophore bearing conidia, **F** with sterile cell **F–H** conidia **I** colony on MEA. Scale bars: 100 µm (**A**); 5 µm (**B–H**).

Notes. *Arthrinium sporophleum* is the only species of *Arthrinium* with lemon-shaped conidia. Kunze (1823) considered that *Sporophleum gramineum* represents a synonym of this species, and Cooke (1954) considered *A. sporophleoides* Fuckel a synonym of this species too. The only sample analyzed in the present work fits the descriptions of this species by Kunze (1823), Ellis et al. (1951), Ellis (1965) and Scheuer (1996). This sample was found in *Juncus* sp., but this remarkable species has been often reported from *Carex* sp. hosts (Ellis 1965). Interestingly, other species occurring in *Carex* sp. present also conidia with unusual shapes, e.g. *A. puccinioides* (polygonal), *A. curvatum* var. *minus* (curved), and *A. caricicola* or *A. japonicum* (fusiform).

Specimens examined. Spain: Balearic Islands: Mallorca, Escorca, on dead leaves of *Juncus* sp., 21 Feb. 2018, *A. Pintos 21218* (MA-Fungi 91749).

Other specimens studied. *Arthrinium arundinis*: Spain: Galicia: Santiago de Compostela, city garden, culms of *Bambusa* sp., 11 Jan. 2018, *A. Pintos 11118A* (MA-Fungi 91722). ***Arthrinium phragmitis*:** Spain: Balearic Islands: Mallorca, Esporles, on dead culms of *Arundo donax*, 29 July 2017, *A. Pintos* (MA-Fungi 91744, AP29717A). Ibidem., on dead stem of *Phragmites australis*, 3 Feb. 2018, *A. Pintos* (MA-Fungi 91743,

AP3218). Jardin Botanico de Soller, on dead culms of *Arundo donax*, 24 Oct. 2017, *A. Pintos* (MA-Fungi 91742, AP2410172A). Puigpunyent, on dead culms of *Phragmites australis*, 28 Dec. 2017, *A. Pintos* (MA-Fungi 91741, AP281217A1). ***Arthrinium rasikravindrii*:** Spain: *Balearic Islands*: Mallorca, Esporlas, on dead culms of *Phyllostachys aurea*, 8 Aug. 2017, *A. Pintos* (MA-Fungi 91747, AP8817). Jardin Botanico de Soller, on dead culms of *Bambusa* sp., 24 Oct. 2017, *A. Pintos* (AP2420171). Soller, on dead culms of *Phyllostachys aurea*, 10 Apr. 2018, *A. Pintos* (MA-Fungi 91748, AP10418).

Discussion

Arthrinium is thought to represent the asexual morph of *Apiospora* because genetic data of *Ap. montagnei* (type species of *Apiospora*, Müller and Arx 1962) grouped together with other species of *Arthrinium* (Crous and Groenewald 2013; Senanayake et al. 2015; Réblová et al. 2016). Unfortunately, no data from the type species of *Arthrinium*, *A. caricicola*, was available to confirm this synonymy. In the present work, a phylogenetic relationship was found between a specimen identified as *A. caricicola* and other species of *Arthrinium* mainly occurring in *Carex* sp., such as *A. curvatum* var. *minus*, *A. japonicum*, *A. puccinioides* and *A. sporohleum*. Moreover, this clade was not significantly related with all other species of *Arthrinium* and *Apiospora* found in other hosts or substrates, suggesting that both clades could be interpreted as independent genera sister to *Nigrospora*. In this case, the synonymy between *Arthrinium* and *Apiospora* could be rejected, requiring new combinations. However, this hypothesis should be further confirmed after the analysis of the remaining known species occurring in Cyperaceae hosts, such as *A. austriacum*, *A. fuckelii*, *A. globosum*, *A. kamtschaticum*, *A. morthieri*, *A. muelleri*, or *A. naviculare*.

Arthrinium species have been found in several different plant hosts (Ramos et al. 2010; Sharma 2014), where they sometimes cause plant diseases (Martínez-Cano et al. 1992; Mavragani et al. 2007; Chen et al. 2014; Li et al. 2016). They are also isolated from lichens (He and Zhang 2012), marine algae (Suryanarayanan 2012), soil (Singh et al. 2013) and can even cause infections in humans (Rai 1989; Zhao et al. 1990; Hoog et al. 2000). In the present study six new species of *Arthrinium* are proposed: *A. balearicum*, *A. descalsii*, *A. esporlense*, *A. ibericum*, *A. italicum*, and *A. piptatheri*, all of them found in the Mediterranean biogeographical region, excepting for *A. ibericum*, which was found in the Atlantic areas of Spain. All these new taxa were found growing on plant hosts of the Poaceae family, such as *Arundo donax* or *Piptatherum miliaceum*. However, *A. marii* was the species most frequently found in the surveys, occurring on the Poaceae grasses *Ampelodesmos mauritanicus* and *Phragmites australis*, in agreement with the data reported by Crous and Groenewald (2013). *Arthrinium phragmitis* was found also on *Phragmites australis* and less commonly in *Arundo donax*, while *A. hysterinum* and *A. rasikravindrae* were associated with the Poaceae bamboos *Phyllostachys aurea* and *Bambusa* sp. Several colonies of *A. rasikravindrae* were found growing on *Phyllostachys aurea* as well, where they developed acervular conidiomata, a feature not observed in the protologue of this species, and therefore not considered diagnostic, in the same way as conidial shape, presence of setae, or lobate sterile cells.

Apiospora tintinnabula (Samuels et al. 1981) is considered a synonym of *A. hysterinum* (Sivanesan 1983; Kirk 1986). Multigenic data from the ex-type culture ICMP 6889 of *Ap. tintinnabula* was obtained so as to compare it with the newly found specimens of *A. hysterinum*, and no significant difference could be found. Interestingly, the collections of *A. hysterinum* studied in the present work presented sterile lobed cells, a feature not mentioned in the protologue of *Ap. tintinnabula*. The genetic data available from *Ap. setosa* and *Ap. bambusae* (28S and tub2) are not significantly different from those of *A. hysterinum* and *Ap. tintinnabula*, although additional markers would be needed to confirm a putative synonymy.

Acknowledgements

We thank Dr Hermann Voglmayr for his valuable advice, Chris Yeates and Martin Bemmann for providing literature, and Äsa Kruys for providing details about type collection of *Arthrinium caricicola*.

References

Altschul SF, Gish W, Miller W, Myers EW, Lipman DJ (1990) Basic local alignment search tool. Journal of Molecular Biology 215: 403–410. https://doi.org/10.1016/S0022-2836(05)80360-2

Arx JA von (1970) The Genera of Fungi Sporulating in Pure Culture (3rd edn). Cramer Vaduz, 424 pp.

Castresana J (2000) Selection of conserved blocks from multiple alignments for their use in phylogenetic analysis. Molecular Biology and Evolution 17: 540–552. https://doi.org/10.1093/oxfordjournals.molbev.a026334

Chen K, Wu XQ, Huang MX, Han YY (2014) First report of brown culm streak of *Phyllostachys praecox* caused by *Arthrinium arundinis* in Nanjing, China. Plant Disease 98: 1274. https://doi.org/10.1094/PDIS-02-14-0165-PDN

Cooke WB (1954) The gennus *Arthrinium*. Mycologia 46 (6) 815–822. https://doi.org/10.1080/00275514.1954.12024418

Crous PW, Groenewald JZ (2013) A phylogenetic re-evaluation of *Arthrinium*. IMA Fungus 4: 133–154. https://doi.org/10.5598/imafungus.2013.04.01.13

Cubeta MA, Echandi E, Abernethy T, Vilgalys R (1991) Characterization of anastomosis groups of binucleate *Rhizoctonia* species using restriction analysis of an amplified ribosomal RNA gene. Phytopathology 81: 1395–1400. https://doi.org/10.1094/Phyto-81-1395

Dai DQ, Jiang HB, Tang LZ, Bhat DJ (2016) Two new species of *Arthrinium* (Apiosporaceae, Xylariales) associated with bamboo from Yunnan, China. Mycosphere 7: 1332–1345. https://doi.org/10.5943/mycosphere/7/9/7

Dai DQ, Phookamsak R, Wijayawardene NN, Li WJ, Bhat DJ, Xu JC, Taylor JE, Hyde KD, Chukeatirote E (2017) Bambusicolous fungi. Fungal Diversity 82: 1–105. https://doi.org/10.1007/s13225-016-0367-8

de Hoog GS, Guarro J, Gené J, Figueras MJ (2000) Atlas of Clinical Fungi (2nd edn). CBS, Utrecht, The Netherlands, and Universitat Rovira i Virgili, Reus, 1126 pp.

Ellis MB, Ellis EA, Ellis JP (1951) British marsh and fen fungi. II. Transactions of the British Mycological Society 34: 497–514. https://doi.org/10.1016/S0007-1536(51)80034-2

Ellis MB (1963) Dematiaceous Hyphomycetes. IV. Mycological Papers 87:1–42.

Ellis MB (1965) Dematiaceous *Hyphomycetes*. VI. Mycological Papers 103: 1–46.

Ellis MB (1971) Dematiaceous *Hyphomycetes*. Commonwealth Mycological Institute, Kew, 608 pp.

Ellis MB (1976) More Dematiaceous *Hyphomycetes*. Commonwealth Mycological Institute, Kew, 507 pp.

Fuckel L (1870) Symbolae mycologicae. Beiträge zur Kenntniss der Rheinischen Pilze. Jahrbücher des Nassauischen Vereins für Naturkunde 23–24: 1–459.

Fuckel L (1874) Symbolae mycologicae. Beiträge zur Kenntniss der rheinischen Pilze Jahrbücher des Nassauischen Vereins für Naturkunde 27–28: 1–99.

Gardes M, Bruns TD (1993) ITS primers with enhanced specificity for *Basidiomycetes*—application to the identification of mycorrhizae and rusts. Molecular Ecology 2: 113–118. https://doi.org/10.1111/j.1365-294X.1993.tb00005.x

Glass NL, Donaldson GC (1995) Development of primer sets designed for use with the PCR to amplify conserved genes from filamentous Ascomycetes. Applied and Environmental Microbiology 61: 1323–1330.

Hawksworth DL, Crous PW, Redhead SA, et al. (2011) The Amsterdam declaration on fungal nomenclature. IMA Fungus 2: 105–112.

He Y, Zhang Z (2012) Diversity of organism in the *Usnea longissima* lichen. African Journal of Microbiology Research 6: 4797–4804.

Hughes SJ (1953) Conidiophores, conidia, and classification. Canadian Journal of Botany 31: 577–659. https://doi.org/10.1139/b53-046

Huhndorf SM, Miller AN, Fernandez FA (2004) Molecular systematics of the *Sordariales*: the order and the family *Lasiosphaeriaceae* redefined. Mycologia 96: 368–387. https://doi.org/10.1080/15572536.2005.11832982

Li GJ, Hyde KD, Zhao RL, Hongsanan S, Abdel-Aziz FA, Abdel-Wahab MA, Alvarado P, Alves-Silva G, Ammirati JF, Ariyawansa HA, Baghela A (2016) Fungal diversity notes 367–490: taxonomic and phylogenetic contributions to fungal taxa. Fungal Diversity 80: 1–270. https://doi.org/10.1007/s13225-016-0373-x

Hyde KD, Fröhlich J, Taylor JE (1998) Fungi from palms. XXXVI. Reflections on unitunicate ascomycetes with apiospores. Sydowia 50: 21–80.

Jaklitsch WM, Voglmayr H (2012) Phylogenetic relationships of five genera of Xylariales and *Rosasphaeria* gen. nov. (Hypocreales). Fungal Diversity 52: 75–98. https://doi.org/10.1007/s13225-011-0104-2

Jiang N, Li J, Tian CM (2018) *Arthrinium* species associated with bamboo and reed plants in China. Fungal Systematics and Evolution 2: 1–9. https://doi.org/10.3114/fuse.2018.02.01

Kirk PM (1986) New or interesting microfungi. XV. Miscellaneous hyphomycetes from the British Isles. Transactions of the British Mycological Society 86: 409–428.https://doi.org/10.1016/S0007-1536(86)80185-1

Kunze G, Schmidt JC (1823) Mykologische Hefte. 2. Vossische Buchhandlung, Leipzig, 176 pp.

Larrondo JV, Calvo MA (1990) Two new species of *Arthrinium* from Spain. Mycologia 82: 396–398. https://doi.org/10.1080/00275514.1990.12025899

Larrondo JV, Calvo MA (1992) New contributions to the study of the genus *Arthrinium*. Mycologia 84: 475–478. https://doi.org/10.1080/00275514.1992.12026164

Li BJ, Liu PQ, Jiang Y, Weng QY, Chen QH (2016) First report of culm rot caused by *Arthrinium phaeospermum* on *Phyllostachys viridis* in China. Plant Disease 100: 1013–1013. https://doi.org/10.1094/PDIS-08-15-0901-PDN

Martínez-Cano C, Grey WE, Sands DC (1992) First report of *Arthrinium arundinis* causing kernel blight on barley. Plant Disease 76: 1077. https://doi.org/10.1094/PD-76-1077B

Mavragani DC, Abdellatif L, McConkey B, Hamel C, Vujanovic V (2007) First report of damping-off of durum wheat caused by *Arthrinium sacchari* in the semi-arid Saskatchewan fields. Plant Disease 91: 469. https://doi.org/10.1094/PDIS-91-4-0469A

Minter DW (1985) A re-appraisal of the relationships between *Arthrinium* and other hyphomycetes. Proceedings of Indian Academy of Sciences (Plant Science) 94: 281–308.

Müller E, Arx JA von (1962) Die Gattungen der didymosporen Pyrenomyceten. Beiträge zur Kryptogamenflora der Schweiz 11: 1–922.

Murray MG, Thompson WF (1980) Rapid isolation of high molecular weight plant DNA. Nucleic Acids Research 8: 4321–4325. https://doi.org/10.1093/nar/8.19.4321

Nylander JAA (2004) MrModeltest v2. Program distributed by the author. Uppsala, Evolutionary Biology Centre, Uppsala University.

O'Donnell K, Cigelnik E (1997) Two divergent intragenomic rDNA ITS2 types within a monophyletic lineage of the fungus *Fusarium* are nonorthologous. Molecular Phylogenetics and Evolution 7: 103–116. https://doi.org/10.1006/mpev.1996.0376

Rai MK (1989) Mycosis in man due to *Arthrinium phaeospermum* var. *indicum*. First case report. Mycoses 32: 472–475. https://doi.org/10.1111/j.1439-0507.1989.tb02285.x

Ramos HP, Braun GH, Pupo MT, Said S (2010) Antimicrobial activity from endophytic fungi *Arthrinium* state of *Apiospora montagnei* Sacc. and *Papulaspora immersa*. Brazilian Archives of Biology and Technology 53: 629–632. https://doi.org/10.1590/S1516-89132010000300017

Réblová M, Miller AN, Rossman AY, et al. (2016) Recommendations for competing sexual-asexually typified generic names in *Sordariomycetes* (except *Diaporthales*, Hypocreales, and *Magnaporthales*). IMA Fungus 7: 131–153. https://doi.org/10.5598/imafungus.2016.07.01.08

Rehner SA, Buckley E (2005) A *Beauveria* phylogeny inferred from nuclear ITS and EF1-a sequences: evidence for cryptic diversification and links to *Cordyceps* teleomorphs. Mycologia 97: 84–98. https://doi.org/10.3852/mycologia.97.1.84

Ronquist F, Huelsenbeck JP (2003) MrBayes 3: Bayesian phylogenetic inference under mixed models. Bioinformatics 19: 1572–1574. https://doi.org/10.1093/bioinformatics/btg180

Samuels GJ, McKenzie EHC, Buchanan DE (1981) Ascomycetes of New Zealand. 3. Two new species of *Apiospora* and their *Arthrinium* anamorphs on bamboo. New Zealand Journal of Botany 19: 137–149. https://doi.org/10.1080/0028825X.1981.10425113

Schmidt JC, Kunze G (1817) Mykologische Hefte. 1. Vossische Buchhandlung, Leipzig, 109 pp.

Seifert K, Morgan-Jones G, Gams W, Kendrick B (2011) The Genera of Hyphomycetes. [CBS Biodiversity Series 9]. CBSKNAW Fungal Biodiversity Centre, Utrecht, 997 pp.

Senanayake IC, Maharachchikumbura SS, Hyde KD, Bhat JD, Jones EG, McKenzie EH, Dai DQ, Daranagama DA, Dayarathne MC, Goonasekara ID, Konta S (2015) Towards unraveling relationships in *Xylariomycetidae* (*Sordariomycetes*). Fungal Diversity 73: 73–144. https://doi.org/10.1007/s13225-015-0340-y

Sharma R, Kulkarni G, Sonawane MS, Shouche YS (2014) A new endophytic species of *Arthrinium* (Apiosporaceae) from *Jatropha podagrica*. Mycoscience 55: 118–123. https://doi.org/10.1016/j.myc.2013.06.004

Singh SM, Yadav LS, Singh PN, Hepat R, Sharma R, Singh SK (2013) *Arthrinium rasikravindrii* sp. nov. from Svalbard, Norway. Mycotaxon 122: 449–460. https://doi.org/10.5248/122.449

Sivanesan A (1983) Studies on Ascomycetes. Transactions of the British Mycological Society 81: 313–332. https://doi.org/10.1016/S0007-1536(83)80084-9

Smith GJD, Liew ECY, Hyde KD (2003) The Xylariales: a monophyletic order containing 7 families. Fungal Diversity 13: 185–218.

Spatafora JW, Sung G-H, Johnson D, Hesse C, O'Rourke B, et al. (2006) A five-gene phylogeny of *Pezizomycotina*. Mycologia 98: 1018–1028. https://doi.org/10.1080/15572536.2006.11832630

Stamatakis A (2006) RAxML-VI-HPC: maximum likelihood-based phylogenetic analyses with thousands of taxa and mixed models. Bioinformatics 22: 2688–2690. https://doi.org/10.1093/bioinformatics/btl446

Suryanarayanan TS (2012) Fungal endosymbionts of seaweeds. In: Raghukumar C (Ed.) Biology of Marine Fungi. Springer, Dordrecht, 53–70. https://doi.org/10.1007/978-3-642-23342-5_3

Swofford DL (2001) PAUP*4.0b10: phylogenetic analysis using parsimony (and other methods). Sinauer Associates, Sunderland.

Tamura K, Peterson D, Peterson N, Stecher G, Nei M, Kumar S (2011) MEGA5: Molecular evolutionary genetics analysis using maximum likelihood, evolutionary distance, and maximum parsimony methods. Molecular Biology and Evolution 28: 2731–2739. https://doi.org/10.1093/molbev/msr121

Vilgalys R, Hester M (1990) Rapid genetic identification and mapping of enzymatically ampliWed ribosomal DNA from several *Cryptococcus* species. Journal of Bacteriology 172: 4238–4246.https://doi.org/10.1128/jb.172.8.4238-4246.1990

Wang M, Liu F, Crous PW, Cai L (2017) Phylogenetic reassessment of *Nigrospora*: ubiquitous endophytes, plant and human pathogens. Persoonia 39: 118–142. https://doi.org/10.3767/persoonia.2017.39.06

Wang M, Tan X-M, Liu F, Cai L (2018) Eight new *Arthrinium* species from China. MycoKeys 34: 1–24. https://doi.org/10.3897/mycokeys.34.24221

White TJ, Bruns TD, Lee S, Taylor JW (1990) Amplification and direct sequencing of fungal ribosomal RNA genes for phylogenetics. In: Innis MA, Gelfand DH, Sninsky J, White TJ (Eds) PCR protocols: A Guide to Methods and Applications. Academic Press, San Diego, 482 pp.

Zhang N, Castlebury LA, Miller AN, Huhndorf SM, Schoch CL, Seifert KA, Rossman AY, Rogers JD, Kohlmeyer J, Volkmann-Kohlmeyer B, Sung GH (2006) An overview of the systematics of the *Sordariomycetes* based on four-gene phylogeny. Mycologia 98: 1076–1087. https://doi.org/10.3852/mycologia.98.6.1076

Zhao YM, Deng CR, Chen X (1990) *Arthrinium phaeospermum* causing dermatomycosis, a new record of China. Acta Mycologica Sinica 9: 232–235.

MycoKeys 49: 49–72 (2019)
doi: 10.3897/mycokeys.49.32034
http://mycokeys.pensoft.net

RESEARCH ARTICLE

A peer-reviewed open-access journal
MycoKeys
Launched to accelerate biodiversity research

Epitypification of the Central African *Cantharellus densifolius* and *C. luteopunctatus* allows for the recognition of two additional species

Bart Buyck[1], Terry W. Henkel[2], Valérie Hofstetter[3]

1 *Institut de Systematique, Evolution, Biodiversite (ISYEB – UMR 7205), Museum national d'Histoire naturelle, Sorbonne Université, CNRS, CP 39, 12 Rue Buffon, F-75005 Paris, France* **2** *Department of Biological Sciences, Humboldt State University, Arcata, California, 95521, USA* **3** *Department of Plant Protection, Agroscope Changins-Wädenswil Research Station ACW, Rte De Duiller, CH-1260 Nyon 1, Switzerland*

Corresponding author: *Terry Henkel* (twh5@humboldt.edu)

Academic editor: *A. Vizzini* | Received 30 November 2018 | Accepted 19 February 2019 | Published 27 March 2019

Citation: Buyck B, Henkel TW, Hofstetter V (2019) Epitypification of the Central African *Cantharellus densifolius* and *C. luteopunctatus* allows for the recognition of two additional species. MycoKeys 49: 49–72. https://doi.org/10.3897/mycokeys.49.32034

Abstract

Cantharellus densifolius and *C. luteopunctatus* are epitypified on the basis of recently collected specimens from the Central African rain forest that correspond in every way to their respective original descriptions. Sequences obtained from these new collections demonstrate that both epitypes represent distinct species that belong in different subclades of *Cantharellus* subg. *Rubrinus*. Previously, the name *C. densifolius* has been consistently misapplied to more or less similar species from the African woodland area, including *C. densilamellatus* **sp. nov.** which is described here, In addition, *C. tomentosoides* **sp. nov.**, a rain forest species that is easily confused with *C. densifolius*, is described.

Keywords

Cantharellales, ectomycorrhizal, *tef*-1, phylogeny, rain forest, taxonomy

Introduction

Tropical African *Cantharellus* species ("chanterelles") have been well-documented compared to other tropical regions. Nonetheless, there is a great need for sequence data to provide the foundation for unambiguous species concepts. This is due to the highly

variable and potentially deceptive macromorphologies, compounded by the limited interspecific micromorphological variation among *Cantharellus* species (Buyck et al. 2014, 2016e, Olariaga et al. 2015).

Despite this need for sequence data, *Cantharellus* has been difficult to work with from a molecular standpoint. *Cantharellus* ribosomal genes have high rates of molecular evolution (Moncalvo et al. 2006) and *Cantharellus* species often have an unusually long ITS sequence, ranging from around 900 to 2200 base pairs. The ITS barcode locus is consequently difficult to obtain for chanterelles (Schoch et al. 2012). This is especially true for old type specimens, due to their degraded DNA and resulting difficulties in extraction, and the frequent failures in the annealing of fungal primers designed to amplify the ITS locus or part of it.

While phylogenetic understanding of *Cantharellus* in Europe and North America has recently improved (Buyck et al. 2016c,d,e,f; Olariaga et al. 2015, 2016), the continuing lack of sequence data for Old World *Cantharellus* has helped to perpetuate taxonomic confusion regarding species delimitation and infrageneric relationships (Buyck et al. 2013, 2014). For Africa, some *Cantharellus* species from Madagascar and the African mainland have been circumscribed by single or multilocus molecular phylogenies (Ariyawansa et al. 2015, Buyck et al. 2014, 2015, 2016a, 2017, Liu et al. 2015, De Kesel et al. 2016). However, species recognition for the majority of chanterelles from the Guineo-Congolian rain forest is still based on morphological descriptions published over half a century ago (Heinemann 1958, 1959, 1966).

Many of the older species names for African chanterelles have been misapplied to morphologically similar specimens gathered in dense, closed-canopy rain forest versus the surrounding seasonal woodlands, or in open woodlands of neighboring Madagascar (Buyck et al. 2016g). As type specimen DNA of these earliest described rain forest chanterelles appears completely degraded (fide De Kesel et al. 2016), epitypification with sequencing of newly collected specimens is the most efficient way for unambiguous species delimitation. Until recently, new, well-documented specimens of rain forest chanterelles have not been available for sequencing. Thanks to renewed collecting efforts for *Cantharellus* in the African rain forest, the limits of species bearing these older names can be assessed, and the epitypification process has begun (Buyck et al. 2016a,b,g, De Kesel et al. 2016, Buyck and Hofstetter 2018).

Here we epitypify *Cantharellus densifolius* Heinem. based on recent collections made ~400 km from the type locality but in the same forest habitat. The chosen epitype, which is in perfect agreement with the original description, clearly demonstrates that the name has been misapplied to different species for decades. The new collections constitute the first records for *C. densifolius* since this species was collected by Mme. Goossens-Fontana in 1929 and later described by Heinemann (1958). In this paper we also epitypify *Cantharellus luteopunctatus* Heinem, previously considered a yellowish color-variant of *C. densifolius* (Eyssartier 2001), but shown here to be a morphologically well-defined, independent species. Additionally, two new species previously confused with *C. densifolius* are described.

Material and methods

Collecting and macromorphology

Basidiomata were collected in the Central African Republic (RCA) during dry conditions in early May 2016 in pure *Gilbertiodendron dewevrei* stands of the Dzangha-Sangha Forest Reserve. In Cameroon, basidiomata were collected during the Aug.-Nov. rainy seasons of 2014, 2016, and 2017 from the Dja Biosphere Reserve, Northwest Sector near the village of Somalomo, Upper Dja River Basin, within a two km radius of a base camp located at 3°21'29.8"N, 12°43'46.9"E, 650 m a.s.l., in forests dominated by *G. dewevrei*. Photographs and descriptions of macromorphological features were made from fresh material in the field. Colors were compared with color plates from Kornerup and Wanscher (1978) and are cited in parentheses. Collections were dried with a self-made drier (RCA) or silica gel (Cameroon). Epitype material and additional specimens are deposited in PC, Museum national d'histoire naturelle, Paris, and for the Cameroon collections also in the following herbaria: YA, Cameroon National Herbarium; HSC, Humboldt State University.

Micromorphology

Microscopic observations and measurements were made from ammoniacal Congo red mounts after a short pretreatment in a 10% aqueous KOH solution to improve tissue dissociation and matrix dissolution. Original drawings for all elements of the hymenium and pileipellis were made at a magnification of 2400× with the aid of a camera lucida. Measurements of basidiospores cite length, width and length/width ratio (Q) in this format: (minimum–) mean minus standard deviation – mean value – mean plus standard deviation (– maximum measured); basidiospore size statistics are based on 20 basidiospores measured per specimen.

Taxon sampling and phylogenetic analyses

Genomic DNA isolation, amplification and sequencing for the transcription elongation factor 1-alpha (*tef*-1) of the new *Cantharellus* collections were obtained as described in Buyck et al. (2014). The *tef*-1 sequence data from other taxa were obtained from our previous publications (Buyck et al. 2014, 2016a, b, 2018; Das et al. 2018). Sequences were assembled and corrected with the software package Sequencher 3.0 (Gene Codes Corp., USA). Alignment of *tef*-1 was performed manually in MacClade 4.05 (Maddison and Maddison 2002). Searches for the optimal tree and branch robustness were conducted with the program PhyML (Guindon and Gascuel 2003), under a GTR nucleotide substitution model, with the search starting from a distance-based

tree and with the proportion of invariable sites, gamma shape parameter and number of substitution categories estimated during the search. Three independent runs were conducted to check for convergence toward the same likelihood value. Branch support was estimated based on 500 bootstrap replicates (ML-bs) and was considered significant when ≥ 70% (Mason-Gamer and Kellogg 1996; Alfaro et al. 2003).

Results

Seven new sequences were produced for this study (five collections of *C. densifolius*, one of *C. tomentosoides*, and one of *C. luteopunctatus*). The alignment used for phylogenetic analyses included sequences of 90 *Cantharellus* specimens and one of *Craterellus tubaeformis* used for outgroup. The full alignment length was 864 base pairs. After exclusion of three spliceosomal introns, the remaining 629 characters were used for the analyses.

The most likely tree (Fig. 1; -ln = 14270.90232) placed *C. densifolius* (ML-bs = 100 %) as sister without support to a highly supported monophyletic group (ML-bs = 100 %) containing *C. tomentosoides* sp. nov. and the typical woodland species *C. tomentosus* (ML-bs = 100 %) (Buyck et al. 2000). *Cantharellus densilamellatus* sp. nov. was not conspecific with *C. densifolius*, instead forming a highly supported terminal clade (ML-bs = 98 %) with the designated epitype of *C. luteopunctatus*, and this clade was supported (ML-bs = 80 %) as sister to a clade containing *C. tanzanicus* and the Malagasy, eucalypt-associated *C. eucalyptorum* Buyck & V. Hofst. (Ariyawansa et al. 2015). These species formed a larger, strongly supported clade (ML-bs = 97 %) within subg. *Rubrinus* with two additional Malagasy species, the woodland endemic *C. albidolutescens* Buyck & V. Hofst. (Buyck et al. 2015), and the eucalypt-associated *C. tricolor* Buyck & V. Hofst. (Ariyawansa et al. 2015).

Taxonomy

Cantharellus densifolius **Heinem., Bull. Jard. bot. État Brux. 28(4): 410. 1958.**
Figs 2, 3

Original diagnosis. "*Pileus carnosulus, infundibuliformis, lobatus, laete ochraceus, squamulosus. Stipes solidus, pileo concolor. Lamellae confertissimae, angustissimae, furcatae, non intervenatae. Caro ochracea, sapore amaro. Sporae breviter ellipsoidae, 5,6–7 × 3,7–4,5 µm.*"

Holotype. DEMOCRATIC REPUBLIC OF THE CONGO. Binga, dispersed on the soil of the dry forest, Aug. 1929, Mme. Goossens-Fontana 879 (BR).

Iconography. Heinemann (1958, fig. 45; 1959, pl. XXVI, fig. 11).

Original description. (freely translated from French) "Pileus ca. 8 cm diam., thin, deeply concave to infundibuliform, with the margin convex to stretched, irregular and wavy; surface ochraceous orange, very finely punctuated with tiny squamules that are easily detached. Stipe ca. 30 × 7 mm, cylindrical, massive, concolorous with the cap.

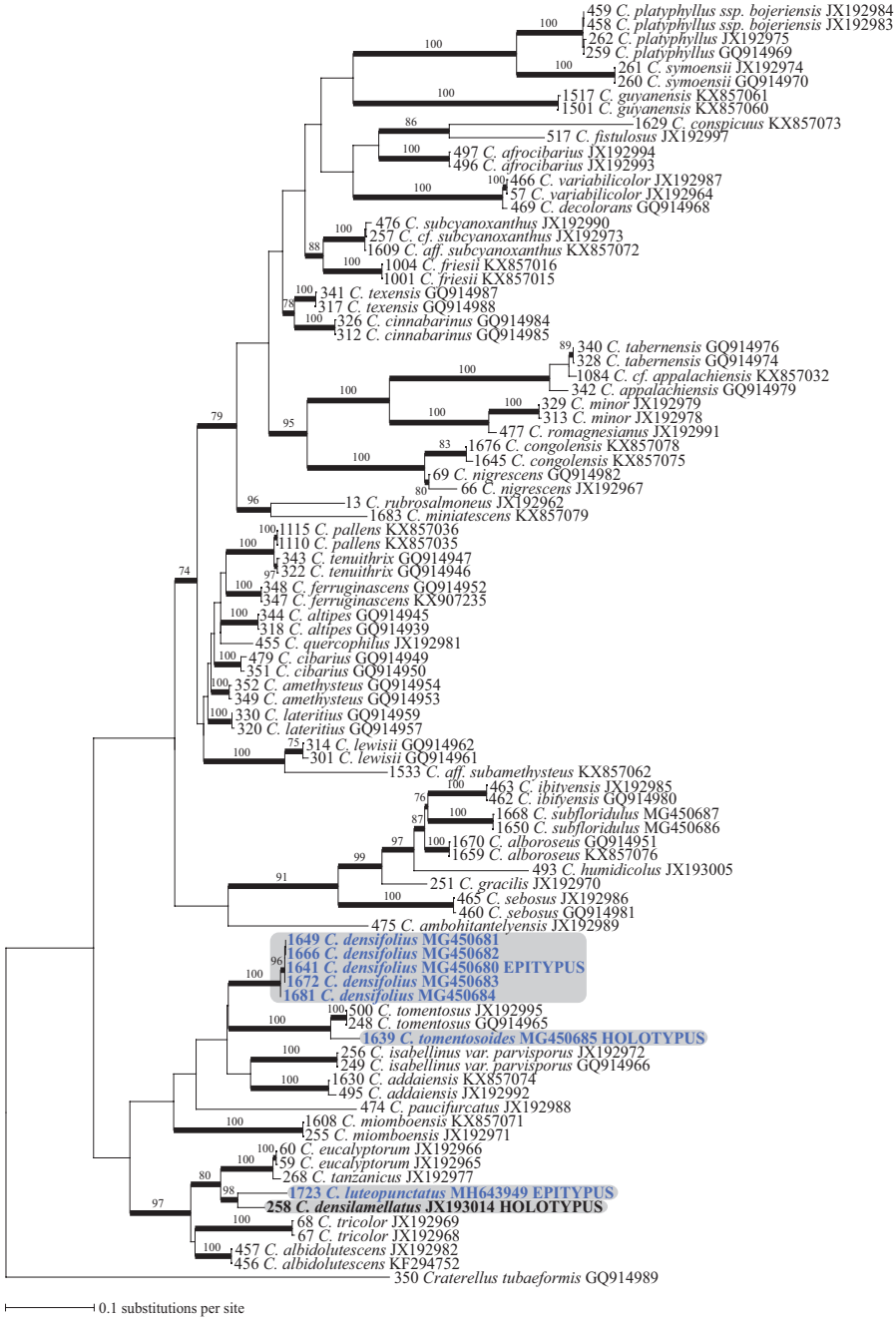

Figure 1. Most likely tree obtained by analysis of the 91 *tef*-1 sequence dataset. Species names are preceded by their extraction number (see Buyck et al. 2014 for corresponding vouchers) and followed by the corresponding GenBank deposit number. Branches that received significant ML bootstrap support are in bold with ML-bs associated values indicated above the branches. Newly produced sequences are in blue and discussed species are in bold.

Hymenophore composed of crowded gill-folds, less than 1 mm high, 1–4 times forking, deeply decurrent, with blunt gill edge, not interveined. Context fibrous, bright ochraceous. Taste bitter. Smell of *C. cibarius*. Spore print white. Exsiccatum with reddish ochre brown color.

Spores hyaline, 5.6–7 × 3.7–4.5 µm, shortly ellipsoid, thin-walled, not amyloid; apiculus small. Basidia slender, 37–48 × 6–8 µm, probably 6-spored. Hymenophoral trama pseudoparenchymatic, slightly bilateral. Pseudoparenchyma very compact. Pileipellis squamulae composed of easily detaching cells that are irregularly cylindrical, often undulating, thick-walled with a very thick yellow wall in ammonium solution; the terminal cells obtusely rounded. Clamp connections rare."

Description of the epitype. *Basidiomata* solitary or in small groups. *Pileus* medium-sized to rather large and up to 100 mm diam., 1–2 mm thick at mid-radius, yet firm and leathery; margin undulating, irregularly waving to strongly lobed, smooth; surface layer remaining more or less continuous in the center, then disrupting toward the margin with expansion of the pileus and forming dark, more or less concentrically arranged squamules or fibres; observed under a hand lens these can be appressed and flat, or forming a woolly-cottony mass of suberect fibers, pale brown (5AB3) to warm chocolate brown or dark brown (5EF7–8, 5F4–8, 5D5–8, 5C5–6) when young, but rapidly tinged with ochraceous orange as a consequence of the exposure of the underlying pileus tissue and the yellowing tendency of the context. *Hymenophore* composed of very crowded (>30/mm) gill folds, which are very low (<1 mm) and thick, not interveined, often transversely fissuring over their entire height, repeatedly forking, strongly decurrent, off-white when young, then darkening to the color of coffee with copious milk, moderately to strongly yellowing upon handling. *Stipe* 40–60 × 4–5 mm, widening toward the hymenophore and there up to 8(–17) mm wide; surface smooth, whitish, pale brown just beneath the hymenophore. *Context* whitish, thin and leathery, fibrous in the stipe, faintly to strongly yellowing upon injury or handling, occasionally turning rusty brown. *Odor* faint. *Taste* mild. *Spore print* off-white.

Basidiospores ellipsoid, (5.8–)6.0–6.46–6.9(–7.1) × (3.5–)3.8–4.19–4.6(–5.0) µm, Q = (1.3–)1.4–1.55–1.7(–1.8), smooth, hyaline. *Basidia* mostly 35–50 × 7–8 µm, (5–)6(–7)-spored; sterigmata stout but rather short. *Subhymenium* forming a very dense layer, not pseudoparenchymatous, but composed of mostly short cells that are not wider than the basidium base. *Cystidia* none. *Pileipellis* of loosely interwoven and much septate hyphal extremities composed of ramifying chains of distinctly thick-walled cells; terminal (but also sometimes subapical) cells subcylindrical, but often more irregularly inflated or sinuous-tortuous in outline, 5–8(–10) µm wide, mostly 25–45 µm long, often narrowing or abruptly constricted near the apex. *Clamp connections* absent.

CENTRAL AFRICAN REPUBLIC. Dzanga-Sangha Forest Reserve, near Bayanga, close to Bai-Hakou base camp, 02.859934N, 16.467492E, in monospecific *Gilbertiodendron dewevrei* forest, on bare sandy soil, 15 May 2016, 1641/Buyck 16.021 (PC 0142486, **epitypus hic designatus**). MycoBank MBT 384669.

Additional specimens examined. CENTRAL AFRICAN REPUBLIC. Dzanga-Sangha Forest Reserve, near Bayanga, in and around Bai-Hakou base camp,

Figure 2. *Cantharellus densifolius*. **a** Field habit of the epitype (BB 16.021), showing the areolate-squamose ochraceous orange pileus surface resulting from the concentrical disruption of a dark tomentum that covered initially the young pileus **b** Detail of the epitype hymenophore showing the remarkably low and thick, crowded, repeatedly forking gill folds without interstitial veination **c** Original watercolor of the holotype by Mme. Goossens-Fontana from Heinemann (1959), reproduced with the permission of Botanic Garden Meise, Belgium **d** Field habit of specimen BB 16.081 showing the variability of the pileus color within a single collection. Photos: B. Buyck.

02.859934N, 16.467492E, in monospecific *Gilbertiodendron dewevrei* forest, on bare sandy soil, 19 May 2016, Buyck 16.081/1656 (PC0142487), Buyck 16.065/1649 (PC0142488); ibid., 24 May 2016, Buyck 16.113/1672 (PC0142490); ibid., 26 May 2016, Buyck 16.137/1681 (PC0142489).

Discussion. *Cantharellus densifolius* was originally described by Heinemann (1958) and was one of three rain forest *Cantharellus* species characterized by crowded gill folds. The other two chanterelles with equally crowded gill folds were the fragile, smaller (pileus < 30 mm diam.), bright orange *C. pseudofriesii* Heinem. and the medium-sized, bright yellow *C. luteopunctatus* Heinem. Eyssartier (2001) re-examined the holotype of each of these three species, and concluded that *C. pseudofriesii* was distinctive due to its possession of clamp connections (contrary to the original description, see also Buyck et al. 2016a), and suggested that *C. luteopunctatus* may be a color variant of *C. densifolius* because of its similar micromorphological features.

The epitype specimen selected here perfectly agrees with the original description of *C. densifolius*. Indeed, Heinemann (l.c.) described it as a medium-sized species with an infundibuliform, ochre-orange and finely squamulose pileus measuring ca. 80 mm diam. and ending in an irregular but stretched margin, with strongly decurrent, crowded, frequently forking and very low gill folds (< 1 mm high) with blunt edges, lacking any intervenation. Heinemann cited shortly ellipsoid basidiospores of near identical size, more precisely given by Eyssartier (2001), as important microscopic features, along with the pileipellis composed of easily disintegrating, very thick-walled hyphal extremities that are sinuous-undulating in outline (compare Heinemann 1958 fig. 45B with our Fig. 3c).

The typical features appear to be quite constant across all specimens of *C. densifolius* examined here, including both the size and shape of basidiospores (Table 1), as well as the undulate, thick-walled, often apically tapered or constricted hyphal extremities (although less so in Buyck 16.137). The ochre-orange color of the pileus described for the holotype was also present in the epitype (Fig. 2a, c) but across collections examined here pileus color ranged from ochraceous yellow over orange to pale brown and even dark chocolate brown, but never to bright lemon yellow as described for *C. luteopunctatus*. This is consistent with the highly variable color within many other *Cantharellus* species (Olariaga et al. 2015, Buyck et al. 2016e). For *C. densifolius*, the general color of the pileus also depends on the degree of yellowing of the context underneath the disrupted surface tomentum, which can vary between or within individual basidiomata.

The form of the hyphal extremities composing the pileal tomentum is very similar to that of various other squamulose species in subg. *Rubrinus* sect. *Isabellinus* Eyssart. & Buyck, in particular those of the African *C. tanzanicus* Buyck & V. Hofst. (Buyck et al. 2013) and the Malagasy *C. eucalyptorum* Buyck & V. Hofst. and *C. tricolor* Buyck & V. Hofst., the latter two species being associates of introduced eucalypts (Liu et al. 2015). The differences in habitat and basidiospore size allow differentiation of *C. densifolius* from these species.

Cantharellus densifolius has repeatedly been reported from the surrounding woodland area in Africa (e.g. Heinemann 1966, Buyck 1994, Buyck et al. 2000, Härkönen

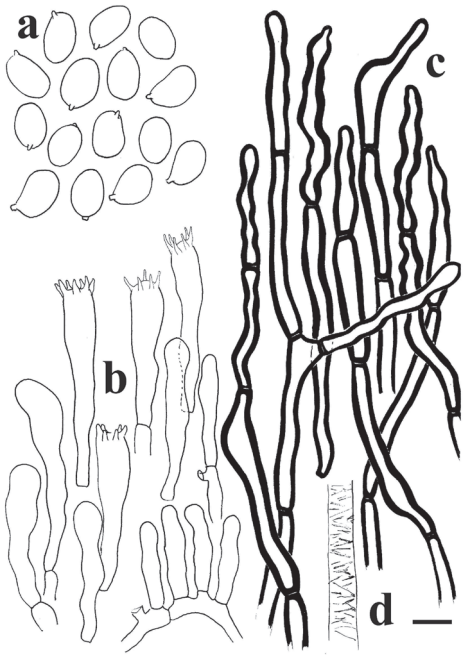

Figure 3. *Cantharellus densifolius* (epitype, BB 16.021). Microscopic features: **a** basidiospores **b** basidia and basidiola **c** distinctly thick-walled and typically sinuous-undulate hyphal extremities of the pileipellis **d** detail of an encrusted hypha from the pileus context. Scale bar: 10 µm but only 5 µm for basidiospores. Drawings B. Buyck.

Table 1. Comparison of basidiospore measurements for the discussed species.

C. densifolius			
Holotype (Heinemann 1958):	5.6–7	3.7–4.5 µm	
Holotype (Eyssartier 2001):	5.5–**6.37**–7	3.5–**4.06**–4.5	1.3–**1.57**–1.8
Epitype:	(5.8–)6.0–**6.46**–6.9(–7.1)	(3.5–)3.8–**4.19**–4.6(–5.0)	(1.3–)1.4–**1.55**–1.7(–1.8)
Buyck 16.137	(5.4–)5.5–**5.78**–6.1(–6.5)	(3.5–)3.9–**4.14**–1.5(–1.6)	(1.2–)1.3–**1.40**–1.5(–1.6)
Buyck 16.081	(4.8–)5.4–**5.78**–6.1(–6.2)	(3.5–)3.8–**4.02**–1.5(–1.7)	(1.2–)1.3–**1.44**–1.5(–1.6)
C. tomentosoides			
Holotype	(5.8–)6.0–**6.36**–6.7(–7.1)	(3.9–)4.0–**4.27**–4.5(–5.0)	(1.3–)1.4–**1.49**–1.6(–1.7)
C. densilamellatus			
Holotype:	6.7–**7.05**–7.4(7.9)	(3.3)3.4–**3.65**–3.9(4.0)	(1.7)1.8–**1.94**–2.1(2.3)
C. luteopunctatus			
Holotype (Heinemann 1958):	4.9–6.0 (7.5)	3.8–4.6 (5) µm	
Holotype (Eyssartier 2001):	5–**5.97**–7	3.5–**4.19**–5	1.2–**1.42**–1.6
Epitype / Henkel 10285	(5.4–)5.7–**6.04**–6.4(–7.1)	(3.9–)4.0–**4.29**–4.6(–5.0)	(1.2–)1.3–**1.41**–1.5(–1.8)
Henkel 10442:	(5.4–)5.4–**5.94**–6.5(–7.3)	(4.1–)4.2–**4.33**–4.5(–4.8)	(1.2–)1.3–**1.37**–1.5

et al. 2015). Our sequence data have now indicated that such woodland specimens merit recognition as independent species. For example, the morphologically similar *C. densilamellatus* sp. nov. described below is unrelated to *C. densifolius* but resolved as sister to *C. luteopunctatus* (Fig. 1).

Cantharellus luteopunctatus **(Beeli) Heinem. Bull. Jard. bot. État Brux. 28(4): 415. 1958.**
Figs 4–6

Basionym. *Lentinus luteopunctatus* Beeli, Bull. Soc Roy Bot Belge 60: 160. 1928.

Original diagnosis. "*Pileo carnoso-coriaceo, centro depresso, margine incurvato, luteo; furfuraceo brunneo, 3,5–4 cm. lato; stipite cylindrico-solido, glabro, concolori, 3 × 0,5–0,7 cm, lamellis deccurentibus, luteis; sporis ovoideis 5–6 × 3,5–4 µm, carne lutea.*"

Holotype. DEMOCRATIC REPUBLIC OF CONGO. Central forest district, near Djongo-Akula, dispersed on the soil of the dry *Gilbertiodendron dewevrei* forest, Dec. 1925, Mme. Goossens-Fontana 502 (BR).

Iconography. HEINEMANN (1958, fig. 47; 1959, pl. XXVI, fig. 6).

Original description. (freely translated from French) "Pileus rather thick, 49 mm diam., soon depressed, concave with rounded, then straight margin, bright lemon yellow, punctuated – particularly in the center – with minute brownish squamules. Stipe 30 × 6 mm, [30–50 × 5–11 mm], cylindrical, solid inside, yellow, finally rusty, faintly covered from brownish scales. Gills very crowded, deeply decurrent, very narrow, 0.5–11 mm wide (sic!), yellow, irregularly forked, interconnected by rather abundant transversal anastomoses. Context firm, bright yellow, more orangish near the stipe base. Taste strong, bitter. Spore print white. Exsiccatum orangish brown-ochre.

Spores hyaline, shortly ellipsoid, 4.9–6.0 (7.5) × 3.8–4.6 (5) µm, granular inside, thin-walled, not amyloid, with a small apiculus. Basidia narrowly clavate, 30–40 × 6.7–9.5 µm, 4-spored, perhaps sometimes 6-spored. Hymenium not or only slightly accrescent. Subhymenium narrow. Pseudoparenchyma composed of very long and slender elements, mixed with some oleiferous hyphae that do not color in Congo Red. Pileipellis undifferentiated; squamules formed of hyphae united in bundles made up of yellowish to pinkish cells; terminal cells lanceolate or clavate, 6–13 µm diam. Hyphae not amyloid."

Description of the epitype. *Basidiomata* scattered to occasionally caespitose. *Pileus* up to 65(–75) mm diam., initially broadly convex with shallow depression, extending outward and upward with age, becoming increasingly infundibuliform with downturned margin, deep golden yellow (2–3A4), beset with minute, conical erect tufts, these flesh-brown, more concentrated over the disc but extending and gradually more widely dispersed toward margin; intervening surface shiny-glabrous; margin irregularly crenulate, slightly wavy. *Hymenophore* composed of very thin, crowded, ridge-like gill folds, creamish to nearly concolorous with the pileus surface (2–3A3), occasionally developing tannish overtones with age (3–4A3), decurrent and fairly abruptly demarcated from the sterile stipe surface, discoloring slowly darker yellow to orangish where injured, repeatedly forking, also abundantly cross-connected between stipe and pileus margin at almost right angles, becoming increasingly tortuous and anastomosed with advanced age; edges even and concolorous. *Stipe* subequal or slightly tapering toward the base, (17–)24–43 × 4–8(–10) mm, concolorous with pileus, beset apically with conical, flesh-brown, erect tufts, longitudinally striate below; extreme base often devel-

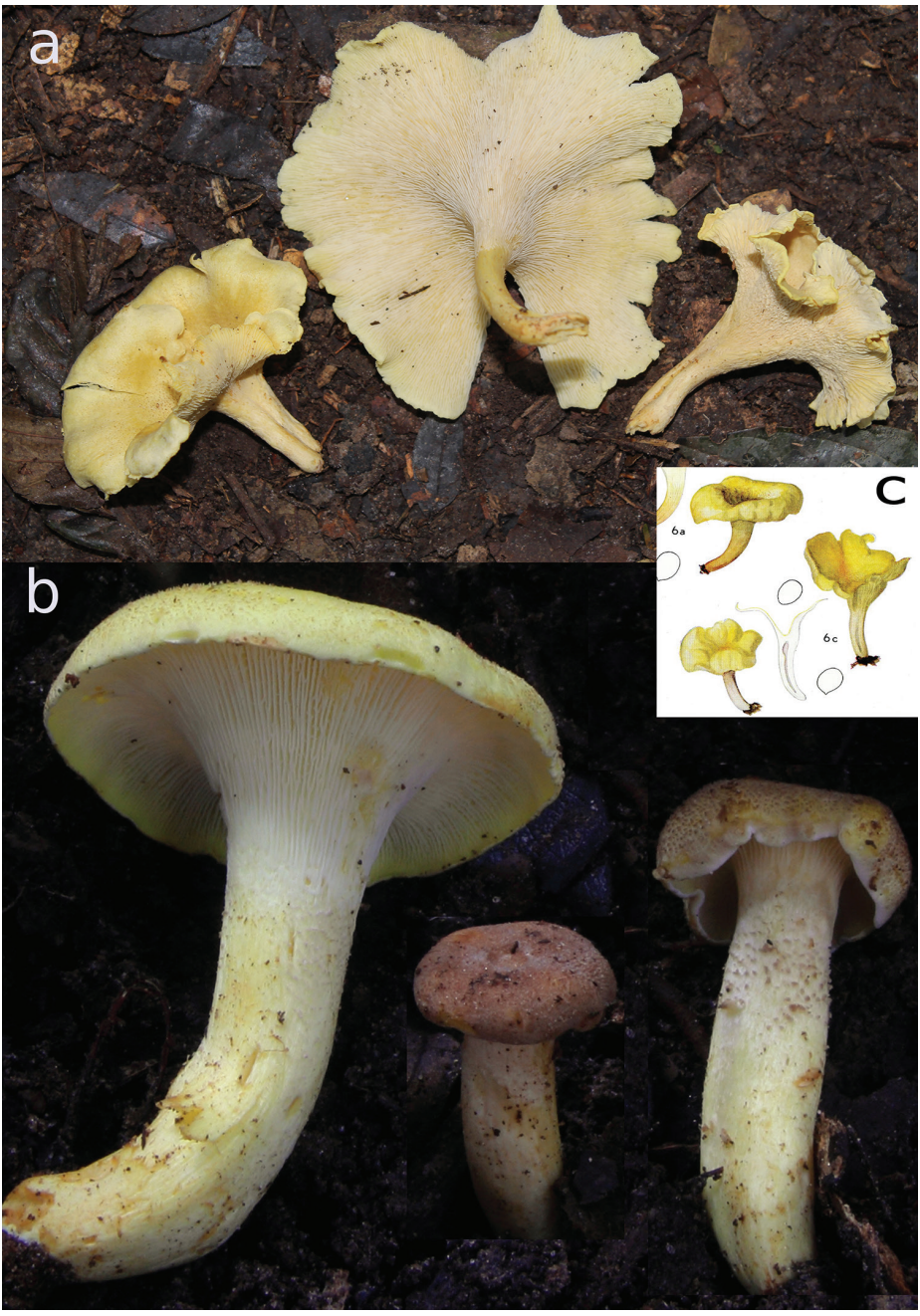

Figure 4. *Cantharellus luteopunctatus*. **a** Field habit of the epitype (TH 10285) **b** details of younger basidiomata from specimen TH 9921, showing the gradual color change of the pileus going from pinkish brown in youngest stages to pale yellow in older stages because of the less dense squamulae; similar squamulae are present on the stipe surface. Composition based on photos by Terry Henkel and Todd Elliott **c** original watercolor of the holotype by Mme. Goossens-Fontana from Heinemann (1959), reproduced with the permission of Botanic Garden Meise, Belgium.

oping some white mycelial tissue at the soil interface. *Context* solid, yellow, unchanging to increasingly yellow. *Odor* mildly chanterelle-like. *Taste* mild, nutty, pleasant, somewhat tardily acrid in young specimens. *Spore print* not obtained.

Basidiospores short-ellipsoid to ellipsoid, (5.4–)5.7–6.04–6.4(–7.1) × (3.9–)4.0–4.29–4.6(–5.0) µm, Q = (1.24)1.29–1.41–1.53(–1.79), smooth. *Basidia* quite short, mostly 30–40(–50) × 6–7 µm, (5–)6-spored. *Cystidia* none. *Subhymenium* cells mostly hardly wider than the basidium base, but locally more inflated parts make it somewhat intermediate between distinctly pseudoparenchymatous and filamentous. *Pileipellis* composed periclinal thin-walled hyphae of variable diameter, but most ca. 10 µm wide, that locally emit anticlinal tufts of short-septate chains of more or less inflated cells, with the largest cells in these chains distinctly zebroid incrusted and the more terminal cells distinctly thick-walled (up to 1 µm thick); terminal cells 30–60 µm long, mostly (6–)10–15 µm wide, subcylindric or clavulate to lageniform, with obtusely rounded to attenuated tips, never remarkably undulate or irregular in outline. *Clamp connections* absent.

CAMEROON. East Region: Dja Biosphere Reserve, Northwest Sector near the village of Somalomo, Upper Dja River Basin, within 2 km radius of Dja base camp located at 3°21'29.8"N, 12°43'46.9"W, 650 m a.s.l., 2 km SW of Dja base camp, under *Gilbertiodendron dewevrei*, coll. T. Henkel, 22 Nov 2016, TH 10285 (YA, **epitypus hic designatus**, duplicates at HSC G1264 and PC). MycoBank MBT 384670.

Additional specimens examined. CAMEROON. East Region: Dja Biosphere Reserve, Northwest Sector near the village of Somalomo, Upper Dja River Basin, 1.4 km SW of Dja base camp, under *G. dewevrei*, coll. T. Henkel, 2 Sep 2014, TH 9921 (YA, HSC G1265, PC); 2 km SW of Dja base camp, under *G. dewevrei*, coll. T. Henkel, 29 Aug 2017, TH 10442 (YA, HSC G1266, PC).

Discussion. *Cantharellus luteopunctatus* has long been considered as "uncomfortably close" to *C. densifolius*. Eyssartier (2001) found no significant microscopic differences between their holotypes, and suggested that *C. luteopunctatus* was likely a more yellowish color form of the latter species. For several decades following its original description *C. luteopunctatus* was not discussed in the literature, until recently by Eyi N'dong et al. (2011) who accepted it as an independent species. Both *C. luteopunctatus* and *C. densifolius* were also maintained as independent entities in a recent identification key to all African chanterelles (De Kesel et al. 2016). Our choice of epitype has been based on the specimen with the highest degree of similarity with the original macro- and microscopic description of *C. luteopunctatus*, and the original watercolor showing a species with a similar stature, color, and laterally compressed stipe (Fig. 4c).

Close reading reveals some differences between the original descriptions for *C. luteopunctatus* and *C. densifolius*. Apart from the difference in pileus color, the second most important difference, also noted by Eyi N'dong et al. (2011), concerns the configuration of the hymenophore. Gill folds were originally described for *C. luteopunctatus* as "irregularly forking and with many interstitial anastomosing veins", versus those of *C. densifolius* which were "1–4 times forking, not interveined" (Heinemann 1958). Although the presence and frequency of anastomoses between gill folds can be highly

Figure 5. *Cantharellus luteopunctatus* (TH 10442). **a** Field habit of a collection that is more intensely yellow with distinctly yellowing context **b** detail of the hymenophore showing the crowded, thin and strongly anastomosing gill folds. Based on photos by Noah Siegel.

variable among and within *Cantharellus* species, it remains nevertheless a very informative feature to characterize those species that appear always to be on one side of the continuum (De Kesel et al. 2016). In this particular case, the macromorphologies of recent collections suggest that this feature is consistent across, and different between, specimens of *C. luteopunctatus* and *C. densifolius*.

Our collections also demonstrate a difference in hymenophore color between the species, something that is not evident from Heinemann's descriptions. Heinemann described *C. luteopunctatus* as having a yellow hymenophore, but does not indicate the color for the hymenophore of *C. densifolius*, although the original watercolor clearly shows it to be more or less ochraceous (see Fig. 2c here, and Heinemann 1959, Plate XXVI, fig. 6). Our collections confirm this ochraceous to dirty isabelline color of the hymenophore of *C. densifolius*, even when still relatively young, whereas the hymenophore color is more variable in *C. luteopunctatus* due to the translucent context above. The hymenophore of *C. luteopunctatus* is pure white when young, but it may also have pinkish tinges when the pileus surface is still densely covered by pinkish brown squamae, and then becomes more yellowish (which is the color mentioned in the original description) with maturation due to the yellowing context and absence of squamae over the expanded pileus margin. As in *C. densifolius*, the yellowing can be of variable intensity; for instance, the exposed context of TH 10442 is more strongly chrome yellow than that of the epitype (Fig. 5a).

Other considerable differences between *C. luteopunctatus* and *C. densifolius* include the surface structures of the pileus and stipe. In *C. luteopunctatus*, distinct central pileal squamae are erect, flesh brown to pinkish brown, and strongly separated and paler toward the margin. The pinkish color of the squamae was also mentioned in the original description of Heinemann (1958). In contrast, the pileus surface of *C. densifolius* is a continuous tomentum that lacks a pinkish flesh color and is woolly-fibrous, before breaking up concentrically in appressed fragments. Furthermore, in *C. luteopunctatus* the upper stipe surface has the same squamae as the pileus center, whereas in *C. densifolius* the stipe surface is smooth (compare Figs 2, 4, 5).

Micromorphologically, the basidiospores are nearly identical in both species (Table 1), but the pileipellis differs dramatically. In *C. luteopunctatus* the pileipellis is composed of fascicles of thin- to slightly thick-walled hyphae (corresponding to the erect squamae) that are recognizable on the background of more or less parallel, thin-walled hyphae of the interstitial surface, whereas in *C. densifolius*, the thicker-walled hyphae are not organized in fascicles. Moreover, in the latter species the distal cells of these thick-walled hyphae are much more undulate-sinuous in outline and narrower than those of *C. luteopunctatus*.

A final remark concerns the edibility of these Central African chanterelles: In Cameroon *C. luteopunctatus* basidiomata are mild-flavored and consumed by the indigenous Baka, while *C. densifolius* slowly develops a very strong bitterness and is not consumed by the Baka (T. Henkel, pers. obs.). While the bitter taste was also noted in the original description (Heinemann 1958), the first author did not detect bitterness for *C. densifolius* specimens from the Central African Republic.

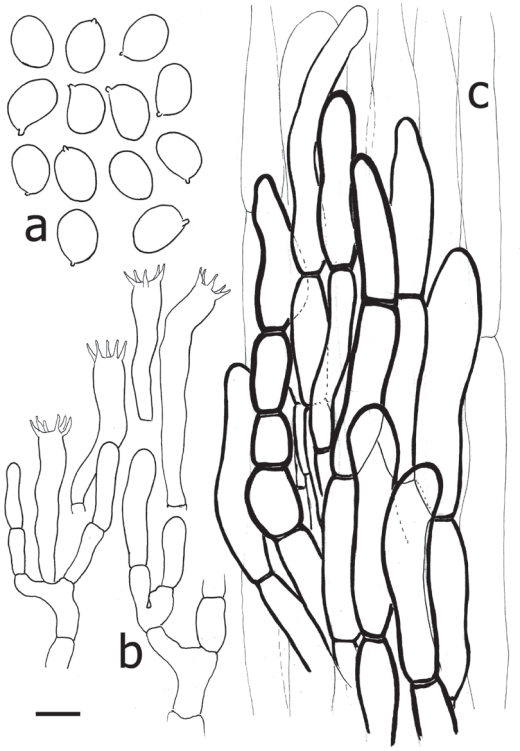

Figure 6. *Cantharellus luteopunctatus*. Microscopic features: **a** basidiospores **b** basidia and basidiola **c** detail of part of a squamula showing the terminal, thin- to slightly thick-walled hyphal extremities overlying the pileipellis. Scale bar: 10 µm but only 5 µm for basidiospores. Drawings: B. Buyck.

Cantharellus tomentosoides **Buyck & V. Hofst., sp. nov.**
MycoBank MB 828890
Figs 7, 8

Diagnosis. *Cantharellus tomentosoides* is similar to *C. densifolius* in its low, blunt and crowded gill folds, overall yellowish brown color, identical basidiospores, and same habitat, but differs in its mostly smaller basidioma size, pileus surface texture, slightly more yellowish olive hymenophore color, and less thick-walled, less sinuous pileipellis extremities.

Gene sequences ex-holotype. MG450685 (*tef*-1).

Etymology. In reference to the species' resemblance to its woodland sister-species, *C. tomentosus*.

Holotype. CENTRAL AFRICAN REPUBLIC. Dzanga-Sangha Forest Reserve, near Bayanga, close to Bai-Hakou base camp, 02.859934N, 16.467492E, in monospecific *Gilbertiodendron dewevrei* forest, on bare sandy soil along trail at the entrance of the camp, 14 May 2016, Buyck 16.007 (PC0142485). MycoBank MBT 828890.

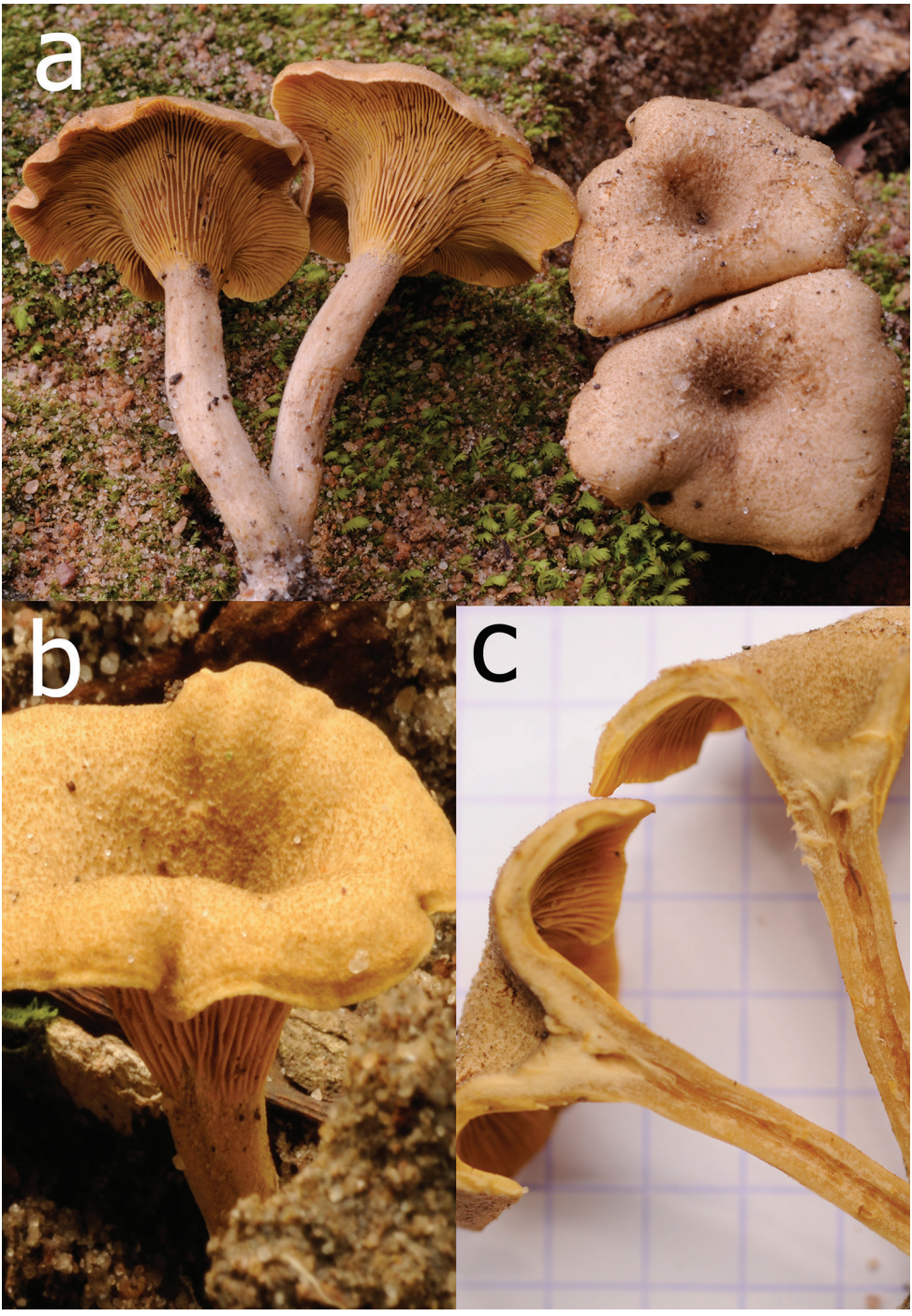

Figure 7. *Cantharellus tomentosoides* (holotypus, Buyck 16.007). **a** Field habit **b** detail of the pileus surface **c** Longitudinal section showing the fistulose stipe. Photos: B. Buyck.

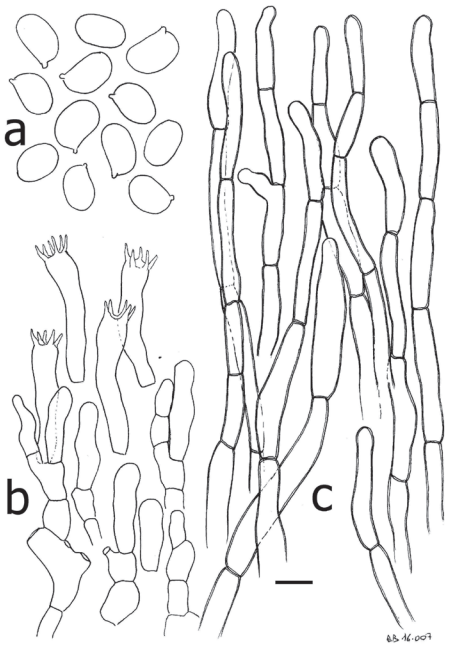

Figure 8. *Cantharellus tomentosoides*. Microscopic features: **a** basidiospores **b** basidia and basidiola **c** densely septate and nearly thin-walled hyphal extremities of the pileipellis. Scale bar: 10 µm but only 5 µm for basidiospores. Drawings: B. Buyck.

Description. *Basidiomata* in small clusters, up to 40 mm high. *Pileus* 20–30 mm diam., thin and leathery, wavy with inrolled margin, young entirely hirsute-rugose, remaining lacerate-fibrillose to cottony in the center, elsewhere slightly rugose but lacking well-defined appressed scales, overall pale grayish brown with dark brown center, very early on becoming narrowly but strongly depressed centrally. *Stipe* slender, 6 mm diam., 20–30 mm high, rapidly elongating while pileus is still small, paler to concolorous with pileus margin, occasionally white at base; interior distinctly fistulose. *Hymenophore* composed of very crowded (up to 40/cm), low but comparatively thick and blunt gill folds, these 1 mm high, repeatedly forking, frequently fissuring over their full height, yellow with brownish tint, transitioning to warm egg-yolk yellow near extreme margin. *Context* leathery, whitish in the pileus, almost concolorous with the stipe surface, yellowing slowly. *Odor* agreeable, typical. *Taste* mild. Spore print not obtained.

Basidiospores short-ellipsoid to ellipsoid, (5.8–)6.0–6.36–6.7(–7.1) × (3.9–)4.0–4.27–4.5(–5.0) µm, Q = (1.3–)1.4–1.49–1.6(–1.7), smooth, hyaline. *Basidia* short and narrow, 30–38 × 6–8 µm, mostly five-spored. *Subhymenium* pseudoparenchymatous, composed of short, barely inflated cells that are slightly wider than the basidium base. *Cystidia* none. *Pileipellis* composed of almost thin-walled to slightly refringent hyphal extremities, mostly 4–8 µm wide; terminal cells rather short, mostly 20–40(–

50) µm long, subcylindrical, regular in outline, broadly rounded at the apex; walls refringent, not thickened. *Clamp connections* absent.

Discussion. *Cantharellus tomentosoides* is a rain forest species that is phylogenetically sister to *C. tomentosus* Eyssart. & Buyck (Fig. 1), for which it was initially mistaken in the field. The latter species was described from miombo woodland in Tanzania and was documented from Burundi by Buyck (1994) under the local name 'nyarumpu'. Apart from its different habitat, *C. tomentosus* differs from *C. tomentosoides* in its slightly narrower basidiospores (6–6.98–8 × 3.5–3.92–4.5 µm, Q = 1.5–1.79–2.1), narrower hyphal extremities of the pileipellis, more brownish gill folds, and its nearly smooth to faintly squamose pileus surface (Buyck et al. 2000).

Cantharellus tomentosoides resembles *C. densifolius* in its similarly crowded gill folds, overall yellowish brown coloration and identical basidiospores, but differs in its mostly smaller size, different texture of pileus surface, slightly different color of hymenophore, and thinner-walled hyphal extremities at the pileus surface. Additionally, these two species are phylogenetically distinct (Fig. 1).

Cantharellus densilamellatus Buyck & V. Hofst., sp. nov.

MycoBank MB 828893
Figs 9, 10

Diagnosis. *Cantharellus densilamellatus* resembles *C. densifolius* in its overall yellowish to orange-brown color, but differs in its thinner and comparatively well-developed gill folds with less blunt edges, smaller size, nearly thin-walled, less undulate hyphal extremities at the pileus surface, more elongate basidiospores, and its seasonal woodland habitat.

Gene sequences ex-holotype. JX193014 (published in Buyck et al. 2014).

Etymology. "densilamellatus"; referring to the relatively close spacing of the gill folds.

Holotype. TANZANIA. Msanga village, in very degraded woodland with *Brachystegia*, 24 April 1998, Buyck 98.013 (PC0084126). MycoBank MBT 828893.

Description. *Basidiomata* small to medium-sized. *Pileus* up to 60 mm diam., first centrally depressed and with a downturned margin, then becoming more depressed as the margin spreads out, fleshy in the center, but increasingly thin fleshed toward the margin and there often striate or radially splitting; margin regular to slightly wavy-lobed; surface dry, with a pale to dark brown to reddish brown tomentum (5DEF6–8) contiguous over disc, toward margin tomentum separating concentrically into a pale yellowish cream (3A2–3) areolate pattern. *Hymenophore* composed of thin, well-developed gill folds, 2–3 mm high, densely spaced (> 10/cm) but not crowded, forking, not anastomosing, often splitting transversely through their entire height, uniformly pale yellow (3A4), brighter than the pileus margin and stipe. *Stipe* central, up to 40 mm long, 6–11 mm wide, subcylindrical to slightly wider near the base, rapidly elongating before the pileus margin starts to spread, concolorous with the pileus margin, distinctly finely squamulose over apical portion, compact in section. *Context* off-white to pale cream, weakly yellowing. *Odor* fruity. *Taste* mild. *Spore print* off-white to very pale yellowish.

Figure 9. *Cantharellus densilamellatus* (holotypus, Buyck 98.013). Aspect of fresh specimens. Photo: B. Buyck.

Basidiospores narrowly ellipsoid to almost elongate, often reniform or peanut shaped, 6.7–7.05–7.4(–7.9) × (3.3–)3.4–3.65–3.9(–4.0) µm, Q = (1.7–)1.8–1.94–2.1(–2.3), smooth. *Basidia* rather short, 35–50(–58) × 6–7 µm, (4–)5–6-spored; basidioles mostly clavate. *Cystidia* none. *Subhymenium* pseudoparenchymatous, composed of irregular, slightly inflated cells. *Pileipellis* a cutis of interwoven hyphal extremities forming slender chains of subcylindrical cells, these quite regular in outline, with thin to very slightly thickened and refringent walls; terminal cells (25–)30–45(–65) × (3–)4–7 µm, subcylindrical or sometimes very slightly inflated in the lower or middle portion, obtusely rounded at the tip or slightly constricted subapically. *Clamp connections* absent.

Discussion. *Cantharellus densifolius* has long been the only available name for yellowish brown, clampless chanterelles in Africa with a squamulose pileus and crowded gill folds. Indeed, the holotype collection of *C. densilamellatus* reported here was initially identified as *C. densifolius* in Buyck et al. (2000) and, in the absence of any reliable concept for Heinemann's species, was even maintained as *C. densifolius* in the multigene *Cantharellus* phylogeny of Buyck et al. (2014). Although more than one woodland species might have been referred to as '*C. densifolius*', *C. densilamellatus* as described here is undoubtedly one of the more common and widespread inhabitants of the Zambezian miombo woodlands. It differs from the true *C. densifolius* not only in its habitat preference, but also in its more elongated basidiospores, which are very similar to those of *C. tomentosus* Eyssart. & Buyck (another, but much less common,

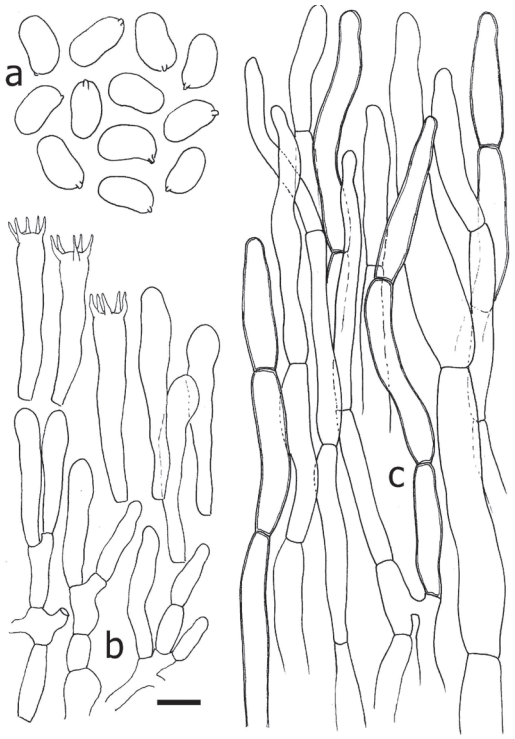

Figure 10. *Cantharellus densilamellatus* (holotypus, Buyck 98.013). Microscopic features: **a** basidiospores **b** basidia and basidiola **c** thin-walled to slightly refringent hyphal extremities of the pileipellis. Scale bar: 10 µm but only 5 µm for basidiospores. Drawings: B. Buyck.

woodland species with crowded gills and much darker pileus surface and hymenophore – see Buyck 1994 [as 'nyarympu', its Kirundi vernacular name] and Buyck et al. 2000). *Cantharellus densilamellatus* further differs micromorphologically from *C. densifolius* in its more regular, less undulate and thinner-walled hyphal extremities of the pileus surface (Fig. 10). While the phylogenetic analysis presented here (Fig. 1) shows a close relationship of *C. densilamellatus* with *C. luteopunctatus*, the latter species differs in its pinkish, erect squamae, bright yellow pileus color, and initially white and strongly anastomosing gill folds.

Conclusion

Phylogenetic analysis including the newly obtained sequence data demonstrated that *C. densifolius* and *C. luteopunctatus*, here epityped, belong in the same subgenus but in different subclades. Additionally, the name *C. densifolius* has been consistently misapplied to at least one, and possibly several, similar taxa from the African woodland area (De Kesel pers. comm., Buyck 1994, Buyck et al. 2000, Härkönen et al. 2015). One of

these woodland species described here, *C. densilamellatus*, is very different morphologically from, but phylogenetically sister to, *C. luteopunctatus*. *Cantharellus tomentosoides* is a new species that is morphologically similar to, but phylogenetically distinct from, *C. densifolius* and is from the same local habitat in the *G. dewevrei* rain forest. These results, along with the continuing discovery of new, morphologically unique African chanterelles, emphasize the importance of Africa as a global diversity hotspot for *Cantharellus* (Buyck 2016, De Kesel et al. 2016, Buyck et al. 2017).

Acknowledgements

B. Buyck thanks the ATM of the Paris' Museum and "l'Institut Ecologie et Environnement" (CNRS-INEE) for funding the field trip with Shelly Masi to Africa; Shelly is thanked for all the practical help and sharing her experience. Terence Fuh and the staff of the Primate Habituation Programme of the Dzanga-Ndoki National Park, Réserve Spéciale de Foret Dense de Dzanga-Sangha at Bayanga, as well as all staff, Aka guides and visitors of the Bai Hokou field station for their logistical support, field assistance and their very enjoyable company during our stay. This research was made possible through research permit 034/MENESR/DIRCAB/DGESRSTI/DRSTSPI/SSSTI/16 from the "Ministère de l'éducation nationale, de l'enseignement supérieur et de la recherche scientifique" of the Central African Republic. Funding was provided to T.W. Henkel by National Geographic Society's Committee for Research and Exploration grant 9235-13 and National Science Foundation grant DEB-1556338. In Cameroon the Ministry of Research and Scientific Innovation issued research permits. The Conservator of the Dja Biosphere Reserve, Mr. Ndinga Hilaire, and his staff greatly assisted the fieldwork in the Dja. Congo Basin Institute staff provided much logistical support. Field assistance in Cameroon was provided by Mei Lin Chin, Todd Elliott, Camille Truong, Bryn Dentinger, Cathie Aime, Rachel Koch, Blaise Jumbam, Olivier Séné, Carolyn Delevich, Kennan Mighell, Jessie Uehling, Noah Siegel, Alamane Gabriel (a.k.a. Sikiro), and Essambe Jean-Pierre (a.k.a. Papa Chef). The first author thanks the Curator of the Herbarium (BR) of the Botanic Garden Meise, Belgium, for permission to reproduce the original watercolors by Mme. Goossens-Fontana.

References

Alfaro M, Zoller S, Lutzoni F (2003) Bayes or bootstrap? A simulation study comparing the performance of Bayesian Markov chain Monte Carlo sampling and bootstrapping inassessing phylogenetic confidence. Molecular Biology and Evolution 20: 255–266. https://doi.org/10.1093/molbev/msg028

Ariyawansa HA, Hyde KD, Jayasiri SC, Buyck B, Chethana, KWT, Dai DQ, Dai YC, Daranagama DA, Jayawardena RS, Lücking R, Ghobad-Nejhad M, Niskanen T, Thambugala KM, Voigt K, Zhao RL, Li GJ, Doilom M, Boonmee S, Yang ZL, Cai Q, Cui

YY, Bahkali AH, Chen J, Cui BK, Chen JJ, Dayarathne MC, Dissanayake AJ, Ekanayaka AH, Hashimoto A, Hongsanan S, Jones EBG, Larsson E, Li WJ, Li QR, Liu JK, Luo ZL, Maharachchikumbura SSN, Mapook A, McKenzie EHC, Norphanphoun C, Konta S, Pang KL, Perera RH, Phookamsak R, Phukhamsakda C, Pinruan U, Randrianjohany E, Singtripop C, Tanaka K, Tian CM, Tibpromma S, Abdel-Wahab MA, Wanasinghe DN, Wijayawardene NN, Zhang JF, Zhang H, Abdel-Aziz FA, Wedin M, Westberg M, Ammirati JF, Bulgakov TS, Lima DX, Callaghan TM, Callac P, Chang CH, Coca LF, Dal-Forno M, Dollhofer V, Fliegerová K, Greiner K, Griffith GW, Ho HM, Hofstetter V, Jeewon R, Kang JC, Wen TC, Kirk PM, Kytövuori I, Lawrey JD, Xing J, Li H, Liu ZY, Liu XZ, Liimatainen K, Lumbsch HT, Matsumura M, Moncada B, Nuankaew S, Parnmen S, Santiago A, Sommai S, Song Y, Souza CAF, Souza-Motta CM, Su HY, Suetrong S, Wang Y, Wei SF, Yuan HS, Zhou LW, Réblová M, Fournier J, Camporesi E, Luangsaard JJ, Tasanathai K, Khonsanit A, Thanakitpipattana D, Somrithipol S, Diederich P, Millanes AM, Common RS, Stadler M, Yan JY, Li XH, Eberhardt U, Simonini G, Wen HA, Chen XH (2015) Fungal diversity notes 111–252 : taxonomic and phylogenetic contributions to fungal taxa. Fungal Diversity 75: 27–274. https://doi.org/10.1007/s13225-015-0346-5

Buyck B (1994) Ubwoba: les champignons comestibles de l'ouest du Burundi. Publications Agricoles 34: 1–123, Admin Gén Coop Dévelopm., Bruxelles.

Buyck B (2016) Special Issue: *Cantharellus*. Editorial: Towards completing the world inventory of *Cantharellus*. Cryptogamie Mycologie 37: 255−258. https://doi.org/10.7872/crym/v37.iss3.2016.255

Buyck B, Eyssartier G, Kivaisi A (2000) Addition to the inventory of the genus *Cantharellus* (Basidiomycotina, Cantharellaceae) in Tanzania. Nova Hedwigia 71: 491–502.

Buyck B, Kauff F, Cruaud C, Hofstetter V (2013) Molecular evidence for novel *Cantharellus* (Cantharellales Basidiomycota) from tropical African miombo woodland and a key to all tropical African chanterelles. Fungal Diversity 58: 281–298. https://doi.org/10.1007/s13225-012-0215-4

Buyck B, Kauff F, Eyssartier G, Couloux A, Hofstetter V (2014) A multilocus phylogeny for worldwide *Cantharellus* (Cantharellales Agaricomycetidae). Fungal Diversity 64: 101–121. https://doi.org/10.1007/s13225-013-0272-3

Buyck B, Kauff F, Randrianjohany E, Hofstetter V (2015) Sequence data reveal a high diversity of *Cantharellus* associated with endemic vegetation in Madagascar. Fungal Diversity 70: 189–208. https://doi.org/10.1007/s13225-014-0314-5

Buyck B, De Crop E, Verbeken A, Hofstetter V (2016a) Untangling the Central African *Cantharellus* sect. *Tenues*: *Cantharellus minutissimus* sp.nov. and epitypification of *Cantharellus alboroseus*. Cryptogamie Mycologie 37: 329–343. https://doi.org/10.7872/crym/v37.iss3.2016.329

Buyck B, Henkel TW, Dentinger BTM, Séné O, Hofstetter V (2016b) Multigene sequencing provides a suitable epitype barcode sequences and a precise systematic position for the enigmatic African *Cantharellus miniatescens*. Cryptogamie Mycologie 37: 269–282. https://doi.org/10.7872/crym/v37.iss3.2016.269

Buyck B, Hofstetter V, Olariaga I (2016c) Setting the record straight on North American *Cantharellus*. Cryptogamie Mycologie 37: 405–417. https://doi.org/10.7872/crym/v37.iss3.2016.405

Buyck B, Moreau P-A, Courtecuisse R, Kong A, Roy M, Hofstetter V (2016d) *Cantharellus coccolobae* sp. nov. and *Cantharellus garnieri* two tropical members of *Cantharellus* subg. *Cinnabarinus*. Cryptogamie Mycologie 37: 391–403. https://doi.org/10.7872/crym/v37.iss3.2016.391

Buyck B, Olariaga I, Justice J, Lewis DP, Roody W, Hofstetter V (2016e) The dilemma of species recognition in the field when sequence data are not in phase with phenotypic variability. Cryptogamie Mycologie 37: 367–389. https://doi.org/10.7872/crym/v37.iss3.2016.367

Buyck B, Olariaga I, Looney B, Justice J, Hofstetter V (2016f) Wisconsin chanterelles revisited and first indications for very wide distributions of *Cantharellus* species in the United States East of the Rocky Mountains. Cryptogamie Mycologie 37: 345–366. https://doi.org/10.7872/crym/v37.iss3.2016.345

Buyck B, Randrianjohany E, Hofstetter V (2016g) Almost one century later… *Cantharellus avellaneus* finally rediscovered! Cryptogamie Mycologie 37: 259–268. https://doi.org/10.7872/crym/v37.iss3.2016.259

Buyck B, Duhem B, Das K, Jayawardena RS, Niveiro N, Pereira OL, Prasher IB, Adhikari S, Albertó EO, Bulgakov TS, Castañeda-Ruiz RF, Hembrom ME, Hyde KD, Lewis DP, Michlig A, Nuytinck J, Parihar A, Popoff OF, Ramirez NA, da Silva M, Verma RK, Hofstetter V (2017) Fungal Biodiversity Profiles 21–30. Cryptogamie Mycologie 38: 101–146. https://doi.org/10.7872/crym/v38.iss1.2017.101

Buyck B, Hofstetter V (2018) *Cantharellus* subgenus *Pseudocantharellus* revisited. Mycosphere 91: 141–148. https://doi.org/10.5943/mycosphere/9/1/3

Das K, Rossi W, Leonard M, Ghosh A, Bera I, Hembrom ME, Bajpai R, Joseph S, Nayaka S, Upreti DK, Wang XH, Hofstetter V, Buyck B (2018) Fungal Biodiversity Profiles 61–70. Cryptogamie Mycologie 39: 381–418. https://doi.org/10.7872/crym/v39.iss4.2018.381

De Kesel A, Amalfi M, Kasongo B, Yorou NS, Raspe O, Degreef J, Buyck B (2016) New and interesting *Cantharellus* from tropical Africa. Cryptogamie Mycologie 37: 283–327. https://doi.org/10.7872/crym/v37.iss3.2016.283

Eyi N'dong HE, Degreef J, De Kesel A (2011) Champignons comestibles des forets denses d'Afrique Centrale. Taxonomie et identification. ABC Taxa 10, 253 pp.

Eyssartier G (2001) Vers une monographie du genre *Cantharellus* Adans.: Fr. Dissertation, National Natural History Museum Paris, 259 pp.

Guindon S, Gascuel O (2003) A simple, fast, and accurate algorithm to estimate large phylogenies by maximum likelihood. Systematic Biology 52: 696–704. https://doi.org/10.1080/10635150390235520

Härkönen M, Niemelä T, Mbindo K, Kotiranta H, Piearce G (2015) Zambian mushrooms and mycology. Norrlinia 29: 1–208. Finnish Museum of Natural History, Helsinki, pl. 1–276.

Heinemann P (1958) Champignons récoltés au Congo Belge par Madame Goossens-Fontana. III. Cantharellineae. Bulletin du jardin botanique de l'État Bruxelles 28: 385–438. https://doi.org/10.2307/3667153

Heinemann P (1959) Cantharellineae. Flore iconographique des champignons du Congo 8: 153–165. [pl. 26–28]

Heinemann P (1966) Cantharellineae du Katanga. Bulletin du jardin botanique de l'État Bruxelles 36: 365–352. https://doi.org/10.2307/3667194

Kornerup A, Wanscher JH (1978) Methuen handbook of colour. 3rd ed. Methuen & Co. Ltd., London, 252 pp.

Liu JK, Hyde KD, Jones EBG, Ariyawansa HA, Bhat DJ, Boonmee S, Maharachchikumbura SSN, McKenzie EHC, Phookamsak R, Phukhamsakda C, Shenoy BD, Abdel-Wahab MA, Buyck B, Chen J, Chethana KWT, Singtripop C, Dai DQ, Dai YC, Daranagama DA, Dissanayake AJ, Doliom M, D'souza MJ, Fan XL, Goonasekara ID, Hirayama K, Hongsanan S, Jayasiri SC, Jayawardena RS, Karunarathna SC, Li WJ, Mapook A, Norphanphoun C, Pang KL, Perera RH, Peršoh D, Pinruan U, Senanayake IC, Somrithipol S, Suetrong S, Tanaka K, Thambugala KM, Tian Q, Tibpromma S, Udayanga D, Wijayawardene NN, Wanasinghe D, Wisitrassameewong K, Zeng XY, Abdel-Aziz FA, Adamčík S, Bahkali AH, Boonyuen N, Bulgakov T, Callac P, Chomnunti P, Greiner K, Hashimoto A, Hofstetter V, Kang JC, Lewis DP, Li XH, Liu ZY, Liu ZY, Matumura M, Mortimer PE, Rambold R, Randrianjohany E, Sato G, Indrasutdhi VS, Tian CM, Verbeken A, Brackel W, Wang Y, Wen TC, Xu JC, Yan JY, Zhao RL, Camporesi E (2015) Fungal Diversity Notes 1–100: Taxonomic and phylogenetic contributions to fungal species. Fungal Diversity 72: 1–197. https://doi.org/10.1007/s13225-015-0324-y

Maddison DR, Maddison WP (2002) MacClade: Analysis of Phylogeny and Character Evolution, version 4.05. Sinauer Associates Inc., Sunderland, Massachusetts, USA.

Mason-Gamer RJ, Kellogg EA (1996) Testing for phylogenetic conflict among molecular data sets in the tribe Triticeae (Gramineae). Systematic Biology 54: 524–545. https://doi.org/10.1093/sysbio/45.4.524

Moncalvo J-M, Nilsson RH, Koster B, Bernauer T, Matheny PB, Porter TM, Margaritescu S, Weiss M, Garnica S, Danell E, Langer G, Langer E, Larsson E, Larsson K-H, Vilgalys R (2006) The cantharelloid clade: dealing with incongruent gene trees and phylogenetic reconstruction methods. Mycologia 98: 937–948. https://doi.org/10.1080/15572536.2006.11832623

Olariaga I, Buyck B, Esteve-Raventos F, Hofstetter V, Manjon JL, Moreno G, Salcedo I (2015) Assessing the taxonomic identity of white and orange specimens of *Cantharellus*: occasional colour variants or independent species? Cryptogamie Mycologie 36: 287–300. https://doi.org/10.7872/crym/v36.iss3.2015.287

Olariaga I, Moreno G, Manjón J-L, Salcedo I, Rodriguez D, Hofstetter V, Buyck B (2016) *Cantharellus* (Cantharellales, Basidiomycota) revisited in Europe through a multigene phylogeny. Fungal Diversity 83: 263–292. https://doi.org/10.1007/s13225-016-0376-7

Schoch CL, Seifert KA, Huhndorf S, Robert V, Spouge JL, Levesque CA, Chen W, and the Fungal Barcoding Consortium (2012) Nuclear ribosomal internal transcribed spacer (ITS) region as a universal DNA barcode marker for *Fungi*. Proceedings of the National Academy of Sciences 109: 6241–6246. https://doi.org/10.1073/pnas.1117018109

MycoKeys 49: 73–97 (2019)
doi: 10.3897/mycokeys.49.33185
http://mycokeys.pensoft.net

RESEARCH ARTICLE

A peer-reviewed open-access journal
MycoKeys
Launched to accelerate biodiversity research

Neoboletus antillanus sp. nov. (Boletaceae), first report of a red-pored bolete from the Dominican Republic and insights on the genus *Neoboletus*

Matteo Gelardi[1], Claudio Angelini[2,3], Federica Costanzo[1], Francesco Dovana[4], Beatriz Ortiz-Santana[5], Alfredo Vizzini[4]

1 *Via Angelo Custode 4A, I-00061 Anguillara Sabazia, RM, Italy* **2** *Via Cappuccini 78/8, I-33170 Pordenone, Italy* **3** *National Botanical Garden of Santo Domingo, Santo Domingo, Dominican Republic* **4** *Department of Life Sciences and Systems Biology, University of Turin, Viale P.A. Mattioli 25, I-10125 Torino, Italy* **5** *US Forest Service, Northern Research Station, Center for Forest Mycology Research, One Gifford Pinchot Drive, Madison, Wisconsin 53726, USA*

Corresponding author: *Alfredo Vizzini* (alfredo.vizzini@unito.it)

Academic editor: *M.P. Martín* | Received 18 January 2019 | Accepted 12 March 2019 | Published 29 March 2019

Citation: Gelardi M, Angelini C, Costanzo F, Dovana F, Ortiz-Santana B, Vizzini A (2019) *Neoboletus antillanus* sp. nov. (Boletaceae), first report of a red-pored bolete from the Dominican Republic and insights on the genus *Neoboletus*. MycoKeys 49: 73–97. https://doi.org/10.3897/mycokeys.49.33185

Abstract

Neoboletus antillanus **sp. nov.** appears to be the only red-pored bolete known from the Dominican Republic to date. It is reported as a novel species to science based on collections gathered in a neotropical lowland mixed broadleaved woodland. A detailed morphological description, color images of fresh basidiomes in habitat and line drawings of the main anatomical features are provided and relationships with phylogenetically and phenotypically similar taxa are discussed. Three genomic regions (nrITS, nrLSU/28S and *rpb2*) have been sequenced in order to reinforce the recognition of the new species and to elucidate its taxonomic affiliation within *Neoboletus*.

Keywords

Boletales, molecular phylogeny, Greater Antilles, neotropical boletes, *Sutorius*, taxonomy

Introduction

In recent times the intensive use of molecular tools applied to the investigation of the systematics of boletoid mushrooms and related groups (order Boletales) has dramatically revolutionized traditional classifications based on morphological traits, facilitating the research process and leading to the establishment of a novel scientific approach with unexpected taxonomic implications (Bruns and Palmer 1989, Binder 1999, Binder and Bresinsky 2002, Binder et al. 2005, Binder and Hibbett 2006, Nuhn et al. 2013, Wu et al. 2014).

In particular, members of the Boletaceae have undergone an extensive reassessment and several new genera have arisen from large, unwieldy and definitely polyphyletic assemblages such as *Boletus* Fr., *Xerocomus* Quél. and *Tylopilus* P. Karst, just to name a few (Wu et al. 2016b). Among these genera, *Neoboletus* Gelardi, Simonini & Vizzini has recently been segregated from *Boletus* s.l. (Vizzini 2014), to include taxa orbiting around the generic type *Boletus luridiformis* Rostk. that were traditionally assigned to either the polyphyletic *Boletus* sect. *Luridi* Fr. emend. Lannoy & Estadès (Lannoy and Estadès 2001), *Boletus* sect. *Erythropodes* Galli pro parte (Galli 2007) or *Boletus* subg. *Luridellus* sect. *Immutabiles* and sect. *Luridiformes* pro parte (nom. inval., art. 39.1) (Watling and Hills 2005). Species included in *Neoboletus* are characterized by boletoid to rarely secotioid habit, tomentose to velvety pileus, yellow-olive tubes, brownish, red to orange or more rarely yellow pores, stipe surface usually finely dotted-punctate, yellowish context, tissues quickly and intensely bluing on handling or exposure, mild taste, olive-brown spore print, ellipsoid-fusiform, smooth basidiospores, trichodermal pileipellis consisting of filamentous hyphae, hymenophoral trama of the "*Boletus*-type", fertile caulohymenium, inamyloid hyphae in the stipe trama, gymnocarpic ontogenetic development and ectomycorrhizal (ECM) association with members of the Pinaceae and Fagaceae (Vizzini 2014, Simonini and Vizzini 2015, Bessette et al. 2016, Wu et al. 2016a). The separation of *Neoboletus* from *Boletus* s. str. and its establishment at the generic rank is phylogenetically strongly supported (Binder and Hibbett 2006, Mello et al. 2006, Halling et al. 2007, 2015; Desjardin et al. 2009, Li et al. 2011, Zeng et al. 2012, Gelardi et al. 2013, 2015; Nuhn et al. 2013, Trappe et al. 2013, Arora and Frank 2014, Vizzini et al. 2014, Wu et al. 2014, Zhao et al. 2014, 2015; Zhu et al. 2014, Chakraborty et al. 2015, Simonini and Vizzini 2015, Smith et al. 2015, Urban and Klofac 2015, Henkel et al. 2016, Liang et al. 2016, Orihara and Smith 2017), the genus being tentatively placed in the "Pulveroboletus group" (Wu et al. 2014), although its taxonomic placement within the Boletaceae still remains uncertain (Nuhn et al. 2013, Wu et al. 2014).

In contrast to the well-known bolete heritage of North America, Europe and to a lesser degree East Asia, the diversity of the fleshy pored mushrooms in the neotropical forests of Central America and adjacent regions have received only relatively limited attention (e.g. Dennis 1970, Singer et al. 1983, 1990, 1991, 1992; Gómez and Singer 1984, Singer and Gómez 1984, Halling 1989, 1997; Gómez 1997, Halling et al. 1999, 2004, 2008, 2012a, b; Flores Arzù and Simonini 2000, Franco-Molano et al. 2000, Halling and Mueller 2002, 2003, 2005; Mata et al. 2003, Mueller et al. 2006, Halling and Ortiz-Santana

2009, Flores Arzù et al. 2012, García-Jiménez 2013, although there are many others). Particularly the Caribbean appear to be little explored from the mycological perspective; information is generally widely dispersed and members of the Boletales (including also lamellate and sequestrate representatives) have only sporadically been reported over the past two centuries (Berkeley and Curtis 1869, Hitchcock 1898, Patouillard 1900 1902; Murrill 1910, 1918, 1921; Baker and Dale 1951, Dennis 1970, Kreisel 1971, Singer and Fiard 1976, Reid 1977, Hosford and Trappe 1980, Alphonse 1981, Pegler 1983, 1987; Miller et al. 2000, Guzmán et al. 2004, Camino Vilaró et al. 2006, Ortiz-Santana 2006, Courtecuisse and Welti 2013, Lécuru and Courtecuisse 2013, Moreau et al. 2013). In the Dominican Republic (Hispaniola), as far as the boletoid fungi are concerned and aside from the recent settlement of the genus *Phylloporopsis* Angelini et al. based on *Phylloporus boletinoides* A.H. Smith & Thiers (Farid et al. 2018) and a few other reports of boletes annotated in general publications (Minter et al. 2001, Lodge et al. 2001), the monographic treatment of Ortiz-Santana et al. (2007) currently remains the sole and as yet most comprehensive taxonomic account dealing with the Boletaceae and Suillaceae for this country.

Neoboletus antillanus is described herein as a new species to science using morphological and three-loci (nrITS, nrLSU/28S and *rpb2*) molecular data, based on multiple collections from a lowland mixed woodland consisting of a number of different neotropical broadleaved trees, in purported ECM association with the widespread, natively sand-growing littoral seagrape, *Coccoloba uvifera* (L.) L. (Polygonaceae), a small woody plant naturally distributed throughout the Caribbean basin (Séne et al. 2015, 2018). This notable species appears to be the first and sole red-pored bolete recorded in the Dominican Republic so far and one of the very few ECM members of the Boletaceae to be found in local lowland deciduous forested ecosystem.

The present paper is one in a series of intended contributions devoted to the study of neotropical Boletales, aiming to provide new insights into the taxonomy, phylogenetic relationships, plant and substrate associations, ecological importance, conservation and biogeographic patterns of the bolete communities occurring in the Dominican Republic, with continued biodiversity investigations of underexplored areas.

Materials and methods

Collection site and sampling

Specimens examined were collected in a hilly forest near the cemetery of Sousa, in Puerto Plata Province, Dominican Republic, and are deposited in the Herbarium of Jardín Botánico Nacional of Santo Domingo, Dr. Rafael Ma. Moscoso (JBSD) (acronym from Thiers 2019), while "ANGE" and "MG" refer to the personal herbarium of Claudio Angelini and Matteo Gelardi, respectively. Herbarium numbers are cited for all collections from which morphological features were examined. Author citations follow the Index Fungorum, Authors of Fungal Names (www.indexfungorum.org/authorsoffungalnames.htm).

Morphological studies

Macroscopic descriptions and ecological information, such as habitat notations, time of fruiting and associated plant communities accompanied the detailed field notes of the fresh basidiomata. Color terms in capital letters (e.g. Myrtle Green, pl. VIII) are from Ridgway (1912). Photographs of collections were taken in the natural habitat using a Nikon Coolpix 8400 digital camera. Microscopic anatomical features were observed and recorded from revived dried material; sections were rehydrated either in water, 5% potassium hydroxide (KOH) or in anionic solution saturated with Congo red. All anatomical structures were observed and measured from preparations in anionic Congo red. Colors and pigments were described after examination in water and 5% KOH. Measurements were made at 1000× using a calibrated ocular micrometer (Nikon Eclipse E200 optical light microscope). Basidiospores were measured directly from the hymenophore of mature basidiomes, dimensions are given as (minimum) average ± standard deviation (maximum), Q = length/width ratio with the extreme values in parentheses, Qm = average quotient (length/width ratio) ± standard deviation and average spore volume was approximated as a rotation ellipsoid [V = (π.L.W2)/6 ± standard deviation]. The notation [n/m/p] indicates that measurements were made on "n" randomly selected basidiospores from "m" basidiomes of "p" collections. The width of each basidium was measured at the widest part, and the length was measured from the apex (sterigmata excluded) to the basal septum. Metachromatic, cyanophilic and iodine reactions were tested by staining the basidiospores in Brilliant Cresyl blue, Cotton blue and Melzer's reagent, respectively. Line drawings of microstructures were traced in free-hand based on digital photomicrographs of rehydrated material.

DNA extraction, PCR amplification and DNA sequencing

Genomic DNA was isolated from 10 mg of four dried herbarium specimen (Table 1), by using the DNeasy PlantMini Kit (Qiagen, Milan Italy) according to the manufacturer's instructions. PCR amplifications were performed with the primers ITS1F/ITS4 for the nrITS region (White et al. 1990, Gardes and Bruns 1993), LR0R and LR5 for the nrLSU region (Vilgalys and Hester 1990) and the reverse complement of bRPB2-6R2 (Matheny et al. 2007) and bRPB2-7.1R2 (5'– CC-CATNGCYTGYTTVCCCATDGC –3') or RPB2-B-F1 and RPB2-B-R (Wu et al. 2014) for partial *rpb2*. Amplification reactions were performed in a PE9700thermal cycler (Perkin-Elmer, Applied Biosystems) following Vizzini et al. (2015). The PCR products were purified with the AMPure XP kit (Beckman Coulter) and sequenced by MACROGEN Inc. (Seoul, Republic of Korea). The sequences were submitted to GenBank (http://www.ncbi.nlm.nih.gov/genbank/) and their accession numbers are reported in Table 1.

Table 1. Samples sequenced for the present study.

Species	GenBank acc. number			Source, date and country
	nrITS	nrLSU (28S)	*rpb2*	
Neoboletus antillanus	MK388290	MK388302	MK488082	JBSD127417 (holotype), 14/12/2014, Dominican Republic
Neoboletus antillanus	MK388291	MK388302	–	JBSD127416, 03/12/2013, Dominican Republic
Neoboletus antillanus	MK388292	–	–	JBSD127418, 01/12/2017, Dominican Republic
Boletus brunneopanoides	MK388293	MK512677	–	BOS 389 (CFMR, holotype), 21/10/2002, Belize

Sequence alignment, data set assembly and phylogenetic analyses

The sequences obtained in this study were checked and assembled using Geneious v. R 11.1.4 (Kearse et al. 2012) and compared to those available in GenBank database (https://www.ncbi.nlm.nih.gov/genbank/) by using the BLASTN algorithm (Altschul et al. 1990). A general combined Maximum likelihood tree including all the Boletaceae sequences present in GenBank and UNITE (http://unite.ut.ee/) databases was generated to detect the phylogenetic position of our collections in the major clades of Boletaceae as circumscribed by Wu et al. (2014) (tree not shown). Consequently, phylogenetic analyses were restricted to the major clade including *Neoboletus* sequences (*Pulveroboletus* group, Fig. 1).

Our datasets consist of sequences of *Neoboletus* and other sequences with greatest similarity available in GenBank selected based on BLASTN search and previous molecular studies including *Neoboletus* collections (Wu et al. 2014, 2016a, b; Smith et al. 2015; Urban and Klofac 2015).

Sequences were aligned with MAFFT v. 7.017 (Katoh et al. 2002) and then manually adjusted using Geneious v. R 11.1.4 (Kearse et al. 2012). Two phylogenetic analyses were performed: the first phylogenetic analysis, based on a combined nrLSU/*rpb1*/*rpb2* dataset, was focused on the intergeneric position of the new species in the *Pulveroboletus* group of the Boletaceae, as delimited by Wu et al. (2014). According to the results by Wu et al. (2014), *Zangia erythrocephala* was chosen as outgroup taxon for the three-loci combined dataset. The second phylogenetic analysis based only on a nrITS sequence dataset was restricted to the taxa closely related to the new species (genus *Neoboletus*). *Costatisporus cyanescens* was used as outgroup taxon for this dataset following Smith et al. (2015).

The GTRGAMMA model of sequence evolution was selected for both analyses. The two phylogenetic analyses were inferred with three partitions: nrLSU(28S)/*rpb1*/*rpb2* and ITS1/5.8S/ITS2, respectively. The datasets were analyzed using Bayesian inference (BI) and Maximum likelihood (ML) criteria. The BI was performed with MrBayes v.3.2 (Ronquist et al. 2012) with four incrementally heated simultaneous Monte Carlo Markov Chains (MCMC) run for 10 million generations, under the selected evolutionary model. Trees were sampled every 1000 generations, resulting in overall

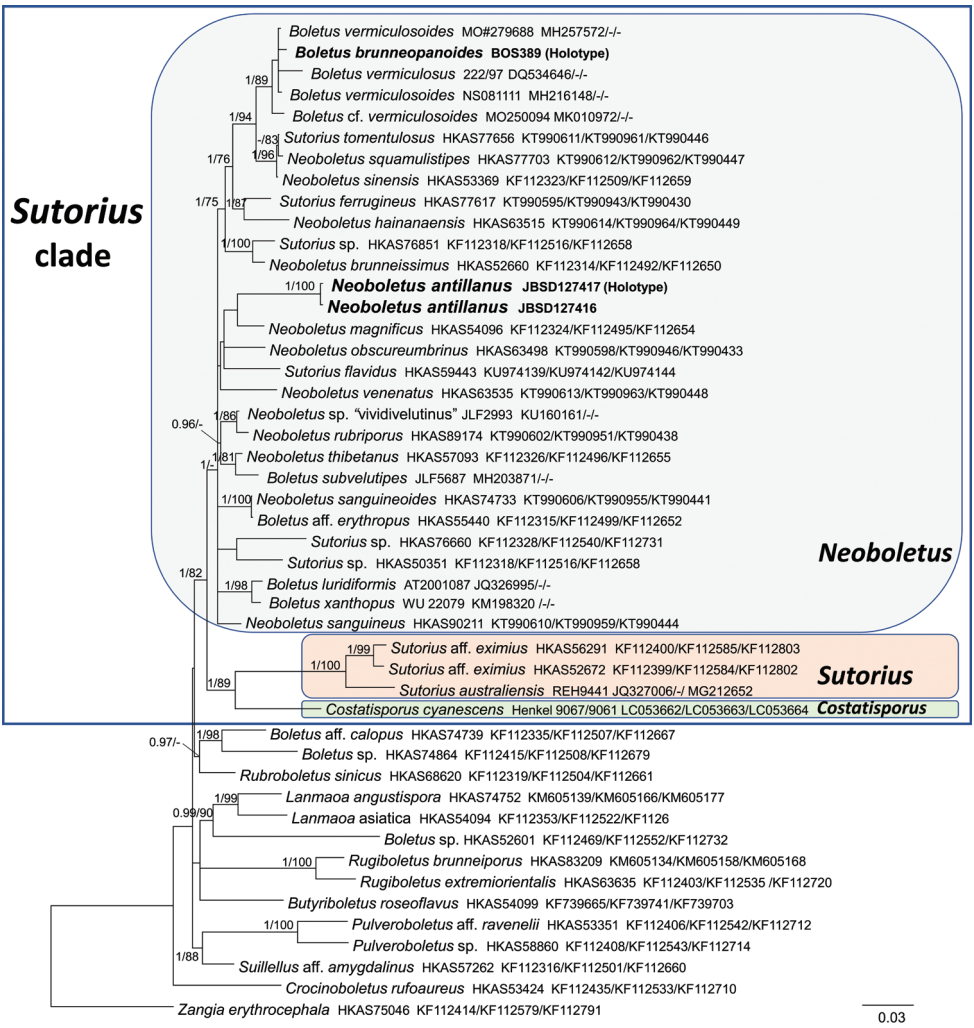

Figure 1. Phylogeny of the *Pulveroboletus* group based on a Bayesian and Maximum-likelihood inference analysis of a matrix of concatenated sequences from three nuclear gene regions (nrLSU/28S, *rpb1* and *rpb2*). *Zangia erythrocephala* was used as outgroup taxon. Values for clades that are supported in either the Bayesian (posterior probabilities, BPP) and Maximum likelihood (ML bootstrap percentage, MLB) analyses are indicated. BPP ≥ 0.95 and MLB ≥ 70% are given above clade branches. Newly sequenced collections are boldfaced in black. For each collection, the specific epithet (as present in GenBank), the herbarium code and GenBank accession numbers of the nrLSU/*rpb1*/*rpb2* sequences are reported.

sampling of 10001 trees; the first 2500 trees were discarded as "burn-in" (25 %). For the remaining trees, a majority rule consensus tree showing all compatible partitions was computed to obtain estimates for Bayesian Posterior Probabilities (BPP). The ML was performed with RAxML v.7.2.8. (Stamatakis 2006) and a total of 1000 bootstrap replicates (Felsenstein 1985) were computed to assess the relative robustness of the

branches. Only BPP values ≥ 0.95 and MLB (Maximum likelihood bootstrap) values ≥ 70 % have been reported in the phylogenetic trees (Figs 1, 2). Pairwise % identity values of the sequences were calculated using Geneious v. R 8.1.2 (Kearse et al. 2012). Alignments and phylogenetic trees are available at Tree-BASE (www.treebase.org, submission number S24011).

Results

Molecular analysis

The combined nrLSU/*rpb1*/*rpb2* data matrix (focused on the *Pulveroboletus* group) comprised 47 sequences and is 2381 bp long. The nrITS data matrix (focused on *Neoboletus*) comprised 41 sequences and is 830 bp long. As the topology and branches support values of all the analyses are consistent, only the Bayesian trees with both BPP and MLB values are shown (Figs 1, 2). In the combined analysis (Fig. 1) a major clade is recognizable (BPP = 1, MLB = 82%), here named as the *Sutorius* clade, where the two sister (BPP = 1, MLB = 89%) genera *Sutorius* and *Costatisporus* are sister (BPP = 1, MLB = 82%) to the genus *Neoboletus*. The two collections of the new species clustered together within the genus *Neoboletus* forming a strongly supported clade (BPP = 1, MLB = 100%) which is sister (with no support) to *N. magnificus*. In the nrITS analysis (Fig. 2) the three collections of the new species (*N. antillanus*) clustered together in a strongly supported clade (BPP = 1, MLB = 100%) which shows no clear phylogenetic affinities with other species. The three nrITS sequences (677 to 683 bp) and the two nrLSU sequences (840 to 857 bp) of *N. antillanus* show a pairwise % identity value of 99.7 and 100, respectively. The type specimen of *Boletus brunneopanoides* from Belize forms: i) a strongly supported clade (BPP = 1, MLB = 89%) with also two collections of *B. vermiculosoides*, one collection of *Boletus* cf. *vermiculosoides* and one of *B. vermiculosus*, in the combined analysis; ii) a strongly supported clade (BPP = 1, MLB = 100%) with also two collections of *B. vermiculosoides*, one collection of *Boletus* cf. *vermiculosoides* and one of Boletales sp. (KY826093), in the nrITS analysis.

Taxonomy

***Neoboletus antillanus* Angelini, Gelardi, Costanzo & Vizzini, sp. nov.**
Figs 3, 4
Mycobank MB829549

Etymology. the specific epithet *antillanus* (Latin) refers to the occurrence of the species in the Antilles islands of the Caribbean.

Original diagnosis. Basidiomes stipitate-pileate with tubular hymenophore characterized by medium-small size, pinkish red to reddish pileus surface, orange-red pores,

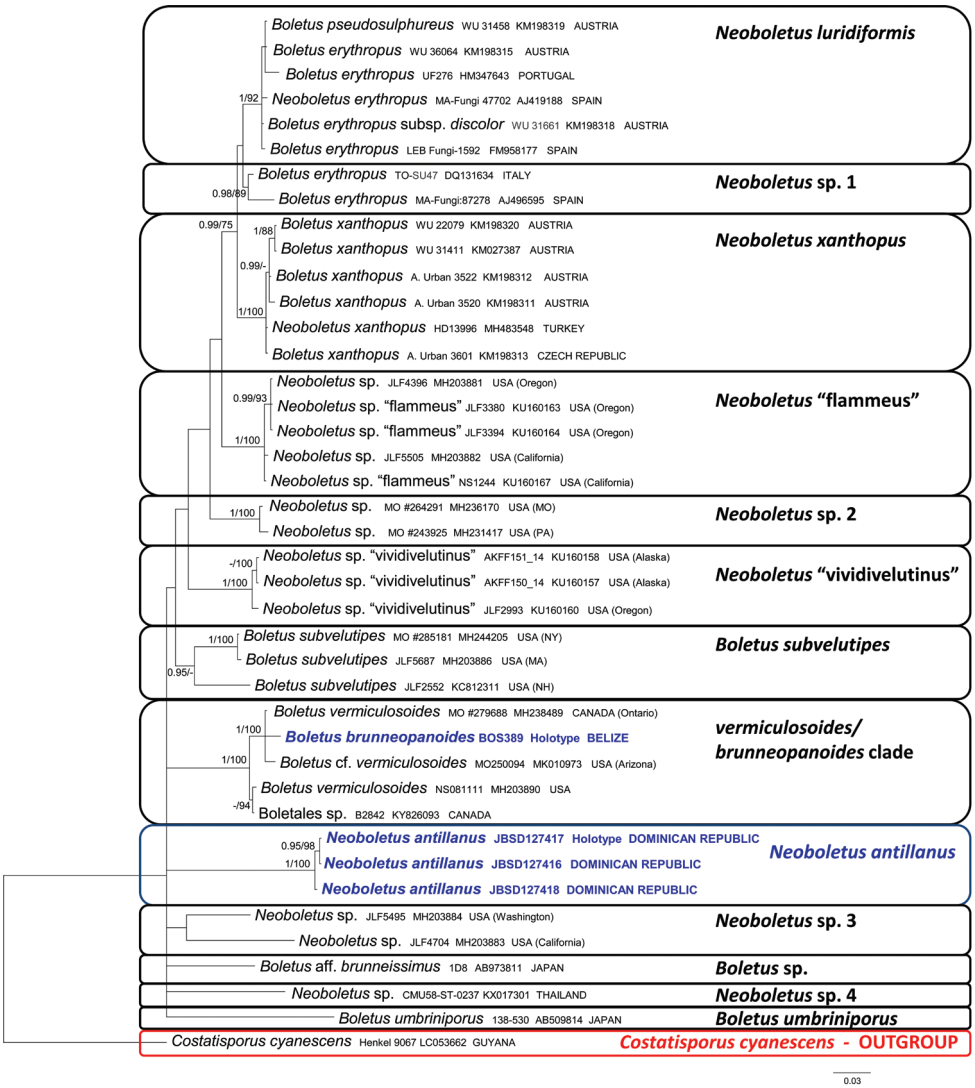

Figure 2. Bayesian phylogram obtained from the nrITS sequence alignment of *Neoboletus* species. *Costatisporus cyanescens* was used as outgroup taxon. Values for clades that are supported in either the Bayesian (posterior probabilities, BPP) and Maximum likelihood (ML bootstrap percentage, MLB) analyses are indicated. BPP ≥ 0.95 and MLB ≥ 70% are given above clade branches. Newly sequenced collections are boldfaced in blue. For each collection, the specific epithet (as present in GenBank), the herbarium code, GenBank accession number of the nrITS sequence and geographical origin (country) are reported.

reddish orange to purple-red punctuations on a yellow stipe surface, golden yellow strigosity at the stipe base, yellow context, tissues bruising dark blue when injured or exposed, ellipsoid-fusiform, smooth basidiospores, ixocutis pileipellis consisting of gelatinized, repent filamentous hyphae and occurrence in neotropical lowland mixed

broadleaved forests in putative ECM association with host species (*Coccoloba uvifera*) other than Fagaceae and Pinaceae.

Holotypus. DOMINICAN REPUBLIC, Municipality of Sousa, Puerto Plata Province, Loc. Cemetery, 19°44'40"N, 70°32'21"W, 100 m a.s.l., 14 Dec 2014, C. Angelini (JBSD127417; *isotypus* ANGE434 and MG719).

Basidiomes medium-small (Fig. 3). *Ontogenetic development* gymnocarpic. *Pileus* (3.0) 3.5–7.5 (8.0) cm broad, at first hemispherical then persistenly convex and finally broadly pulvinate-flattened, sometimes slightly depressed at centre, regularly to hardly unevenly shaped, moderately fleshy, firm at the beginning but progressively softer with age, flabby in old basidiomes; margin steady to faintly wavy-lobed, initially involute then curved downwards, extending beyond the tubes up to 1 mm; surface matt, dry but slightly greasy with moist weather, very finely tomentose, not cracked; cuticle somewhat variable in color, ranging from wine red, dark red or reddish pink to pastel pink (Pomegranate Purple, pl. XII; Spinel Red, pl. XXVI; Pinkish Vinaceous, pl. XXVII; Carmine, Eosine Pink, Geranium Pink, Rose Doree, pl. I; Alizarine Pink, Jasper Pink, Old Rose, pl. XIII), gradually fading with age and becoming pinkish cream to pale ochraceous pink (Flesh Pink, pl. XIII; Pale Ochraceous-Salmon, Pale Ochraceous-Buff, Light Buff, Light Ochraceous-Buff, Warm Buff, pl. XV) with olive-brown to brownish shades (Dresden Brown, pl. XV; Olive Lake, pl. XVI; Light Yellowish Olive, Buffy Olive, pl. XXX) tending to progressively spread from the center towards the peripheral zone; slowly bluing (Methy Green, Sea Green, Prussian Green, pl. XIX; Motmot Blue, Capri Blue, pl. XX) on handling or when injured; subcuticular layer cream-yellowish (Citrine Yellow, pl. XVI). *Tubes* at first thin then increasingly broader and as long as or slightly longer than the thickness of the pileus context at maturity (up to 1.0 cm long), adnate but soon deeply depressed around the stipe apex, occasionally subdecurrent, bright yellow (Lemon Chrome, pl. IV) to olive-yellow (Yellowish Citrine, pl. XVI), turning blue (Prussian Green, Duck Green, Invisible Green, pl. XIX) when cut and eventually fading to drab yellowish (Aniline Yellow, Pyrite Yellow, pl. IV). *Pores* initially forming a concave then flat surface, at first small then gradually wider (up to 1 mm in diam.), simple, roundish to barely angular at maturity, at first bright orange-red to orange (Scarlet Red, Scarlet, pl. I) although concolorous with the tubes (Lemon Chrome, pl. IV) towards the margin, soon becoming yellowish orange (Flame Scarlet, Orange Chrome, pl. II) and finally yellowish olive (Yellowish Citrine, pl. XVI) with very pale orange hues (Orange, pl. III), quickly and intensely turning blue (Prussian Green, Duck Green, Invisible Green, pl. XIX) on bruising or when injured. *Stipe* (3.5) 4.0–9.0 (9.5) × (1.0) 1.5–2.0 (2.5) cm, longer than or as long as the pileus diameter at maturity, central to slightly off-center, solid, firm, dry, straight or curved, at first ventricose-fusiform, later cylindrical but either sligthly swollen towards the base to decidedly clavate or tapering downwards, not to barely rooting, evelate; surface at the apex or in the upper third usually smooth to occasionally very faintly reticulate due to the sub-decurrence of the hymenophore in some specimens and bright yellow (Lemon Chrome, pl. IV) to lemon yellow (Strontian Yellow, pl. XVI), elsewhere showing a fine, purple-red, dark red to orange-red (Indian Lake, pl. XXVI; Amaranth Purple, pl.

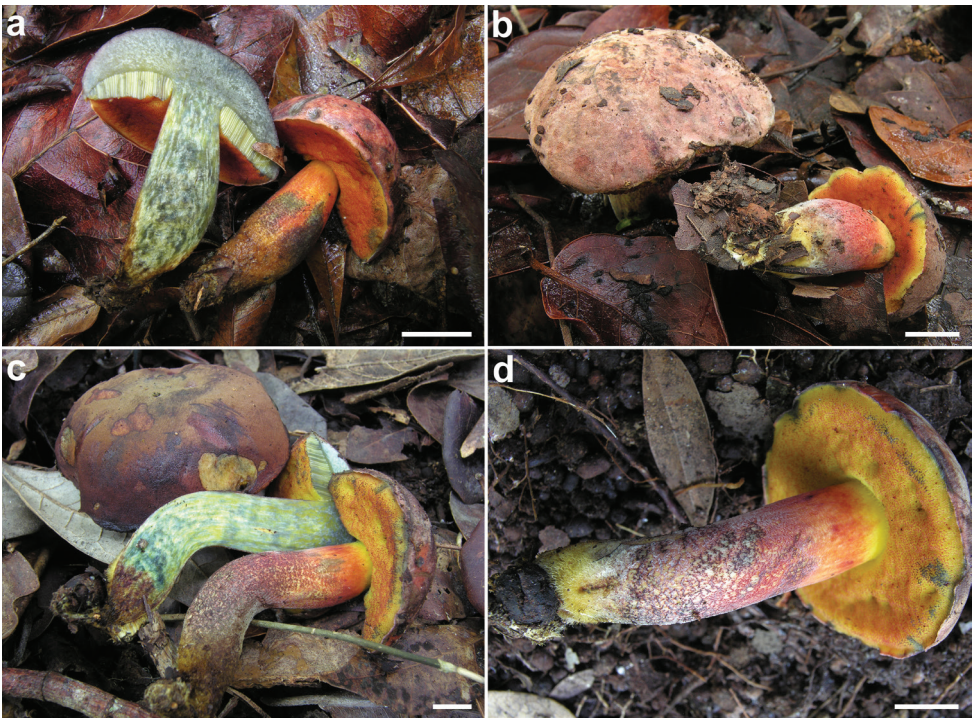

Figure 3. *Neoboletus antillanus*. Basidiomata in situ. **a** JBSD127416 **b** JBSD127417 (holotype) **c, d** JBSD127418. Scale bars: 1 cm. Photos by C. Angelini.

XII; Carmine, Scarlet Red, pl. I) punctuation (Fig. 2d) partly hiding the bright yellow (Lemon Chrome, pl. IV) ground color; the base is typically wrapped by a conspicuous golden yellow to brownish yellow strigosity (Fig. 2d) (Raw Sienna, pl. III; Yellow Ocher, pl. XV); bruising greenish blue (Light Blue Green, Blue Green, Forest Green, pl. XVII) throughout when pressed; *basal mycelium* golden yellow (Raw Sienna, pl. III; Yellow Ocher, pl. XV). *Context* firm when young, later soft textured and eventually flabby in the pileus (up to 1.0 cm thick in the central zone), a little more fibrous in the stipe, lemon yellow (Strontian Yellow, pl. XVI) throughout, usually with purple-brown (Indian Lake, pl. XXVI; Amaranth Purple, pl. XII) spots in the stipe, especially at the extreme base; turning blue (Methy Green, Sea Green, Prussian Green, pl. XIX; Motmot Blue, Capri Blue, pl. XX) more or less evenly when exposed to air and finally fading to drab yellowish (Aniline Yellow, Pyrite Yellow, pl. IV); subhymenophoral layer lemon yellow (Strontian Yellow, pl. XVI). *Odour* and *taste* not distinctive. *Spore-print* not obtained but likely olive-brown.

Basidiospores [102/5/3] (8.8) 11.1 ± 0.78 (12.7) × (4.1) 4.9 ± 0.26 (6) µm, Q= (1.85) 1.96–2.54 (2.57), Qm= 2.24 ± 0.12, V= 143 ± 23 µm³, inequilateral, ellipsoid-fusiform to ellipsoid in side view, ellipsoid in face view, smooth, apex rounded, with a short apiculus and with a shallow suprahilar depression, moderately thick-walled (0.5–0.9 µm), honey yellow colored in water and 5% KOH, having one or two large

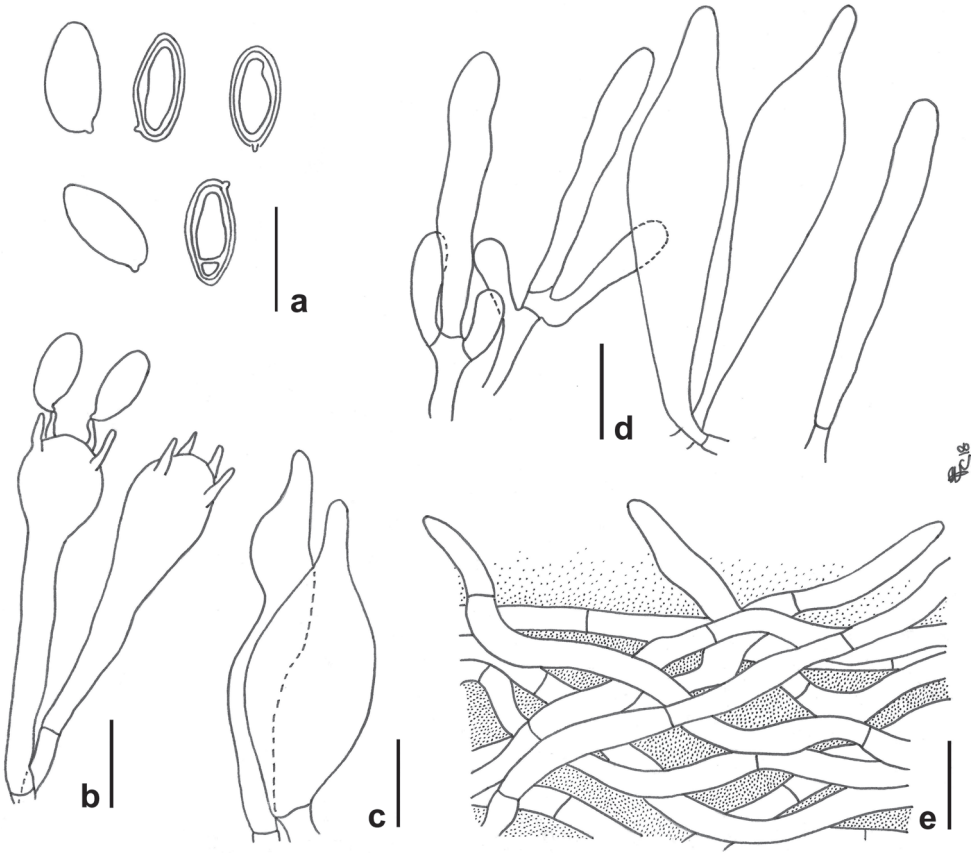

Figure 4. *Neoboletus antillanus*. Micromorphological features (JBSD127417) **a** Basidiospores **b** Basidia **c** Caulocystidia **d** Cheilo- and pleurocystidia **e** Elements of the pileipellis. Scale bars: 10 μm (**a–d**); 20 μm (**e**). Drawings by F. Costanzo.

oil droplets when mature, rarely pluri-guttulate, inamyloid to very faintly dextrinoid, acyanophilic and with an ortochromatic to very faint metachromatic reaction (Fig. 4a). *Basidia* 24–48 × 10–13 μm (n= 26), cylindrical-clavate to clavate, moderately thick-walled (0.5–0.8 μm), predominantly 4-spored but also 1- or 2-spored, usually bearing relatively short sterigmata (2–6 μm), hyaline to pale yellowish and containing straw-yellow oil guttules in water and 5% KOH, bright yellow (inamyloid) in Melzer's, without basal clamps (Fig. 4b); basidioles subcylindrical to faintly clavate, similar in size to basidia. *Cheilocystidia* (19) 21–56 × 4–9 (11) μm (n= 23), very common, moderately slender, projecting straight to sometimes flexuous, irregularly cylindrical or cylindrical-fusiform, fusiform to narrowly lageniform, showing a narrow and long neck, with rounded to subacute tip, smooth, moderately thin- to slightly thick-walled (0.3–0.9 μm), hyaline to pale yellowish in water and 5% KOH, bright yellow (inamyloid) in Melzer's, without epiparietal encrustations (Fig. 4d). *Pleurocystidia* (41) 44–55 × 5–11 μm (n= 14), uncommon, shape, color and chemical reactions similar to but

usually longer than cheilocystidia (Fig. 4d). *Pseudocystidia* not recorded. *Pileipellis* (Fig. 4e) an ixocutis consisting of strongly interwoven, elongated, filamentous and sinuous, frequently branched, repent to occasionally erect hyphae heavily embedded in gelatinous matter; terminal elements 20–72 × 3–9 µm, long and slender, cylindrical, apex pointed, moderately thick-walled (up to 1 µm), pale yellow to golden yellow in water and 5% KOH, inamyloid in Melzer's, smooth to sometimes ornamented by a subtle zebra-like epiparietal encrustation; subterminal elements similar in shape, size and color to terminal elements. *Stipitipellis* a texture of slender, parallel to subparallel and longitudinally running, smooth-walled, adpressed hyphae, 3–11 µm wide, hyaline to yellowish in water and 5% KOH; the stipe apex covered by a well-developed caulohymenial layer consisting of sterile clavate caulobasidioles, abundant, predominantly 4- or 2-spored, fertile caulobasidia and projecting, irregularly cylindrical or cylindrical-fusiform, ventricose-fusiform to fusiform, sublageniform to rarely short mucronate *caulocystidia* (Fig. 4c) similar in shape and color to but slightly broader than hymenial cystidia, (23) 25–45 (54) × 5–13 (15) µm (n= 16), having a wall up to 0.8 µm thick. *Lateral stipe stratum* under the caulohymenium present and well differentiated from the stipe trama, of the "boletoid type", at the stipe apex a (20) 30–40 (50) µm thick layer consisting of divergent, inclined and running towards the external surface, loosely intermingled and branched hyphae remaining separate and embedded in a gelatinous substance. *Stipe-trama* composed of densely arranged, subparallel to moderately interwoven, frequently septate, cylindrical to filamentous, smooth, inamyloid hyphae, 4–13 µm broad. *Basal tomentum hairs* 40–150 µm thick, consisting of tightly adpressed, parallel to subparallel, septate, filamentous, occasionally branched, relatively thick-walled (up to 0.8 µm) hyphae, 2–5.5 µm wide, terminal elements with blunt apex, pale yellow to honey yellow in water and 5 % KOH. *Hymenophoral trama* bilateral divergent of the "*Boletus*-type", with slightly to strongly divergent, recurved-arcuate and loosely arranged, often branched, restricted at septa, gelatinous hyphae (lateral strata hyphae in transversal section not touching each other, (2) 4–8 (10) µm apart, 3–13 µm broad), hyaline to very pale yellowish in water and 5% KOH, inamyloid in Melzer's; lateral strata (20) 30–50 (60) µm thick, mediostratum (20) 30–60 (70) µm thick, axially arranged, consisting of a tightly adpressed, non-gelatinous bundle of hyphae, 3–10 µm broad; in Congo Red the mediostratum is darker than the lateral strata. *Thrombopleroous hyphae* (= oleiferous hyphae sensu Clémençon 2004) very common and particularly frequent in the hymenophore, golden yellow in 5% KOH. *Clamp-connections* absent everywhere. *Hyphal system* monomitic.

Ecology. solitary to gregarious, growing on limestone among litter in a seasonally dry and moist anthropised lowland mixed stand under a large array of neotropical broadleaved trees, including *Coccoloba uvifera*, which represents its probable ECM host tree. See Parra et al. (2018) for further details on vegetation.

Edibility. Unknown.

Examined material. DOMINICAN REPUBLIC, Municipality of Sousa, in Puerto Plata Province, Loc. Cemetery, 19°44'40"N, 70°32'21"W, 100 m a.s.l., a single middle-aged specimen, 03 Dec 2014, C. Angelini (JBSD127416, ANGE425

and MG718); same loc., two young to mature specimens, 14 Dec 2014, C. Angelini (JBSD127417, Holotype, ANGE434 and MG719, Duplo); same loc., several dozens of specimens, most of which heavily parasitized by *Hypomyces* sp., 01 Dec 2017, C. Angelini (JBSD127418, ANGE958 and MG720).

Known distribution. Presently only known from the type locality in the Dominican Republic (Greater Antilles, Caribbean).

Discussion

Neoboletus antillanus phylogeny and interspecific relationships

Phylogenetic analyses corroborate the proposal of the new species *N. antillanus* (Figs 1, 2). It forms an independent evolutive line within *Neoboletus* with no evident phylogenetic relationships (it is sister to the Chinese *N. magnificus* in the combined analysis, but without statistical support) to allied congeneric taxa. According to the same analyses, *B. brunneopanoides*, a Belizean red-pored bolete species phylogenetically nested in *Neoboletus*, clustered in the same clade with collections named *B. vermiculosus*/*B. vermiculosoides* from North America. Should future molecular work prove conspecificity among these three species, *B. vermiculosus* Peck would have priority.

Taxonomic circumscription of *N. antillanus*

The genus *Neoboletus* currently encompasses fewer than ten species geographically restricted to the northern hemisphere and essentially distributed in temperate and tropical regions. However, judging from morphological traits, there might be an additional number of species, up to three times as many in fact, belonging to the same genus, most of which have not yet been molecularly investigated. It is worth noting that a group of Chinese researchers after having firstly accepted *Neoboletus* as an independent genus (Wu et al. 2016a), have subsequently reduced it in synonymy with *Sutorius* Halling, Nuhn & Fechner based on a wider interpretation of the generic boundaries within the Boletaceae (Wu et al. 2016b). As previously pointed out by Gelardi (2018), we presently disagree with this broad circumscription of *Sutorius* since it is, judging from the original description, easily separated from *Neoboletus* based on the overall dark colors, different stipe ornamentation pattern, different spore print color, pores stuffed in early developmental stages like those of *Boletus* s. str. and *Butyriboletus* Arora & J.L. Frank and non-bluing tissues (Halling et al. 2012b). Enough, in our opinion, to state they are not the same thing especially because they cluster in two different (although with a low statistical support) sister clades. Moreover, molecular studies carried out by Smith et al. (2015) on false-truffle fungi from north-eastern South America (Guyana) and our nrLSU/*rpb1*/*rpb2* analy-

sis (Fig. 1) indicate the sequestrate genus *Costatisporus* T.W. Henkel & M.E. Smith as the sister taxon to *Sutorius*. *Costatisporus*, *Neoboletus* and *Sutorius* form the *Sutorius* clade (Fig. 1).

Neoboletus antillanus is easily identifiable among other species of the same genus based on the following set of unique morphologically informative features: 1) medium-small size, 2) reddish to pinkish red then pinkish cream pileus surface, 3) pores orange red to yellowish orange, 4) stipe ornamented over the lower three fourth by purple-red to reddish orange punctuations on a yellow background, 5) lowermost part of the stipe prominently strigose with golden yellow to brownish yellow hairs, 6) yellow context, 7) tissues bruising dark blue when injured, 8) ellipsoid-fusiform, smooth basidiospores, 9) ixocutis pileipellis consisting of gelatinized, repent filamentous hyphae and 10) occurrence in neotropical lowland mixed broadleaved forests. To date, *N. antillanus* has never been found with host species other than local autoctonous broadleaved trees and does not appear to be associated with either Pinaceae or Fagaceae (the latter plant family is not present in Dominican Republic). Moreover, such a purported ECM association of *N. antillanus* with the endemic *C. uvifera* might implicate a neotropical origin. Further suggestion supporting a symbiotic relationship between *N. antillanus* and *C. uvifera* is the co-occurrence at the same locality with *Cantharellus coccolobae* Buyck, P.-A. Moreau and Courtec., which is strictly associated with seagrape in tropical America (Buyck et al. 2016).

Among the other endemic red-pored boletes reported from Central America, *Boletus pyrrhosceles* Halling, *B. guatemalensis* R. Flores & Simonini, *B. dupainii* Boudier and *B. paulae* J. García, Singer & F. Garza-Ocañas superficially resembles *N. antillanus*. However, *B. pyrrhosceles* is easily separated by the reddish brown to brownish orange pileus surface, adnate to subdecurrent hymenophore, shallow tubes (up to 5 mm deep), brownish red pores, tomentose and reticulate stipe that is entirely brownish red to deep red, slightly smaller basidiospores (9.1–11.2 × 4.2–4.9 µm, Qm= 2.3), trichodermal pileipellis and association with *Quercus humboldtii* Bompl. in Colombia (Halling 1992). *Boletus guatemalensis* has a whitish to pale yellow context with yellowish green spots towards the stipe base, radially elongated angular pores, stipe surface with brownish green fibrils in the lower half and a smooth, whitish base, white basal mycelium, unchanging tissues, mostly 2- or 3-spored basidia, a cutis pileipellis consisting of non-gelatinized hyphae, hymenophoral trama intermediate between the "*Boletus*-type" and the "*Phylloporus*-type" and is associated with *Pinus caribaea* Morelet in Guatemala, Belize and Mexico (Flores Arzù and Simonini 2000, Ortiz-Santana et al. 2007, García-Jiménez et al. 2013). *Boletus dupainii* s. Ortiz-Santana et al. differs in the larger size (pileus up to 13 cm broad), polish and shiny, carmine red to crimson red pileus surface, deep red pores, stipe base devoid of strigosity, longer spores (12.8–14.4 × 4–5.6 µm, Qm= 2.9), smaller basidia (24–29.6 × 9.6–10.4 µm), shorter pleuro-, cheilo- and caulocystidia (26.4–47.2 × 7.2–8.8 µm, 16–30.4 × 4.8–8 µm and 16–36.8 × 5.6–11.2 µm, respectively), thinner pileipellis hyphae (up to 6.5 µm diam.) and growth in symbiosis with *Quercus* spp. in Belize

(Ortiz-Santana et al. 2007). This species has recently been assigned to *Rubroboletus* Kuan Zhao & Zhu L. Yang on account of morphological and molecular evidence (Zhao et al. 2014). It was originally described from Europe (Boudier 1902) where it appears to be widespread although uncommon, but in recent times it has also been reported from the New World (McConnell and Both 2002, Ortiz-Santana et al. 2007, Both et al. 2009, García-Jiménez 2013, Bessette et al. 2016). However, the conspecificity of the European material with that from the western hemisphere is yet to be confirmed and a comparative analysis is currently under examination. Finally, *B. paulae* exhibits a deep red, vinaceous red to strawberry red pileus surface, smooth stipe base, whitish gray basal mycelium, pale whitish yellow and erratically bluing context on exposure, hymeniform pileipellis consisting of chains of inflated to subglobose elements up to 34 µm broad and ECM association with oaks in Mexico (García-Jiménez et al. 2013).

Although *N. antillanus* exhibits some superficial morphological affinities with *Boletus vermiculosus* Peck, *B. vermiculosoides* A.H. Smith & Thiers and *B. brunneopanoides* B. Ortiz, these three species have larger basidiome size (pileus 7–18 cm broad and stipe 9–14 cm long in *B. vermiculosus*, pileus up to 12 cm and 16 cm broad in *B. vermiculosoides* and *B. brunneopanoides*, respectively), subtomentose to velvety, yellowish brown or grayish brown to dark brown pileus surface, brownish orange to amber brown or dark brown pore surface fading brownish yellow with age, extremely fine brownish punctuations on stipe surface and stipe base without hairs. *B. vermiculosus* also differs from *N. antillanus* in the trichodermal pileipellis devoid of gelatinous matter, longer basidiospores [(11) 12.6–14 (15) × (4) 4.9–5.6 (6) µm, Qm= 2.6] and the occurrence under Fagaceae. *B. vermiculosoides* is further distinguished by the paler, whitish-yellow stipe surface, narrower basidiospores [9–12 × 3–3.5 (4) µm], smaller basidia (20–26 × 7–9 µm) and association with Fagaceae, whereas *B. brunneopanoides* is also separated by the whitish stipe surface, narrower basidiospores (8.8–12.8 × 4 µm), smaller basidia (20.4–32× 8–8.8 µm) and the occurrence with Pinaceae (*P. caribaea*) (Coker and Beers 1943, Smith and Thiers 1971, Both 1993, Bessette et al. 2000, 2016; Halling and Mueller 2005, Ortiz-Santana et al. 2007). *Boletus vermiculosus* and *B. vermiculosoides* were originally described from eastern North America but the former is also encountered in Central America south to Belize and Costa Rica (Bessette et al. 2000, 2016; Halling and Mueller 2005), while *B. brunneopanoides* was only found in Belize (Ortiz-Santana et al. 2007). Up to now, neither of these species has been reported from the Dominican Republic.

At least two additional North American boletes might be confused with *N. antillanus*, namely *Boletus subluridus* (Murrill) Murrill and *B. fairchildianus* (Singer) Singer. The combination of yellowish orange, orange-pink to purplish red pileus surface, dark red pores, non-strigose stipe base, slightly longer basidiospores [(8.5) 9–14(14.5) × (3.5) 4–6(7) µm], smaller basidia (20–25.5 × 7.5–10 µm and occurrence with oaks and pines in south-eastern USA differentiate *B. subluridus* from *N. antillanus* (Murrill 1938, Singer 1945, 1947, both as *B. miniato-olivaceus* var. *subluridus* Singer; Both

1993, Bessette et al. 2000; 2016), whereas *B. fairchildianus* is distinguished by the larger size (pileus up to 15 cm broad), stipe base without strigosity, larger basidiospores [(12.5) 13–18.8 (19.7) × (4.5) 5–8 µm] and the association with *Quercus* spp. in south-eastern USA and Mexico (Singer 1945, 1947, both as *B. rubricitrinus* var. *fairchildianus* Singer; Both 1993, Bessette et al. 2000, 2016; García-Jiménez 2013).

Neoboletus luridiformis (Rostk.) Gelardi, Simonini & Vizzini (= *Boletus erythropus* Pers. s. Fr. et auct. p.p. non s. Pers.) differs significantly from *N. antillanus* in the large sized basidiomes (pileus up to 25–30 cm in diam.), dark chocolate brown to umber brown, velvety pileus surface, bright red pores, stout, fleshy stipe (up to 15 × 8 cm), non-strigose stipe base, longer basidiospores [(12.8) 13.3–15.5 (16.5) × 4.2–5.5 µm, Qm= 2.95], trichodermal pileipellis with interwoven erect, non-gelatinous hyphae and occurrence in Europe in temperate regions (Pilát and Dermek 1974, Alessio 1985, Breitenbach and Kranzlin 1991, Lannoy and Estadès 2001, Muñoz 2005, Watling and Hills 2005, Klofac 2007, Knudsen and Taylor 2012; pers. obs.).

The eastern Asian species *N. brunneissimus* (W.F. Chiu) Gelardi, Simonini & Vizzini and *N. antillanus* share some common features such as basidiome size, presence of golden yellow to brownish yellow strigosity at the stipe base, yellowish context and dark blue staining of tissues by auto-oxidation but the former is readily separated by the velvety and rusty brown to umber-brown pileus cuticle, rusty brown to reddish-brown pores, denser and rusty-brown punctuation on stipe surface, trichoderm pileipellis consisting of non-gelatinized erect hyphae with slightly shorter and narrower terminal elements [23–45 (58) × 3.5–5 (7) µm] and the occurrence in East Asia in association with Fagaceae and Pinaceae (Chiu 1948, 1957; Bi et al. 1997, Mao 2000, 2009; Wang and Liu 2002, Wang 2004, Wang et al. 2004; Zang 2006, Wu et al. 2016a, Gelardi 2018).

The Chinese *N. magnificus* (W.F. Chiu) Gelardi, Simonini & Vizzini, *Sutorius sanguineoides* G. Wu & Zhu L. Yang and *S. sanguineus* G. Wu & Zhu L. Yang are three additional eastern Asian species that may be confused with *N. antillanus*. Aside from the different geographical distribution and the ECM deciduous and coniferous host associates (Fagaceae and Pinaceae), the former species is also delimited by the dark red to reddish brown pores in the early developmental stages, a decidedly clavate to bulbous stipe base (up to 6 cm broad) that is devoid of or sometimes with inconspicuous strigosity and non-gelatinized trichodermal pileipellis with broader end elements (up to 16 µm wide) (Chiu 1948, 1957; Bi et al. 1997, Mao 2000, 2009; Wang 2004, Wang et al. 2004, Zang 2006, Wu et al. 2016a), whereas *S. sanguineoides* and *S. sanguineus* are both separated from *N. antillanus* on account of the deep red, blood red to brownish red pileus surface, dark red to brownish red pores, non-strigose stipe base, non-gelatinized trichodermal pileipellis and the occurrence in subalpine forests at very high elevations (over 3000 m alt.) (Wu et al. 2016b). Furthermore, *S. sanguineoides* differs in its decidedly larger basidiospores [13.5–17 (21) × 5–7 µm, Qm= 2.56] while *S. sanguineus* also exhibits an evenly red stipe surface, slightly longer basidiospores [10–14 (15) × 5–6 (7) µm, Qm= 2.14] and broader cystidioid pileipellis terminal cells (9–15 µm wide) (Wu et al. 2016b).

Acknowledgments

CA wishes to thank Ricardo G. García, Francisco Jiménez, Brígido Peguero, Yuley E. Piñeyro and Alberto Veloz (Jardín Botánico Nacional Dr. Rafael M. Moscoso, Santo Domingo, Dominican Republic) for their interest and encouragement in studying fungi of the Dominican Republic and for their active cooperation in providing herbarium material preserved in their institution. Roy E. Halling (New York Botanical Garden, New York, USA) is acknowledged for providing valuable bibliography concerning Central American boletes.

References

Alessio C (1985) *Boletus* Dill. ex L. Fungi Europaei 2, Giovanna Biella, Saronno, 705 pp.

Alphonse ME (1981) Les champignons comestible d'Haiti. Faculte d' Agronomie et de Medecine Veterinaire, Damien, Port au Prince.

Altschul SF, Gish W, Miller W, Myers EW, Lipman DJ (1990) Basic local alignment search tool. Journal of Molecular Biology 215: 403–410. https://doi.org/10.1016/S0022-2836(05)80360-2

Arora D, Frank JL (2014) Clarifying the butter Boletes: a new genus, *Butyriboletus*, is established to accommodate *Boletus* sect. *Appendiculati*, and six new species are described. Mycologia 106(3): 464–480. https://doi.org/10.3852/13-052

Baker RED, Dale WT (1951) Fungi of Trinidad and Tobago. Mycological Papers 33: 1–123

Berkeley MJ, Curtis M (1868) ("1869") Fungi Cubenses (Hymenomycetes). Journal of the Linnean Society, Botany 10: 280–392. https://doi.org/10.1111/j.1095-8339.1868.tb00529.x

Bessette AE, Roody WC, Bessette AR (2000) North American boletes. A color guide to the fleshy pored mushrooms. Syracuse University Press, Syracuse, 400 pp.

Bessette AE, Roody WC, Bessette AR (2016) Boletes of eastern North America. Syracuse University Press, Syracuse, 469 pp.

Bi Z-S, Li T-H, Zhang W-M, Song B (1997) A preliminary agaric flora of Hainan Province. Guangdong Higher Education Press, Guangzhou, 388 pp. (in Chinese)

Binder A (1999) Zur molekularen Systematische der Boletales: Boletineae und Sclerodermatineae subordo nov. PhD Dissertation, Universität Regensburg, Regensburg, 149 pp.

Binder M, Bresinsky A (2002) Derivation of a polymorphic lineage of Gasteromycetes from boletoid ancestors. Mycologia 94(1): 85–98. https://doi.org/10.2307/3761848

Binder M, Hibbet DS, Larsson KH, Larsson E, Langer E, Langer G (2005) The phylogenetic distribution of resupinate forms across the major clades of mushroom-forming fungi (Homobasidiomycetes). Systematics and Biodiversity 3(2): 113–157. https://doi.org/10.1017/S1477200005001623

Binder M, Hibbett DS (2006) Molecular systematics and biological diversification of Boletales, Mycologia 98(6): 971–981. https://doi.org/10.3852/mycologia.98.6.971

Both EE (1993) The boletes of North America. A compendium. Buffalo Museum of Science, Buffalo, 436 pp.

Both EE, Brown S, Ortiz-Santana B (2009) The second record of the European species, *Boletus dupainii*, in North America. Bulletin of the Buffalo Society of Natural Sciences 38: 1–4.

Boudier ELÉ (1902) Champignons nouveaux de France. Bulletin de la Société Mycologique de France 18: 137–146.

Breitenbach J, Kränzlin F (1991) Pilze der Schweiz. Band 3. Röhrlinge und Blätterpilze 1 – Fungi of Switzerland. Vol. 3. Boletes and agarics 1. Verlag Mykologia, Luzern, 361 pp.

Bruns TD, Palmer JD (1989) Evolution of mushroom mitochondrial DNA: *Suillus* and related genera. Journal of Molecular Evolution 28(4): 349–362. https://doi.org/10.1007/BF02103431

Buyck B, Moreau P-A, Courtecuisse R, Kong A, Roy M, Hofstetter V (2016) *Cantharellus coccolobae* sp. nov. and *Cantharellus garnieri*, two tropical members of *Cantharellus* subg. *Cinnabarinus*. Cryptogamie, Mycologie. 37(3): 391–403. https://doi.org/10.7872/crym/v37.iss3.2016.391

Camino Vilaró M, Mena Portales J, Minter DW (2006) Fungi of Cuba. www.cybertruffle.org.uk/cubafung

Chakraborty D, Das K, Baghela A, Singh SK, Dentinger BTM (2015) *Boletus recapitulatus* (Boletaceae), a new species from India with peculiar mushroom-shaped cells. Phytotaxa 236(2): 150–160. https://doi.org/10.11646/phytotaxa.236.2.4

Chiu W-F (1948) The Boletes of Yunnan. Mycologia 40(2): 199–231. https://doi.org/10.1080/00275514.1948.12017700

Chiu W-F (1957) Atlas of the Yunnan Boletes – Bolete Flora of Yunnan. Science Press, Beijing, 154 pp. [In Chinese]

Clémençon H (2004) Cytology and plectology of the Hymenomycetes. Bibliotheca Mycologica 199: 1–488.

Coker WC, Beers AH (1943) The Boletaceae of North Carolina. University of North Carolina Press, Chapel Hill, 96 pp.

Courtecuisse R, Welti S (2013) Liste préliminaire des Fungi recensés dans les îles françaises des Petites Antilles : Martinique, Guadeloupe et dépendances. II – Basidiomycètes non lamellés (espèces gastéroïdes, rouilles et charbons exclus). Documents Mycologiques 35: 47–173.

Dennis RWG (1970) Fungus flora of Venezuela and adjacent countries. Kew Bulletin Additional Series 3, Royal Botanic Garden, Kew, 531 pp.

Desjardin DE, Binder M, Roekring S, Flegel T (2009) *Spongiforma*, a new genus of gastroid boletes from Thailand. Fungal Diversity 37: 1–8.

Farid A, Gelardi M, Angelini C, Franck AR, Costanzo F, Kaminsky L, Ercole E, Baroni TJ, White AL, Garey JR, Smith ME, Vizzini A (2018) *Phylloporus* and *Phylloboletellus* are no longer alone: *Phylloporopsis* gen. nov. (Boletaceae), a new smooth-spored lamellate genus to accommodate the American species *Phylloporus boletinoides*. FUSE 2: 341–359. https://doi.org/10.3114/fuse.2018.02.10

Felsenstein J (1985) Confidence limits on phylogenies: an approach using the bootstrap. Evolution 39: 783–791. https://doi.org/10.2307/2408678

Flores Arzù R, Simonini G (2000) Contributo alla conoscenza delle Boletales del Guatemala. Rivista di Micologia 43(2): 121–145.

Flores Arzú R, Comandini O, Rinaldi AC (2012) A preliminary checklist of macrofungi of Guatemala, with notes on edibility and traditional knowledge. Mycosphere 3(1): 1–21. https://doi.org/10.5943/mycosphere/3/1/1

Franco-Molano AE, Aldana-Gómez R, Halling RE (2000) Setas de Colombia. Agaricales, Boletales y otros hongos: guía de campo. Colciencias, Universidad de Antioquia Medellín, Colombia, 156 p.

Galli R (2007) I Boleti, Atlante pratico-monografico per la determinazione dei boleti (3rd ed.). Dalla Natura, Milano, 296 pp.

García-Jiménez J (2013) Diversidad de macromicetos en el estado de Tamaulipas, México. PhD en Ciencias Naturales, Facultad de Ciencias Forestales, Universidad Autónoma de Nuevo León, Linares, México, 254 pp.

García-Jiménez J, Singer R, Estrada E, Garza-Ocañas F, Valenzuela R (2013) Dos especies nuevas del género *Boletus* (Boletales: Agaricomycetes) en México. Revista Mexicana de Biodiversidad 84: 152–162. https://doi.org/10.7550/rmb.31988

Gardes M, Bruns TD (1993) ITS primers with enhanced specificity for Basidiomycetes-application to the identification of mycorrhizae and rusts. Molecular Ecology 2: 113–118. https://doi.org/10.1111/j.1365-294X.1993.tb00005.x

Gelardi M (2018) Contribution to the knowledge of Chinese boletes. II. *Aureoboletus thibetanus* s. l., *Neoboletus brunneissimus*, *Pulveroboletus macrosporus* and *Retiboletus kauffmanii* (Part I), Rivista Micologica Romana 102(3): 13–30.

Gelardi M, Vizzini A, Ercole E, Voyron S, Sun J-Z , Liu X-Z (2013) *Boletus sinopulverulentus*, a new species from Shaanxi Province (central China) and notes on *Boletus* and *Xerocomus*, Sydowia 65(1): 45–57.

Gelardi M, Simonini G, Ercole E, Davoli P, Vizzini A (2015) *Cupreoboletus* (Boletaceae, Boletineae), a new monotypic genus segregated from *Boletus* sect. *Luridi* to reassign the Mediterranean species *B. poikilochromus*. Mycologia 107(6): 1254–1269. https://doi.org/10.3852/15-070

Gómez LD, Singer R (1984) *Veloporphyrellus*, a new genus of Boletaceae from Costa Rica. Brenesia 22: 293–298.

Gómez LD (1996) ("1997") Basidiomicetes de Costa Rica: *Xerocomus*, *Chalciporus*, *Pulveroboletus*, *Boletellus*, *Xanthoconium* (Agaricales: Boletaceae). In: Carranza J, Mueller GM (Eds) Fungi of Costa Rica: selected studies on ecology and biodiversity. Revista de Biología Tropical 44 (suppl. 4): 59–89.

Guzmán G, Ramírez-Guillén F, Miller Jr OK, Lodge DJ, Baroni TJ (2004) *Scleroderma stellatum* versus *Scleroderma bermudense*: the status of *Scleroderma echinatum* and the first record of *Veligaster nitidum* from the Virgin Islands. Mycologia 96(6): 1370–1379. https://doi.org/10.1080/15572536.2005.11832886

Halling RE (1989) A synopsis of Colombian Boletes. Mycotaxon 34: 93–113.

Halling RE (1992) A new species of *Boletus* section *Luridi* from Colombia. Brittonia 44(3): 322–325. https://doi.org/10.2307/2806931

Halling RE (1996) ("1997") Boletaceae (Agaricales): Latitudinal biodiversity and biological interactions in Costa Rica and Colombia. In: Carranza J, Mueller GM (Eds) Fungi of Costa Rica: selected studies on ecology and biodiversity. Revista de Biologia Tropical 44 (Suppl. 4): 111–114.

Halling RE, Mueller GM, Dallwitz MJ (1999) A new *Phylloporus* (Basidiomycetes, Boletaceae) with a key to species in Colombia and Costa Rica. Mycotaxon 63: 63–68.

Halling RE, Mueller GM (2002) Agarics and Boletes of Neotropical Oakwoods. In: Watling R, Frankland JC, Ainsworth AM, Isaac S, Robinson CH (Eds) Tropical Mycology. Vol. 1. Macromycetes, CAB International, Wallingford, 1–10.

Halling RE, Mueller GM (2003) *Leccinum* (Boletaceae) in Costa Rica. Mycologia 95(3): 488–499. https://doi.org/10.2307/3761891

Halling RE, Mata M, Mueller GM (2004) Three new boletes for Costa Rica. Memoirs of the New York Botanical Garden 89: 141–147.

Halling RE, Mueller GM (2005) Common Mushrooms of the Talamanca Mountains, Costa Rica. Memoirs of the New York Botanical Garden Vol. 90, New York Botanical Garden Press, Bronx, 195 p.

Halling RE, Baroni TJ, Binder M (2007) A new genus of Boletaceae from eastern North America. Mycologia 99(2): 310–316. https://doi.org/10.3852/mycologia.99.2.310

Halling RE, Osmundson TW, Neves MA (2008) Pacific boletes: implications for biogeographic relationships. Mycological Research 112: 437–447. https://doi.org/10.1016/j.mycres.2007.11.021

Halling RE, Ortiz-Santana B (2009) A revision of *Boletellus* sect. *Ixocephali*. Mycological Progress 8: 237–244. https://doi.org/10.1007/s11557-009-0595-3

Halling RE, Nuhn M, Osmundson TW, Fechner NA, Trappe JM, Soytong K, Arora D, Hibbett DS, Binder M (2012a) Affinities of the *Boletus chromapes* group to *Royoungia* and the description of two new genera, *Harrya* and *Australopilus*. Australian Systematic Botany 25: 418–431. https://doi.org/10.1071/SB12028

Halling RE, Nuhn M, Fechner N, Osmundson TW, Soytong K, Arora D, Hibbett DS, Binder M (2012b) *Sutorius*: a new genus for *Boletus eximius*. Mycologia 104(4): 951–961. https://doi.org/10.3852/11-376

Halling RE, Fechner N, Nuhn M, Osmundson TW, Soytong K, Arora D, Binder M, Hibbett DS (2015) Evolutionary relationships of *Heimioporus* and *Boletellus* (Boletales), with an emphasis on Australian taxa including new species and new combinations in *Aureoboletus*, *Hemileccinum* and *Xerocomus*. Australian Systematic Botany 28: 1–22. https://doi.org/10.1071/SB14049

Henkel TW, Obase K, Husbands D, Uehling JK, Bonito G, Aime MC, Smith ME (2016) New Boletaceae taxa from Guyana: *Binderoboletus segoi* gen. and sp. nov., *Guyanaporus albipodus* gen. and sp. nov., *Singerocomus rubriflavus* gen. and sp. nov., and a new combination for *Xerocomus inundabilis*. Mycologia 108(1): 157–173. https://doi.org/10.3852/15-075

Hitchcock AS (1898) List of cryptogams collected in the Bahamas, Jamaica and Grand Cayman. Annals and Reports of the Missouri Botanical Garden 9: 111–120. https://doi.org/10.2307/2992138

Hosford DR, Trappe JM (1980) Taxonomic studies on the genus *Rhizopogon*, II. Notes and new records of species from México and Caribbean countries. Boletin de la Sociedad Mexicana de Micología 14: 3–15.

Katoh K, Misawa K, Kuma K, Miyata T (2002) MAFFT: a novel method for rapid multiple sequence alignment based on fast Fourier transform. Nucleic Acids Research 30: 3059–3066. https://doi.org/10.1093/nar/gkf436

Kearse M, Moir R, Wilson A, Stones-Havas S, Cheung M, Sturrock S, Buxton S, Cooper A, Markowitz S, Duran C, Thierer T, Ashton B, Meintjes P, Drummond A (2012) Geneious Basic: an integrated and extendable desktop software platform for the organization and analysis of sequence data. Bioinformatics 28: 1647–1649. https://doi.org/10.1093/bioinformatics/bts199

Klofac W(2007) Schlüssel zur Bestimmung von Frischfunden der europäischen Arten der Boletales mit röhrigem Hymenophor. Österreichische Zeitschrift für Pilzkunde 16: 187–279.

Knudsen H, Taylor AFS (2012) Boletales E.-J. Gilbert. In: Knudsen H, Vesterholt J (Eds) Funga Nordica – Agaricoid, boletoid and cyphelloid genera, Nordsvamp, Copenhagen, 149–179.

Kreisel K (1971) Clave para la identificacion de los macromicetos de Cuba. Ciencias Biológicas 16, Universidad de La Habana, Habana, 101 pp.

Lannoy G, Estadès A (2001) Flore Mycologique d'Europe 6 - Les Bolets. Documents Mycologiques, Mém. Hors Série 6, Lille, 163 pp.

Lécuru C, Courtecuisse R (2013) Liste préliminaire des Fungi recensés dans les îles françaises des Petites Antilles: Martinique, Guadeloupe et dépendances. III. Espèces gastéroïdes épigées relevant des Agaricomicetideae. Documents Mycologiques 35: 175–189.

Li Y-C, Feng B, Yang Z-L (2011) *Zangia*, a new genus of Boletaceae supported by molecular and morphological evidence. Fungal Diversity 49(1): 125–143. https://doi.org/10.1007/s13225-011-0096-y

Liang Z-Q, An D-Y, Jiang S, Su M-S, Zeng N-K (2016) *Butyriboletus hainanensis* (Boletaceae, Boletales), a new species from tropical China. Phytotaxa 267(4): 256–262. https://doi.org/10.11646/phytotaxa.267.4.2

Lodge DJ, Baroni TJ, Miller Jr OK, Halling RE (2001) Emerging biogeographic patterns among macrobasidiomycete fungi in the Greater Antilles. In: Zanoni T (Ed.) Biogeography of Plants in the Greater Antilles, New York Botanical Garden, New York.

Mao X-L (2000) The Macrofungi of China. Henan Science and Technology Press, Zhengzhou, 719 pp. [In Chinese]

Mao X-L (2009) Macromycetes of China. Science Press, Beijing, 816 p. [In Chinese]

Mata M, Halling RE, Mueller GM (2003) Macrohongos de Costa Rica. Vol. 2. INBio, Santo Domingo, Costa Rica. 240 pp.

Matheny PB, Wang Z, Binder M, Curtis JM, Lim YW, Nilsson RH et al. (2007) Contributions of rpb2 and tef1 to the phylogeny of mushrooms and allies (Basidiomycota, Fungi). Molecular Phylogenetics and Evolution 43: 430–451. https://doi.org/10.1016/j.ympev.2006.08.024

McConnell OL, Both EE (2002) *Boletus dupainii* in North America. Field Mycology 3(3): 103–104. https://doi.org/10.1016/S1468-1641(10)60162-4

Mello A, Ghignone S, Vizzini A, Sechi C, Ruiu P, Bonfante P (2006) ITS primers for identification of marketable Boletes. Journal of Biotechnology 121: 318–329. https://doi.org/10.1016/j.jbiotec.2005.08.022

Miller Jr OK, Lodge DJ, Baroni TJ (2000) New and interesting ectomycorrhizal fungi from Puerto Rico, Mona, and Guana Islands. Mycologia 92(3): 558–570. https://doi.org/10.2307/3761516

Minter DW, Rodríguez-Hernández M, Mena-Portales J (2001) Fungi of the Caribbean. An annotated checklist, PDMS Publishing, Isleworth, 950 pp.

Moreau P-A, Paz Conde A, Lavoise C, Curtecuisse R (2011) ("2013") Les rhizomorphes de *Diplocystis guadalupensis* (Boletales, Sclerodermataceae). Bulletin de la Société Mycologique de France 127(3–4): 213–224.

Mueller GM, Halling RE, Carranza J, Mata M, Schmit JP (2006) Saprotrophic and ectomycorrhizal Macrofungi of Costa Rican oak forests. In: Keppelle M (Ed) Ecology and conservation of Neotropical montane oak forests. Springer-Verlag, Heidelberg, 55–68. https://doi.org/10.1007/3-540-28909-7_5

Muñoz JA (2005) *Boletus* s.l. (excl. *Xerocomus*). Fungi Europaei 2, Edizioni Candusso, Alassio, 952 pp.

Murrill WA (1910) A new *Boletus* from Jamaica. Mycologia 2(6): 305. https://doi.org/10.2307/3753294

Murrill WA (1918) The Agaricaceae of Tropical North America – VIII. Mycologia 10(2): 62–85. https://doi.org/10.2307/3753227

Murrill WA (1921) Notes and brief articles – A new bolete from Porto Rico. Mycologia 13(1): 60–61.

Murrill WA (1938) New boletes. Mycologia 30(5): 520–525. https://doi.org/10.1080/00275514.1938.12017294

Nuhn ME, Binder M, Taylor AFS, Halling RE, Hibbett DS (2013) Phylogenetic overview of the Boletineae. Fungal Biology 117(7–8): 479–511. https://doi.org/10.1016/j.funbio.2013.04.008

Orihara T, Smith ME (2017) Unique phylogenetic position of the African truffle-like fungus, *Octaviania ivoryana* (Boletaceae, Boletales), and the proposal of a new genus, *Afrocastellanoa*. Mycologia 109(2): 323–332. https://doi.org/10.1080/00275514.2017.1301750

Ortiz-Santana B (2006) Phylogeny and biogeography of Caribbean Boletales. PhD Dissertation, University of Puerto Rico.

Ortiz-Santana B, Lodge DJ, Baroni TJ, Both EE (2007) Boletes from Belize and the Dominican Republic. Fungal Diversity 27: 247–416.

Parra AL, Angelini C, Ortiz-Santana B, Mata G, Billette C, Rojo C, Chen J, Callac P (2018) The genus *Agaricus* in the Caribbean. Nine new taxa mostly based on collections from the Dominican Republic. Phytotaxa 345(3): 219–271. https://doi.org/10.11646/phytotaxa.345.3.2

Patouillard NT (1900) Champignons de la Guadeloupe. Bulletin de la Société Mycologique de France 16: 175–188.

Patouillard NT (1902) Champignons de la Guadeloupe, recueillis par le R.P. Duss. Bulletin de la Société Mycologique de France 18: 171–186.

Pegler DN (1983) Agaric flora of the Lesser Antilles. Kew Bulletin Additional Series 9, HMSO, London, 668 pp.

Pegler DN (1987) Revision of Agaricales of Cuba. Kew Bulletin 42(3): 501–585. https://doi.org/10.2307/4110064

Pilát A, Dermek A (1974) Hríbovité huby. Československé hríbovité a sliziakovité huby (Boletaceae – Gomphidiaceae). Veda, Bratislava, 207 pp.

Reid DA (1977) Some Gasteromycetes from Trinidad and Tobago. Kew Bulletin 31(3): 657–690. https://doi.org/10.2307/4119418

Ridgway R (1912) Color standards and color nomenclature. Self-published, Washington D.C. https://doi.org/10.5962/bhl.title.144788

Ronquist F, Teslenko M, van der Mark P, Ayres DL, Darling A, Höhna S, Larget B, Liu L, Suchard MA, Huelsenbeck JP (2012) MrBayes 3.2: efficient Bayesian phylogenetic inference and model choice across a large model space. Systematic Biology 61: 539–542. https://doi.org/10.1093/sysbio/sys029

Séne S, Avril R, Chaintreuil C, Geoffroy A, Ndiaye C, Diédhiou AG, Sadio O, Courtecuisse R, Sylla SN, Selosse M-A, Bâ A (2015) Ectomycorrhizal fungal communities of *Coccoloba uvifera* (L.) L. mature trees and seedlings in the neotropical coastal forests of Guadeloupe (Lesser Antilles). Mycorrhiza 25(7): 547–559. https://doi.org/10.1007/s00572-015-0633-8

Séne S, Selosse M-A, Forget M, Lambourdière J, Cissé K, Diédhiou AG, Rivera-Ocasio E, Kodja H, Kameyama N, Nara K, Vincenot L, Mansot J-L, Weber J, Roy M, Sylla SN, Bâ A (2018) A pantropically introduced tree is followed by specific ectomycorrhizal symbionts due to pseudo-vertical transmission.The ISME Journal 12: 1806–1816. https://doi.org/10.1038/s41396-018-0088-y

Simonini G, Vizzini A (2015) *Boletus mendax*, una specie recentemente descritta in Italia ed i nuovi orientamenti sulla sistematica della sez. *Luridi* del genere *Boletus*. Numero speciale XL Mostra Reggiana del Fungo: 3–24.

Singer R (1945) New Boletaceae from Florida (a preliminary communication). Mycologia 37: 797–799. https://doi.org/10.2307/3755143

Singer R (1947) The Boletoideae of Florida. The Boletineae of Florida with notes on extralimital species III. The American Midland Naturalist 37(1): 1–135. https://doi.org/10.2307/2421647

Singer R, Fiard JP (1976) Agaricales nouvelles des Antilles françaises. Bulletin de la Société Mycologique de France 92(4): 445–447.

Singer R, Araujo I, Ivory MH (1983) The ectotrophically mycorrizal Fungi of the neotropical lowlands, especially Central Amazonia (Litter decomposition and ectomycorrhiza in Amazonian forests 2.). Beihefte zur Nova Hedwigia 77: 1–352.

Singer R, Gómez LD (1984) The Basidiomycetes of Costa Rica. III. The genus *Phylloporus* (Boletaceae). Brenesia 22: 163–181.

Singer R, García J, Gómez LD (1990) The Boletineae of Mexico and Central America I & II. Beihefte zur Nova Hedwigia 98: 1–70.

Singer R, García J, Gómez LD (1991) The Boletineae of Mexico and Central America III. Beihefte zur Nova Hedwigia 102: 1–99.

Singer R, García J, Gómez LD (1992) The Boletineae of Mexico and Central America IV. Beihefte zur Nova Hedwigia 105: 1–62.

Smith ME, Amses KR, Elliott TF, Obase K, Aime MC, Henkel TW (2015) New sequestrate fungi from Guyana: *Jimtrappea guyanensis* gen. sp. nov., *Castellanea pakaraimophila* gen. sp. nov., and *Costatisporus cyanescens* gen. sp. nov. (Boletaceae, Boletales), IMA Fungus 6(2): 297–317. https://doi.org/10.5598/imafungus.2015.06.02.03

Stamatakis A (2006) RAxML-VI-HPC: maximum likelihood-based phylogenetic analyses with thousands of taxa and mixed models. Bioinformatic 22: 2688–2690. https://doi.org/10.1093/bioinformatics/btl446

Thiers B (2019) (continuously updated): Index Herbariorum: a global directory of public herbaria and associated staff. New York botanical garden's virtual herbarium. http://sweetgum.nybg.org/ih/

Trappe JM, Castellano MA, Halling RE, Osmundson TW, Binder M, Fechner N, Malajczuk N (2013) Australasian sequestrate fungi. 18: *Solioccasus polychromus* gen. and sp. nov., a richly colored, tropical to subtropical, hypogeous fungus, Mycologia 105(4): 888–895. https://doi.org/10.3852/12-046

Urban A, Klofac W (2015) *Neoboletus xanthopus*, a sibling species of *Neoboletus luridiformis* and similar boletes with yellowish pileus colors. Sydowia 67: 175–187. https://doi.org/10.12905/0380.sydowia67-2015-0175

Vilgalys R, Hester M (1990) Rapid genetic identification and mapping of enzymatically amplified ribosomal DNA from several *Cryptococcus* species. Journal of Bacteriology 172: 4238–4246. https://doi.org/10.1128/jb.172.8.4238-4246.1990

Vizzini A (2014) Nomenclatural novelties. Index Fungorum 192: 1.

Vizzini A, Simonini G, Ercole E, Voyron S (2014) *Boletus mendax*, a new species of *Boletus* sect. *Luridi* from Italy, and insights on the *B. luridus* complex. Mycological Progress 13(1): 95–109. https://doi.org/10.1007/s11557-013-0896-4

Vizzini A, Consiglio G, Setti L, Ercole E (2015) *Calocybella*, a new genus for *Rugosomyces pudicus* (Agaricales, Lyophyllaceae) and emendation of the genus *Gerhardtia*. IMA Fungus 6(1): 1–11. https://doi.org/10.5598/imafungus.2015.06.01.01

Wang Q-B (2004) Taxonomy and molecular systematics of *Boletus* in China. PhD Dissertation, Systematic Mycology and Lichenology Laboratory, Institute of Microbiology, Chinese Academy of Sciences, Beijing, 214 pp. (in Chinese)

Wang X-H, Liu P-G (2002) Notes on several boleti from Yunnan, China. Mycotaxon 84: 125–134.

Wang X-H, Liu P-G, Yu F-Q (2004) Color atlas of wild commercial mushrooms in Yunnan. Yunnan Science and Technology Press, Kunming, 136 pp. [In Chinese]

Watling R, Hills AE (2005) Boletes and their allies - Boletaceae, Strobilomycetaceae, Gyroporaceae, Paxillaceae, Coniophoraceae, Gomphidiaceae (revised and enlarged edition). In: Henderson DM, Watling R (Eds) British Fungus Flora, Agarics and Boleti, vol. 1, HMSO, Edinburgh, 174 pp.

White TJ, Bruns TD, Lee S, Taylor J (1990) Amplification and direct sequencing of fungal ribosomal RNA genes for phylogenetics. In: Innis MA, Gelfand DH, Sninsky JJ, White TJ (Eds) PCR protocols, a guide to methods and applications. Academic press, Orlando, 315–322. https://doi.org/10.1016/B978-0-12-372180-8.50042-1

Wu G, Feng B, Xu J-P, Zhu X-T, Li Y-C, Zeng N-K, Hosen I, Yang Z-L (2014) Molecular phylogenetic analyses redefine seven major clades and reveal 22 new generic clades in the fungal family Boletaceae. Fungal Diversity 69(1): 93–115. https://doi.org/10.1007/s13225-014-0283-8

Wu G, Zhao K, Li Y-C, Zeng N-K, Feng B, Halling RE, Yang Z-L (2016a) Four new genera of the fungal family Boletaceae. Fungal Diversity 81(1): 1–24. https://doi.org/10.1007/s13225-015-0322-0

Wu G, Li Y-C, Zhu X-T, Zhao K, Han L-H, Cui Y-Y, Li F, Xu J-P, Yang Z-L (2016b) One hundred noteworthy boletes from China. Fungal Diversity 81(1): 25–188. https://doi.org/10.1007/s13225-016-0375-8

Zang M (2006) Boletaceae (I). Flora Fungorum Sinicorum Vol. 22, Science Press, Beijing, 205 pp. [In Chinese]

Zeng N-K, Cai Q, Yang Z-L (2012) *Corneroboletus*, a new genus to accommodate the southeast Asian *Boletus indecorus*. Mycologia 104(6): 1420–1432. https://doi.org/10.3852/11-326

Zhao K, Wu G, Yang Z-L (2014) A new genus, *Rubroboletus*, to accommodate *Boletus sinicus* and its allies. Phytotaxa 188(2): 61–77. https://doi.org/10.11646/phytotaxa.188.2.1

Zhao K, Wu G, Halling RE, Yang Z-L (2015) Three new combinations of *Butyriboletus* (Boletaceae). Phytotaxa 234(1): 51–62. https://doi.org/10.11646/phytotaxa.234.1.3

Zhu X-T, Li Y-C, Wu G, Feng B, Zhao K, Gelardi M, Kost G-W, Yang Z-L (2014) The genus *Imleria* (Boletaceae) in East Asia. Phytotaxa 191(1): 81–98. https://doi.org/10.11646/phytotaxa.191.1.5

MycoKeys 49: 99–129 (2019)
doi: 10.3897/mycokeys.49.30886
http://mycokeys.pensoft.net

RESEARCH ARTICLE

A peer-reviewed open-access journal
MycoKeys
Launched to accelerate biodiversity research

Striatiguttulaceae, a new pleosporalean family to accommodate *Longicorpus* and *Striatiguttula* gen. nov. from palms

Sheng-Nan Zhang[1,2,3,4], Kevin D. Hyde[4], E.B. Gareth Jones[5], Rajesh Jeewon[6], Ratchadawan Cheewangkoon[3], Jian-Kui Liu[1,2]

1 *Center for Bioinformatics, School of Life Science and Technology, University of Electronic Science and Technology of China, Chengdu 611731, P.R. China* **2** *Guizhou Key Laboratory of Agricultural Biotechnology, Guizhou Academy of Agricultural Science, Guiyang 550006, P.R. China* **3** *Department of Entomology and Plant Pathology, Faculty of Agriculture, Chiang Mai University, Chiang Mai 50200, Thailand* **4** *Center of Excellence in Fungal Research, Mae Fah Luang University, Chiang Rai 57100, Thailand* **5** *Nantgaredig 33B St. Edwards Road, Southsea, Hants, UK* **6** *Department of Health Sciences, Faculty of Science, University of Mauritius, Reduit, Mauritius, 80837, Mauritius*

Corresponding author: *Jian-Kui Liu* (ljiankui@gmail.com)

Academic editor: *G. Mugambi* | Received 28 October 2018 | Accepted 29 January 2019 | Published 1 April 2019

Citation: Zhang S-N, Hyde KD, Jones EBG, Jeewon R, Cheewangkoon R, Liu J-K (2019) Striatiguttulaceae, a new pleosporalean family to accommodate *Longicorpus* and *Striatiguttula* gen. nov. from palms. MycoKeys 49: 99–129. https://doi.org/10.3897/mycokeys.49.30886

Abstract

Palms represent the most morphological diverse monocotyledonous plants and support a vast array of fungi. Recent examinations of palmicolous fungi in Thailand led to the discovery of a group of morphologically similar and interesting taxa. A polyphasic approach based on morphology, multi-gene phylogenetic analyses and divergence time estimates supports the establishment of a novel pleosporalean family Striatiguttulaceae, which diversified approximately 39 (20–63) MYA (crown age) and 60 (35–91) MYA (stem age). Striatiguttulaceae is characterized by stromata or ascomata with a short to long neck, trabeculate pseudoparaphyses and fusiform to ellipsoidal, 1–3-septate ascospores, with longitudinal striations and paler end cells, surrounded by a mucilaginous sheath. Multi-gene phylogenetic analysis showed that taxa of Striatiguttulaceae form a well-supported and distinct monophyletic clade in Pleosporales, and related to Ligninsphaeriaceae and Pseudoastrosphaeriellaceae. However, these families can be morphologically demarcated by the slit-like ascomata and extremely large ascospores in Ligninsphaeriaceae and the rather narrow fusiform ascospores in Pseudoastrosphaeriellaceae. Eight strains of Striatiguttulaceae formed two monophyletic sub-clades, which can be recognized as *Longicorpus* **gen. nov.** and *Striatiguttula* **gen. nov.** Morphologically, the genus *Longicorpus* can be differentiated from *Striatiguttula* by its elongated immersed

ascomata and fusiform ascospores with relatively larger middle cells and paler end cells. Two new species *Striatiguttula nypae* and *S. phoenicis*, and one new combination, *Longicorpus striataspora* are introduced with morphological details, and phylogenetic relationships are discussed based on DNA sequence data.

Keywords
6 new taxa, divergence times, Dothideomycetes, epitype, sexual morphs

Introduction

Fungi associated with palms have been intensively investigated by Hyde and his co-workers (Goh and Hyde 1996, Fröhlich and Hyde 2000, Hyde and Alias 2000, Hyde et al. 2000, Yanna et al. 2001a,b,c, Taylor and Hyde 2003, Hyde et al. 2007), and provided a significant contribution to their diversity and taxonomy. There have been a number of interesting studies on palm fungi. For example, Fröhlich and Hyde (1999) reviewed the biodiversity of palm fungi in the tropics, and proposed the ratio of host specific fungi to palm species as 33 to 1 rather than the general ratio of 6 to 1 for all plants proposed by Hawksworth (1991). Taylor et al. (2000) investigated biogeographical distribution of microfungi from temperate and tropical palms, and found different fungal assemblages from these two regions, and also revealed that the difference was more related to climatic influences than hosts sampled. Subsequently, Yanna et al. (2001b, 2002) studied fungal communities and succession of palms, and pointed out that fungal species compositions were distinct on different hosts and at different sites, and even differed from different palm tissues. In addition, some studies were dedicated to endophytic palmicolous fungi (Rodrigues and Samuels 1990, Taylor et al. 1999, Fröhlich et al. 2000, Hyde and Soytong 2008, Pinruan et al. 2010a, Mahmoud et al. 2017) and pathogens (Fröhlich et al. 1997, Hyde and Cannon 1999, Elliott et al. 2010, Mohammadi 2014). Other studies have focused on fungi on peat swamp palms (Pinruan et al. 2002, 2007, 2008, 2010b, 2014, Pinnoi et al. 2003) and from mangrove palms (Suetrong et al. 2009, Loilong et al. 2012, Zhang et al. 2018). All these examples indicate that species are diverse and palms harbour numerous undescribed microfungi.

Ascomycetes from palms are a very diverse assemblage and the best represented family is Xylariaceae (Xylariales, Sordariomycetes), with three commonly recorded genera *Anthostomella* (Xylariaceae), *Linocarpon* (Linocarpaceae) and *Oxydothis* (Oxydothidaceae) (Taylor and Hyde 2003, Hidayat et al. 2006, Konta et al. 2016b, 2017). In recent years, a series of Dothideomycetes from palms were described as new on the basis of morphology and phylogenetic analyses, such as astrosphaeriella-like species (recognized as three groups: *Astrosphaeriellopsis*, Astrosphaeriellaceae and Pseudoastrosphaeriellaceae) and species of *Botryosphaeria* (Botryosphaeriaceae), *Fissuroma* (Aigialaceae), *Neodeightonia* (Botryosphaeriaceae) and *Roussoella* (Roussoellaceae) (Liu et al. 2010, 2011a,b, 2012, 2014, Phookamsak et al. 2015, Konta et al. 2016a,c, Wanasinghe et al. 2018). The diversity of palmicolous ascomycetes recovered can in part be due to the wide range of hosts and habitats sampled, the latter including terrestrial, freshwater, and marine or mangrove ecosystems. There are four palm species encoun-

tered as mangrove associates in Asia (Tomlinson 1986): *Calamus erinaceus* (Becc.) J.Dransf., *Nypa fruticans* Wurmb., *Oncosperma tigillarium* (Jack) Ridl. and *Phoenix paludosa* Roxb. Loilong et al. (2012) documented the greatest biodiversity of fungi on *N. fruticans* listing 135 taxa (90 Ascomycota, three Basidiomycota and 42 asexual taxa), of which 97 taxa were described (Hyde 1992a,b, Hyde et al. 1999, Hyde and Alias 2000, Pilantanapak et al. 2005, Hyde and Sarma 2006) with support from DNA sequence data (Suetrong et al. 2015). Nevertheless, few studies have focused on fungi growing on *Phoenix paludosa*, where *Lignincola conchicola*, *Kirschsteiniothelia phoenicis* and *Acuminatispora palmarum* were recently reported (Liu et al. 2011a, Hyde et al. 2018, Zhang et al. 2018).

Nypa fruticans is an ancient palm that grows in brackish water, while *Phoenix paludosa* is found in the upper parts of mangroves and tolerates salt water, with both occurring in Thailand mangrove sites. In an ongoing study on the taxonomy of fungi occurring on palms, we collected fungi colonizing these two palm hosts from different mangrove sites in Thailand. Interestingly, a group of ascomycetes recovered appears to be new to science based on morphology and multi-gene phylogenetic evidence. The aim of this study was to characterize the novel taxa and investigate their phylogenetic relationships in the order Pleosporales, as well as apply the divergence times as additional evidence, especially in higher taxa ranking, for the establishment of new family Striatiguttulaceae.

Materials and methods

Specimen collection, examination and single spore isolation

Decayed rachides or petioles of *Nypa fruticans* and *Phoenix paludosa* were collected from Chanthaburi, Krabi and Ranong provinces in Thailand. The collected specimens were washed under running water and examined via laboratory procedures as outlined by Jones and Hyde (1988). Morphological characters were observed using a Carl Zeiss stereo microscope fitted with an AxioCam ERC 5S camera and photographed by a Nikon ECLIPSE 80i compound microscope fitted with a Canon EOS 600D digital camera. Free hand sections of fruiting bodies were made into slides within water mounts and observed under Motic SMZ 168 stereo microscope. Measurements were taken by Tarosoft Image Frame Work program v. 0.9.7 and images used for figures processed with Adobe Photoshop CS6 Extended v. 13.0 software. Isolations were obtained from single spores as described in Choi et al. (1999). New taxa were established based on recommendations outlined by Jeewon and Hyde (2016). The strains isolated in this study were deposited in Mae Fah Luang University Culture Collection (MFLUCC) and Guizhou Culture Collection (GZCC). Herbarium specimens were deposited at the herbaria of Mae Fah Luang University (MFLU), Chiang Rai, Thailand and Kunming Institute of Botany Academia Sinica (HKAS), Kunming, China. MycoBank numbers (Crous et al. 2004) and Facesoffungi numbers (Jayasiri et al. 2015) are provided.

DNA extraction, PCR amplification and sequencing

Fungal genomic DNA was extracted from fresh mycelia scraped from the margin of a colony on PDA that was incubated at 25 °C–28 °C for 30 days, followed by the Ezup Column Fungi Genomic DNA Purification Kit (Sangon Biotech (Shanghai) Co., Ltd, China) following the manufacturer's instructions. Two partial rDNA genes and two protein coding genes were used in this study: the large subunit of the nuclear ribosomal RNA genes (LSU), the small subunit of the nuclear ribosomal RNA (SSU), the translation elongation factor 1-alpha (*TEF1a*) and the second largest subunit of RNA polymerase II (*RPB2*). The primers used were LR0R and LR5 for LSU (Vilgalys and Hester 1990), NS1/NS4 for SSU (White et al. 1990), EF1-983F/EF1-2218R for *TEF1a* (Rehner and Buckley 2005) and fRPB2-5F/fRPB2-7cR for *RPB2* (Liu et al. 1999). The amplification reactions were performed in 25μL of PCR mixtures containing 9.5μL ddH_2O, 12.5μL 2× PCR MasterMix (TIANGEN Co., China), 1μL DNA temple and 1μL of each primer. The PCR thermal cycle program for LSU, SSU and *TEF1a* amplification were as follows: initial denaturing step of 94 °C for 3 min, followed by 40 cycles of denaturation at 94 °C for 45 seconds, annealing at 56 °C for 50 seconds, elongation at 72 °C for 1 min, and final extension at 72 °C for 10 min. The PCR thermal cycle program for the partial RNA polymerase second largest subunit (*RPB2*) was followed as initially 95 °C for 5 min, followed by 40 cycles of denaturation at 95 °C for 1 min, annealing at 52 °C for 2 min, elongation at 72 °C for 90 seconds, and final extension at 72 °C for 10 min. Purification and sequencing of PCR products were carried out with primers mentioned above at Sangon Biotech (Shanghai) Co., Ltd, China.

Sequence alignment and phylogeny analyses

A concatenated data set of LSU, SSU, *TEF1a* and *RPB2* sequences was used for phylogenetic analyses with the inclusion of reference taxa from GenBank (Table 1). Sequences were aligned using MAFFT v.7 (http://mafft.cbrc.jp/alignment/server/) (Katoh and Standley 2013) and then checked visually and manually optimized using BioEdit v.7.0.9 (Hall 1999). Representative families in Pleosporales and several major groups in Dothideomycetes were included in our analyses, and taxa in Arthoniomycetes were selected as outgroup. A maximum likelihood (ML) analysis was performed at the CIPRES web portal (Miller et al. 2010) using RAxML v.7.2.8 as part of the "RAxML-HPC Blackbox (8.2.10)" tool (Stamatakis 2006, Stamatakis et al. 2008). A general time-reversible model (GTR) was applied with a discrete GAMMA distribution and four rate classes. Fifty thorough ML tree searches were carried out in RAxML v.7.2.7 under the same model. One thousand non-parametric bootstrap iterations were run with the GTR model and a discrete gamma distribution. The resulting replicates were plotted on to the best scoring tree obtained previously.

Table 1. Taxa used in this study and their GenBank accession numbers. The type species of each genus are marked with superscript T and ex-type strains are in bold.

Taxa	Strain / Culture	GenBank Accession numbers			
		LSU	SSU	*TEF1α*	*RPB2*
Acrocordiopsis patilii	BCC28167	GU479773	GU479737	–	GU479812
Acrocordiopsis patilii[T]	BCC28166	GU479772	GU479736	–	GU479811
Acuminatispora palmarum	MFLUCC 18-0460	MH390438	MH390402	MH399249	MH399252
Acuminatispora palmarum[T]	MFLUCC 18-0264	MH390437	MH390401	MH399248	–
Aigialus grandis[T]	BCC18419	GU479774	GU479738	GU479838	GU479813
Aigialus mangrovei	BCC33563	GU479776	GU479741	GU479840	GU479815
Aigialus parvus	BCC 18403	GU479778	GU479744	GU479842	GU479817
Aigialus rhizophorae	BCC 33572	GU479780	GU479745	GU479844	GU479819
Alternaria alternata	CBS 916.96	DQ678082	DQ678031	DQ677927	DQ677980
Amniculicola lignicola[T]	Ying01	EF493861	EF493863	–	EF493862
Anteaglonium abbreviatum[T]	ANM 925a	GQ221877	–	GQ221924	–
Anteaglonium globosum	ANM 925.2	GQ221879	–	GQ221925	–
Antealophiotrema brunneosporum[T]	CBS 123095	LC194340	–	LC194382	LC194419
Aquasubmersa japonica	KT 2862	LC061587	LC061582	–	LC194421
Aquasubmersa mircensis[T]	MFLUCC 11-0401	JX276955	JX276956	–	–
Arthonia dispersa	UPSC2583	AY571381	AY571379	–	–
Ascocratera manglicola[T]	BCC 09270	GU479782	GU479747	GU479846	GU479821
Astrosphaeriella fusispora[T]	MFLUCC 10-0555	KT955462	–	–	KT955413
Astrosphaeriella neofusispora	MFLUCC 11-0161	KT955463	KT955444	–	KT955418
Astrosphaeriella stellata	KT998	AB524592	AB524451	–	–
Astrosphaeriellopsis bakeriana	MFLUCC 11-0027	JN846730	–	–	–
Astrosphaeriellopsis bakeriana[T]	CBS 115556	GU301801	–	GU349015	–
Bimuria novae-zelandiae[T]	CBS 107.79	AY016356	AY016338	DQ471087	DQ470917
Botryosphaeria dothidea	CMW 8000	KF766319	KF766233	–	–
Byssothecium circinans[T]	CBS 675.92	AY016357	–	GU349061	DQ767646
Capnodium coffeae	CBS 147.52	DQ247800	DQ247808	DQ471089	DQ247788
Caryospora minima	–	EU196550	EU196551	–	–
Caryospora aquatica	MFLUCC 11-0008	MH057847	MH057850	–	–
Cladosporium herbarum	CBS 399.80	DQ678074	DQ678022	DQ677918	DQ677971
Cryptocoryneum condensatum	CBS 122629	LC194351	LC194309	LC096139	LC194433
Cryptocoryneum pseudorilstonei	CBS 113641	LC194364	LC194322	LC096152	LC194446
Delitschia chaetomioides	SMH 3253.2	GU390656	–	–	–
Delitschia didyma	UME 31411	DQ384090	AF242264	–	–
Delitschia winteri	CBS 225.62	DQ678077	–	–	DQ677975
Dendrographa decolorans	Ertz 5003 (BR)	NG_027622	AY548809	–	–
Didymella exigua[T]	CBS 183.55	EU754155	EU754056	–	–
Didymosphaeria rubi-ulmifolii	MFLUCC 14-0023	KJ436586	KJ436588	–	–
Dissoconium aciculare	CBS 204.89	GU214419	GU214523	–	–
Dothidotthia aspera	CPC 12933	EU673276	EU673228	–	–
Dothidotthia symphoricarpi[T]	CPC 12929	EU673273	EU673224	–	–
Extremus antarcticus	CCFEE 5312	KF310020	–	–	KF310086
Fissuroma bambusae	MFLUCC 11-0160	KT955468	KT955448	KT955430	KT955417
Halotthia posidoniae[T]	BBH 22481	GU479786	–	–	–
Hermatomyces iriomotensis	MAFF 245730	LC194367	–	LC194394	LC194449
Hypsostroma caimitalense	GKM 1165	GU385180	–	–	–
Hypsostroma saxicola[T]	SMH 5005	GU385181	–	–	–
Hysterium angustatum	CBS 236.34	FJ161180	GU397359	FJ161096	–
Hysterobrevium smilacis	CBS 114601	FJ161174	FJ161135	FJ161091	–
Latorua caligans[T]	CBS 576.65	KR873266	–	–	–

Taxa	Strain / Culture	GenBank Accession numbers			
		LSU	SSU	*TEF1α*	*RPB2*
Latorua grootfonteinensis	CBS 369.72	KR873267	–	–	–
Lecanactis abietina	Ertz 5068 (BR)	AY548812	AY548805	–	–
Longicorpus striataspora[T]	MFLUCC 18-0267	MK035988	MK035973	MK034428	MK034436
Longicorpus striataspora	MFLUCC 18-0268	MK035989	MK035974	MK034429	MK034437
Longicorpus striataspora	MFLUCC 17-2515	MK035990	MK035975	MK034430	MK034438
Longicorpus striataspora	MFLUCC 17-2516	MK035991	MK035976	MK034431	MK034439
Lepidosphaeria nicotiae	CBS 101341	DQ678067	–	–	DQ677963
Leptosphaeria doliolum[T]	CBS 505.75	GU301827	GU296159	GU349069	–
Leptoxyphium fumago	CBS 123.26	GU301831	GU214535	GU349051	GU371741
Ligninsphaeria jonesii	GZCC 15-0080	KU221038	–	–	–
Ligninsphaeria jonesii[T]	MFLUCC 15-0641	KU221037	–	–	–
Lindgomyces cinctosporae	R56-1	AB522431	AB522430	–	–
Lindgomyces ingoldianus[T]	ATCC 200398	AB521736	AB521719	–	–
Lindgomyces rotundatus	KT1096	AB521740	AB521723	–	–
Lophiostoma macrostomoides	GKM1033	GU385190	–	–	–
'Lophiotrema' boreale	CBS 114422	LC194375	–	LC194402	LC194457
Lophiotrema lignicola	CBS 122364	GU301836	GU296166	GU349072	–
Lophiotrema nucula[T]	CBS 627.86	GU301837	GU296167	GU349073	GU371792
Macrodiplodiopsis desmazieri[T]	CPC 24971	KR873272	–	–	–
Massaria anomia	CBS 591.78	GU301839	GU296169	–	GU371769
Massaria gigantispora	M26	HQ599397	HQ599447	HQ599337	–
Massaria inquinans[T]	M19	HQ599402	HQ599444	HQ599342	HQ599460
Massarina eburnea[T]	CBS 473.64	GU301840	GU296170	GU349040	GU371732
Mauritiana rhizophorae[T]	BCC 28866	GU371824	–	GU371817	GU371796
Melanomma pulvis-pyrius[T]	CBS 124080	GU456323	GU456302	GU456265	GU456350
Murispora rubicunda[T]	IFRD 2017	FJ795507	GU456308	–	–
Mycosphaerella graminicola	CBS 292.38	DQ678084	DQ678033	–	DQ677982
Neoastrosphaeriella krabiensis[T]	MFLUCC 11-0025	JN846729	JN846739	–	–
Neodeightonia palmicola	MFLUCC10-0822	HQ199222	HQ199223	–	–
Neotestudina rosatii	CBS 690.82	DQ384107	DQ384069	–	–
Nigrograna mackinnonii[T]	CBS 674.75	GQ387613	–	–	KF015703
Nigrograna marina	CY 1228	GQ925848	–	–	GU479823
Phaeosphaeria oryzae[T]	CBS 110110	GQ387591	GQ387530	–	KF252193
Phoma herbarum[T]	CBS 276.37	DQ678066	DQ678014	DQ677909	DQ677962
Piedraia hortae var. *hortae*	CBS 480.64	GU214466	AY016349	–	DQ677990
Pleomassaria siparia[T]	CBS 279.74	DQ678078	DQ678027	–	DQ677976
Pleospora herbarum[T]	CBS 191.86	DQ247804	DQ247812	DQ471090	DQ247794
Polyplosphaeria fusca[T]	KT 1616	AB524604	AB524463	–	–
Preussia funiculata[T]	CBS 659.74	GU301864	–	–	–
Prosthemium orientale	KT1669	AB553748	AB553641	–	–
Pseudoastrosphaeriella africana	MFLUCC 11-0176	KT955474	KT955454	KT955436	KT955421
Pseudoastrosphaeriella bambusae	MFLUCC 11-0205	KT955475	–	KT955437	KT955414
Pseudoastrosphaeriella longicolla	MFLUCC 11-0171	KT955476	–	KT955438	KT955420
Pseudoastrosphaeriella thailandensis[T]	MFLUCC 11-0144	KT955478	KT955457	KT955440	KT955416
Pseudotetraploa curviappendiculata[T]	HC 4930	AB524608	AB524467	–	–
Quadricrura septentrionalis[T]	HC 4984	AB524616	AB524475	–	–
Racodium rupestre	L346	EU048583	EU048575	–	–
Roccella fuciformis	Tehler 8171	FJ638979	–	–	–
Roussoella nitidula[T]	MFLUCC 11-0182	KJ474843	–	KJ474852	KJ474859
Roussoellopsis macrospora	MFLUCC 12-0005	KJ474847	–	KJ474855	KJ474862

Taxa	Strain / Culture	GenBank Accession numbers			
		LSU	SSU	*TEF1α*	*RPB2*
Salsuginea ramicola	KT2597.2	GU479801	GU479768	GU479862	GU479834
Salsuginea ramicola[T]	KT 2597.1	GU479800	GU479767	GU479861	GU479833
Striatiguttula nypae[T]	MFLUCC 18-0265	MK035992	MK035977	MK034432	MK034440
Striatiguttula nypae	MFLUCC 17-2517	MK035993	MK035978	MK034433	MK034441
Striatiguttula nypae	MFLUCC 17-2518	MK035994	MK035979	MK034434	–
Striatiguttula phoenicis[T]	MFLUCC 18-0266	MK035995	MK035980	MK034435	MK034442
Tetraplosphaeria sasicola[T]	KT563	AB524631	AB524490	–	
Trematosphaeria pertusa[T]	CBS 122371	FJ201992	–	–	GU371801
Triplosphaeria maxima[T]	KT 870	AB524637	AB524496	–	–
Ulospora bilgramii[T]	CBS 101364	DQ678076	DQ678025	DQ677921	DQ677974
Verruculina enalia[T]	BCC 18401	GU479802	–	GU479863	GU479835
Wicklowia aquatica	AF289-1	GU045446	–	–	–
Wicklowia aquatica[T]	F76-2	GU045445	GU266232	–	–
Zopfia rhizophila[T]	CBS 207.26	DQ384104	–	–	–

Abbreviations: **ATCC**: American Type Culture Collection, Virginia, USA; **BBH**: Biotec Bangkok Herbarium, Thailand; **BCC**: BIOTEC Culture Collection, Bangkok, Thailand; **CBS**: Centraal bureau voor Schimmel cultures, Utrecht, The Netherlands; **CPC**: Collection of Pedro Crous housed at CBS; **DAOM**: Plant Research Institute, Department of Agriculture (Mycology), Ottawa, Canada; **GZCC**: Guizhou Culture Collection; **IFRDCC**: Culture Collection, International Fungal Research & Development Centre, Chinese Academy of Forestry, Kunming, China; **JCM**: the Japan Collection of Microorganisms, Japan; **MAFF**: Ministry of Agriculture, Forestry and Fisheries, Japan; **MFLU**: Mae Fah Luang University Herbarium Collection; **MFLUCC**: Mae Fah Luang University Culture Collection, Chiang Rai, Thailand. **ANM**: A.N. Miller; **GKM**: G.K. Mugambi; **JK**: J. Kohlmeyer; **KT**: K. Tanaka; **SMH**: S.M. Huhndorf.

Maximum parsimony (MP) analyses were performed using the heuristic search option with 1000 random taxa additions and tree bisection and reconnection (TBR) as the branch-swapping algorithm. All characters were unordered and of equally weight; gaps were treated as missing data. Maxtrees setting was 1000, and zero-length branches were collapsed, and all parsimonious trees were saved. Clade stability was assessed using a bootstrap (BT) analysis with 1000 replicates, each with 10 replicates of random stepwise addition of taxa (Hillis and Bull 1993). Tree length [TL], Consistency index [CI], Retention index [RI], Rescaled consistency index [RC], Homoplasy index [HI] were calculated.

The Bayesian analysis was performed using PAUP v.4.0b10 (Swofford 2002) and MrBayes v.3.1.2 (Ronquist and Huelsenbeck 2003). The best model for different genes partition in the concatenated data set was determined by MrModeltest 2.3 (Nylander 2004). Posterior probabilities (Rannala and Yang 1996) were determined by Markov Chain Monte Carlo sampling (MCMC) (Larget and Simon 1999) in MrBayes v.3.1.2. Four simultaneous Markov chains were run for 10 million generations and trees were sampled every 1000th generation, thus 10,000 trees were obtained. The suitable burn-in phases were determined by inspecting likelihoods and parameters in Tracer version 1.6 (Rambaut et al. 2013). Based on the tracer analysis, the first 1,000 trees representing 10% were discarded as the burn-in phase in the analysis. The remaining trees were used to calculate posterior probabilities in the majority rule consensus tree (critical value for the topological convergence diagnostic set to 0.01). Phylogenetic tree was visualized by FigTree v.1.4.2 (Rambaut 2014), and the alignment is deposited in TreeBASE under the accession number TB2: S23392 (http://purl.org/phylo/treebase/phylows/study/TB2:S23392).

Divergence times estimates

One secondary data and two fungal fossil calibrations were used in this study. The split between Arthoniomycetes and Dothideomycetes was selected as a secondary calibration point referring to previous evolutionary molecular studies (Gueidan et al. 2011, Prieto and Wedin 2013, Beimforde et al. 2014, Pérez-Ortega et al. 2016, Phukhamsakda et al. 2016), with a mean of 300 MYA and standard deviation (SD) of 50 MYA in a normal posterior distribution. Simultaneously, one ascomycete fossil Metacapnodiaceae (Schmidt et al. 2014), was used as the common ancestor of *Capnodiales*, with constraint of mean 100 MYA and SD 150 MYA in a normal posterior distribution (Pérez-Ortega et al. 2016, Hongsanan et al. 2016, Phukhamsakda et al. 2016, Liu et al. 2017). Whereas the fossil *Margaretbarromyces dictyosporus* (Mindell et al. 2007, Berbee and Taylor 2010, Taylor et al. 2015) was used to calibrate the *Aigialus* (Aigialaceae) crown, with an offset of 35 MYA in a gamma distribution (Phukhamsakda et al. 2016). Divergence time estimates were carried out by BEAST v 1.8.0 (Drummond et al. 2012). Aligned sequence data were partitioned separately for LSU, SSU, *TEF1a* and *RPB2* data set, and loaded to prepare an XML file constructed with BEAUti v1.8.0. The substitution models, clock models and the tree prior parameters were set to be linked. The nucleotide substitution model was set to GTR (Generalized Time Reversible) + Gamma + Invariant sites, with estimated base frequencies, four gamma categories and without partitions. An uncorrelated relaxed clock model (Drummond et al. 2007) with a lognormal distribution of rates for each gene estimate was used for the analyses. We used a Yule tree prior, which assumes a constant speciation rate per lineage, and a randomly generated starting tree. The analysis was run for 100 million generations and parameters were sampled every 10,000 generations. Tracer v.1.6 (Rambaut et al. 2013) was used to analyze the trace files, and the acceptable effective sample sizes (ESS) values were greater than 200. Maximum clade creditability (MCC) trees were annotated using TreeAnnotator v1.8.0 and then visualized in FigTree v.1.4.2 (Rambaut 2014).

Results

Phylogenetic results

The multi-gene dataset comprised 113 taxa and 4113 characters after alignment (LSU: 919 bp; SSU: 1245 bp; *TEF1a*: 929 bp; *RPB2*: 1020 bp) including gaps. RAxML, MP and Bayesian analyses were conducted and resulted in generally congruent topologies, and the familial assignments are similar to previous work (Hashimoto et al. 2017, Liu et al. 2017). Maximum parsimony analyses indicated that 2,302 characters were constant, 355 variable characters parsimony uninformative and 1,456 characters are parsimony-informative. A heuristic search yield four equally most parsimonious trees (TL = 10905, CI = 0.278, RI = 0.561, RC = 0.156, HI = 0.722). The combined dataset provided higher confidence values for the familial level than those of the individual gene trees

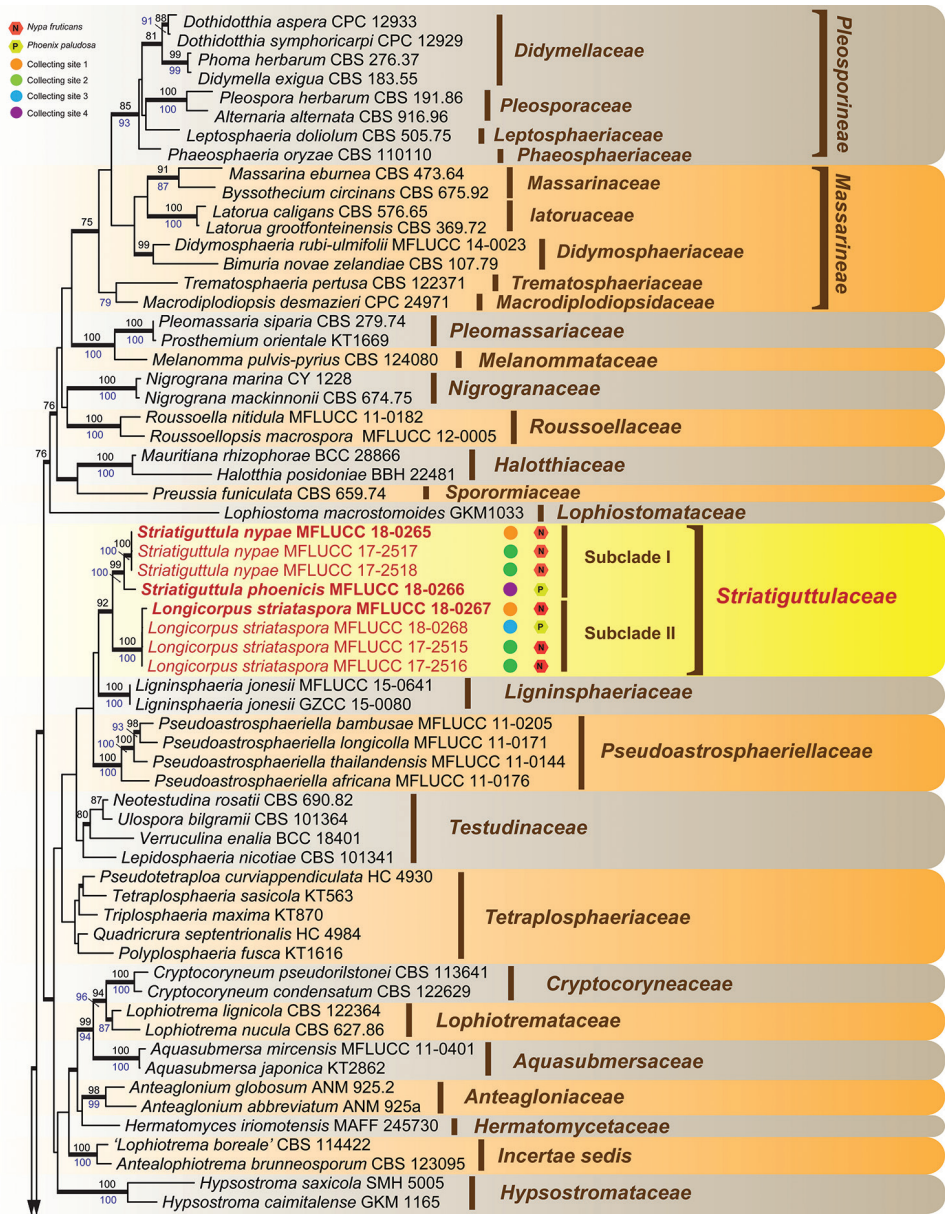

Figure 1. RAxML tree of Pleosporales based on analysis of combined LSU, SSU, *TEF1a* and *RPB2* sequence data. Bootstrap values for ML and MP equal to or greater than 75% are placed above and below the branches respectively. Branches with Bayesian posterior probabilities (PP) from MCMC analysis equal or greater than 0.95 are in bold. Newly generated sequences are indicated in red.

(data not shown), and RAxML analysis based on LSU, SSU, *TEF1a* and *RPB2* yielded a best sorting tree (Figure 1) with a final optimization likelihood value of -52455.532059.

The eight newly generated strains clustered together and positioned outside the two suborders (Massarineae and Pleosporineae) of Pleosporales, and formed a well-supported

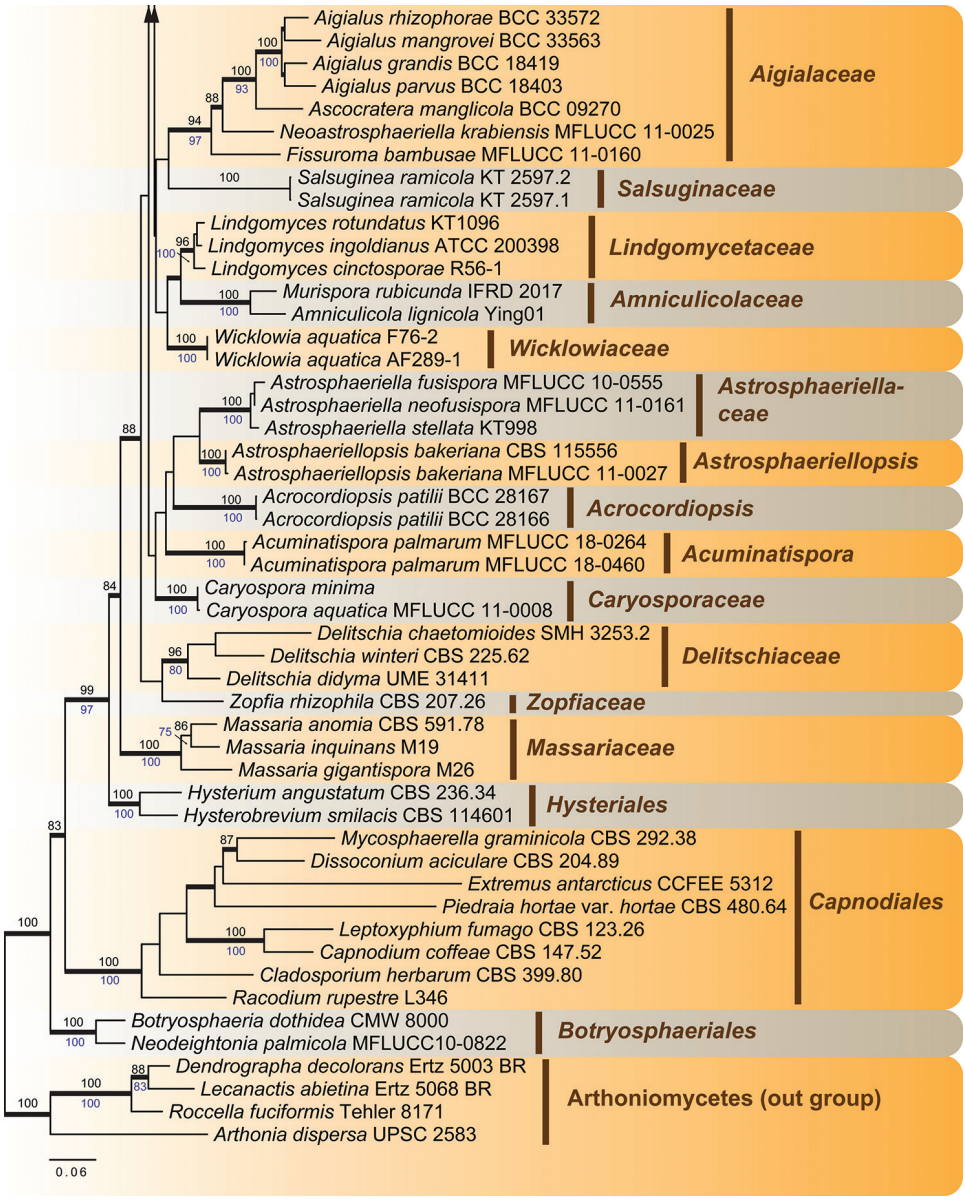

Figure 1. Continued.

monophyletic clade and represented as a new linage of Pleosporales. The phylogeny also revealed that this clade is close to Ligninsphaeriaceae, Pseudoastrosphaeriellaceae, Testudinaceae and Tetraplosphaeriaceae, and can be recognized as a novel family (Striatiguttulaceae). Furthermore, the eight strains formed two well-supported monophyletic sub-clades, which can be identified as two new genera (*Longicorpus* and *Striatiguttula*) with three species (*Longicorpus striataspora*, *Striatiguttula nypae* and *S. phoenicis*).

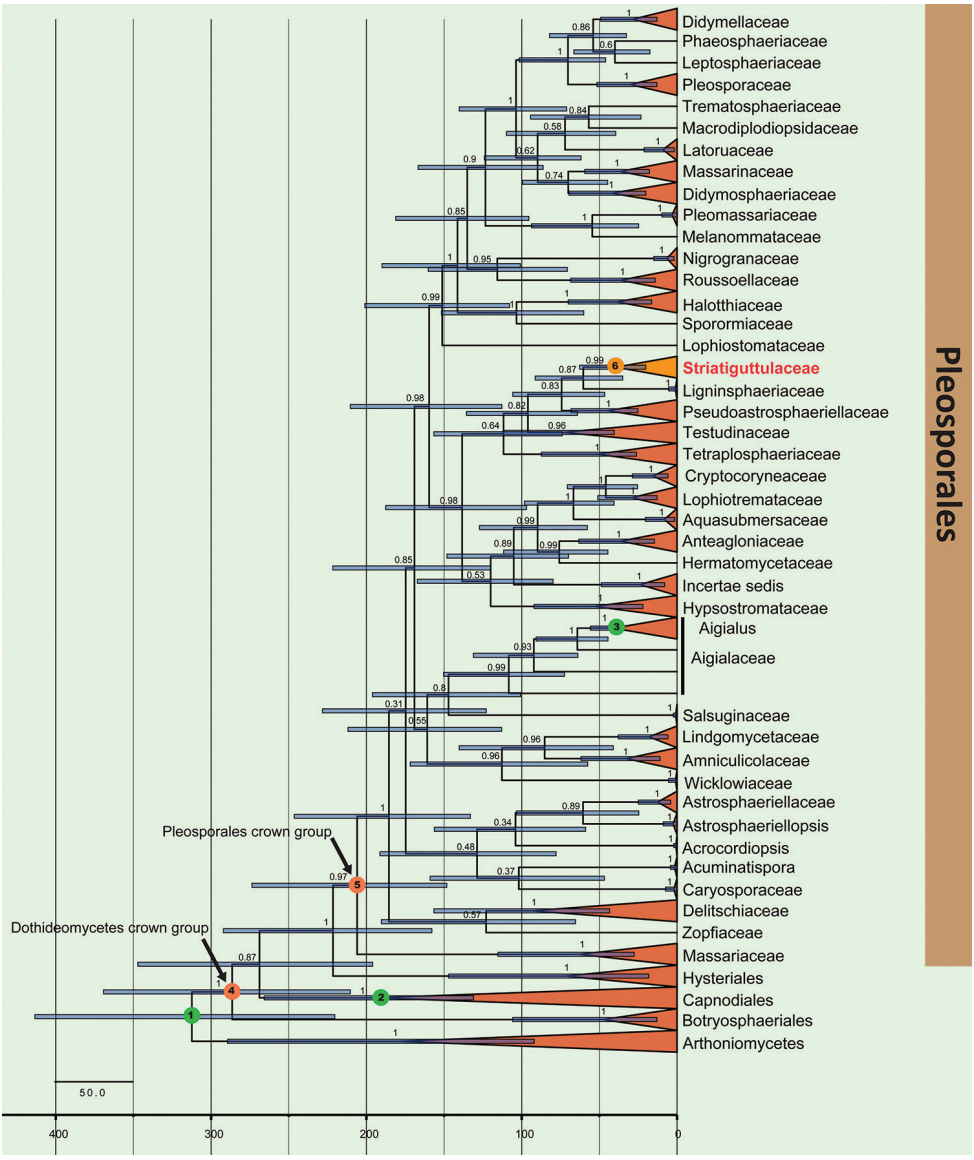

Figure 2. Maximum clade credibility (MCC) tree with divergence times estimates for Pleosporales and selected groups in Dothideomycetes, obtained from a Bayesian approach (BEAST) using one secondary and two fossil calibrations. Numbers at nodes indicate posterior probabilities (pp) for node support; bars correspond to the 95% highest posterior density (HPD) intervals. Numbers inside green circles indicate nodes used for calibrations: 1) the split of Arthoniomycetes and Dothideomycetes; 2) Metacapnodiaceae; 3) *Margaretbarromyces dictyosporus*.

Table 2. Divergence time estimates of Pleosporales and selected lineages of Dothideomycetes obtained from a Bayesian approach (BEAST) on basis of three calibrations. For each divergence, the median and the 95% highest posterior density (HPD) are provided. Divergence times are provided in millions of years (MYA).

Nodes	Crown group	Divergence times				
		This study		Phukhamsakda et al. (2016)	Liu et al. (2017)	Liu et al. (2018)
		Crown age	Stem age	Crown age		
1	Arthoniomycetes-Dothideomycetes	312 (220–413)	–	317	–	310–320
2	*Capnodiales*	195 (131–266)	269 (196–347)	147	216/ (151–283)	~120
3	*Aigialus*	41 (35–56)	64 (44–91)	39	–	~50
4	Dothideomycetes	286 (210–369)	312 (220–413)	293 ~(210–370)	341 (257–425)	255 (166–344)
5	*Pleosporales*	206 (148–274)	221 (158–292)	211 ~(140–270)	204 (148–260)	195 (124–271)
6	Striatiguttulaceae	39 20–63)	60 (35–91)	–	–	–

Divergence time estimates

The maximum clade credibility (MCC) tree with divergence estimates (Figure 2) obtained through BEAST was topologically identical to those recovered by Bayesian and ML procedures with regards to the placement Pleosporales and several major lineages within Dothideomycetes. The mean dates of Pleosporales crown corroborate reported estimates (Phukhamsakda et al. 2016, Liu et al. 2017, 2018) are provided in Table 2. The results showed that the new family Striatiguttulaceae diverged approximately 60 (35–91) MYA, which is line with recommendations for ranking families proposed in related studies (Hyde et al. 2017, Liu et al. 2017).

Taxonomy

Striatiguttulaceae S.N.Zhang, K.D.Hyde & J.K.Liu, fam. nov.
MycoBank: MB828272
Facesoffungi: FoF 05032

Etymology. Name refers to the name of the type genus.

Description. *Saprobic* on palms distributed in mangrove habitats. **Sexual morph**: *Stromata* black, scattered to gregarious, immersed beneath host epidermis, and erumpent to superficial, with a papilla or a short to long neck, ampulliform, subglobose or conical, uni-loculate or bi-loculate, coriaceous to carbonaceous, ostiolate, periphysate, papillate, clypeate or not clear, glabrous or somewhat interwoven pale brown hyphae or setae. *Peridium* composed of several brown to hyaline cell layers. *Hamathecium* of trabeculate pseudoparaphyses. *Asci* 8-spored, bitunicate, cylindric-clavate, pedicellate. *Ascospores* hyaline to brown, uniseriate to biseriate or triseriate, fusiform or ellipsoidal, 1–3-septate, striate, guttulate, with paler end cells and surrounded by a mucilaginous sheath. **Asexual morph**: Undetermined.

Type genus. *Striatiguttula* S.N.Zhang, K.D.Hyde & J.K.Liu.

Notes. The family Striatiguttulaceae is introduced to accommodate two new genera *Longicorpus* and *Striatiguttula*, characterized by the immersed, and erumpent to superficial stromata, with a papilla or a short to long neck, trabeculate pseudoparaphyses, bitunicate asci, and hyaline to brown, fusiform to ellipsoidal, striate, guttulate, 1–3-septate ascospores, with paler end cells and surrounded by a mucilaginous sheath. Members of Striatiguttulaceae are morphologically similar to the genera *Leptosphaeria* and *Trematosphaeria*, but they are phylogenetically distinct and also differ in ascospores characteristics and the latter two have coriaceous, heavily pigmented thick-walled peridium. Multi-gene phylogenetic analyses revealed a close relationship of Striatiguttulaceae to Ligninsphaeriaceae and Pseudoastrosphaeriellaceae. However, Striatiguttulaceae differs from Pseudoastrosphaeriellaceae as the latter has 1–3-septate or 2–5-septate ascospores, which are narrowly fusiform with acute ends and all cells are concolorous. The slit-like ascomata and broad fusiform, 1-septate, rather large ascospores (79–121 × 14–23 µm) in Ligninsphaeriaceae (Zhang et al. 2016) are distinct from those found in Striatiguttulaceae. Additionally, a divergence time estimate analysis indicated that the crown age 39 (20–63) MYA and stem age 60 (35–91) MYA of Striatiguttulaceae, match with the recommendations of using divergence times to recognize families in Liu et al. (2017). Attempts were made to culture the asexual morph in order to build comprehensive familial concept for Striatiguttulaceae, but it was not successful. Further morphological investigations together with more molecular data are needed.

***Striatiguttula* S.N.Zhang, K.D.Hyde & J.K.Liu, gen. nov.**
MycoBank: MB828273
Facesoffungi: FoF 05033

Etymology. Name refers to the striate and guttulate ascospores.

Description. *Saprobic* on palms which are distributed in mangrove habitats. **Sexual morph**: *Stromata* black, scattered to gregarious, immersed beneath host epidermis, and erumpent to superficial, with a papilla or a short to long neck, ampulliform, subglobose or conical, uni-loculate or bi-loculate, coriaceous to carbonaceous, ostiolate, periphysate, papillate, clypeate or not, glabrous or somewhat interwoven pale brown hyphae or setae, lying at apex of the neck. *Peridium* thin, composed of several pale brown to hyaline angular cells. Wall of the neck having elongated angular cells. *Hamathecium* filament thin, trabeculate pseudoparaphyses, septate, branched, anastomosing, embedded in a gelatinous matrix. *Asci* 8-spored, bitunicate, cylindric-clavate, pedicellate, apically rounded, with an ocular chamber. *Ascospores* hyaline to brown, uniseriate to biseriate or triseriate, fusiform to ellipsoidal, 1–3-septate, constrict, the middle cells slightly swollen towards the central septa, striate, guttulate, end cells slightly paler or not, surrounded by a mucilaginous sheath. **Asexual morph**: Undetermined.

Type species. *Striatiguttula nypae* S.N.Zhang, K.D.Hyde & J.K.Liu.

Striatiguttula nypae **S.N.Zhang, K.D.Hyde & J.K.Liu, sp. nov.**
MycoBank number: MB828274
Facesoffungi number: FoF 05034
Figure 3

Etymology. The epithet reflects the genus name of the host plant *Nypa fruticans*, from which the specimens were collected.

Type. THAILAND. Ranong: Ranong, on decayed rachis of *Nypa fruticans* Wurmb (Arecaceae), 3 December 2016, S.N.Zhang, SNT44 (holotype: MFLU 18–1576; isotype: HKAS 97480; ex-type living culture MFLUCC 18–0265 = GZCC 18–0005).

Description. *Saprobic* on mangrove palm *Nypa fruticans*. **Sexual morph**: *Stromata* in vertical section 240–380 μm high, 195–385 μm diameter, ($\bar{x}$ = 318.2 × 289.0 μm, n = 15), black, scattered, gregarious, immersed beneath host epidermis, and erumpent to superficial, with a papilla or short to long neck up to 550 μm, subglobose or conical, uni-loculate or bi-loculate, coriaceous to carbonaceous, ostiolate, periphysate, papillate and clypeate, glabrous or somewhat interwoven pale brown hyphae or with setae, lying at apex of the neck. *Peridium* 9–16 μm thin, composed of several pale brown to hyaline angular cells, compressed and pallid inwardly. Wall of the clypeus composed of brown cells of *textura* epidermoidea and dark brown host tissue. Wall of the neck with thicker and elongated angular cells. *Hamathecium* 1–2 μm wide, trabeculate pseudoparaphyses, septate, branched, filamentous, anastomosing, embedded in a gelatinous matrix. *Asci* 64–145 × 8–17 μm, ($\bar{x}$ = 106.3 × 13.8 μm, n = 30), 8-spored, bitunicate, fissitunicate, cylindric-clavate, pedicellate, apically rounded, with an ocular chamber. *Ascospores* 18–26 × 4–6 μm, ($\bar{x}$ = 22.2 × 5.3 μm, n = 50), hyaline to brown, uniseriate to biseriate or triseriate, fusiform, 1–3-septate, constricted at the central septum, the upper middle cell slightly swollen towards the central septum, straight or slightly curved, striate, guttulate, end cells slightly paler, surrounded by a mucilaginous sheath. **Asexual morph**: Undetermined.

Culture characteristics. Colonies on PDA attaining 15 mm diam. within 21 days at 25 °C under natural light, velvety, centrally raised, greenish grey or greyish olivaceous, reverse dull green or grey olivaceous, with a margin of translucent, milky white to hyaline mycelia.

Additional specimens examined. Thailand. Krabi: near Pali, Mueang Krabi District, on submerged decaying rachis of *Nypa fruticans* Wurmb (Arecaceae), 30 August 2017, S.N.Zhang, SNT207 (paratype: MFLU 18–1577; living culture MFLUCC 17–2517 = GZCC 18–0006); Thailand. Krabi: near Pali, Mueang Krabi District, on submerged decaying rachis of *Nypa fruticans* Wurmb (Arecaceae), 30 August 2017, S.N.Zhang, SNT208 (paratype: MFLU 18–1578; living culture MFLUCC 17–2518 = GZCC 18–0007).

Habitat and distribution. Inhabiting Thai mangrove forests, Andaman sea (west) coastline, Thailand.

Notes. *Striatiguttula nypae* varies in ascomatal appearance, mostly immersed beneath the plant surface, sometimes visible as a papilla or dome-shaped area on the

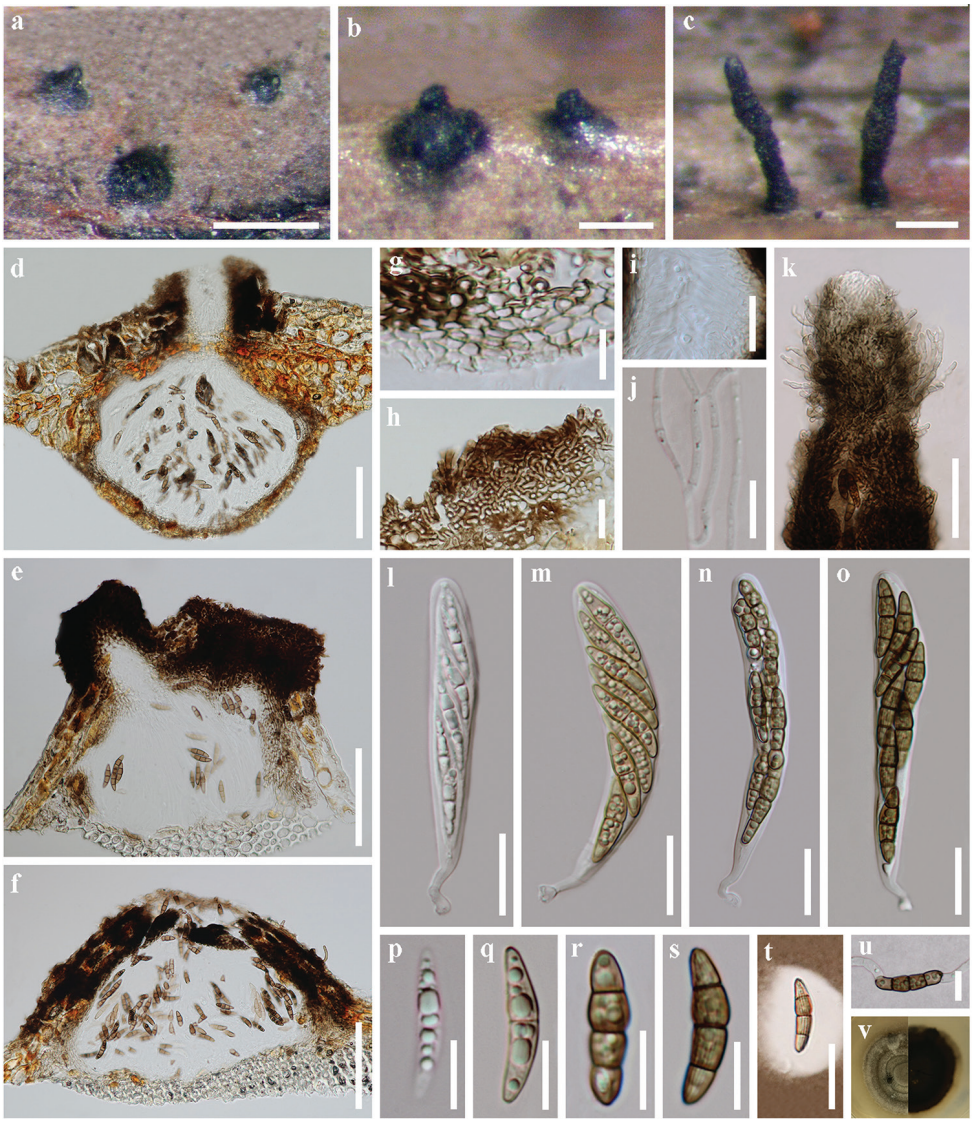

Figure 3. *Striatiguttula nypae* (holotype MFLU 18–1576, paratype MFLU 18–1578). **a–c** Appearance of stromata on host surface **d–f** vertical section through a stroma **g** structure of peridium **h** structure of clypeus near the ostiole, composed of epidermoidea cells and host tissue **i** ostiole with periphyses **j** pseudoparaphyses **k** apex of the neck, with somewhat interwoven pale brown hyphae or setae **l–o** ascus **p–s** ascospores **t** ascospore in India ink and presenting a clear mucilaginous sheath **u** germinating ascospore **v** colony on PDA. Scale bars: 500 μm (**a**), 200 μm (**b, c**), 100 μm (**d–f**), 10 μm (**g, p–s, u**), 20 μm (**h, i, l–o, t**), 50 μm (**k**).

plant surface, and becomes erumpent to superficial, with a papilla or a short to long neck. The typical morphological characters of *S. nypae* are the appearance of stromata, with interwoven pale brown hyphae or setae at the apex of the neck, and the hyaline

Table 3. Morphological comparison of three new species to *Trematosphaeria lineolatispora*, *T. mangrovis* and *T. striataspora*.

Taxa	Ascomata		Peridium (µm)	Pseudoparaphyses (µm)	Asci (µm)	Ascospores		References
	Ascomata morphology	(high × diam. µm)				Ascospores morphology	Ascospores size (µm)	
Longicorpus striataspora	Immersed, erumpent, ampulliform, subglobose or conical, CA	300–500 × 230–560	11–15	1.5	85–160 × 10–17	Fusiform, 1–3-septate, CC	24–45 × 7–8.8	This study
Striatiguttula nypae	Immersed and erumpent to superficial, subglobose or conical, uni-loculate or bi-loculate, CA	240–380 × 195–385	9–16	1–2	64–145 × 8–17	Fusiform, 1–3-septate, CC	18–26 × 4–6	This study
Striatiguttula phoenicis	Immersed, erumpent, ampulliform, subglobose, uni-loculate, CB	195–580 × 135–390	10–24	1–2	89–141 × 12–18	Fusiform to ellipsoidal, 1–3-septate, CC but nearly concolorous	20–29 × 6–10	This study
Trematosphaeria lineolatispora K.D. Hyde	Immersed with a flattened base, conical to subglobose, clypeate, ostiolate, papillate	90–180 × 216–360	up to 25	2–4	120–204 × 14–18	Fusiform, mostly 5-septate; CC	34–48 × 7–10	Hyde 1992b
Trematosphaeria mangrovis Kohlm.	Semi-immersed, conical or subglobose, papillate	380–750 × 450–800	64–88	1.6–2.2	190–220 × 20–22	Broad fusiform or ellipsoidal, 3-septate, CC but no striations	30–35.6–41 × 10–11.8–13 (–16.5)	Kohlmeyer 1968
Trematosphaeria striataspora K.D. Hyde	Developing amongst the host cortical cells beneath the host epidermis, ampulliform, subglobose or conical, CA	176–355 × 352–528	42–57 (clypeus), thin-walled	0.8–2.1	99–173 × 11–23	Fusiform, 3(–6)-septate, CC	31–38 × 6–9	Hyde 1988

CA: (Characteristics A) clypeate, ostiolate, periphysate, papillate;
CB: (Characteristics B) ostiolate, periphysate, papillate;
CC: (Characteristics C) central cells larger, brown, end cells smaller and paler, ascospore wall covered in distinct longitudinal striations, and surrounded by a sheath.

to brown, 1–3-septate, fusiform ascospores, striate, guttulate, with slightly paler end cells and a mucilaginous sheath. We have compared *Striatiguttula nypae* to previously encountered species on *Nypa fruticans*, and several morphologically similar mangrove fungal species. However, the striation of ascospores can be a reliable morphological character to distinguish *Striatiguttula nypae* from *Astrosphaeriella nipicola* (Hyde and Fröhlich 1998), *A. nypae* (Hyde 1992a) and *Leptosphaeria* spp. (Spegazzini 1881, Cribb and Cribb 1955, Hyde et al. 1999, Pang et al. 2011), which are characterized by one or three septa and hyaline or brown ascospores. The presence of erumpent to superficial stromata, the number of septa and size of ascospores in *S. nypae* are also different from *Trematosphaeria* spp. (Table 3), despite being quite similar in ascospore morphology. In addition, the phylogenetic analysis showed that the three isolates of *Striatiguttula nypae* clustered together and were distinct from *S. phoenicis*.

Striatiguttula phoenicis **S.N.Zhang, K.D.Hyde & J.K.Liu, sp. nov.**
MycoBank: MB828275
Facesoffungi: FoF 05035
Figure 4

Etymology. The epithet referring to the host on which the fungus was collected.

Type. THAILAND. Ranong: Amphoe Mueang Ranong, Tambon Ngao, on decayed rachis of *Phoenix paludosa* Roxb. (Arecaceae), 6 December 2016, S.N.Zhang, SNT51 (holotype: MFLU 18–1579; isotype: HKAS 97481; ex-type culture MFLUCC 18–0266 = GZCC 18–0008).

Description. *Saprobic* on mangrove date palm *Phoenix paludosa*. **Sexual morph**: *Ascomata* in vertical section 195–580 µm high, 135–390 µm diameter, ($\bar{x}$ = 396.0 × 230.3 µm, n = 15), black, scattered, rarely gregarious, immersed, and erumpent through host epidermis by a papilla or a short neck, ampulliform, subglobose, uni-loculate, coriaceous to carbonaceous, ostiolate, periphysate, papillate, glabrous or somewhat interwoven pale brown hyphae or setae, lying around apex of the neck. *Peridium* 10–24 µm thin, composed of several pale brown to hyaline cells of *textura angularis*, compressed and pallid inwardly. Wall of the neck composed thick and elongated angular pale brown to brown cells with hyaline inner layers. *Hamathecium* of 1–2 µm wide, septate, branched, filamentous, anastomosing, trabeculate pseudoparaphyses, embedded in a gelatinous matrix. *Asci* 89–141 × 12–18 µm, ($\bar{x}$ = 120.5 × 15.4 µm, n = 20), 8-spored, bitunicate, fissitunicate, cylindric-clavate, pedicellate, apically rounded, with an ocular chamber. *Ascospores* 20–29 × 6–10 µm, ($\bar{x}$ = 24.5 × 7.8 µm, n = 40), hyaline to brown (all cells nearly concolorous), uniseriate to biseriate, fusiform to ellipsoidal, 1–3-septate, constricted at the central septum, the upper middle cell slightly swollen and larger, straight or slightly curved, striate, guttulate, surrounded by an irregular mucilaginous sheath. **Asexual morph**: Undetermined.

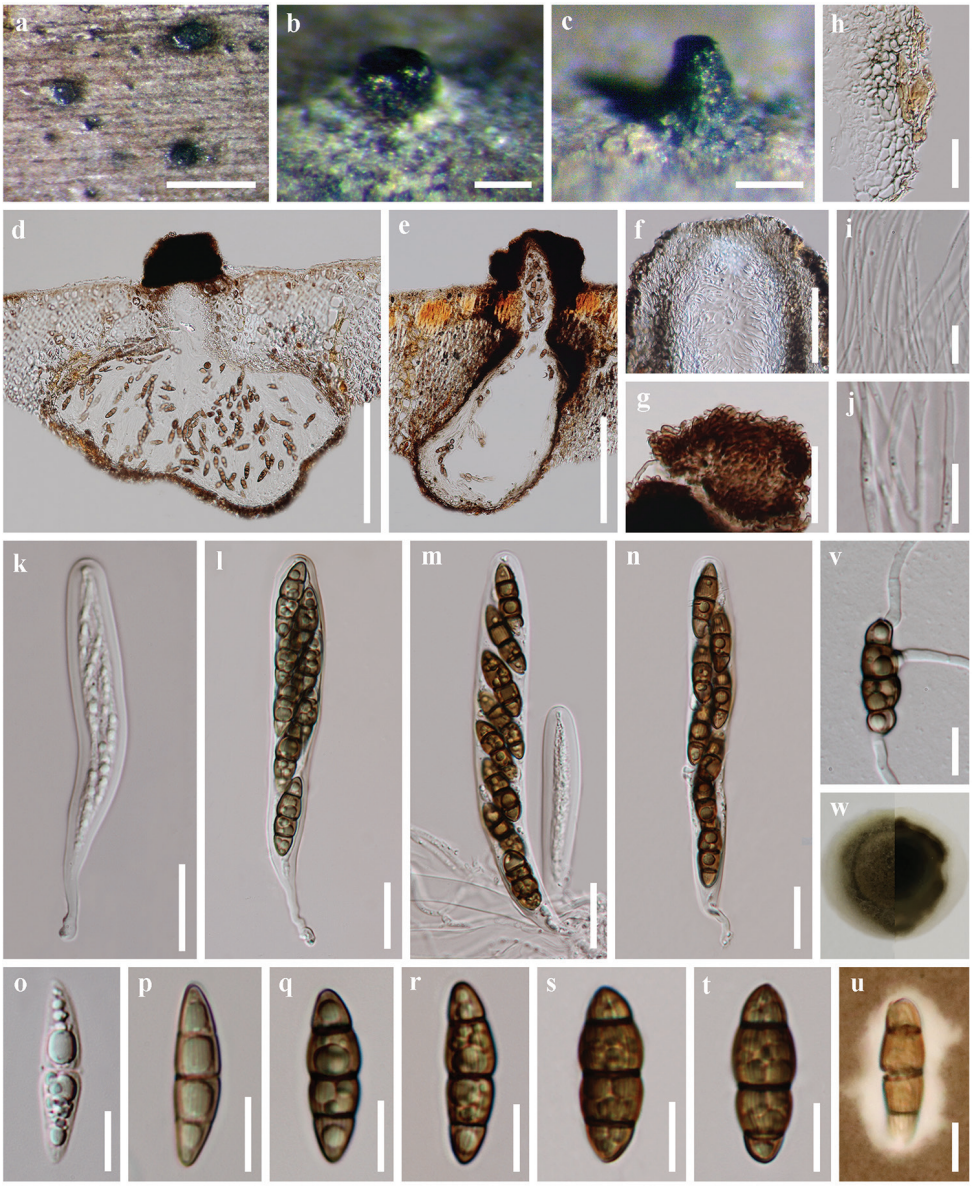

Figure 4. *Striatiguttula phoenicis* (holotype MFLU 18–1579). **a–c** Appearance of ascoma on host surface **d, e** vertical section through an ascoma **f** ostiole **g** apex of the neck, with somewhat interwoven pale brown hyphae or setae **h** structure of peridium **i, j** pseudoparaphyses **k–n** asci **o–t** ascospores **u** ascospore in India ink and presenting a clear mucilaginous sheath **v** germinating ascospore **w** colony on PDA. Scale bars: 500 μm (**a**), 100 μm (**b, c**), 200 μm (**d, e**), 50 μm **(f, g**), 20 μm (**h, k–n**), 10 μm (**i, j, o–v**).

Culture characteristics. Colonies on PDA attaining 14 mm diam within 21 days at 25 °C under natural light, velvety, centrally raised, greenish grey or greyish olivaceous, reverse dull olivaceous or grey, with a margin of translucent, milky white to hyaline mycelium.

Habitat and distribution. Inhabiting Thai mangrove forests, Andaman sea (west) coastline, Thailand.

Notes. The fusiform to ellipsoidal, 1–3-septate ascospores of *Striatiguttula phoenicis* is similar to those of *Trematosphaeria mangrovis*, associated with submerged roots of mangrove trees. However, *Striatiguttula phoenicis* differs from *T. mangrovis* (Kohlmeyer 1968) as the latter has larger ascospores and lacks striations (Table 3). *Striatiguttula phoenicis* is morphologically different from *S. nypae* as it has ellipsoidal ascospores which are broader in width. Currently, the erumpent to superficial stromata have not been found in *S. phoenicis*. The phylogenetic analysis also confirms that they are distinct species. There are 26 noticeable nucleotide differences across the 474 nucleotides (Suppl. material 1) of ribosomal ITS sequence data (strains: MFLUCC 18–0266 vs. MFLUCC 18–0265, MFLUCC 17–2517 and MFLUCC 17–2518).

***Longicorpus* S.N.Zhang, K.D.Hyde & J.K.Liu, gen. nov.**
MycoBank: MB828276
Facesoffungi: FoF 05036

Etymology. Name refers to the elongated ascomata and ascospores.

Description. *Saprobic* on mangrove palms. **Sexual morph**: *Ascomata* black, scattered to gregarious, immersed, and erumpent through host epidermis by a papilla or a short to long neck, sometimes visible as a slightly raised, dome-shaped area, with a clypeus comprises host tissue and fungal hyphae, ampulliform, subglobose or conical, uni-loculate, coriaceous to carbonaceous, ostiolate, periphysate, papillate, glabrous or somewhat interwoven pale brown hyphae or setae. *Peridium* composing of pale brown or brown angular cells. *Hamathecium* of septate, branched, thin, anastomosing trabeculate pseudoparaphyses, embedded in a gelatinous matrix. *Asci* 8-spored, bitunicate, cylindric-clavate, pedicellate, apically rounded, with an ocular chamber. *Ascospores* uniseriate to biseriate, hyaline to brown, fusiform, 1–3-septate, the upper middle cell slightly swollen towards the central septum, and the end cells paler and smaller, striate, guttulate, surrounded by a mucilaginous sheath. **Asexual morph**: Undetermined.

Type species. *Longicorpus striataspora* (K.D.Hyde) S.N.Zhang, K.D.Hyde & J.K.Liu.

Notes. *Longicorpus* differs from *Striatiguttula* in having elongate, fusiform ascospores with relatively larger middle cells and paler end cells (Figures 3–5). Multigene phylogeny also strongly supports the establishment of two genera. *Longicorpus* is sister to *Striatiguttula* but forms a distinct phylogenetic sub-clade (Figure 1). There are noticeable differences (nucleotide substitutions) at specific positions in the large subunit nuclear ribosomal DNA: 51, 428, 436, 465 (T substituted by C); 53, 55, 102, 153, 163, 166, 251, 367, 369, 427, 435, 440, 446, 448, 466, 504, 550, 654 (C substituted by T); 130 (G substituted by A); 362, 406 (G substituted by T); 370 (C substituted by A); 547 (A substituted by C).

Longicorpus striataspora **(K.D.Hyde) S.N.Zhang, K.D.Hyde & J.K.Liu, comb. nov.**
MycoBank: MB828277
Facesoffungi: FoF 05037
Figure 5

Trematosphaeria striataspora K.D.Hyde, Botanical Journal of the Linnean Society 98(2): 142. 1988.

Astrosphaeriella striataspora (K.D.Hyde) K.D.Hyde, Botanical Journal of the Linnean Society 110(2): 97. 1992. Type: North Sumatra. K.D.Hyde (holotype: IMI 312390).

Epitype. THAILAND. Ranong: Ranong, on decayed rachis of *Nypa fruticans* Wurmb (Arecaceae), 6 December 2016, S.N. Zhang, SNT93 (epitype designated here: MFLU 18–1580; epi-isotype designated here: HKAS 97479; ex-epitype living culture MFLUCC 18–0267 = GZCC 18–0009).

Description. *Saprobic* on mangrove palms. **Sexual morph**: *Ascomata* in vertical section (including short papilla) 300–500 µm high, 230–560 µm diameter, ($\bar{x}$ = 405.3 × 376.6 µm, n = 15), long neck up to 1285 µm, black, scattered to gregarious, immersed, and erumpent through host epidermis by a papilla or a short to long neck, sometimes visible as a slightly raised, dome-shaped area, with a clypeus comprises host tissue and fungal hyphae, ampulliform, subglobose or conical, uni-loculate, coriaceous to carbonaceous, ostiolate, periphysate, papillate, glabrous or somewhat interwoven pale brown hyphae or setae, lying at apex of the neck. *Peridium* 11–15 µm wide, composing of brown to pale brown angular cells, thicker at the rim towards the apex. *Hamathecium* comprising up to 1.5 µm wide, septate, branched, filamentous, trabeculate, anastomosing pseudoparaphyses, embedded in a gelatinous matrix. *Asci* 85–160 × 10–17 µm ($\bar{x}$ = 122.7 × 13.7 µm, n = 22), 8-spored, bitunicate, cylindric-clavate, pedicellate, apically rounded, with an ocular chamber. *Ascospores* 24–45 × 7–8.8 µm, ($\bar{x}$ = 34.2 × 7 µm, n = 40), uniseriate to biseriate, hyaline to brown, fusiform, 1–3-septate, the upper middle cell slightly swollen towards the central septate, middle cells larger and longer, end cells paler and smaller, straight or slightly curved, striate, guttulate, surrounded by a mucilaginous sheath. **Asexual morph**: Undetermined.

Culture characteristics. Colonies on PDA attaining 12 mm diameter within 21 days at 25 °C under natural light, velvety, centrally raised, irregular to circular in shape, greenish grey and mixed with milky white mycelium at the edge of a colony, the reverse dull green or grey olivaceous.

Additional specimens examined. Thailand. Chanthaburi, 12°26'43"N, 102°15'47"E, on rachis of *Phoenix paludosa* Roxb. (Arecaceae), immersed mangrove mud and water, 25 April 2017, S.N.Zhang, SNT130 (epi-paratype MFLU 18–1581; living culture MFLUCC 18–0268 = GZCC 18–0010); Thailand. Krabi, near Pali, on decayed rachis of *Nypa fruticans* Wurmb (Arecaceae), immersed mangrove mud and water, 30 August 2017, S.N.Zhang, SNT195 (epi-paratype MFLU 18–1582; living culture MFLUCC 17–2515 = GZCC 18–0011; MFLUCC 17–2516 = GZCC 18–0012).

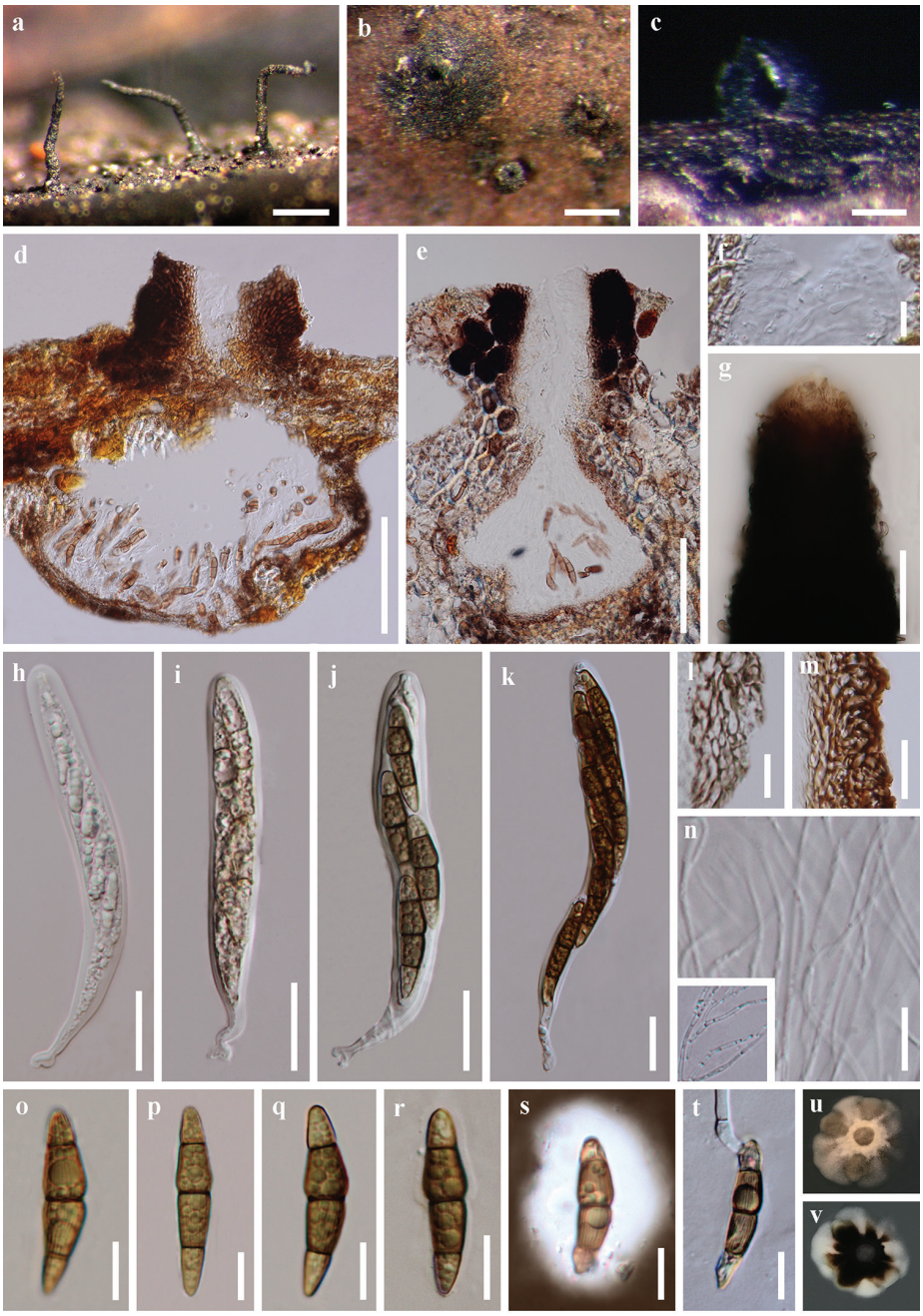

Figure 5. *Longicorpus striataspora* (epitype MFLU 18–1580, epi-paratype MFLU 18–1582). **a, b** Appearance of ascoma on host surface **c–e** vertical section through an ascoma, with a clypeus near the ostiole **f** ostiole with periphyses **g** apex of the neck, with somewhat interwoven pale brown hyphae or setae **h–k** ascus **l** peridium in vertical section **m** vertical section of the neck, with thicker angular cells **n** pseudoparaphyses **o–r** ascospores **s** ascospore in India ink and presenting a clear mucilaginous sheath **t** germinating ascospore **u, v** Colony on PDA. Scale bars: 500 μm (**a**), 200 μm (**b**), 100 μm (**c–e**), 10 μm (**f, l, n–t**), 50 μm (**g**), 20 μm (**h–k, m**).

Habitat and distribution. Inhabiting in Thai mangrove forests, the Andaman sea (west) coastline and the Gulf of Thailand (east).

Notes. *Longicorpus striataspora* was found on two mangrove palm species, *Nypa fruticans* and *Phoenix paludosa*. The typical characteristics of *L. striataspora* are the deeply immersed, carbonaceous ascomata with a long neck, and the striate, guttulate, fusiform, 1–3-septate ascospores, with larger middle cells and relatively smaller and paler end cells, surrounded by a mucilaginous sheath. However, such characteristics are similar to *Trematosphaeria* spp. (Table 3), and match with *Trematosphaeria striataspora* (Hyde 1988), the holotype collected from intertidal wood of *Nypa fruticans* in North Sumatra. *Trematosphaeria striataspora* was later accommodated in *Astrosphaeriella* Syd. & P. Syd. (Hyde 1992a) with proposals for recollection and further phylogenetic studies (Liu et al. 2011b, Phookamsak et al. 2015). We have compared the fresh collections of *Longicorpus striataspora* with the type material of *Trematosphaeria striataspora*, and concluded that the two are identical in morphology. On the other hand, the genus *Trematosphaeria* Fuckel has been assigned to the family Trematosphaeriaceae K.D. Hyde, Y. Zhang ter, Suetrong & E.B.G. Jones, based on molecular data of its type species *T. pertusa* Fuckel. Therefore, we follow Ariyawansa et al. (2014) and designate an epitype for *Longicorpus striataspora* in this study.

Discussion

A novel pleosporalean family, Striatiguttulaceae is introduced herein, which has been compared to several morphologically similar genera and species recovered from mangroves. This study introduces three novel species including an epitypification. The use of divergence times as an additional evidence for ranking taxa (especially in higher taxa ranking) has become possible and several studies have been carried out across different fungal groups (Phukhamsakda et al. 2016, Samarakoon et al. 2016, Divakar et al. 2017, Hongsanan et al. 2017, Hyde et al. 2017, Liu et al. 2017, Zhao et al. 2017). To better understand the placement of Striatiguttulaceae, divergence time was also estimated and this study supports taxonomic schemes proposed earlier. The recent study of ranking a family with divergence time estimates is Liu et al. (2018), who introduced Lentimurisporaceae, a new pleosporalean family. We have recovered essentially similar phylogenetic topology, and in an extensive dataset that included berkleasmium-like taxa (referred to Liu et al. 2018), phylogenies generated were also topologically identical to those recovered herein (Figure 1). The monotypic family Ligninsphaeriaceae is sister to Striatiguttulaceae, and berkleasmium-like taxa are close to Aquasubmersaceae, Hermatomycetaceae and Salsuginaceae respectively. In this study, the ages of most families in Pleosporales, especially those positioned outside the two suborders were estimated in our divergence time analysis, and the results are comparable to other studies. However, Ligninsphaeriaceae, Pseudoastrosphaeriellaceae and Testudinaceae have relatively younger stem ages than that in Liu et al. (2017), presumably due to different taxa sampling in our phylogeny.

The nature of the pseudoparaphyses (*sensu* Liew et al. 2000) is worth considering here and may provide evidence for separate lineages. The family Striatiguttulaceae, currently with three species, have trabeculate pseudoparaphyses, but also appearing septate. Phylogenetically closely related families of Ligninsphaeriaceae and Pseudoastrosphaeriellaceae are characterized by cellular pseudoparaphyses and trabeculate pseudoparaphyses respectively.

Considering the ecology of these Striatiguttulaceae species in relation to the mangrove ecosystem, salinity may be an important contributor to their presence. Loilong et al. (2012) have compared fungal community from *Nypa fruticans* at different salinities, and found freshwater species in lower salinity and marine species at higher salinity. Although no salinity was measured during our collections, *Longicorpus striataspora*, *Striatiguttula nypae* and *S. phoenicis* can be considered as manglicolous, because they are found from decayed rachides/petioles of palms, which are perennials submerged in soft mangrove mud and salty water, and well adapted to the varying salinity in mangroves by tidal water. On the other hand, their ascospores have mucilaginous sheaths and lack elaborate appendages, which are also typical characteristics of most mangrove fungi (Jones 2000).

Acknowledgements

We are grateful to the grant the Thailand Research Fund for supporting collection and research facilities (Grant No. RSA5980068). Jian-Kui Liu thanks the National Natural Science Foundation of China (NSFC 31600032) and Science and Technology Foundation of Guizhou Province (LH [2015]7061). Kevin D. Hyde would like to thank the Thailand Research Grants (No. RDG6130001 and No. 60201000201). The authors would like to thank the staff of Ngao Mangrove Forest Research Center for their assistance in the sample's collection. We are also grateful to Dr. Shaun Pennycook (Manaaki Whenua Landcare Research, New Zealand) for advising on fungal nomenclature. Ning-Guo Liu is acknowledged for assisting in molecular experiments. We also thank the University of Mauritius for its support.

References

Ariyawansa HA, Hawksworth DL, Hyde KD, Jones EBG, Maharachchikumbura SSN, Manamgoda DS, Thambugala KM, Udayanga D, Camporesi Erio, Daranagama A, Jayawardena R, Liu JK, McKenzie EHC, Phookamsak R, Senanayake IC, Shivas RG, Tian Q, Xu JC (2014) Epitypification and neotypification: guidelines with appropriate and inappropriate examples. Fungal Diversity 69: 57–79. https://doi.org/10.1007/s13225-014-0315-4

Beimforde C, Feldberg K, Nylinder S, Rikkinen J, Tuovila H, Dörfelt H, Gube M, Jackson DJ, Reitner J, Seyfullah LJ, Schmidt AR (2014) Estimating the Phanerozoic history of the Ascomycota lineages: combining fossil and molecular data. Molecular Phylogenetics and Evolution 78: 386–398. https://doi.org/10.1016/j.ympev.2014.04.024

Berbee ML, Taylor JW (2010) Dating the molecular clock in fungi – how close are we? Fungal Biology Reviews 24: 1–16. https://doi.org/10.1016/j.fbr.2010.03.001

Choi YW, Hyde KD, Ho W (1999) Single spore isolation of fungi. Fungal Diversity 3: 29–38.

Cribb AB, Cribb JW (1955) Marine fungi from Queensland-1. University Queensland Papers, Department of Botany 3: 77–81.

Crous PW, Gams W, Stalpers JA, Robert V, Stegehuis G (2004) MycoBank: an online initiative to launch mycology into the 21st century. Studies in Mycology 50(1): 19–22.

Divakar PK, Crespo A, Kraichak E, Leavitt SD, Singh G, Schmitt I, Lumbsch HT (2017) Using a temporal phylogenetic method to harmonize family- and genus-level classification in the largest clade of lichen-forming fungi. Fungal Diversity 84: 101–117. https://doi.org/10.1007/s13225-017-0379-z

Drummond AJ, Rambaut A (2007) BEAST: Bayesian evolutionary analysis by sampling trees. BMC Evolutionary Biology 7: 214. https://doi.org/10.1186/1471-2148-7-214

Drummond AJ, Suchard MA, Xie D, Rambaut A (2012) Bayesian phylogenetics with BEAUti and the BEAST 1.7. Molecular biology and evolution 29(8): 1969–1973. https://doi.org/10.1093/molbev/mss075

Elliott ML, Des Jardin EAD, O'Donnell K, Geiser DM, Harrison NA, Broschat TK (2010) *Fusarium oxysporum* f. sp. *palmarum*, a novel forma specialis causing a lethal disease of *Syagrus romanzoffiana* and *Washingtonia robusta* in Florida. Plant Disease 94: 31–38. https://doi.org/10.1094/PDIS-94-1-0031

Fröhlich J, Hyde KD, Guest DI (1997) Fungi associated with leaf spots of palms in north Queensland, Australia. Mycological Research 101(6): 721–732. https://doi.org/10.1017/S095375629600322X

Fröhlich J, Hyde KD (1999) Biodiversity of palm fungi in the tropics: are global fungal diversity estimates realistic? Biodiversity and Conservation 8: 977–1004. https://doi.org/10.1023/A:1008895913857

Fröhlich J, Hyde KD (2000) Palm microfungi. Fungal Diversity Press, 393 pp.

Fröhlich J, Hyde KD, Petrini O (2000) Endophytic fungi associated with palms. Mycological Research 104(10): 1202–1212. https://doi.org/10.1017/S095375620000263X

Goh TK, Hyde KD (1996) A new species of *Nectria* on *Mauritia flexuosa* (Arecaceae) in Ecuador and a key to *Nectria* and allied genera on palms. Mycoscience 37: 277–282. https://doi.org/10.1007/BF02461298

Gueidan C, Ruibal C, De Hoog GS, Schneider H (2011) Rock-inhabiting fungi originated during periods of dry climate in the late Devonian and middle Triassic. Fungal biology 115: 987–996. https://doi.org/10.1016/j.funbio.2011.04.002

Hall TA (1999) BioEdit: a user-friendly biological sequence alignment editor and analysis program for Windows 95/98/NT. Nucleic Acids Symposium Series 41:95–98.

Hashimoto A, Matsumura M, Hirayama K, Tanaka K (2017) Revision of Lophiotremataceae (*Pleosporales*, *Dothideomycetes*): Aquasubmersaceae, Cryptocoryneaceae, and Hermatomycetaceae fam. nov. Persoonia 39: 51–73. https://doi.org/10.3767/persoonia.2017.39.03

Hawksworth DL (1991) The fungal dimension of biodiversity: magnitude, significance, and conservation. Mycological Research 95(6): 641–655. https://doi.org/10.1016/S0953-7562(09)80810-1

Hidayat I, Jeewon R, To-anua C, Hyde KD (2006) The genus *Oxydothis*: new palmicolous taxa and phylogenetic relationships within the *Xylariales*. Fungal Diversity 23: 159–179.

Hillis DM, Bull JJ (1993) An empirical test of bootstrapping as a method for assessing confidence in phylogenetic analysis. Systematic Biology 42(2): 182–192. https://doi.org/10.1093/sysbio/42.2.182

Hongsanan S, Sánchez-Ramirez S, Crous PW, Ariyawansa HA, Zhao RL, Hyde KD (2016) The evolution of fungal epiphytes. Mycosphere 7(11): 1690–1712. https://doi.org/10.5943/mycosphere/7/11/6

Hongsanan S, Maharachchikumbura SS, Hyde KD, Samarakoon MC, Jeewon R, Zhao Q, Al-Sadi AM, Bahkali AH (2017) An updated phylogeny of Sordariomycetes based on phylogenetic and molecular clock evidence. Fungal Diversity 84: 25–41. https://doi.org/10.1007/s13225-017-0384-2

Hyde KD, Goh TK, Lu BS, Alias SA (1999) Eleven new intertidal fungi from *Nypa fruticans*. Mycological Research 103(11): 1409–1422. https://doi.org/10.1017/S0953756299008667

Hyde KD, Sarma VV (2006) Biodiversity and ecological observations on filamentous fungi of mangrove palm *Nypa fruticans* Wurumb (Liliopsida–Arecales) along the Tutong River, Brunei. Indian Journal of Marine Sciences 35(4): 297–307.

Hyde KD, Chaiwan N, Norphanphoun C, Boonmee S, Camporesi E, Chethana KWT, Dayarathne MC, de Silva NI, Dissanayake AJ, Ekanayaka AH, Hongsanan S, Huang SK, Jayasiri SC, Jayawardena RS, Jiang HB, Karunarathna A, Lin CG, Liu JK, Liu NG, Lu YZ, Luo ZL, Maharachchikumbura SSN, Manawasinghe IS, Pem D, Perera RH, Phukhamsakda C, Samarakoon MC, Senwanna C, Shang QJ, Tennakoon DS, Thambugala KM, Tibpromma S, Wanasinghe DN, Xiao YP, Yang J, Zeng XY, Zhang JF, Zhang SN, Bulgakov TS, Bhat DJ, Cheewangkoon R, Goh TK, Jones EBG, Kang JC, Jeewon R, Liu ZY, Lumyong S, Kuo CH, Mckenzie EHC, Wen TC, Yan JY, Zhao Q (2018) Mycosphere notes 169–224. Mycosphere 9(2): 271–430. https://doi.org/10.5943/mycosphere/9/2/8

Hyde KD (1992a) Fungi from decaying intertidal fronds of *Nypa fruticans*, including three new genera and four new species. Botanical Journal of the Linnean Society 110: 95–110. https://doi.org/10.1111/j.1095-8339.1992.tb00284.x

Hyde KD (1992b) Intertidal mangrove fungi from the west coast of Mexico, including one new genus and two new species. Mycological Research 96(1): 25–30. https://doi.org/10.1016/S0953-7562(09)80992-1

Hyde KD (1988) Studies on the tropical marine fungi of Brunei. Botanical Journal of the Linnean Society 98: 135–151. https://doi.org/10.1111/j.1095-8339.1988.tb01700.x

Hyde KD, Fröhlich J (1998) Fungi from palms XXXVII. The genus *Astrosphaeriella*, including ten new species. Sydowia 50(1): 81–132.

Hyde KD, Cannon PF (1999) Fungi causing tar spots on palms. Mycological Papers 175: 1–114.

Hyde KD, Alias SA (2000) Biodiversity and distribution of fungi associated with decomposing *Nypa fruticans*. Biodiversity and Conservation 9: 393–402. https://doi.org/10.1023/A:1008911121774

Hyde KD, Taylor JE, Fröhlich J (2000) Genera of Ascomycetes from palm. Fungal Diversity Press, 1–247.

Hyde KD, Bussaban B, Paulus B, Crous PW, Lee S, Mckenzie EHC, Photita W, Lumyong S (2007) Diversity of saprobic microfungi. Biodiversity and Conservation 16: 7–35. https://doi.org/10.1007/s10531-006-9119-5

Hyde KD, Soytong K (2008) The fungal endophyte dilemma. Fungal Diversity 33: 163–173.

Hyde KD, Maharachchikumbura SSN, Hongsanan S, Samarakoon MC, Lücking R, Pem D, Harishchandra D, Jeewon R, Zhao RL, Xu JC (2017) The ranking of fungi: a tribute to David L. Hawksworth on his 70th birthday. Fungal Diversity 84: 1–23. https://doi.org/10.1007/s13225-017-0383-3

Jayasiri SC, Hyde KD, Ariyawansa HA, Bhat J, Buyck B, Cai L, Dai YC, Abd-Elsalam KA, Ertz D, Hidayat I, Jeewon R, Jones EBG, Bahkali AH, Karunarathna SC, Liu JK, Luangsa-ard JJ, Lumbsch HT, Maharachchikumbura SSN, McKenzie EHC, Moncalvo JM, Ghobad-Nejhad M, Nilsson H, Pang KL, Pereira OL, Phillips AJL, Raspé O, Rollins AW, Romero AI, Etayo J, Selçuk F, Stephenson SL, Suetrong S, Taylor JE, Tsui CKM, Vizzini A, Abdel-Wahab MA, Wen TC, Boonmee S, Dai DQ, Daranagama DA, Dissanayake AJ, Ekanayaka AH, Fryar SC, Hongsanan S, Jayawardena RS, Li WJ, Perera RH, Phookamsak R, de Silva NI, Thambugala KM, Tian Q, Wijayawardene NN, Zhao RL, Zhao Q, Kang JC, Promputtha I (2015) The Faces of Fungi database: fungal names linked with morphology, phylogeny and human impacts. Fungal Diversity 74: 3–18. https://doi.org/10.1007/s13225-015-0351-8

Jeewon R, Hyde KD (2016) Establishing species boundaries and new taxa among fungi: recommendations to resolve taxonomic ambiguities. Mycosphere 7(11): 1669–1677. https://doi.org/10.5943/mycosphere/7/11/4

Jones EBG, Hyde KD (1988) Methods for the study of mangrove marine fungi from the mangroves. In: Agate AD, Subramanian CV, Vannucci M (Eds) Mangrove microbiology. Role of Microorganisms in Nutrient Cycling of Mangrove Soils and Waters. UNDP/UNESCO, New Delhi, 9–27.

Jones EBG (2000) Marine fungi: some factors influencing biodiversity. Fungal Diversity 4: 53–73.

Katoh K, Standley DM (2013) MAFFT multiple sequence alignment software version 7: improvements in performance and usability. Molecular Biology and Evolution 30(4): 772–780. https://doi.org/10.1093/molbev/mst010

Kohlmeyer J (1968) A new *Trematosphaeria* from roots of *Rhizophora racemosa*. Mycopathologia et Mycologia Applicata 34: 1–5. https://doi.org/10.1007/BF02050837

Konta S, Hongsanan S, Phillips AJL, Jones EBG, Boonmee S, Hyde KD (2016a) Botryosphaeriaceae from palms in Thailand II – two new species of *Neodeightonia*, *N. rattanica* and *N. rattanicola* from *Calamus* (rattan palm). Mycosphere 7(7): 950–961. https://doi.org/10.5943/mycosphere/si/1b/6

Konta S, Hongsanan S, Tibpromma S, Thongbai B, Maharachchikumbura SSN, Bahkali AH, Hyde KD, Boonmee S (2016b) An advance in the endophyte story: Oxydothidaceae *fam. nov*. with six new species of *Oxydothis*. Mycosphere 7(9): 1425–1446. https://doi.org/10.5943/mycosphere/7/9/15

Konta S, Phillips AJL, Bahkali AH, Jones EBG, Eungwanichayapant DP, Hyde KD, Boonmee S (2016c) Botryosphaeriaceae from palms in Thailand – *Barriopsis archontophoenicis* sp. nov, from *Archontophoenix alexandrae*. Mycosphere (special issue): 921–932.

Konta S, Hongsanan S, Eungwanichayapant PD, Liu JK, Jeewon R, Hyde KD, Maharachchikumbura SSN, Boonmee S (2017) *Leptosporella* (Leptosporellaceae fam. nov.) and *Linocarpon* and *Neolinocarpon* (Linocarpaceae fam. nov.) are accommodated in Chaetosphaeriales. Mycosphere 8(10): 1943–1974. https://doi.org/10.5943/mycosphere/8/10/16

Larget B, Simon DL (1999) Markov chain Monte Carlo algorithms for the Bayesian analysis of phylogenetic trees. Molecular Biology and Evolution 16(6): 750–759. https://doi.org/10.1093/oxfordjournals.molbev.a026160

Liew ECY, Aptroot A, Hyde KD (2000) Phylogenetic significance of the pseudoparaphyses in Loculoascomycete taxonomy. Molecular Phylogeny and Evolution 16(3): 392–402. https://doi.org/10.1006/mpev.2000.0801

Liu JK, Chomnunti P, Cai L, Phookamsak R, Chukeatirote E, Jones EBG, Moslem M, Hyde KD (2010) Phylogeny and morphology of *Neodeightonia palmicola* sp. nov. from palms. Sydowia 62(2): 261–276.

Liu JK, Jones EBG, Chukeatirote E, Bahkali AH, Hyde KD (2011a) *Lignincola conchicola* from palms with a key to the species of *Lignincola*. Mycotaxon 117: 343–349. https://doi.org/10.5248/117.343

Liu JK, Phookamsak R, Jones EBG, Zhang Y, Ko-Ko TW, Hu HL, Boonmee S, Doilom M, Chukeatirote E, Bahkali AH, Wang Y, Hyde KD (2011b) *Astrosphaeriella* is polyphyletic, with species in *Fissuroma* gen. nov., and *Neoastrosphaeriella* gen. nov. Fungal Diversity 51: 135–154. https://doi.org/10.1007/s13225-011-0142-9

Liu JK, Phookamsak R, Doilom M, Wikee S, Li YM, Ariyawansha H, Boonmee S, Chomnunti P, Dai DQ, Bhat JD, Romero AI, Zhuang WY, Monkai J, Jones EBG, Chukeatirote E, Ko Ko TW, Zhao YC, Wang Y, Hyde KD (2012) Towards a natural classification of *Botryosphaeriales*. Fungal Diversity 57: 149–210. https://doi.org/10.1007/s13225-012-0207-4

Liu JK, Phookamsak R, Dai DQ, Tanaka K, Jones EBG, Xu JC, Chukeatirote E, Hyde KD (2014) Roussoellaceae, a new pleosporalean family to accommodate the genera *Neoroussoella* gen. nov., *Roussoella* and *Roussoellopsis*. Phytotaxa 181(1): 1–33. https://doi.org/10.11646/phytotaxa.181.1.1

Liu JK, Hyde KD, Jeewon R, Phillips AJL, Maharachchikumbura SSN, Ryberg M, Liu ZY, Zhao Q (2017) Ranking higher taxa using divergence times: a case study in Dothideomycetes. Fungal Diversity 84: 75–99. https://doi.org/10.1007/s13225-017-0385-1

Liu NG, Lin CG, Liu JK, Samarakoon MC, Hongsanan S, Bhat DJ, Hyde KD, McKenzie EHC, Jumpathong J (2018) Lentimurisporaceae, a new Pleosporalean family with divergence times estimates. Cryptogamie, Mycologie 39(2): 259–282. https://doi.org/10.7872/crym/v39.iss2.2018.259

Liu YJ, Whelen S, Hall BD (1999) Phylogenetic relationships among ascomycetes: evidence from an RNA polymerse II subunit. Molecular Biology and Evolution 16(12): 1799–1808. https://doi.org/10.1093/oxfordjournals.molbev.a026092

Loilong A, Sakayaroj J, Rungjindamai N, Choeyklin R, Jones EBG (2012) Biodiversity of fungi on the palm *Nypa fruticans*. In: Jones EBG, Pang KL (Eds) Marine Fungi: and Fungal-like Organisms, De Gruyter, Berlin, 273–290. https://doi.org/10.1515/9783110264067.273

Mahmoud FM, Krimi Z, Maciá-Vicente JG, Errahmani MB, Lopez-Llorca LV (2017) Endophytic fungi associated with roots of date palm (*Phoenix dactylifera*) in coastal dunes. Revista Iberoamericana de Micología 34:116–120. https://doi.org/10.1016/j.riam.2016.06.007

Miller MA, Pfeiffer W, Schwartz T (2010) Creating the CIPRES Science Gateway for inference of large phylogenetic trees. In: Proceedings of the Gateway Computing Environments Workshop (GCE) 2010, New Orleans, Louisiana, 1–8. https://doi.org/10.1109/GCE.2010.5676129

Mindell RA, Stockey RA, Beard G, Currah RS (2007) *Margaretbarromyces dictyosporus* gen. sp. nov.: a permineralized corticolous ascomycete from the Eocene of Vancouver Island, British Columbia. Mycological Research III: 680–684. https://doi.org/10.1016/j.mycres.2007.03.010

Mohammadi H (2014) *Phaeoacremonium* spp. and *Botryosphaeriaceae* spp. associated with date palm (*Phoenix dactylifera* L.) decline in Iran. Journal of Phytopathology 162: 575–581. https://doi.org/10.1111/jph.12229

Nylander JAA (2004) MrModeltest v2. Program distributed by the author. Evolutionary Biology Centre, Uppsala University.

Pang KL, Jheng JS, Jones EBG (2011) Marine mangrove fungi of Taiwan. National Taiwan Ocean University

Pérez-Ortega S, Garrido-Benavent I, Grube M, Olmo R, de los Ríos A (2016) Hidden diversity of marine borderline lichens and a new order of fungi: *Collemopsidiales* (*Dothideomyceta*). Fungal Diversity 80: 285–300. https://doi.org/10.1007/s13225-016-0361-1

Phookamsak R, Norphanphoun C, Tanaka K, Dai DQ, Luo ZL, Liu JK, Su HY, Bhat DJ, Bahkali AH, Mortimer PE, Xu JC, Hyde KD (2015) Towards a natural classification of *Astrosphaeriella*-like species; introducing Astrosphaeriellaceae and Pseudoastrosphaeriellaceae fam. nov. and *Astrosphaeriellopsis*, gen. nov. Fungal Diversity 74: 143–197. https://doi.org/10.1007/s13225-015-0352-7

Phukhamsakda C, Hongsanan S, Ryberg M, Ariyawansa HA, Chomnunti P, Bahkali AH, Hyde KD (2016) The evolution of Massarineae with Longipedicellataceae *fam. nov*. Mycosphere 7(11): 1713–1731. https://doi.org/10.5943/mycosphere/7/11/7

Pilantanapak A, Jones EBG, Eaton RA (2005) Marine fungi on *Nypa fruticans* in Thailand. Botanica Marina 48: 365–373. https://doi.org/10.1515/bot.2005.049

Pinnoi A, Jones EBG, McKenzie EHC, Hyde KD (2003) Aquatic fungi from peat swamp palms: *Unisetosphaeria penguinoides* gen. et sp. nov., and three new *Dactylaria* species. Mycoscience 44: 377–382. https://doi.org/10.1007/S10267-003-0124-1

Pinnoi A, Lumyong S, Hyde KD, Jones EBG (2006) Biodiversity of fungi on the palm *Eleiodoxa conferta* in Sirindhorn peat swamp forest, Narathiwat, Thailand. Fungal Diversity 22: 205–218.

Pinruan A, Pinnoi A, Hyde KD, Jones EBG (2014) Tropical peat swamp fungi with special reference to palms. In: Jones EBG, Hyde KD, Pang KL (Eds) Freshwater Fungi: and Fungal-like Organisms, Dee Gruyter, Berlin, 371–386. https://doi.org/10.1515/9783110333480.371

Pinruan U, Jones EBG, Hyde KD (2002) Aquatic fungi from peat swamp palms: *Jahnula appendiculata* sp. nov. Sydowia 54(2): 242–247.

Pinruan U, Hyde KD, Lumyong S, McKenzie EHC, Jones EBG (2007) Occurrence of fungi on tissues of the peat swamp palm *Licuala longicalycata*. Fungal Diversity 25: 157–173.

Pinruan U, Sakayaroj J, Hyde KD, Jones EBG (2008) *Thailandiomyces bisetulosus* gen. et sp. nov. (*Diaporthales*, *Sordariomycetidae*, *Sordariomycetes*) and its anamorph *Craspedodidymum*, is described based on nuclear SSU and LSU rDNA sequences. Fungal Diversity 29: 89–98.

Pinruan U, Rungjindamai N, Choeyklin R, Lumyong S, Hyde KD, Jones EBG (2010a) Occurrence and diversity of basidiomycetous endophytes from the oil palm, *Elaeis guineensis* in Thailand. Fungal Diversity 41: 71–88. https://doi.org/10.1007/s13225-010-0029-1

Pinruan U, Rungjindamai N, Sakayaroj J, Lumyong S, Hyde KD, Jones EBG (2010b) *Baipadisphaeria* gen. nov., a freshwater ascomycete (Hypocreales, Sordariomycetes) from decaying palm leaves in Thailand. Mycosphere 1: 53–63.

Prieto M, Wedin M (2013) Dating the diversification of the major lineages of Ascomycota (Fungi). PLoS ONE 8(6): e65576. https://doi.org/10.1371/journal.pone.0065576

Rambaut A (2014) FigTree 1.4.2. http://tree.bio.ed.ac.uk/software/figtree

Rambaut A, Suchard MA, Xie D, Drummond AJ (2013) Tracer version 1.6. http://tree.bio.ed.ac.uk/software/tracer

Rannala B, Yang ZH (1996) Probability distribution of molecular evolutionary trees: a new method of phylogenetic inference. Journal of Molecular Evolution 43: 304–311. https://doi.org/10.1007/BF02338839

Rehner SA, Buckley E (2005) A Beauveria phylogeny inferred from nuclear ITS and EF1-α sequences: evidence for cryptic diversification and links to Cordyceps teleomorphs. Mycologia 97(1): 84–98. https://doi.org/10.1080/15572536.2006.11832842

Ronquist F, Huelsenbeck JP (2003) MrBayes3: Bayesian phylogenetic inference under mixed models. Bioinformatics 19(12): 1572–1574. https://doi.org/10.1093/bioinformatics/btg180

Rodrigues KF, Samuels GJ (1990) Preliminary study of endophytic fungi in a tropical palm. Mycological Research 94: 827–830. https://doi.org/10.1016/S0953-7562(09)81386-5

Samarakoon MC, Hyde KD, Promputtha I, Ariyawansa HA, Hongsanan S (2016) Divergence and ranking of taxa across the kingdoms Animalia, Fungi and Plantae. Mycosphere 7: 1678–1689. https://doi.org/10.5943/mycosphere/7/11/5

Schmidt AR, Beimforde C, Seyfullah LJ, Wege SE, Dörfelt H, Girard V, Grabenhorst H, Gube M, Heinrichs J, Nel A, Patricia N, Perrichot V, Reitner J, Rikkinen J (2014) Amber fossils of sooty moulds. Review of Palaeobotany and Palynology 200: 53–64. https://doi.org/10.1016/j.revpalbo.2013.07.002

Spegazzini CL (1881) Fungi Argentini additis nonnullis Brasiliensibus Montevideensibusque. Anales de la Sociedad Cientifica Argentina 12(4): 174–189.

Stamatakis A (2006) RAxML-VI-HPC: maximum likelihood-based phylogenetic analyses with thousands of taxa and mixed models. Bioinformatics 22(21): 2688–2690. https://doi.org/10.1093/bioinformatics/btl446

Stamatakis A, Hoover P, Rougemont J (2008) A rapid bootstrap algorithm for the RAxML web servers. Systematic Biology 57(5): 758–771. https://doi.org/10.1080/10635150802429642

Suetrong S, Schoch CL, Spatafora JW, Kohlmeyer J, Volkmann-Kohlmeyer B, Sakayaroj J, Phongpaichit S, Tanaka K, Hirayama K, Jones EBG (2009) Molecular systematics of the marine *Dothideomycetes*. Studies in Mycology 64: 155–173. https://doi.org/10.3114/sim.2009.64.09

Suetrong S, Klaysuban A, Sakayaroj J, Preedanon S, Ruang-Areerate P, Phongpaichit S, Pang KL, Jones EBG (2015) Tirisporellaceae, a new family in the order Diaporthales (Sordariomycetes, Ascomycota). Cryptogamie, Mycologie 36(3): 319–330. https://doi.org/10.7872/crym/v36.iss3.2015.319

Swofford DL (2002) PAUP*. Phylogenetic analysis using parsimony (*and other methods). Version 4. Sinauer Associates, Sunderland, Massachusetts, USA.

Taylor JE, Hyde KD, Jones EBG (1999) Endophytic fungi associated with the temperate palm, *Trachycarpus fortunei*, within and outside its natural geographic range. New Phytologist 142: 335–346. https://doi.org/10.1046/j.1469-8137.1999.00391.x

Taylor JE, Hyde KD, Jones EBG (2000) The biogeographical distribution of microfungi associated with three palm species from tropical and temperate habitats. Journal of Biogeography 27: 297–310. https://doi.org/10.1046/j.1365-2699.2000.00385.x

Taylor JE, Hyde KD (2003) Microfungi of tropical and temperate palms. Fungal Diversity Press, 1–459.

Taylor TN, Krings M, Taylor EL (2015) Fossil fungi. Academic Press, 129–171. https://doi.org/10.1016/B978-0-12-387731-4.00008-6

Tomlinson P (1986) The botany of mangroves. Cambridge tropical biology series. Cambridge University Press, Cambridge, 1–432.

Vilgalys R, Hester M (1990) Rapid genetic identification and mapping of enzymatically amplified ribosomal DNA from several Cryptococcus species. Journal of Bacteriology 172(8): 4238–4246. https://doi.org/10.1128/jb.172.8.4238-4246.1990

Wanasinghe DN, Jeewon R, Jones EBG, Boonmee S, Kaewchai S, Manawasinghe IS, Lumyong S, Hyde KD (2018) Novel palmicolous taxa within Pleosporales: multigene phylogeny and taxonomic circumscription. Mycological Progress 17(5): 571–590. https://doi.org/10.1007/s11557-018-1379-4

White TJ, Bruns T, Lee S, Taylor J (1990) Amplification and direct sequencing of fungal ribosomal RNA genes for phylogenetics. In: Innis MA, Gelfand DH, Sninsky JJ, White TJ (Eds) PCR protocols: a guide to methods and applications. Academic Press, Inc., New York, 315–322.

Yanna, Ho WH, Hyde KD, Goh TK (2001a) Occurrence of fungi on tissues of *Livistona chinensis*. Fungal Diversity 6: 167–180.

Yanna, Ho WH, Hyde KD (2001b) Fungal communities on decaying palm fronds in Australia, Brunei, and Hong Kong. Mycological Research 105(12): 1458–1471. https://doi.org/10.1017/S0953756201005214

Yanna, Ho WH, Hyde KD, McKenzie EHC (2001c) *Sporidesmiella oraniopsis*, a new species of dematiaceous hyphomycete from North Queensland, Australia and synopsis of the genus. Fungal Diversity 8: 183–190.

Yanna, Ho WH, Hyde KD (2002) Fungal succession on fronds of *Phoenix hanceana* in Hong Kong. Fungal Diversity 10: 185–211.

Zhang JF, Liu JK, Hyde KD, Liu YX, Bahkali AH, Liu ZY (2016) Ligninsphaeria jonesii gen. et. sp. nov., a remarkable bamboo inhabiting ascomycete. Phytotaxa 247(2): 109–117. https://doi.org/10.11646/phytotaxa.247.2.2

Zhang SN, Hyde KD, Jones EBG, Cheewangkoon R, Liu JK (2018) *Acuminatispora palmarum* gen. et sp. nov. from mangrove habitats. Mycological progress 17: 1173–1188. https://doi.org/10.1007/s11557-018-1433-2

Zhao RL, Li GJ, Sánchez-Ramírez S, Stata M, Yang ZL, Wu G, Dai YC, He SH, Cui BK, Zhou JL, Wu F, He MQ, Moncalvo JM, Hyde KD (2017) A six-gene phylogenetic overview of *Basidiomycota* and allied phyla with estimated divergence times of higher taxa and a phyloproteomics perspective. Fungal Diversity 84: 43–74. https://doi.org/10.1007/s13225-017-0381-5

Supplementary material 1

Phylogenetic analysis

Authors: Sheng-Nan Zhang, Kevin D. Hyde, E.B. Gareth Jones, Rajesh Jeewon, Ratchadawan Cheewangkoon, Jian-Kui Liu

Link: https://doi.org/10.3897/mycokeys.49.30886.suppl1